Computational Mechanics of Interfaces

Multi-scale fracture and model order reduction Pierre Kerfriden, Lars Beex, Jack Hale, Olivier Goury, Daniel Alves Paladim, Elisa Schenone, Davide Baroli

Advanced discretisation techniques Xuan Peng, Haojie Lian, Sundararajan Natarajan

Error estimation Pierre Kerfriden, Satyendra Tomar, Daniel Alves Paladim…

Biomechanics applications Alexandre Bilger, Hadrien Courtecuisse

Stéphane P.A. Bordas stephane.bordas@alum.northwestern.edu

http://legato-team.eu

Presentation for Ostrava


10 km
10 miles
ARDENNES
Clervaux
BELGIUM
Wiltz
Vianden
GERMANY
Diekirch
MULLERTHAL
Echternach
LUXEMBOURG
Grevenmacher
LUXEMBOURG
MOSELLE
VALLEY
Moselle
Petange
Differdange
Modorf-les-Bains
Esch
Budelange
FRANCE
© wordtravels.com

A M

echanics

Materials

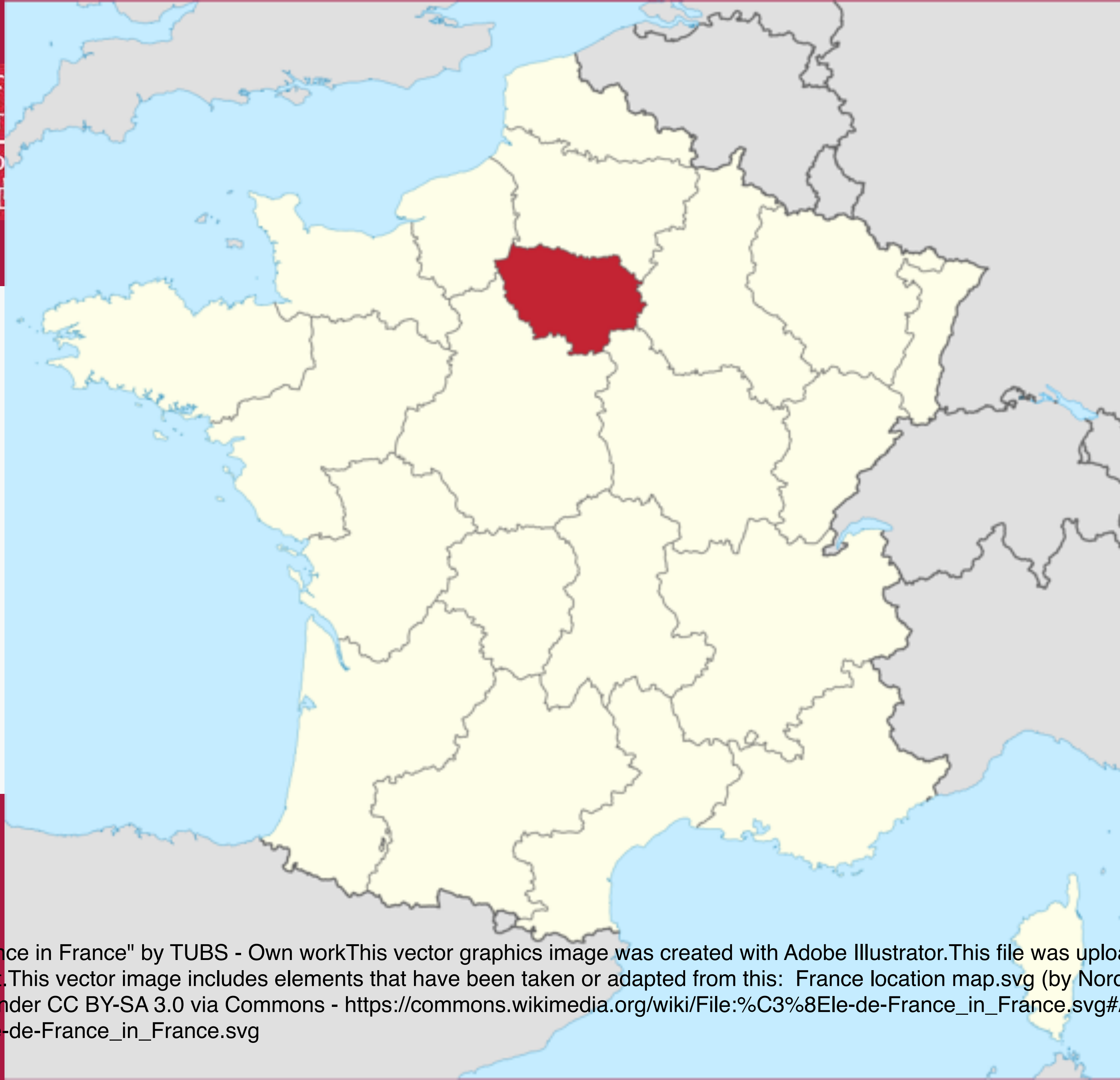

"Île-de-France in France" by TUBS - Own workThis vector graphics image was created with Adobe Illustrator.This file was uploaded with Commonist.This vector image includes elements that have been taken or adapted from this: France location map.svg (by NordNordWest).. Licensed under CC BY-SA 3.0 via Commons - https://commons.wikimedia.org/wiki/File:%C3%8Ele-de-France_in_France.svg#/media/File:%C3%8Ele-de-France_in_France.svg

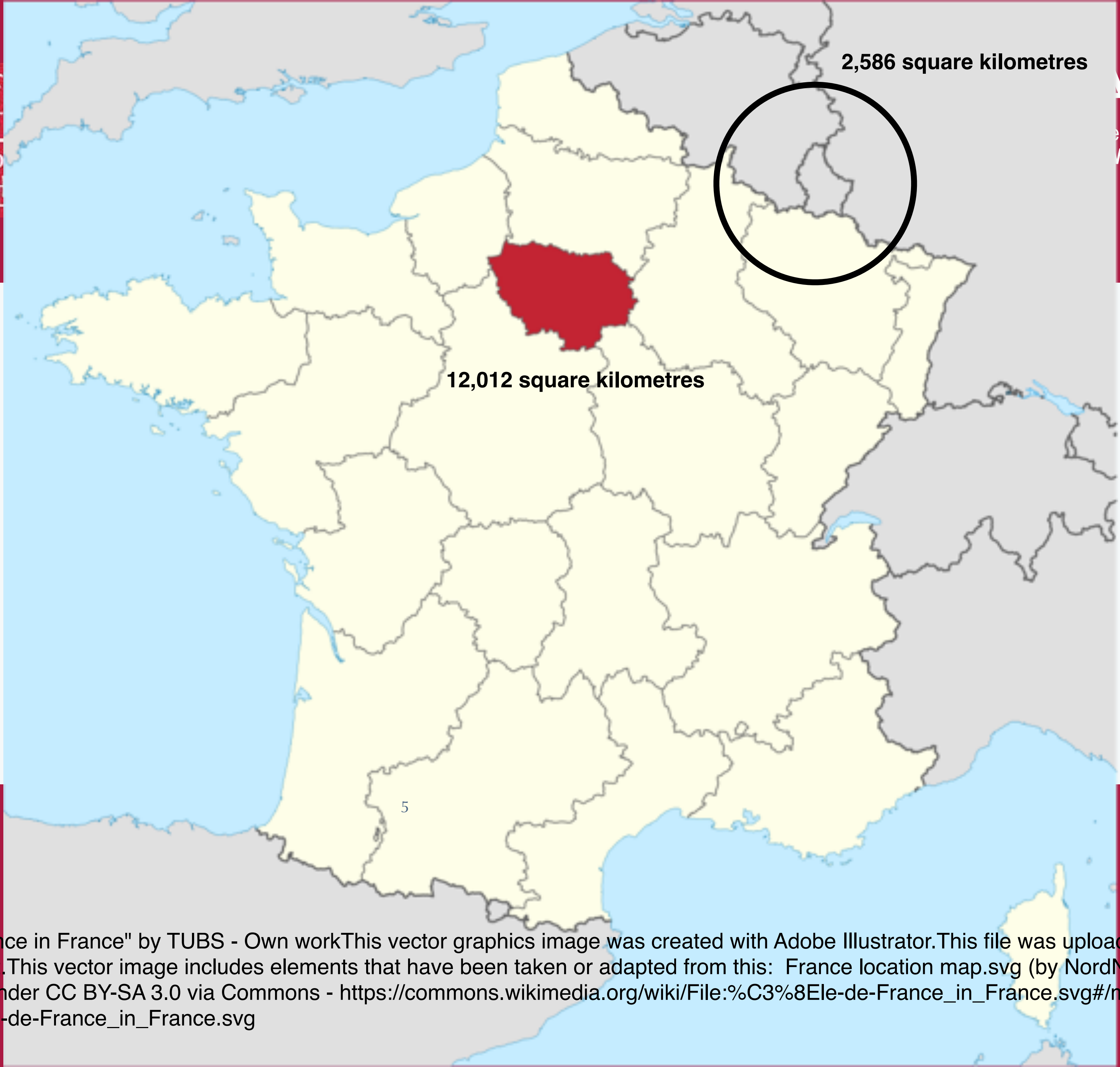
2,586 square kilometres
12,012 square kilometres


odic Table of the Finite Elements
O'NEILL

Discontinuities

Discontinuities

1

Large scale

Small scale

Discontinuities

Large scale

Small scale

Discontinuities

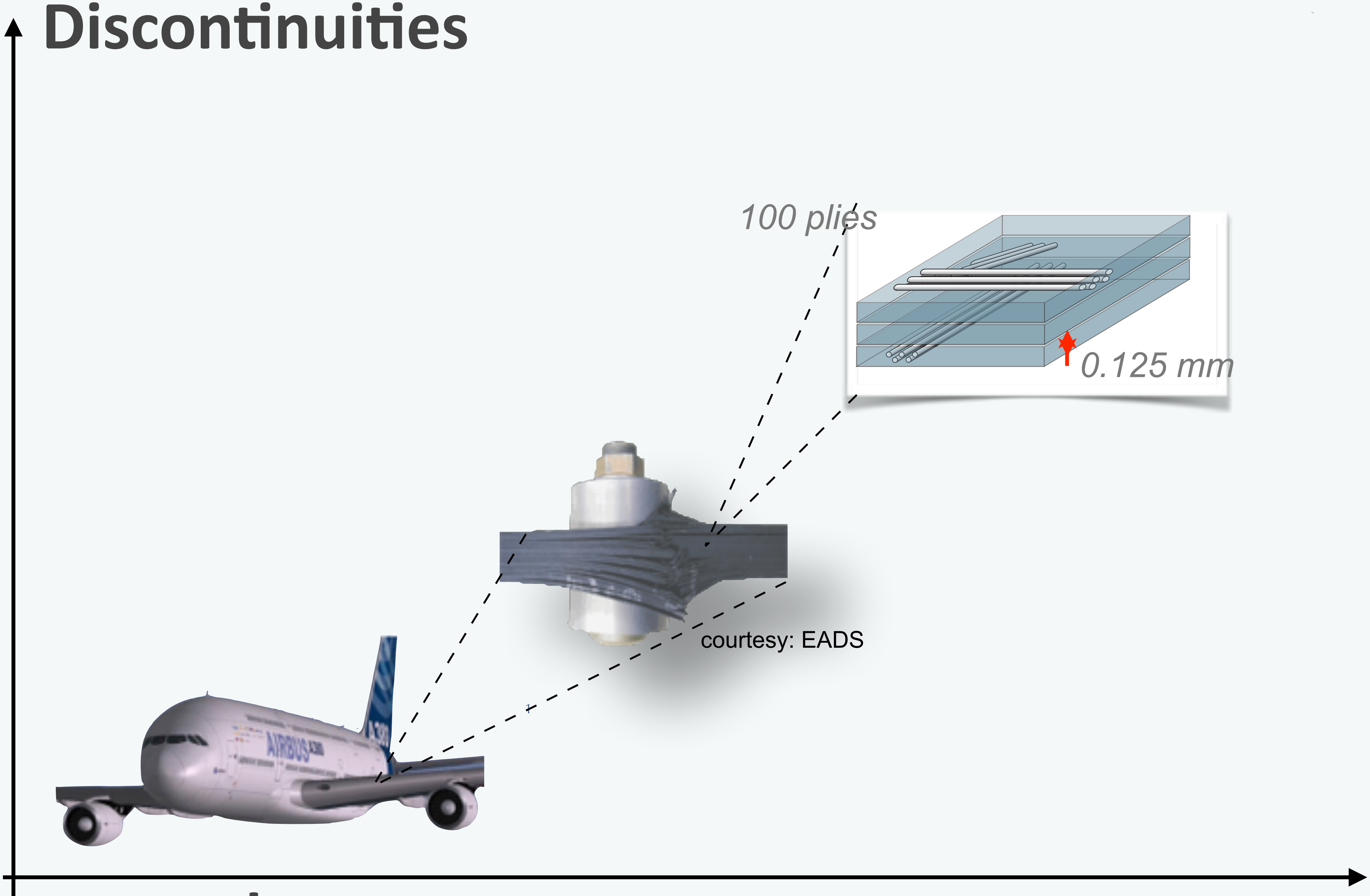

Large scale

Small scale

Mechanics of interfaces - or free boundary problems (Avner Friedman)

FEM

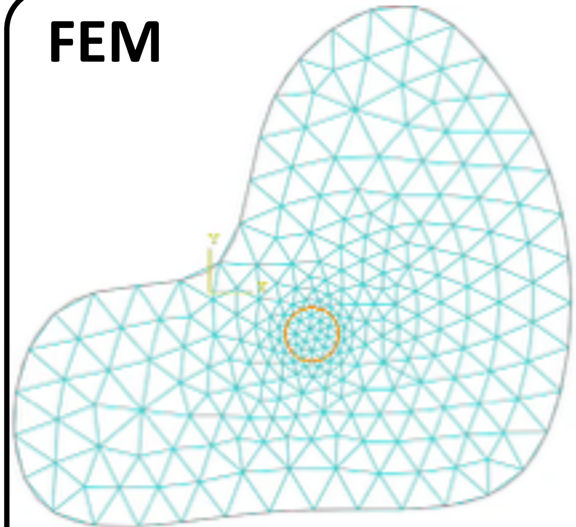

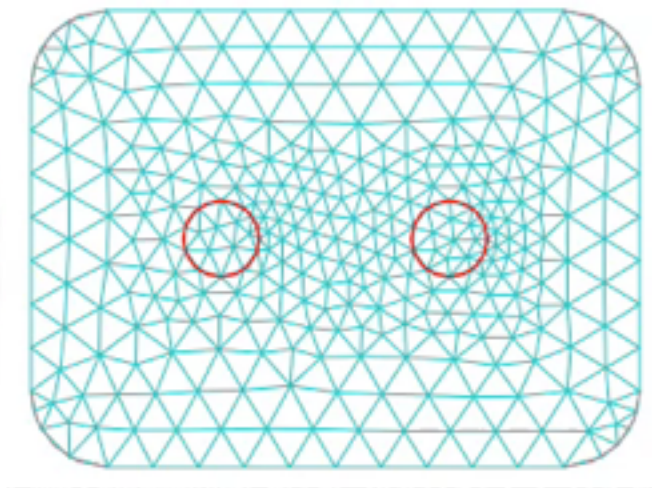

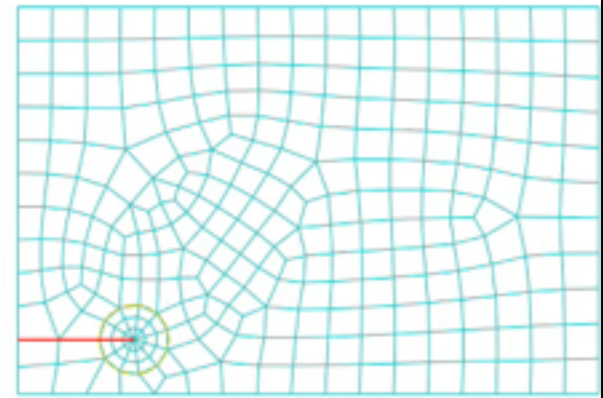

XFEM

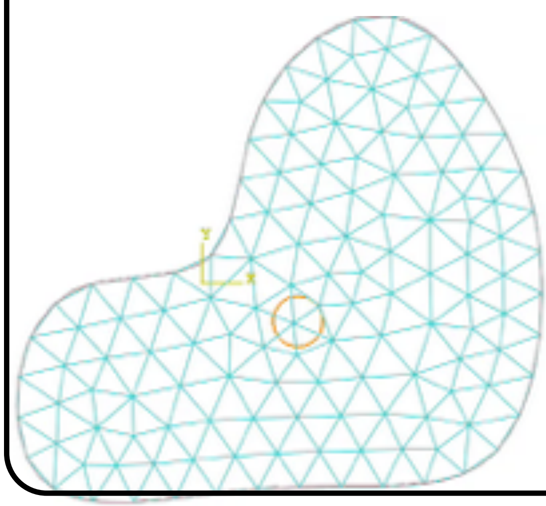

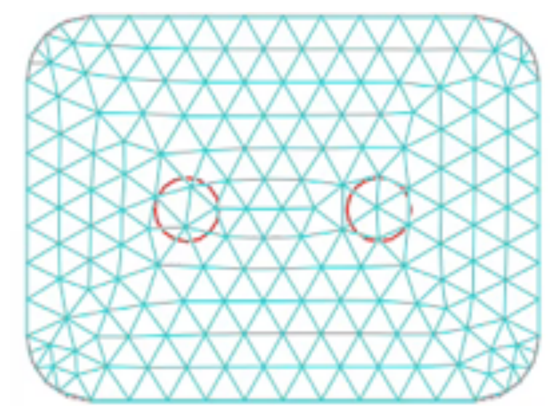

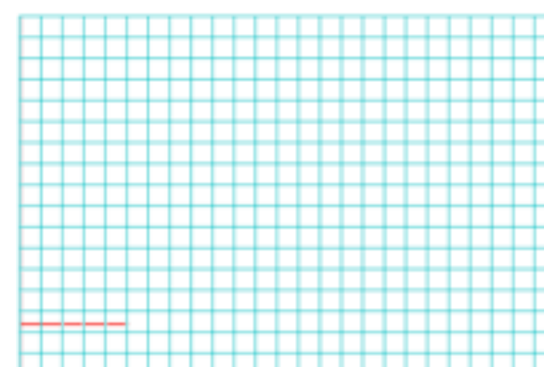

Interfaces in practical engineering simulations

PHASES

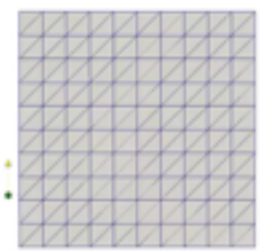

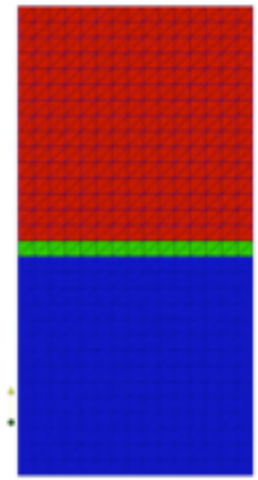

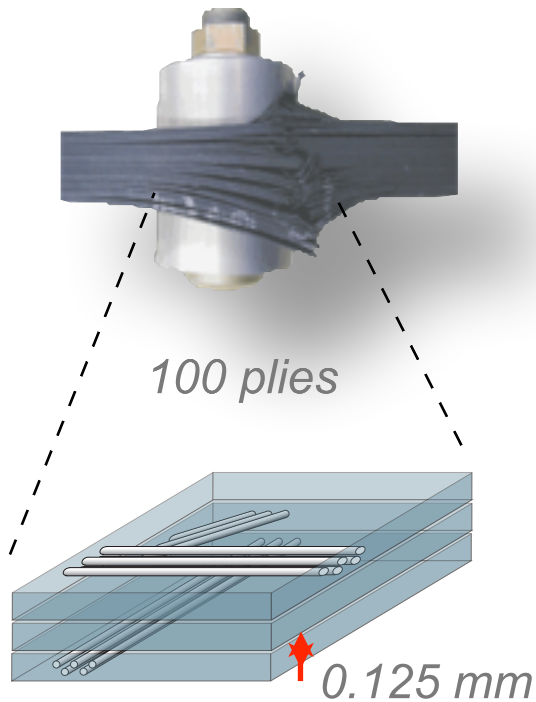

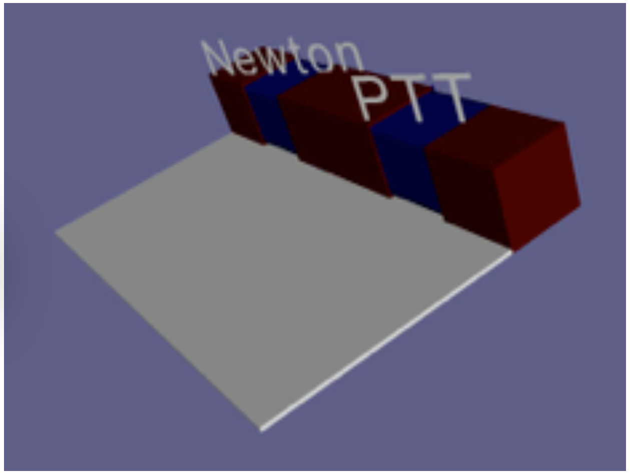

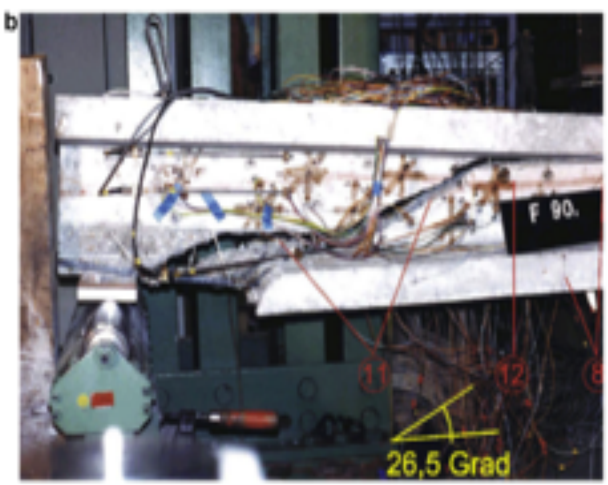

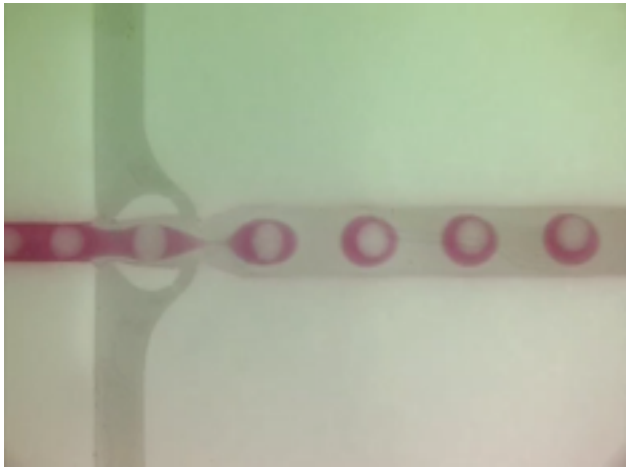

Interfaces in practical engineering simulations

CRACKS & CUTS

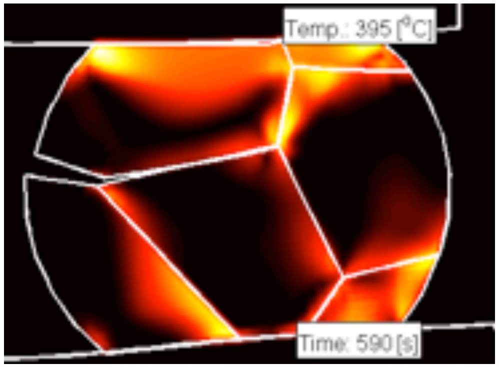

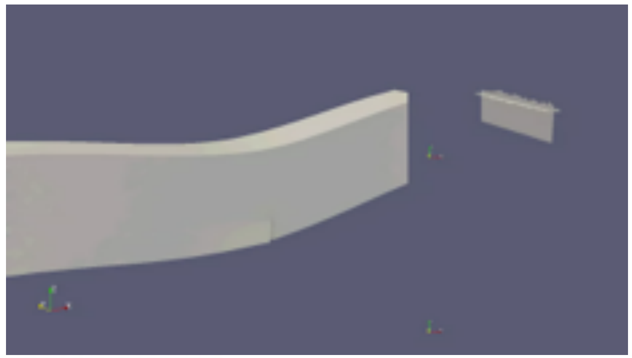

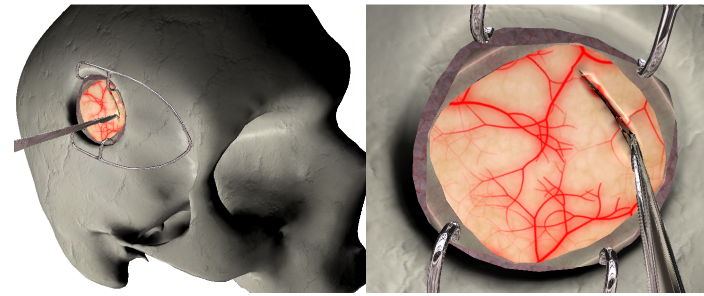

Real-time simulation of cutting during brain surgery

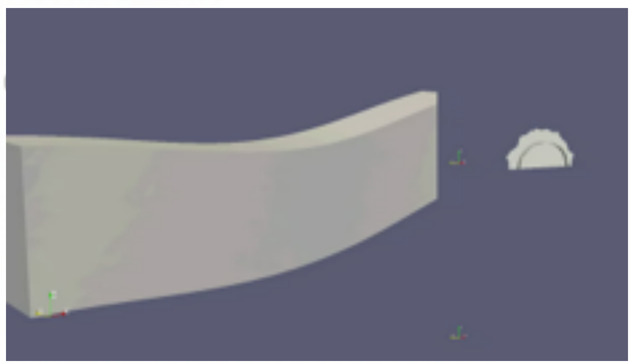

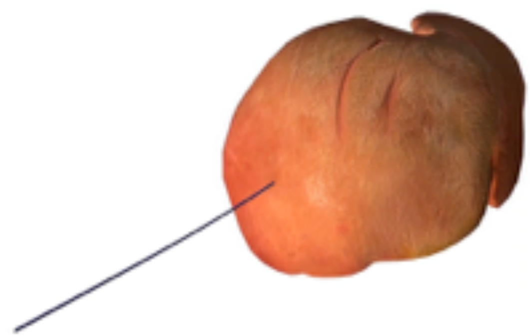

Needle tissue interaction with breathing motion

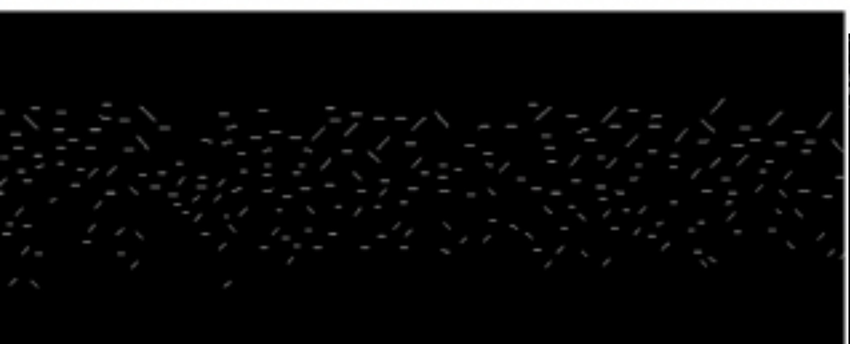

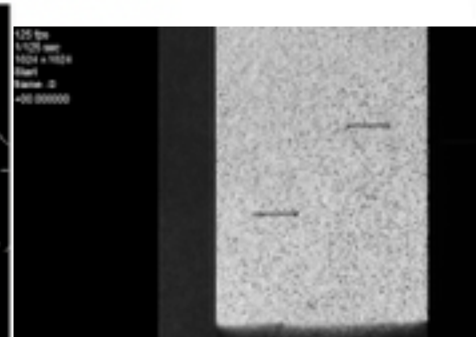

Interfaces in practical engineering simulations

MODELS

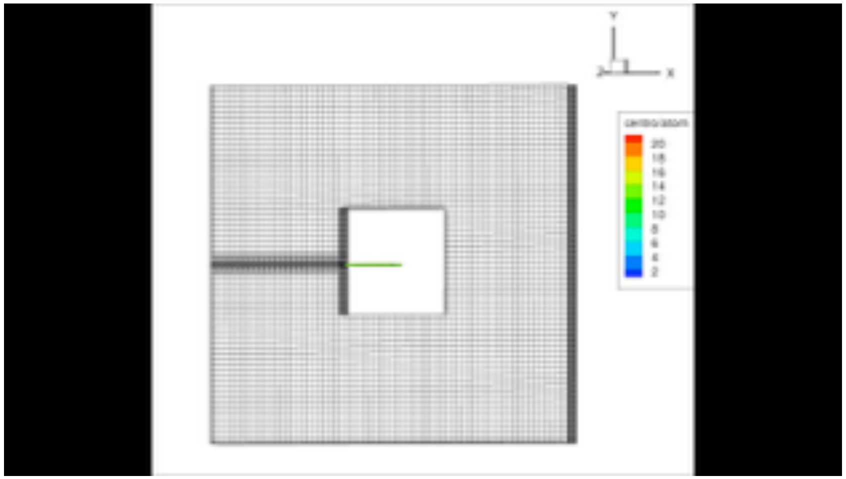

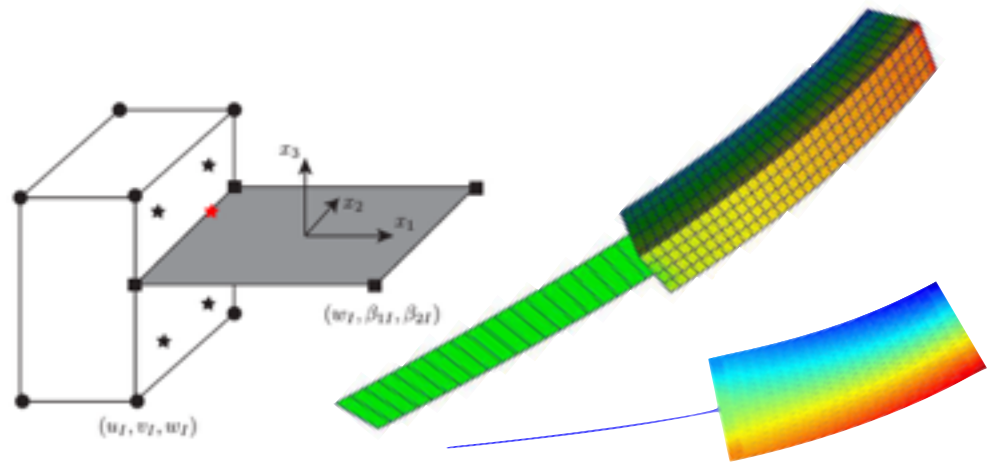

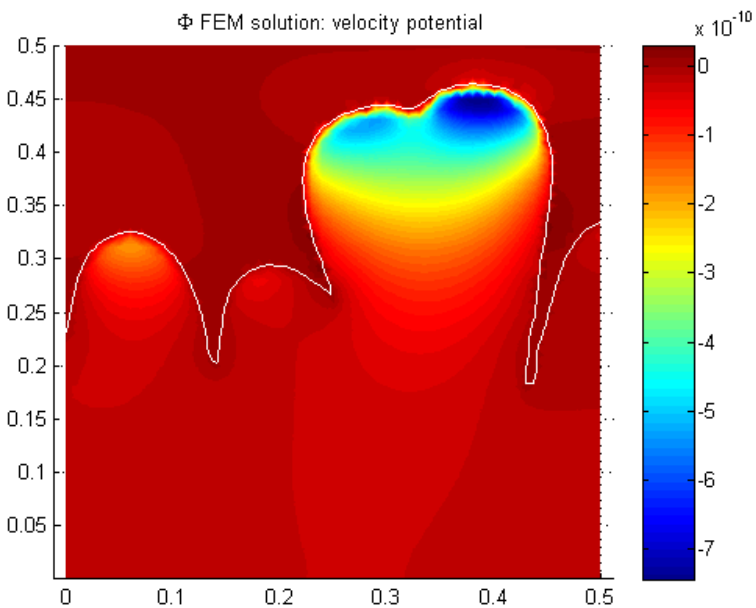

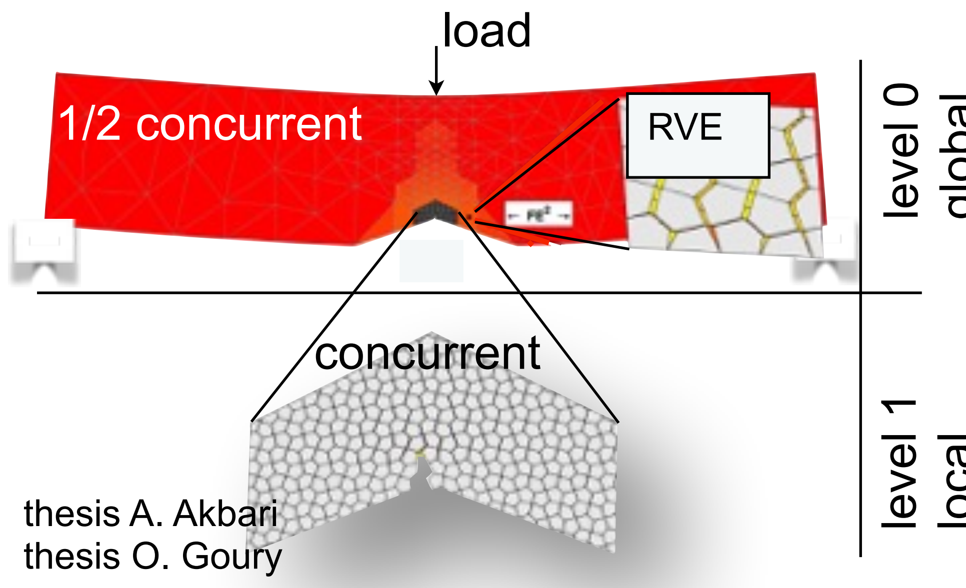

thesis A. Akbari
thesis O. Goury

DISCRETISATION

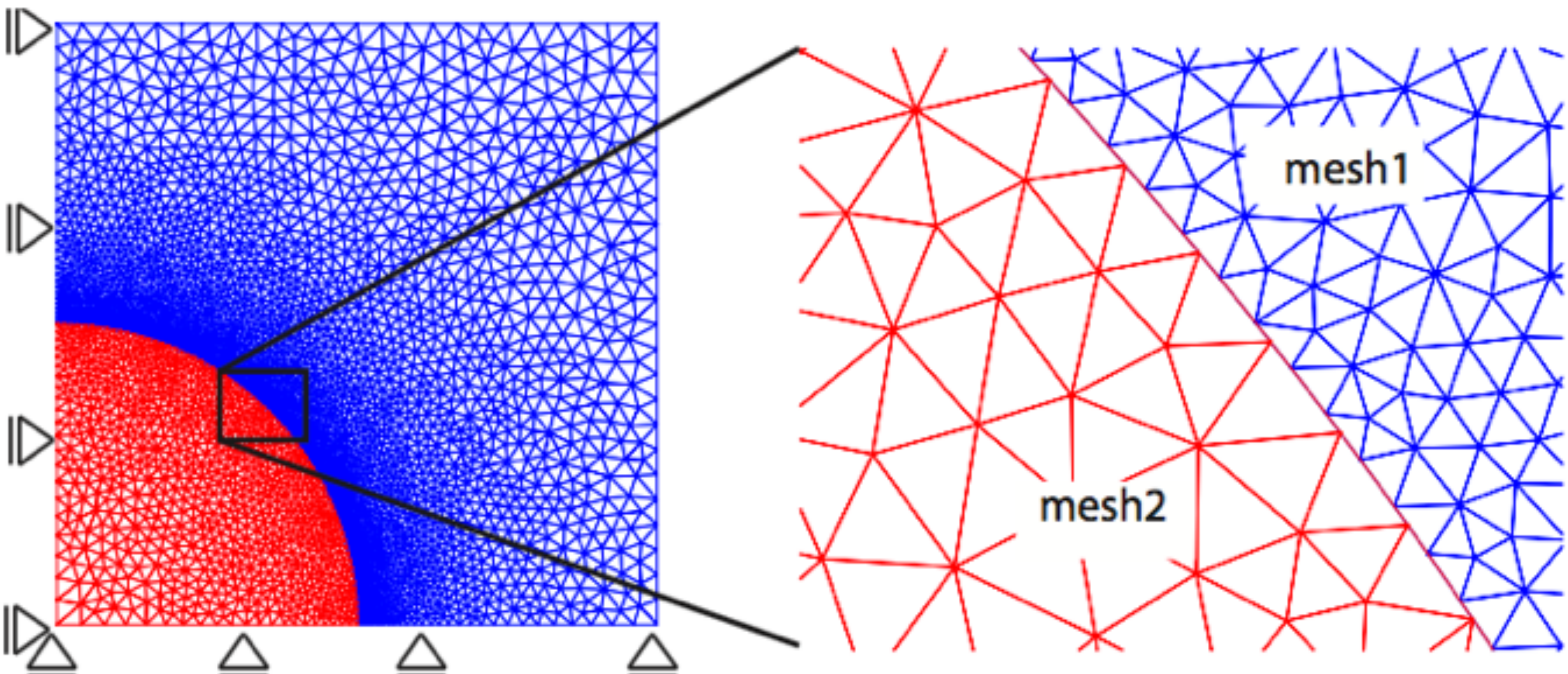

Computational mechanics & computational materials sciences Multiscale/field interface problems

COMPETENCES

DISCRETISATION
discrete and continuum approaches

MULTI-SCALE FRACTURE
aerospace composites, polycrystalline materials

COUPLED PROBLEMS
biofilms, liquid crystals, fluid-structure, batteries

QUALITY & ERROR CONTROL
optimise computational time given an accuracy level

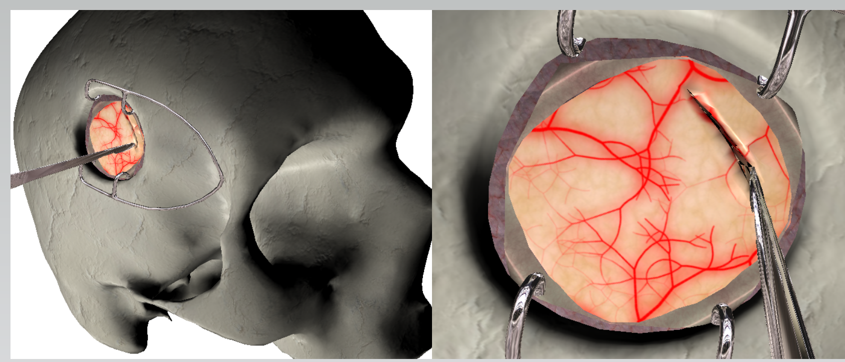

Real-time simulation of cutting during brain surgery

INTERACTIVITY
Reduce computational costs by several orders of magnitude

APPLICATIONS

PERSONALISED MEDICINE

- *Computer-aided surgery*
- *Computer-aided diagnostics*

ENGINEERING

- *Durability & Sustainability*
- *Energy*
- *Aerospace*

http://legato-team.eu — stephane.bordas@uni.lu S. Bordas, B. Peters, A. Zilian and S. Belouettar (LIST)

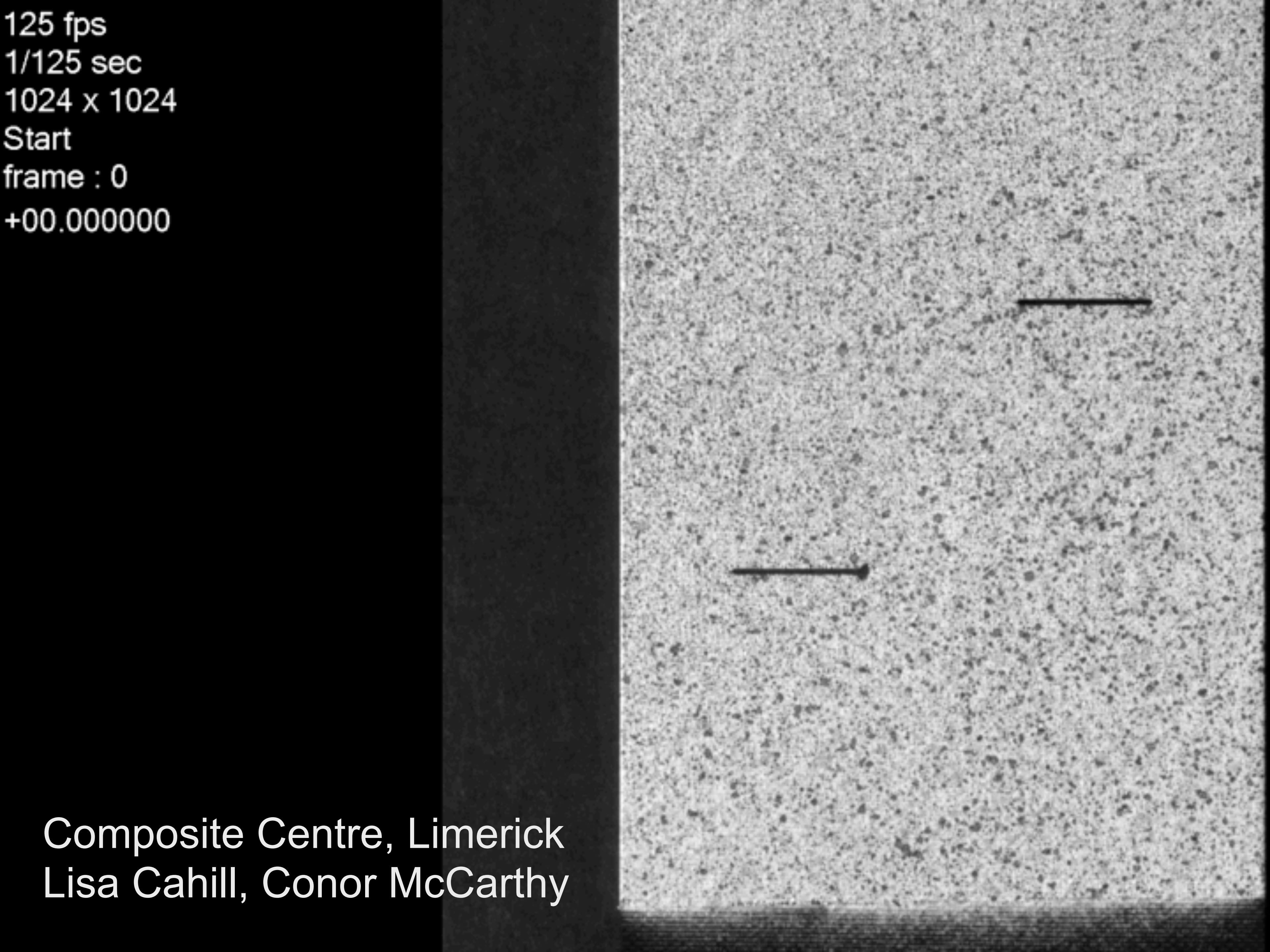
125 fps
1/125 sec
1024 x 1024
Start
frame : 0
+00.000000
Composite Centre, Limerick
Lisa Cahill, Conor McCarthy

Discretisation

Fracture over multiple scales

Coupled problems

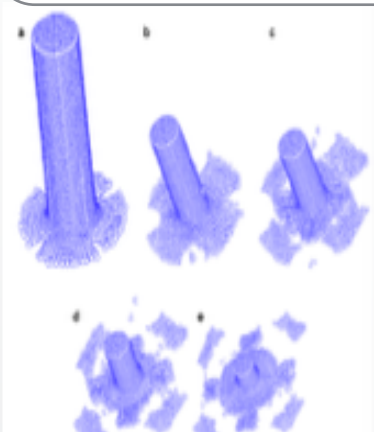

Mesh-free and discrete approaches to fracture

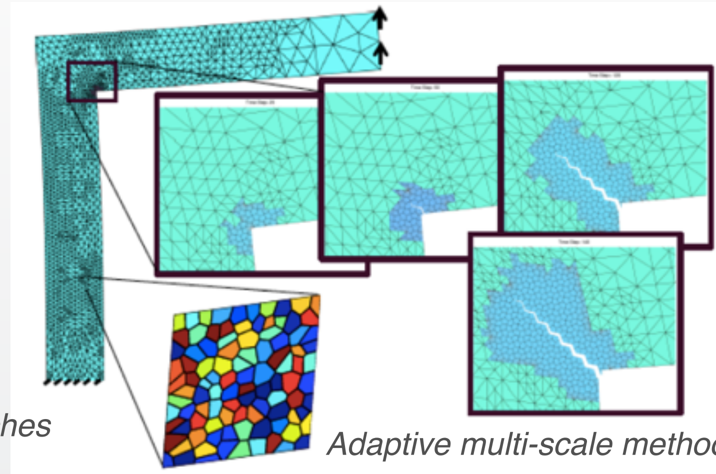

Adaptive multi-scale methods

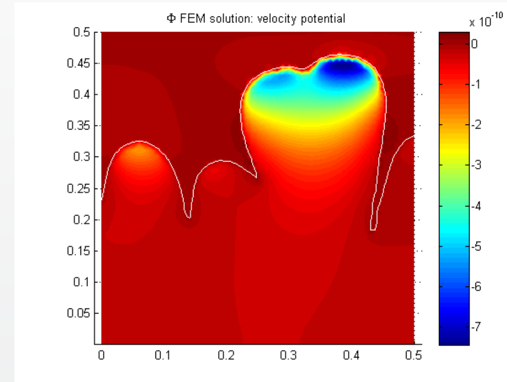

Biofilm growth

Quality and error control

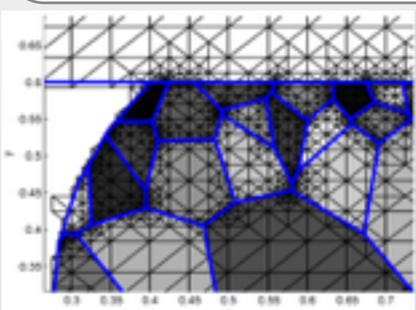

Durability of Pb-free solders

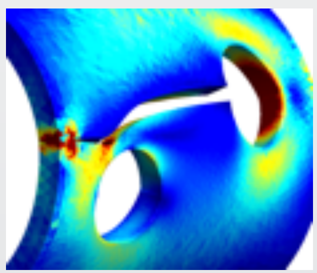

Error estimates for fracture

Interactivity and model order reduction

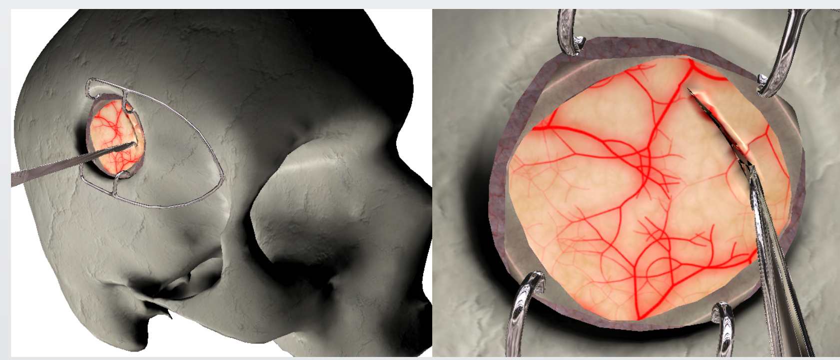

APPLICATIONS

Personalised Medicine

Engineering

Computer-aided surgery

Computer-aided diagnostics

Durability & Sustainability

Energy

Aerospace

Motivation: fracture of engineering structures and materials

- **Limerick**: unidirectional composites

thesis L. Cahill, 2014

- **China/USA**: hydraulic fracturing (shale gas)

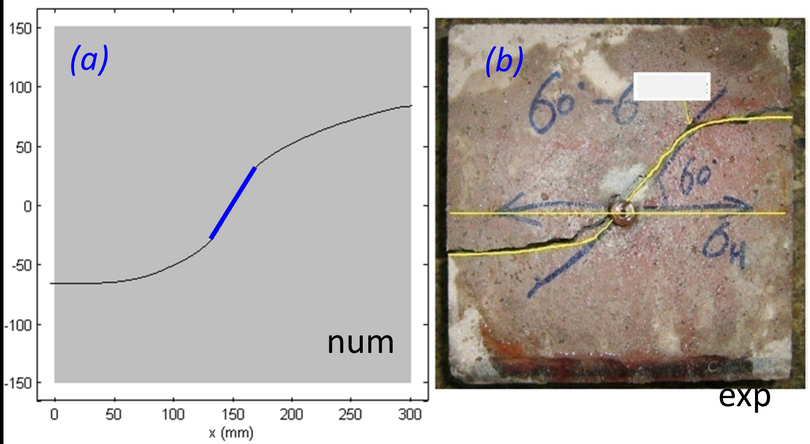

thesis M. Sheng, USA, China, 2016

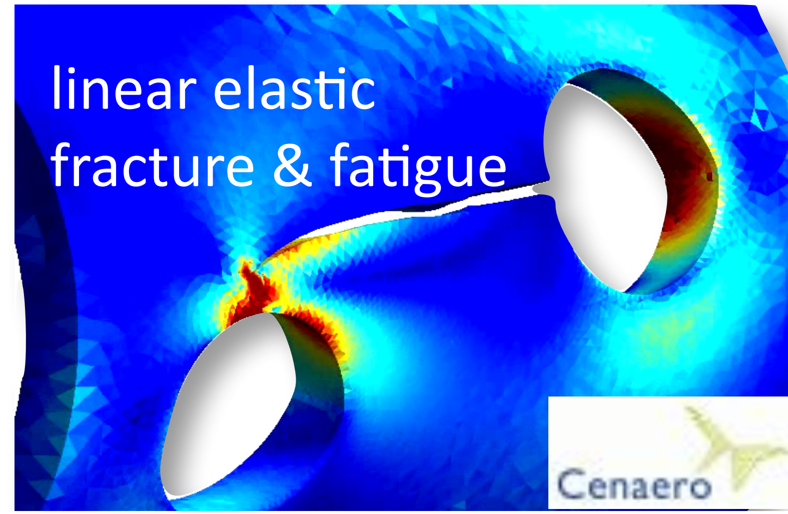

dynamics
ductile

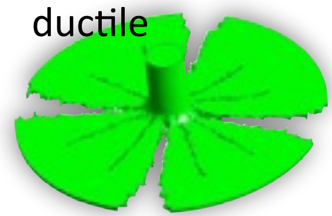

dynamics/brittle

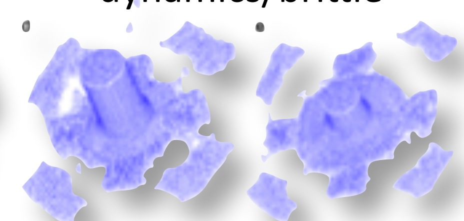

Solder joint durability (microelectronics), Bosch GmbH

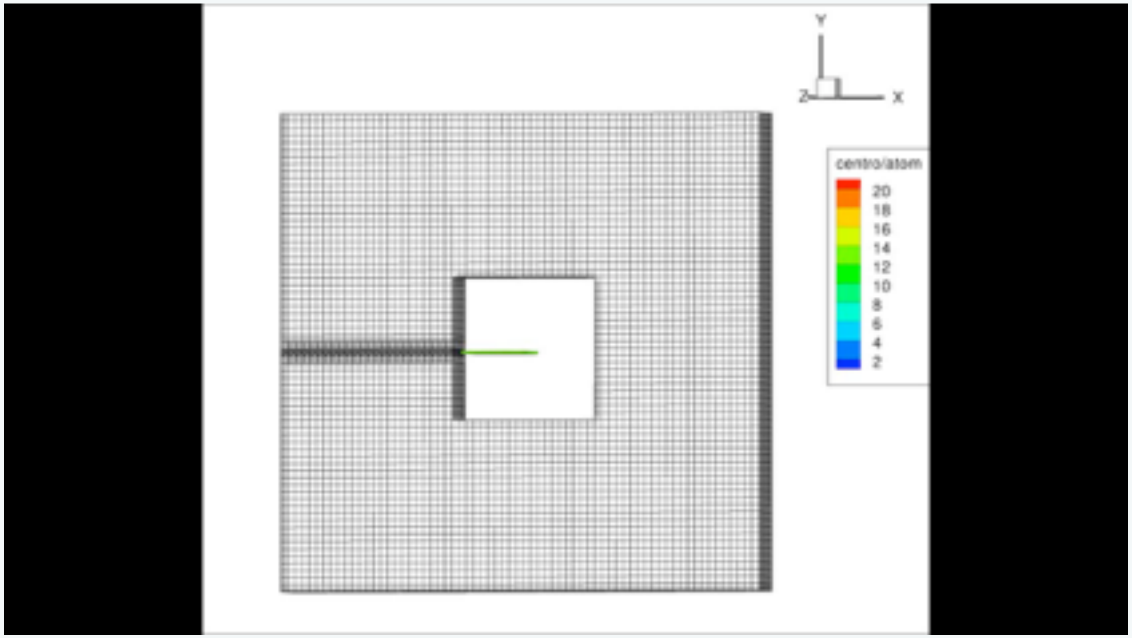

Motivation: multiscale fracture of engineering structures and materials

Practical early-stage design simulations (interactive)

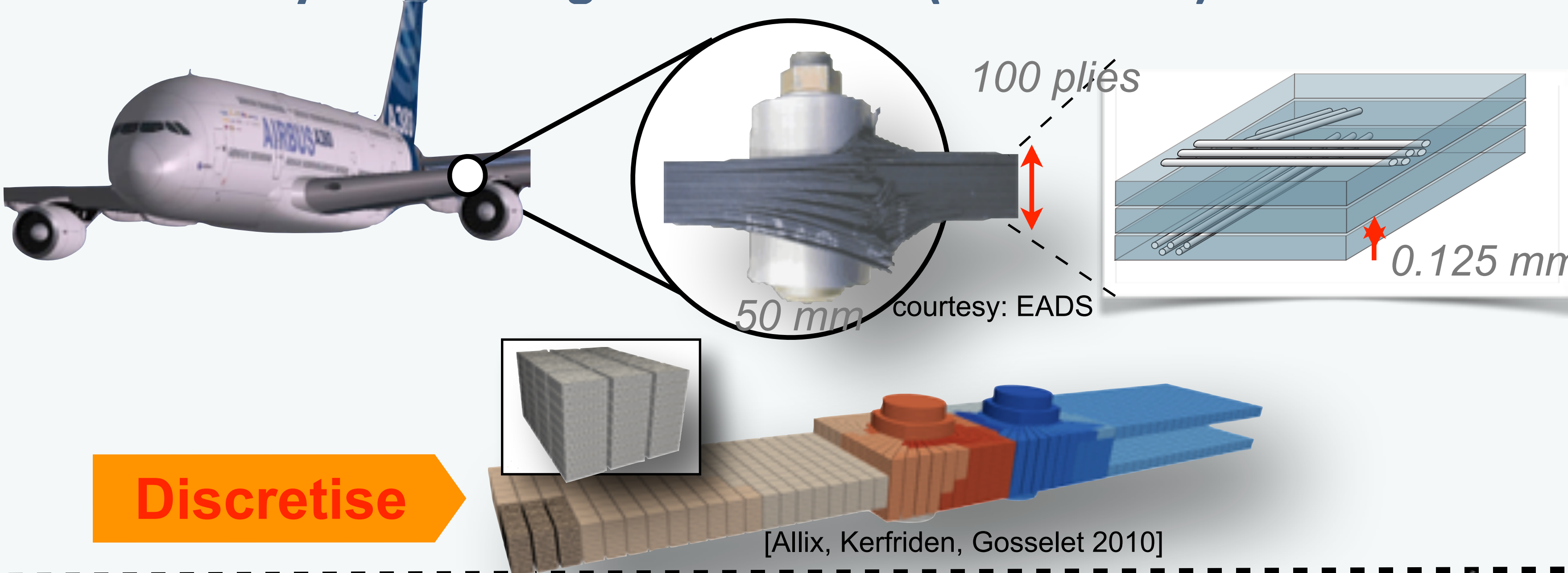

Surgical simulation

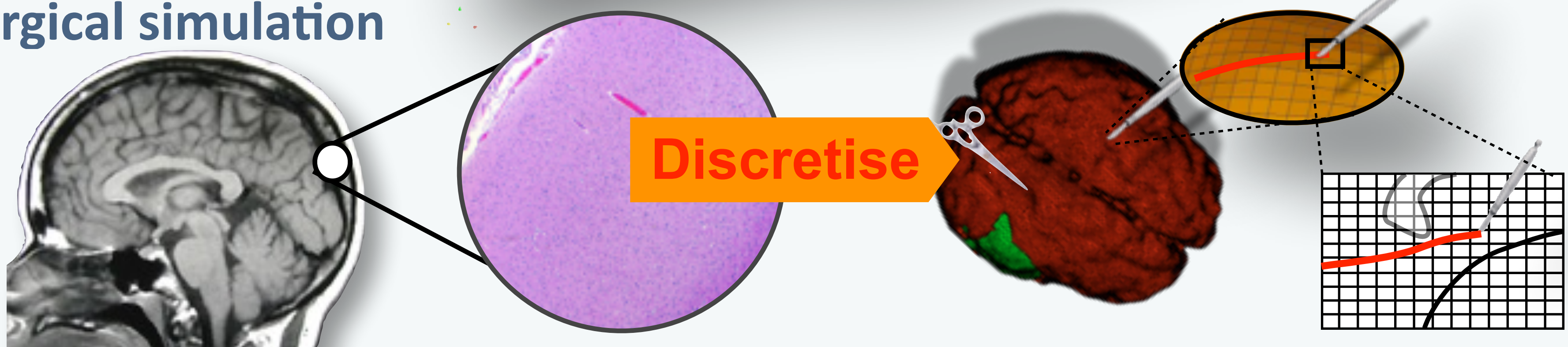

- Reduce the problem size while controlling the error (in QoI) when solving very large (multiscale) mechanics problems

Why enrich approximation spaces?

(board discussion)

ERROR ESTIMATION

Reality

Mathematical model

Truth (Continuum) $u \in \widetilde{V}$

Refined (Reference) $\hat{u} \in \hat{V}$

Coarse $u^h \in V^h$

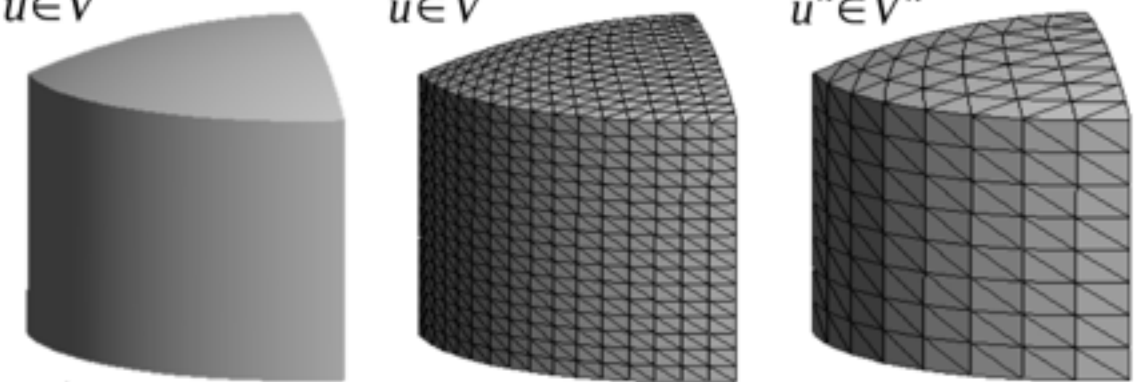

Model error

Discretization error 1

Discretization error 2

Weak form

$$\int_\Omega (\nabla\widetilde{\partial u}\cdot(\underline{\underline{D}}\nabla u)+\widetilde{\partial u}\cdot b\cdot u)\,d\Omega =: a(u,\widetilde{\partial u}) = l(\widetilde{\partial u}) := \int_\Omega \widetilde{\partial u}\cdot f\,d\Omega + \int_{\Gamma_n}\widetilde{\partial u}\cdot g_n\,d\Gamma_n, \quad \forall\,\widetilde{\partial u}\in\widetilde{V}$$

Exact expression for the discretization error (residual form).

$$a(u,\widetilde{\partial u}) - a(u^h,\widetilde{\partial u}) = l(\widetilde{\partial u}) - a(u^h,\widetilde{\partial u}) \qquad a(\widetilde{e},\widetilde{\partial u}) = R(\widetilde{\partial u}) \qquad \textit{where} \quad \widetilde{e} = u - u^h$$

- By Galerkin orthogonality the error in the coarse space is zero
- We need a richer discrete space, to compute any error

Why error estimation?

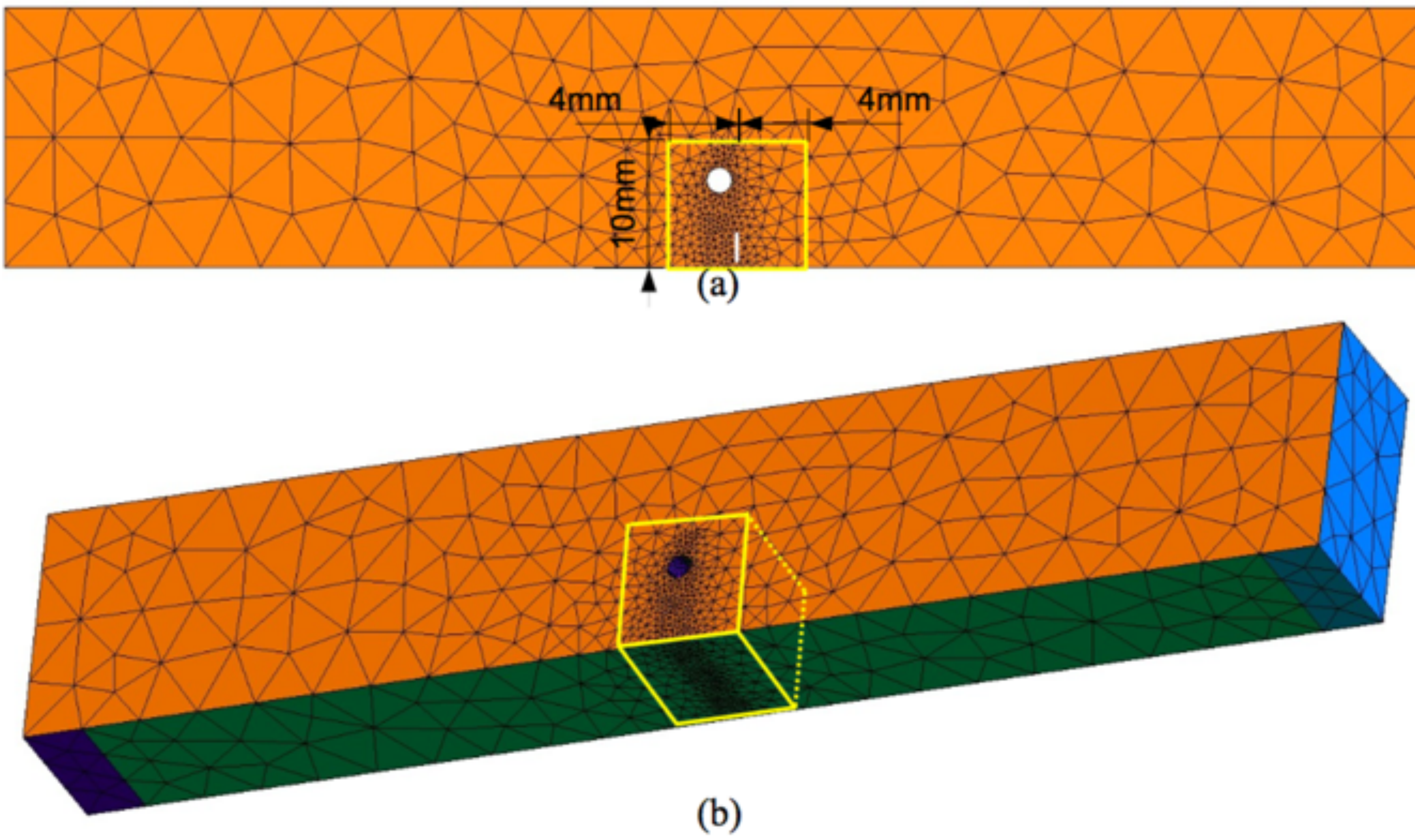

Why error estimation?

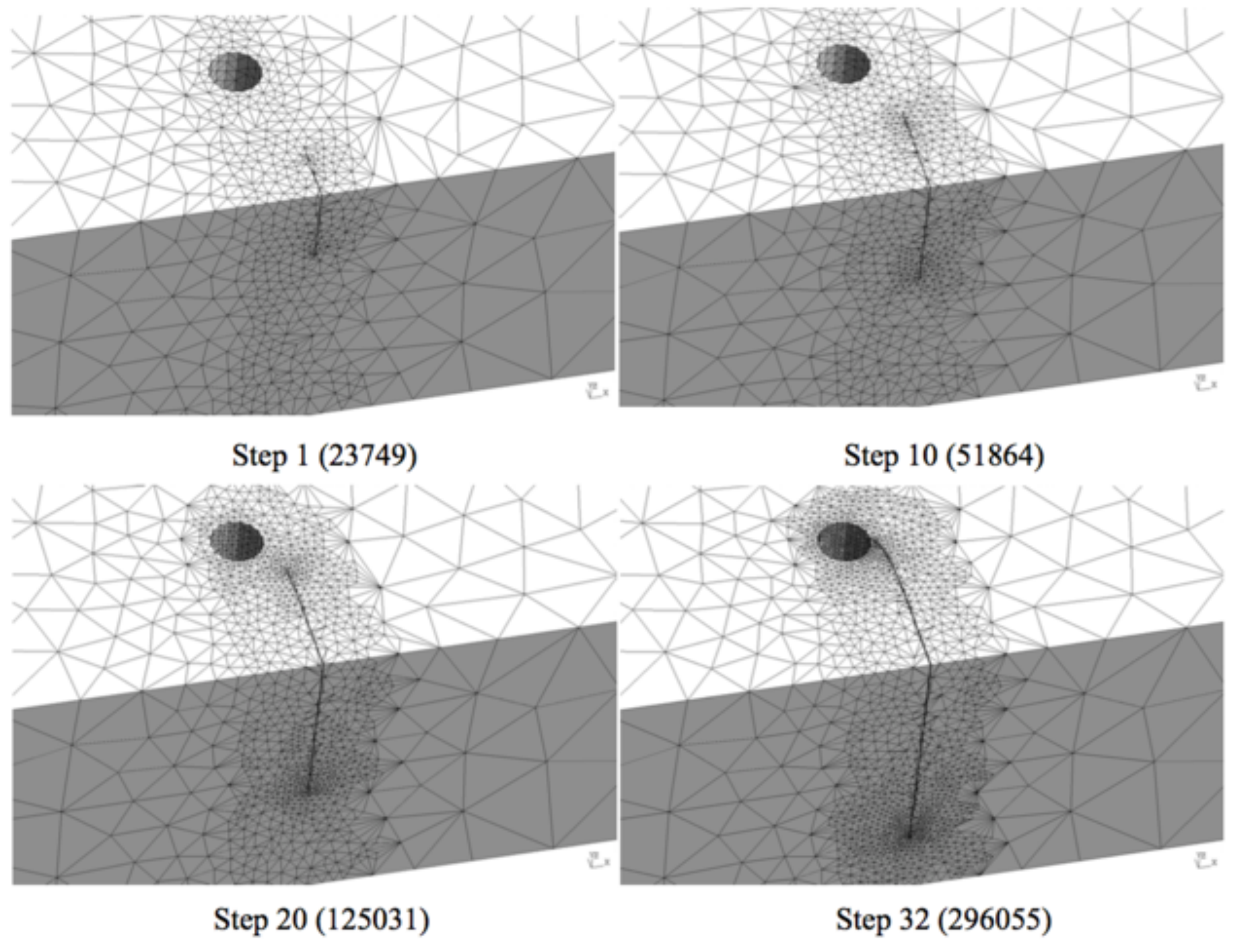

Step 1 (23749)

Step 10 (51864)

Step 20 (125031)

Step 32 (296055)

Why error estimation?

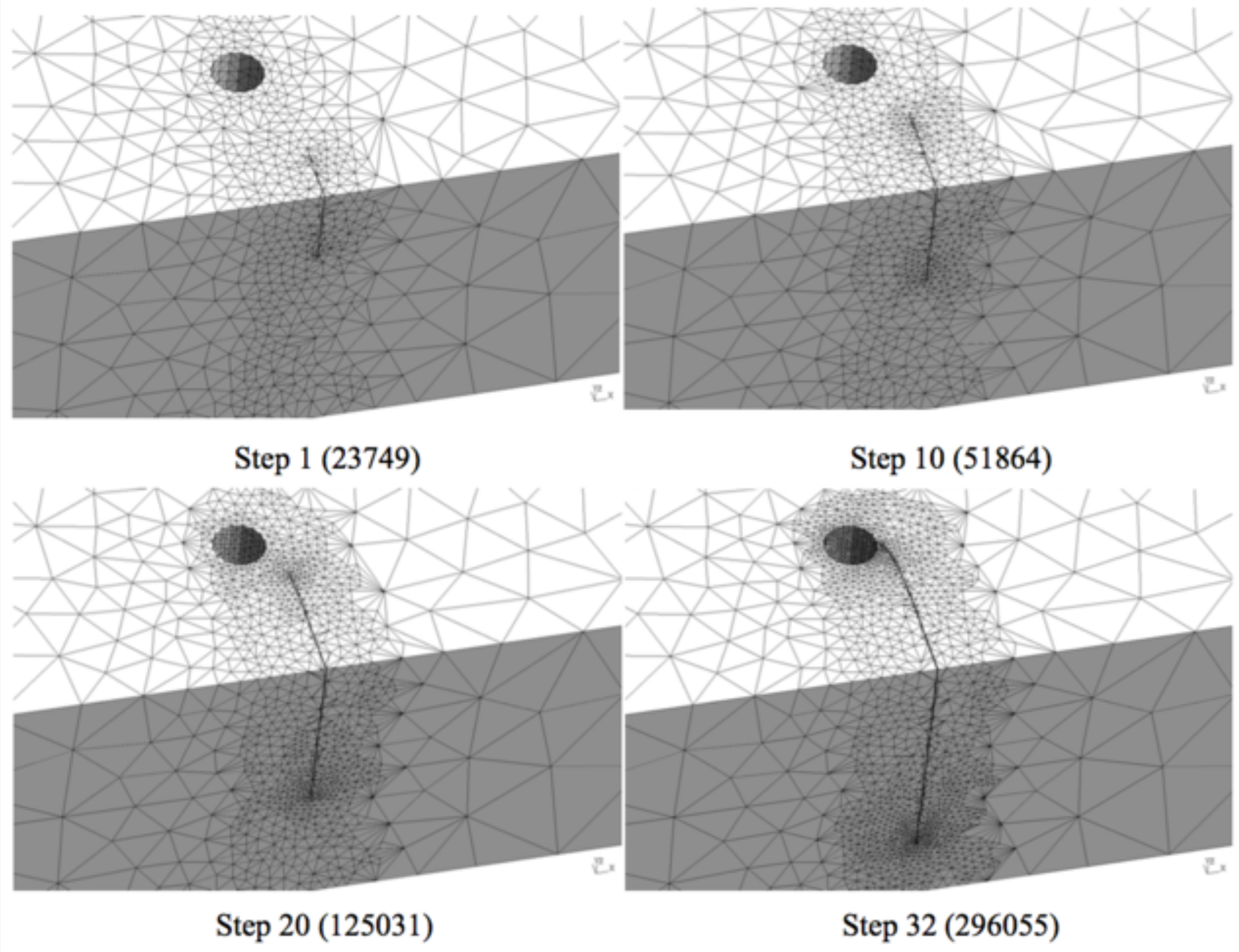

Step 1 (23749) Step 10 (51864)

Step 20 (125031) Step 32 (296055)

Why error estimation?

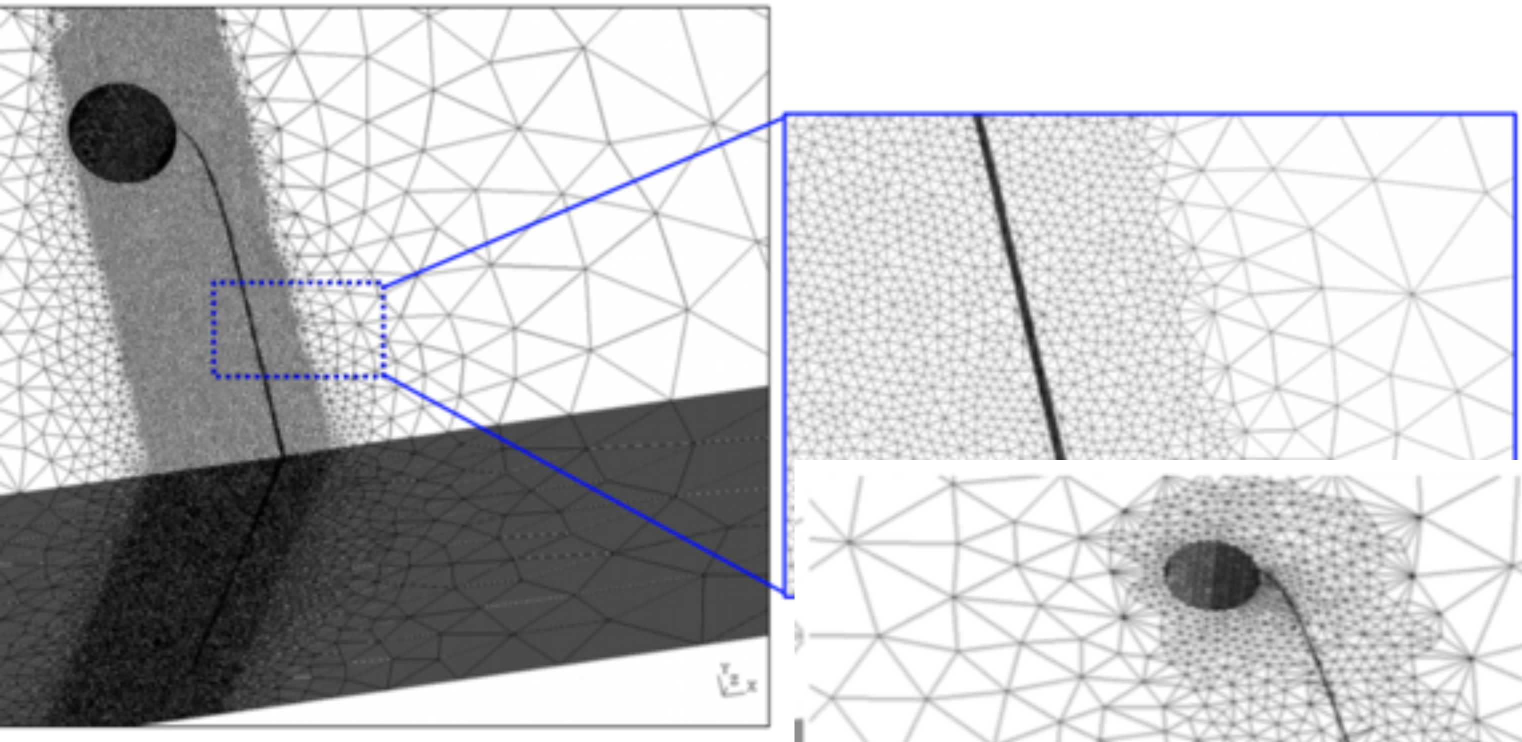

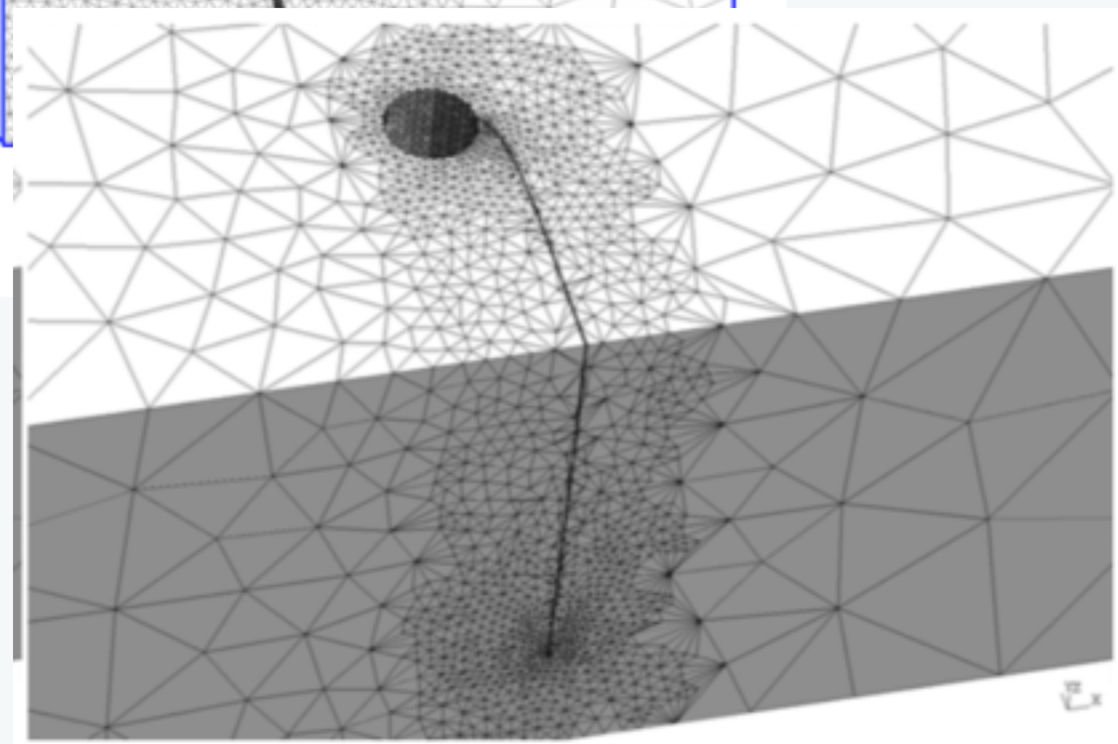

Step 32 (296055)

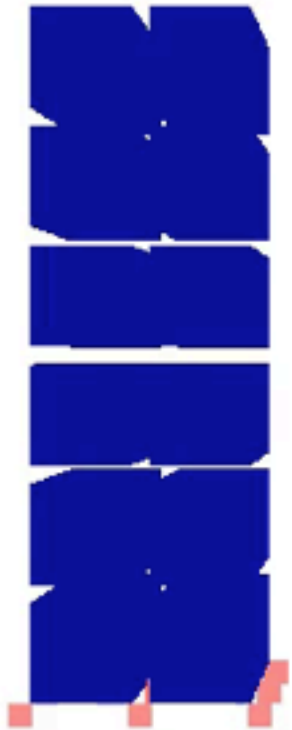

physical problem

Modelling and simulation of materials and structures

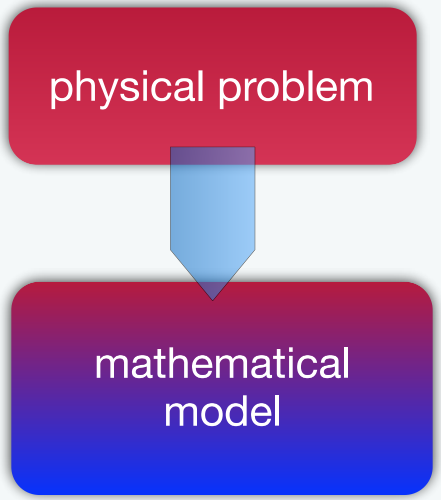

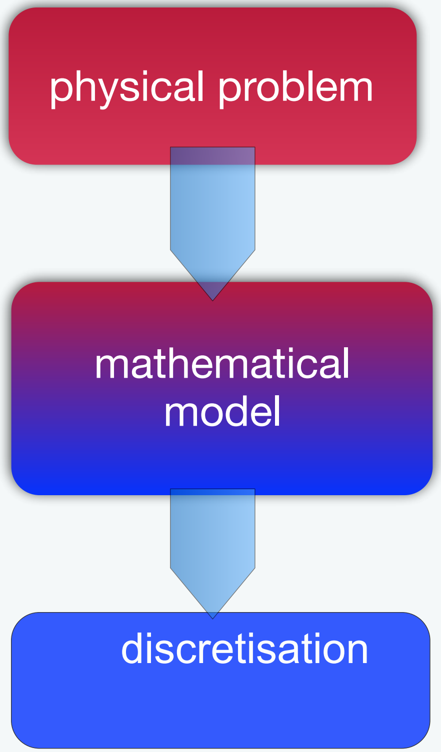
physical problem
mathematical model
discretisation

Modelling and simulation of materials and structures

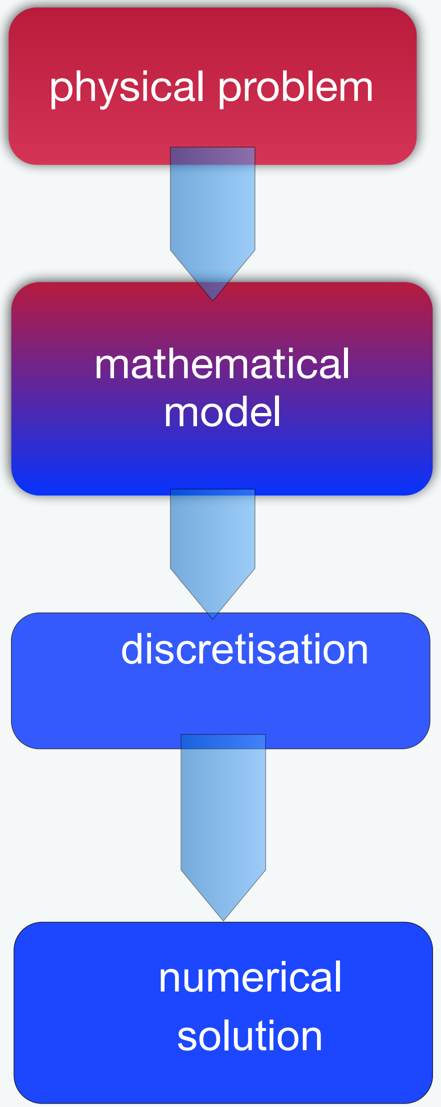

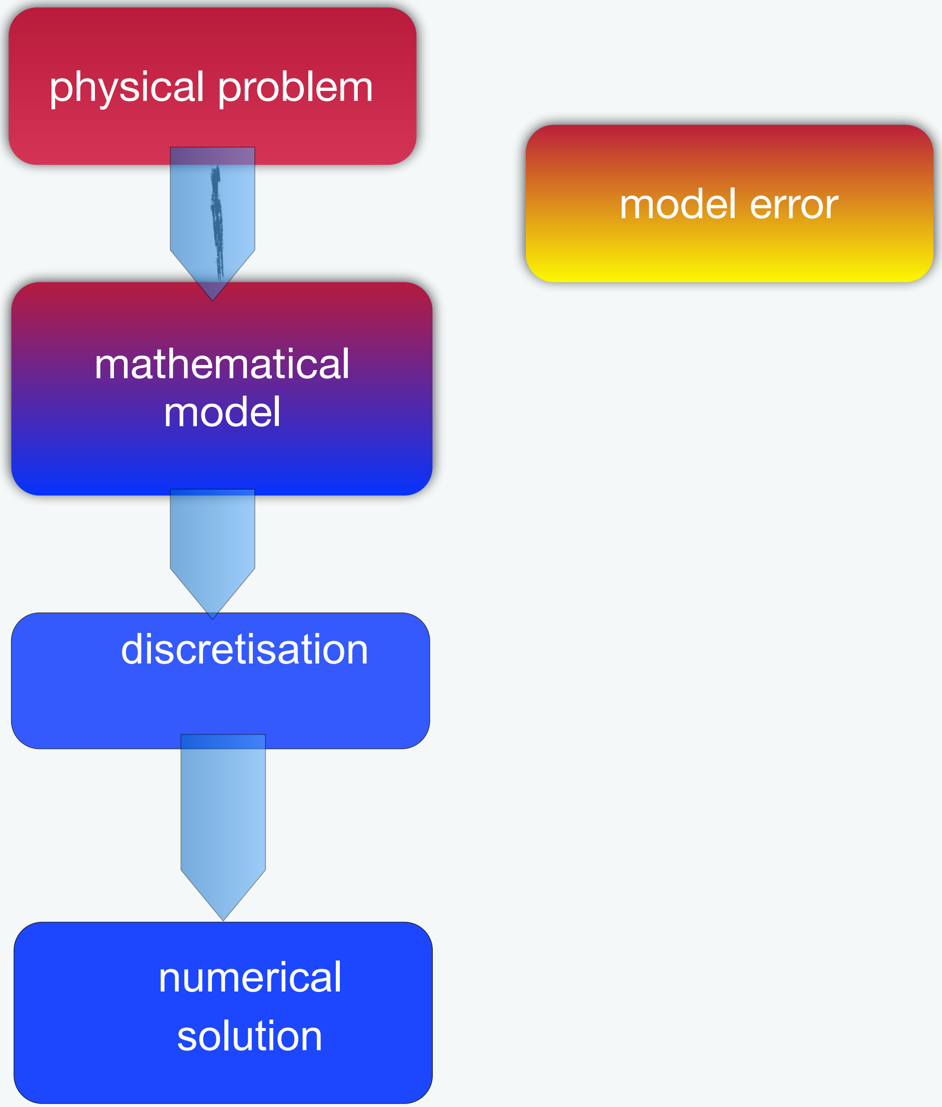
physical problem
model error
mathematical model
discretisation
numerical solution

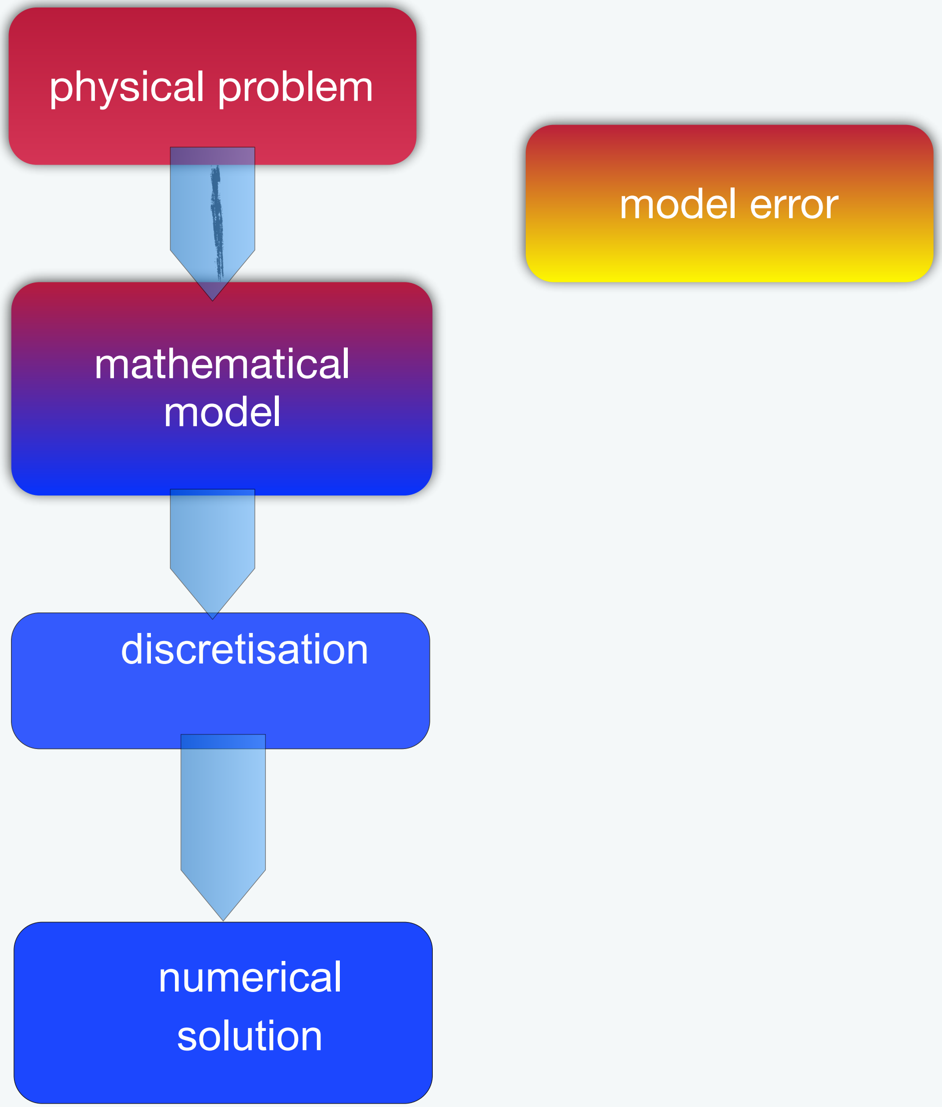
physical problem
model error
mathematical model
discretisation
numerical solution

Modelling and simulation of materials and structures

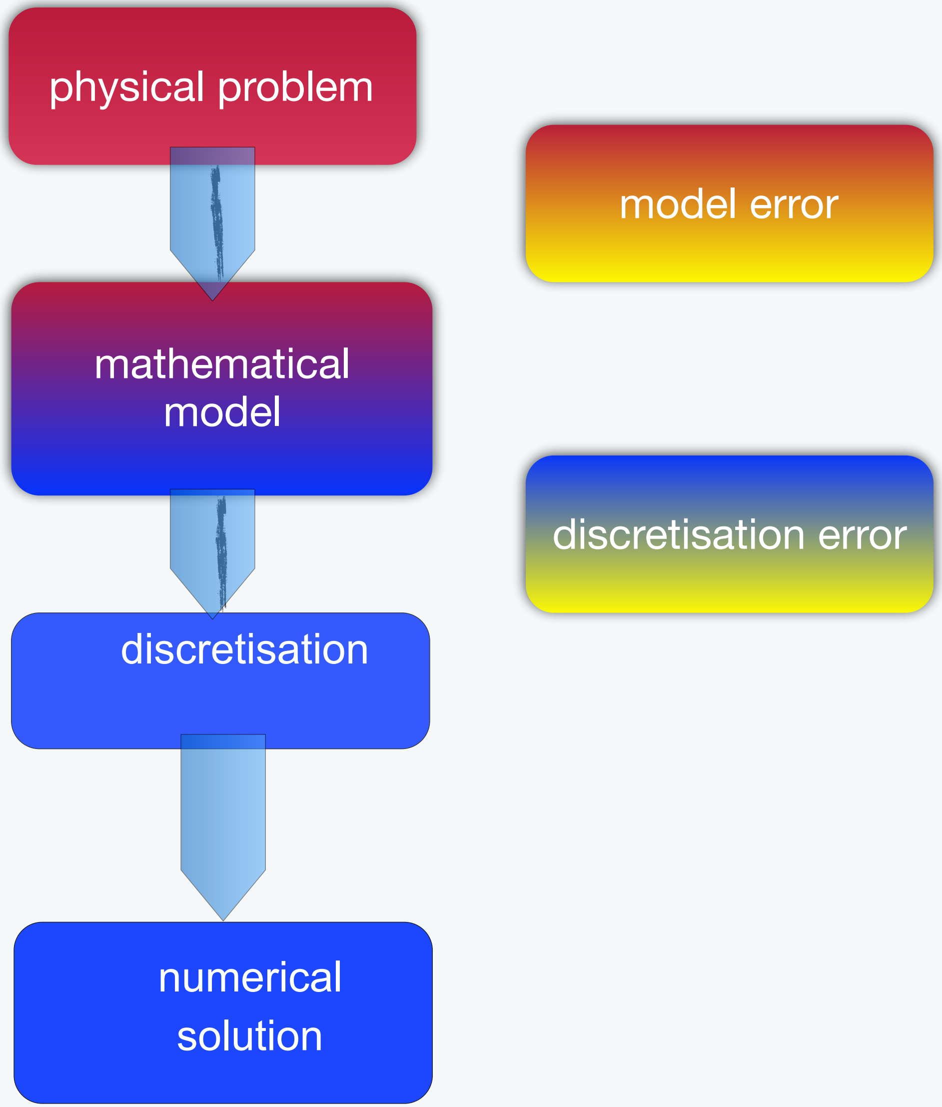

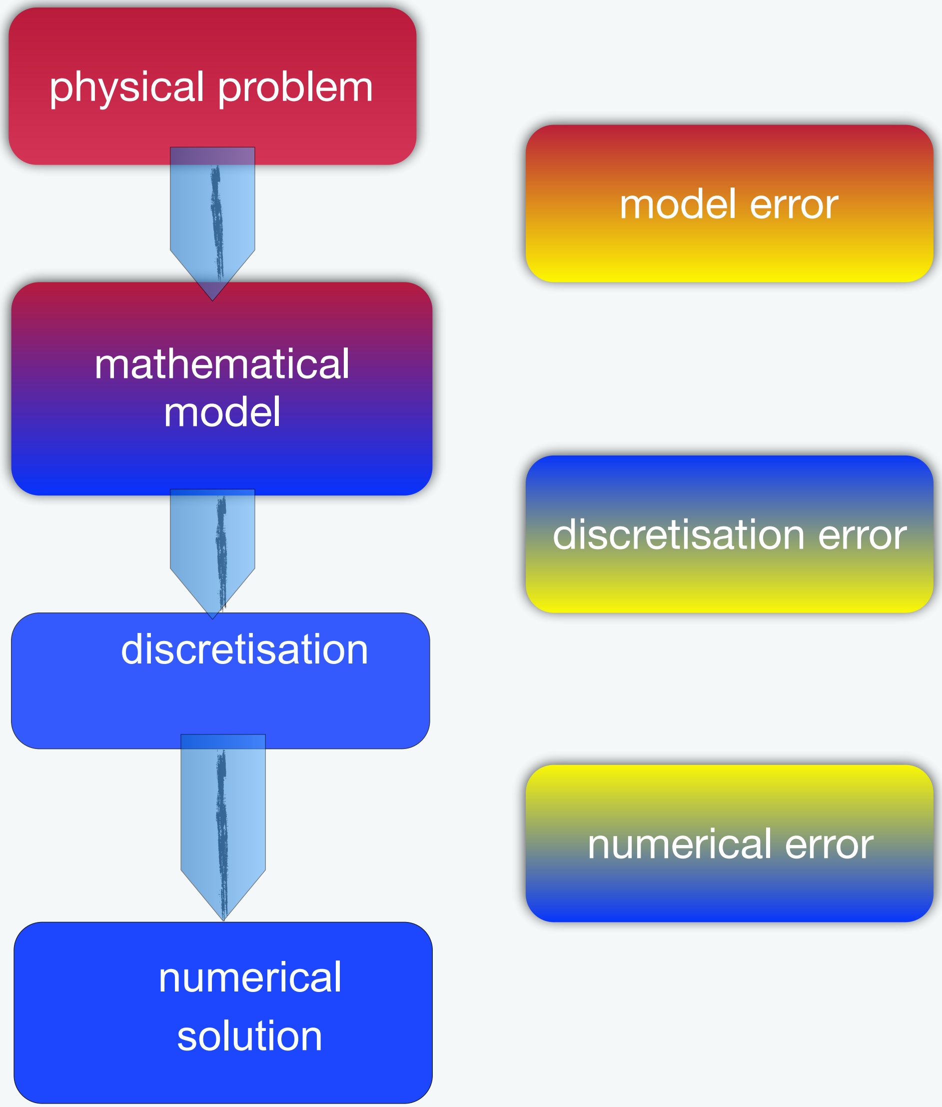
physical problem
mathematical model
discretisation
numerical solution
model error
discretisation error
numerical error

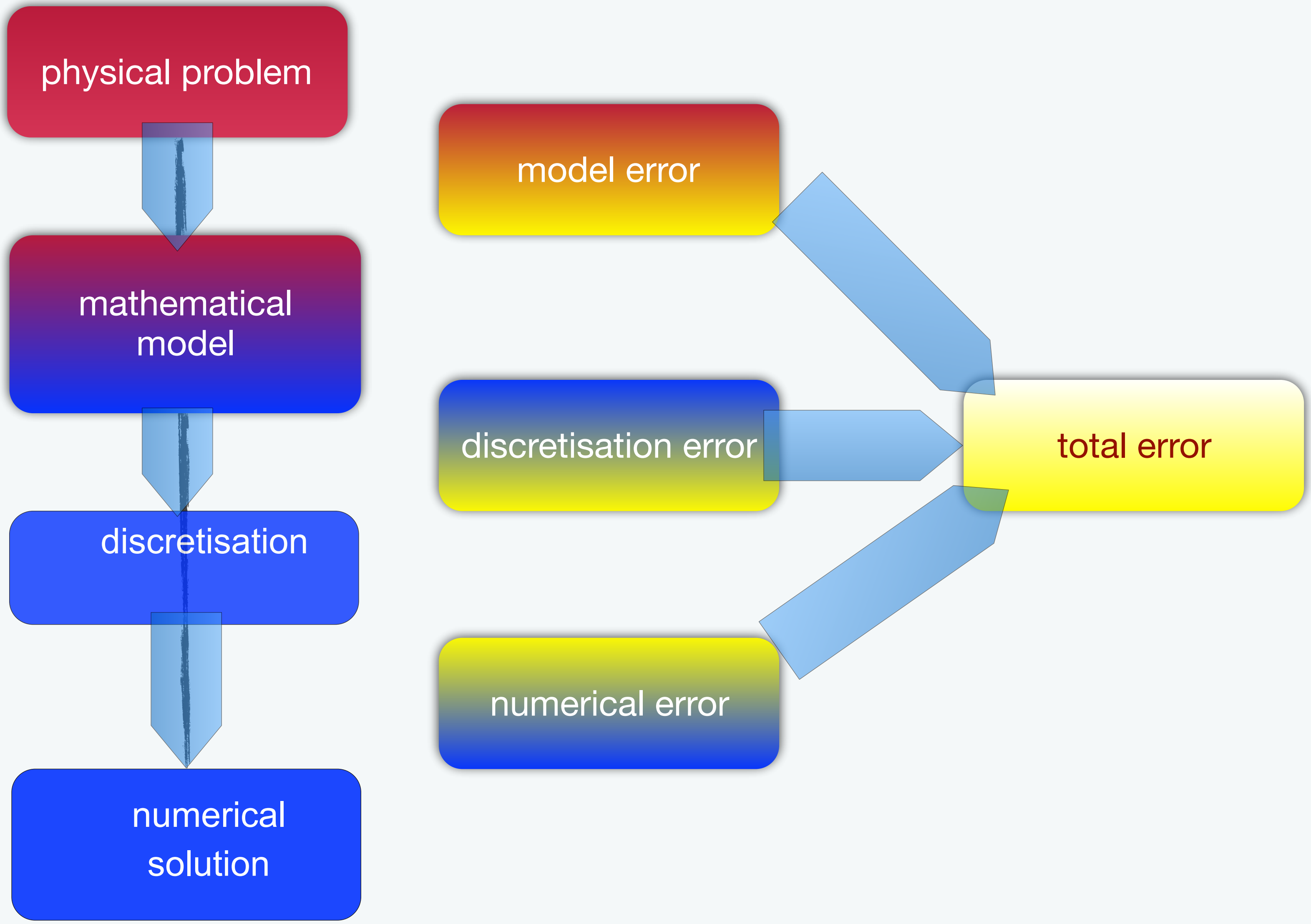
physical problem
mathematical model
discretisation
numerical solution
model error
discretisation error
numerical error
total error

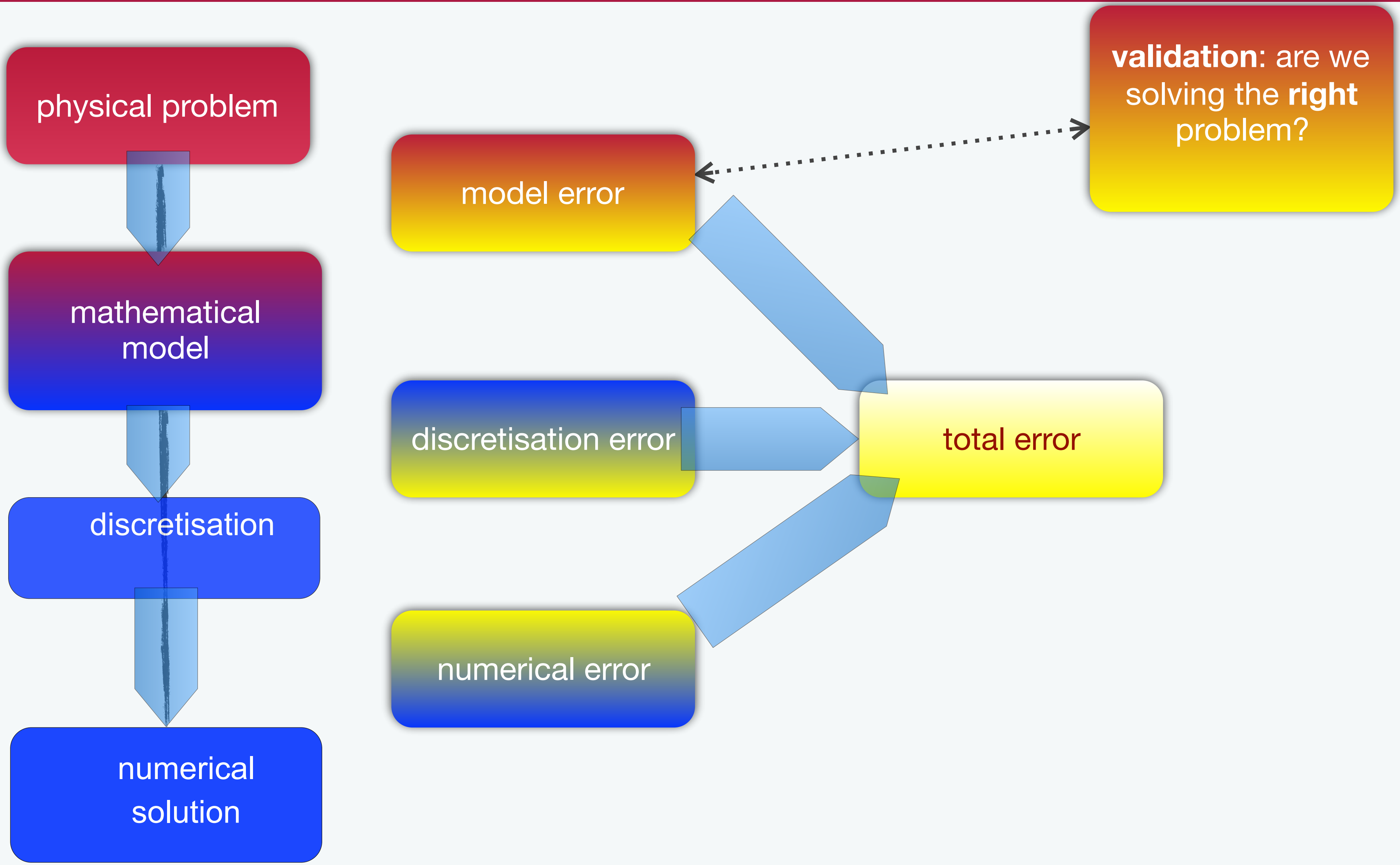
physical problem
mathematical model
discretisation
numerical solution
model error
discretisation error
numerical error
total error
validation: are we solving the right problem?

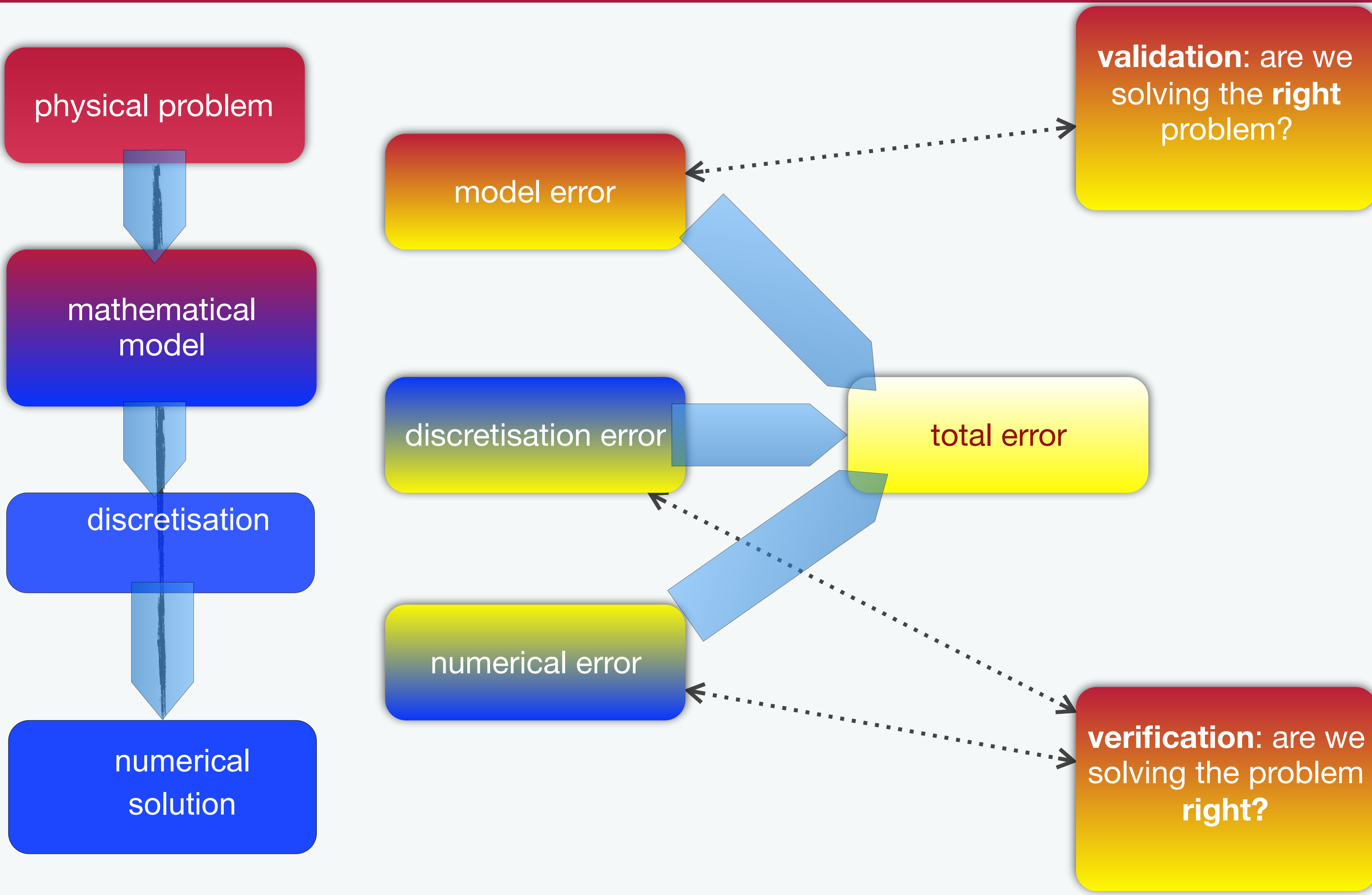
physical problem
mathematical model
discretisation
numerical solution
model error
discretisation error
numerical error
total error
validation: are we solving the right problem?
verification: are we solving the problem right?

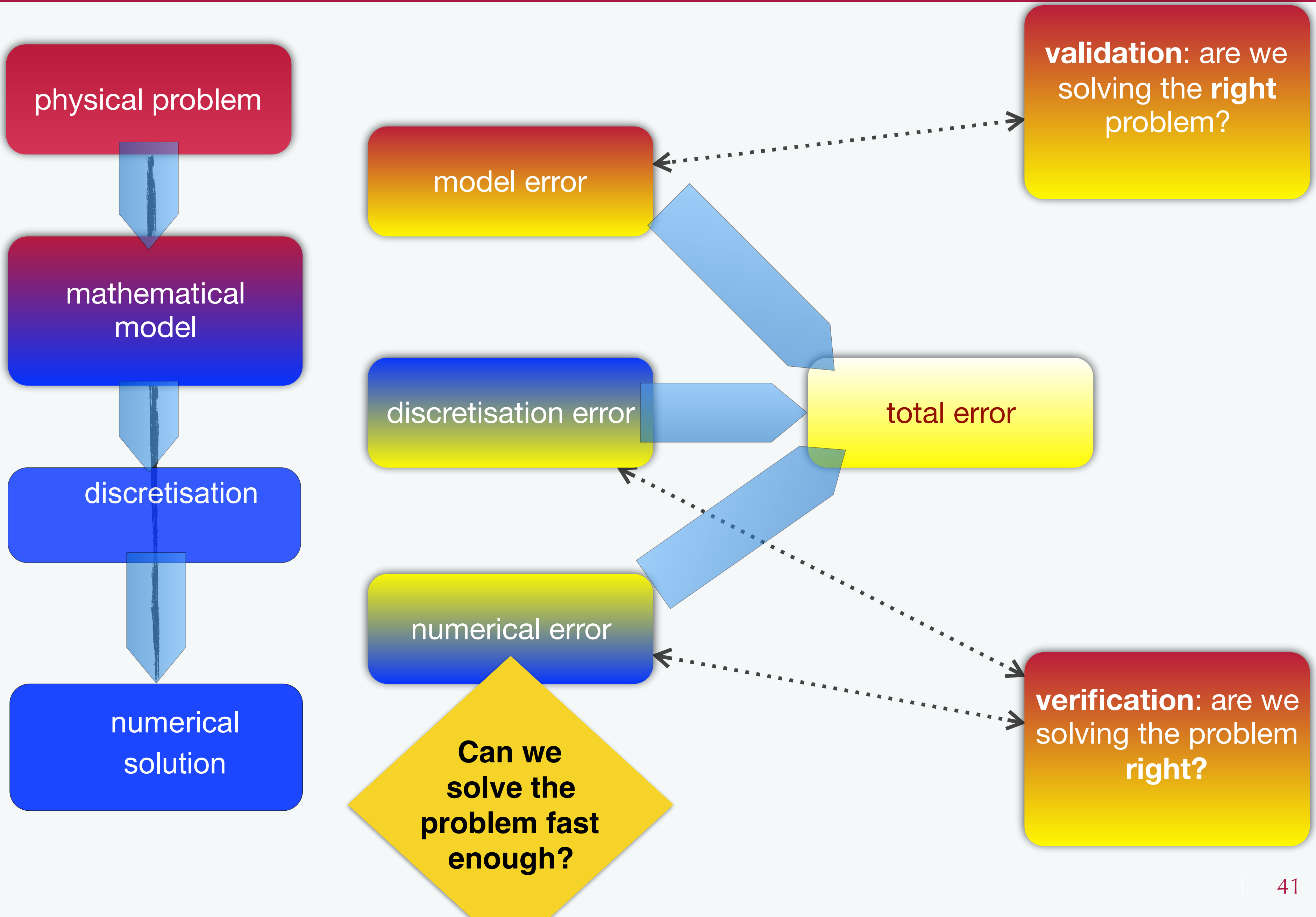
physical problem
mathematical model
discretisation
numerical solution
model error
discretisation error
numerical error
total error
validation: are we solving the right problem?
verification: are we solving the problem right?
Can we solve the problem fast enough?

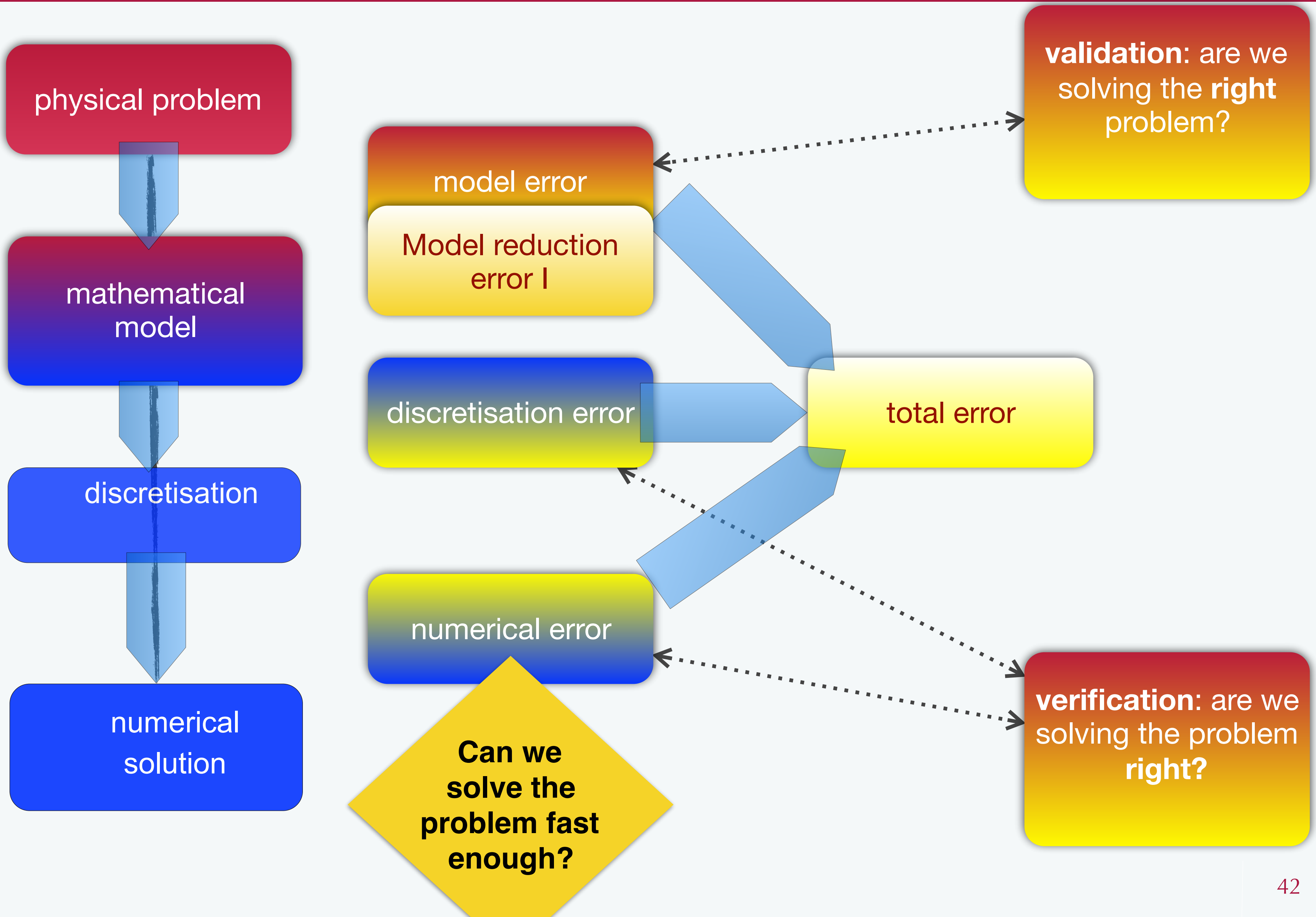
physical problem
mathematical model
discretisation
numerical solution
model error
Model reduction error I
discretisation error
numerical error
total error
validation: are we solving the right problem?
verification: are we solving the problem right?
Can we solve the problem fast enough?

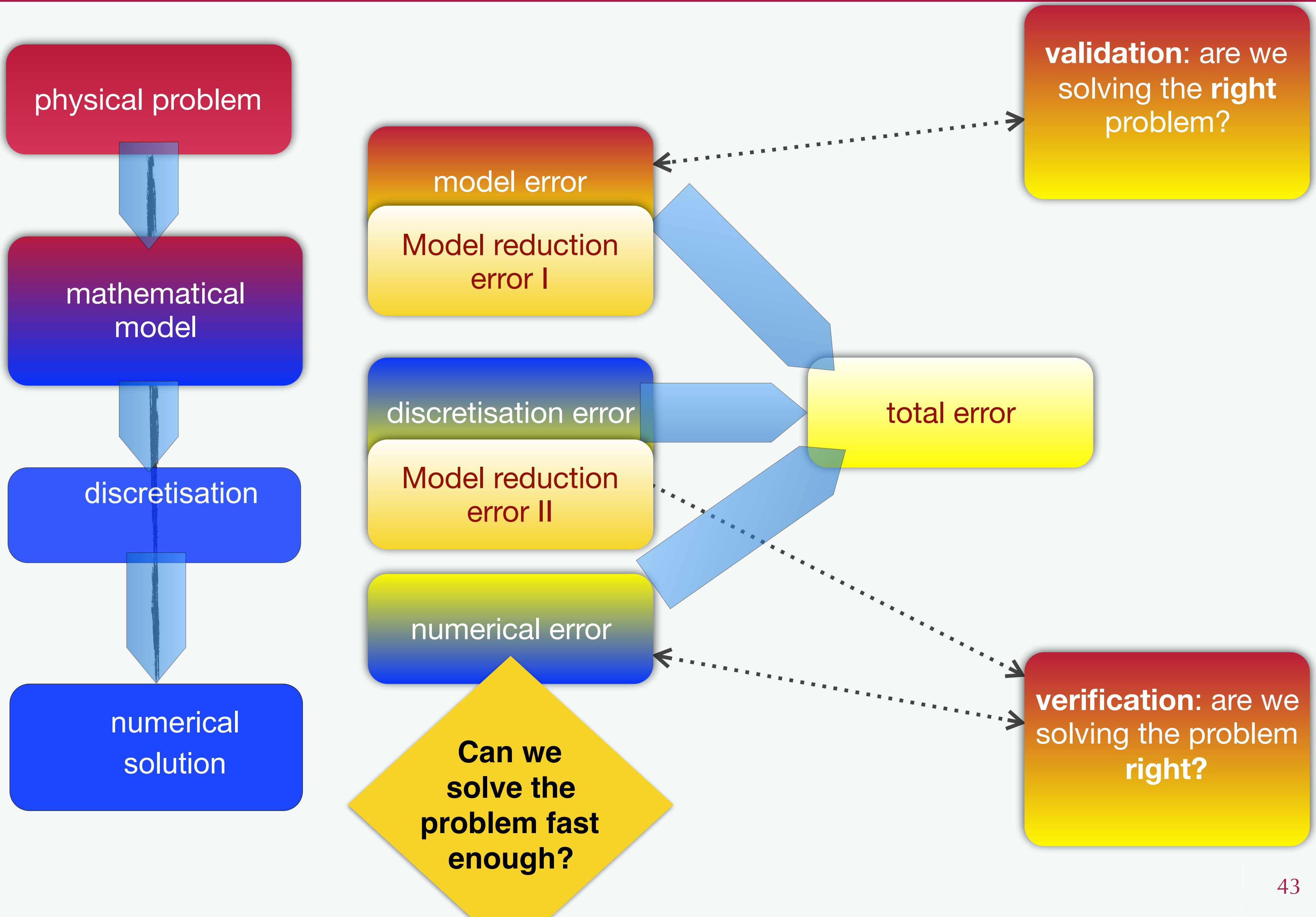
physical problem
mathematical model
discretisation
numerical solution
model error
Model reduction error I
discretisation error
Model reduction error II
numerical error
total error
validation: are we solving the right problem?
verification: are we solving the problem right?
Can we solve the problem fast enough?

Part 0. Enrichment of the finite element method

Enrichment

- When the standard finite element method is unable to efficiently reproduce certain features of the sought solution:

1.	Discontinuities	-	cracks, *material interfaces*
2.	Large gradients	-	*yield lines, shock waves*
3.	Singularities	-	*notches, cracks, corners*
4.	Boundary layers	-	*fluid-fluid, fluid-solid*
5.	Oscillatory behavior	-	*vibrations, impact*

- The approximation space can be extended by introducing of an *a priori* knowledge about the sought solution, and thereby:

1. Rendering the mesh independent of any phenomena
2. reducing error of the approximation locally and globally
3. improving convergence rates

Classification of discontinuities

Strong discontinuities

- The primal field of the solution is discontinuous, e.g. cracks lead to strong discontinuities in the displacement field.

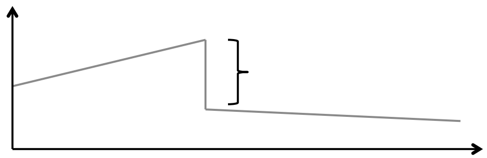

Weak discontinuities

- The first derivative of the solution is discontinuous, e.g. discontinuities in the strain field through a material interface.

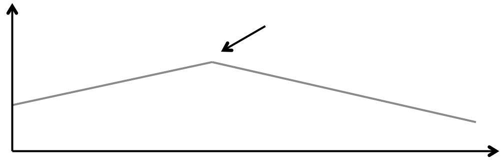

Classification of enrichments

Global enrichment

- The enrichment is employed on the global level, over the **entire domain**.
- Useful for problems that can be considered as **globally non-smooth** e.g. high-frequency solutions (Helmholtz equation)

Local enrichment

- This enrichment scheme is adopted locally, over a **local subdomain**.
- Useful for problems that only involve **locally non-smooth** phenomena, e.g. solutions with discontinuities.

Classification of enrichments

Extrinsic enrichment

- Associated with additional degrees of freedom and additional shape functions to augment the standard approximation basis.

1.	Extended finite element method (XFEM)	- Moës et al.	(1999)
2.	Generalised finite element method (GFEM)	- Strouboulis et al.	(2000a)
3.	Enriched element free Galerkin	- Ventura et al.	(2002)
4.	*hp* – clouds (Meshless/Hybrid)	- Duarte and Oden	(1996)

Intrinsic enrichment

- Not accompanied by additional degrees of freedom. Instead, some standard functions are replaced with special (problem specific) functions.

1.	Enriched moving least squares (Meshless)	- Fleming et al.	(1997)
2.	Enriched weight function (Meshless)	- Duflot et al.	(2004b)
3.	Intrinsic partition of unity methods	- Fries, Belytschko	(2006)
4.	Elements with embedded discontinuities		

Singular elements (Barsoum, 1974)

For simulating the crack tip singular field in LEFM

- A simple way how to introduce a singularity of $1/\sqrt{r}$ in isoperimetric finite elements is by displacing the mid-side nodes of two adjacent edges to one quarter of the element edge length from the node where the singularity is desired.

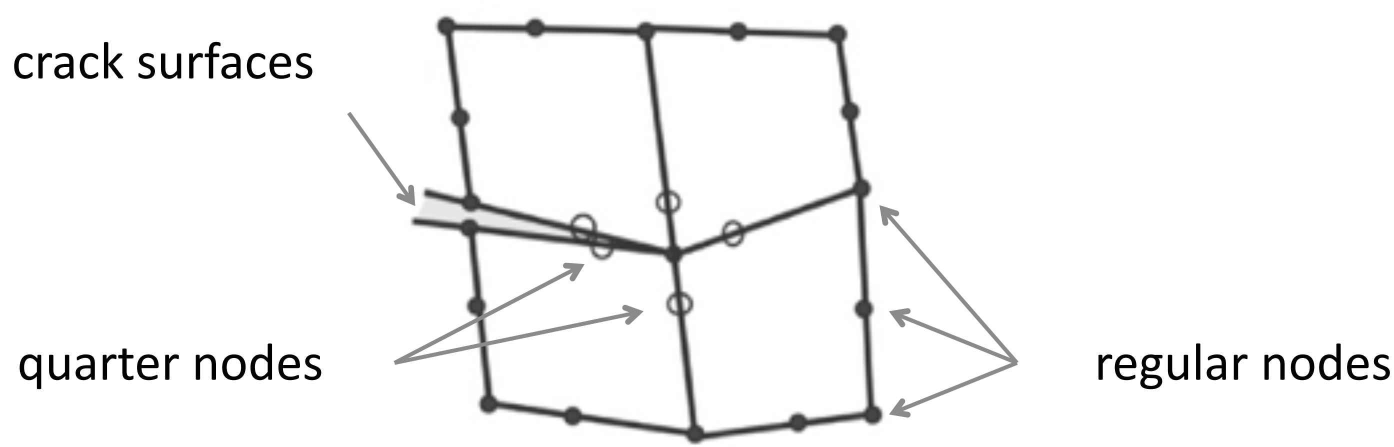

Partition of unity (PU)

- A set of functions ϕ_i whose sum at any point $\boldsymbol{x}$ inside a domain Ω is equal to unity:

$$\forall \mathbf{x} \in \Omega, \mathbf{x} : \sum_{I=1} \phi_I(\mathbf{x}) = 1$$

- Example PU functions are the finite element “hat” functions:

$$N_1(x) = \frac{x_2 - x}{x_2 - x_1}, x \in [x_1, x_2] \qquad N_2(x) = \frac{x - x_1}{x_2 - x_1}, x \in [x_1, x_2]$$

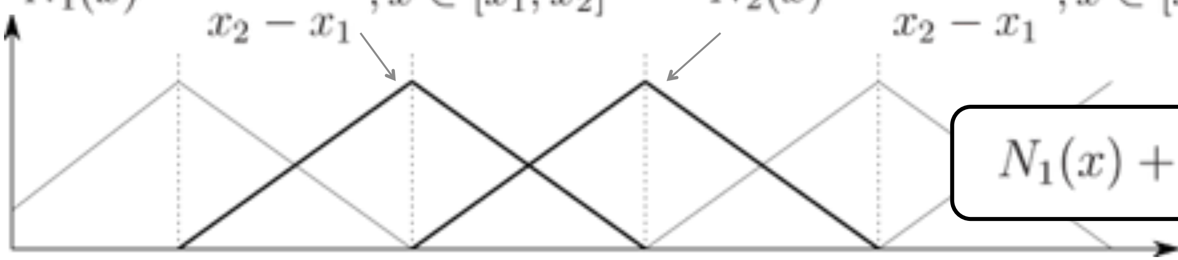

$$N_1(x) + N_2(x) = 1$$

Partition of unity finite element method (PUFEM)

Reproducibility of PU

- Any function $\boldsymbol{p}(\boldsymbol{x})$ can be reproduced by a product of that function and the partition of unity functions:

$$\sum_{I=1} \phi_I(\mathbf{x}) p(\mathbf{x}) = p(\mathbf{x})$$

- The function can be adjusted if the sum is modified by introducing parameters $\boldsymbol{q_I}$:

$$\sum_{I=1} \phi_I(\mathbf{x}) p(\mathbf{x}) q_I = \bar{p}(\mathbf{x})$$

- Reproducibility of $\boldsymbol{p}(\boldsymbol{x})$ can be controlled and localised to arbitrary regions where $\boldsymbol{q_I} \neq \mathbf{0}$

Partition of unity finite element method (PUFEM)

Formulation of PUFEM (example)

- Find the solution to the following 1D boundary value problem (BVP):

$$\forall x \in [0, l] : \frac{\mathrm{d}^2 u}{\mathrm{d}x^2} + f = 0$$

$$\text{with BC} : u(0) = 0, \; u(l) = u_l$$

- If we define two bilinear forms:

$$a(w, u) = \int_0^l \frac{\mathrm{d}w}{\mathrm{d}x} \frac{\mathrm{d}u}{\mathrm{d}x} \, \mathrm{d}x \qquad (w, f) = \int_0^l w f \, \mathrm{d}x$$

- The discrete variational problem can be stated as:

find $u^h \in U^h$ satisfying the BC such that for all $w^h \in W^h$:

$$a(w^h, u^h) = (w^h, f)$$

Partition of unity finite element method (PUFEM)

Formulation of PUFEM (example)

- The approximation/trial function in PUFEM:

$$u^h(x) = \underbrace{\sum_{I=1} N_I(x) u_I}_{\text{standard FE}} + \underbrace{\sum_{J=1} \phi_J(x)\psi(x) q_J}_{\text{PU enriched}}$$

- By choosing $w^h = \delta u^h$, leads to the discrete system of equations:

$$a(\delta u^h, u^h) = (\delta u^h, f)$$

$$\Downarrow$$

$$\begin{bmatrix} \mathbf{K}^{\mathrm{ss}} & \mathbf{K}^{\mathrm{se}} \\ \mathbf{K}^{\mathrm{es}} & \mathbf{K}^{\mathrm{ee}} \end{bmatrix} \begin{Bmatrix} \mathbf{u}^s \\ \mathbf{q}^e \end{Bmatrix} = \begin{Bmatrix} \mathbf{f}^s \\ \mathbf{f}^e \end{Bmatrix}$$

$$\mathbf{K}_{ij}^{ss} = \int_0^l \frac{\mathrm{d}N_i}{\mathrm{d}x}\frac{\mathrm{d}N_j}{\mathrm{d}x}\,\mathrm{d}x$$

$$\mathbf{K}_{ij}^{se} = \int_0^l \frac{\mathrm{d}N_i}{\mathrm{d}x}\frac{\mathrm{d}(\phi_j\psi)}{\mathrm{d}x}\,\mathrm{d}x$$

$$\mathbf{K}_{ij}^{es} = \int_0^l \frac{\mathrm{d}(\phi_i\psi)}{\mathrm{d}x}\frac{\mathrm{d}N_j}{\mathrm{d}x}\,\mathrm{d}x$$

$$\mathbf{K}_{ij}^{ee} = \int_0^l \frac{\mathrm{d}(\phi_i\psi)}{\mathrm{d}x}\frac{\mathrm{d}(\phi_j\psi)}{\mathrm{d}x}\,\mathrm{d}x$$

$$f_i^s = \int_0^l N_i f_x\,\mathrm{d}x$$

$$f_i^e = \int_0^l (\phi_i\psi) f_x\,\mathrm{d}x$$

Partition of unity finite element method (PUFEM)

Remarks

- Allows to introduce an arbitrary function $\boldsymbol{\psi}(\boldsymbol{x})$ in the approximation space by splitting the approximation into a **standard** and **enriched** parts.
- Enrichment can be **localised** to a small region around the features of interest – computationally advantageous.
- Provides a systematic means of introducing multiple enrichments.

References:

- Melenk and Babuska (1996)
- Duarte and Oden (1996)

The Generalised Finite Element Method (GFEM)

GFEM

- Originally associated with global PU enrichment
- Shape functions in the enriched part are usually different from the shape functions in the standard part i.e. $\phi_I(x) \neq N_I(x)$
- Introduced numerically generated enrichment functions, e.g. a solution in the vicinity of a bifurcated crack as enrichment

References:

- Melenk (1995)
- Melenk and Babuška (1996)
- Strouboulis et al. (2000)

The Extended Finite Element Method (XFEM)

XFEM

- Associated with local discontinuous PU enrichment e.g.:

  a. propagation of cracks
  b. evolution of dislocations
  c. phase boundaries

- Both GFEM and XFEM are essentially identical in their application, i.e. extrinsic PU enrichment

References:

- Belytschko and Black (1999)
- Moës et. al. (1999)
- Dolbow (1999)

Formulation for crack growth:

$$\mathbf{u}^h(\mathbf{x}) = \underbrace{\sum_{I\in\mathcal{N}_I} N_I(\mathbf{x})\mathbf{u}^I}_{\text{standard part}} + \underbrace{\sum_{J\in\mathcal{N}_J} N_J(\mathbf{x})H(\mathbf{x})\mathbf{a}^J}_{\text{discontinuous enrichment}} + \underbrace{\sum_{K\in\mathcal{N}_K} N_K(\mathbf{x})\sum_{\alpha=1}^{4} f_\alpha(\mathbf{x})\mathbf{b}^{K\alpha}}_{\text{singular tip enrichment}}$$

$$H(\mathbf{x}) = \begin{cases} +1 & \text{if } \mathbf{x} \text{ above crack} \\ -1 & \text{if } \mathbf{x} \text{ below crack} \end{cases}$$

$$\{f_\alpha(r,\theta), \alpha = 1,4\} = \left\{\sqrt{r}\sin\frac{\theta}{2}, \sqrt{r}\cos\frac{\theta}{2}, \sqrt{r}\sin\frac{\theta}{2}\sin\theta, \sqrt{r}\cos\frac{\theta}{2}\sin\theta\right\}$$

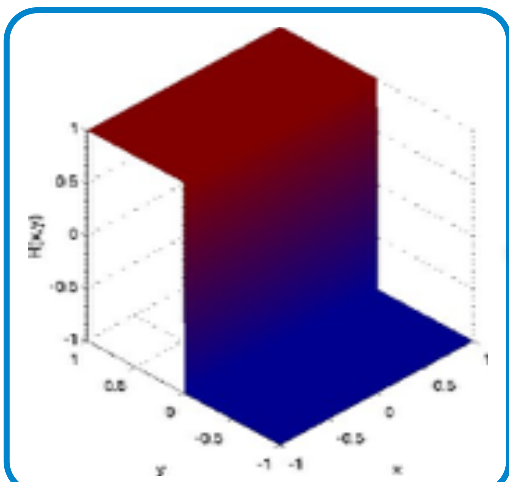

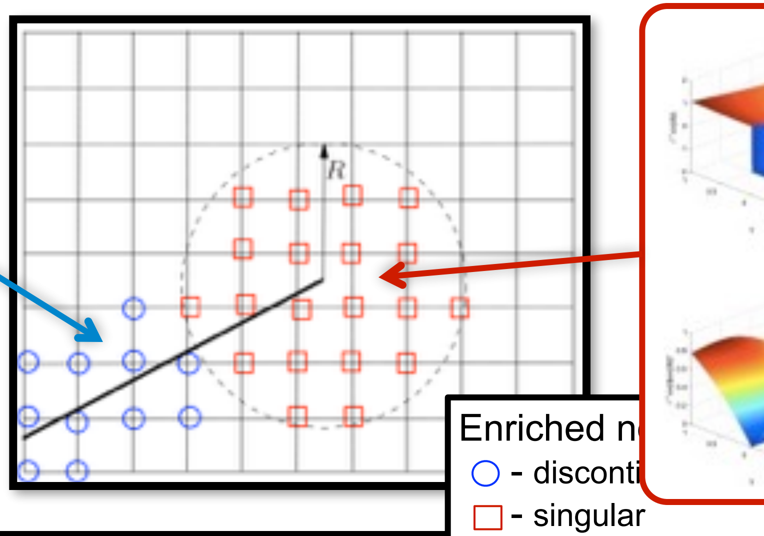

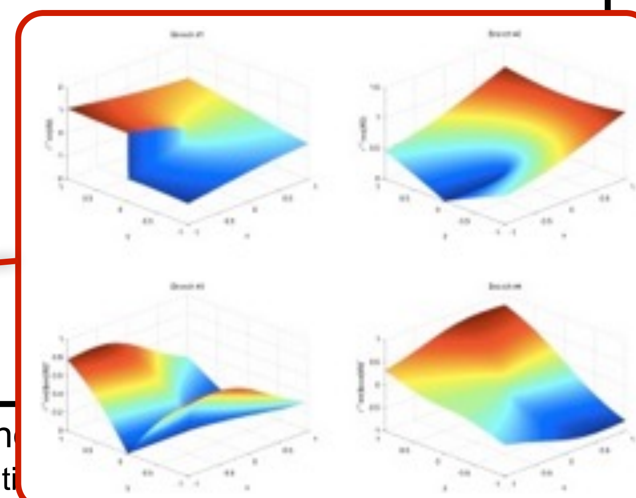

Extended finite element method (XFEM)

$$u_i^h(\mathrm{x}) = \sum_{\substack{I \\ n_I \subset \mathrm{N}}} N_I(\mathrm{x}) u_{iI} + \sum_{\substack{J \\ n_J \subset \mathrm{N}^c}} N_J(\mathrm{x}) a_{iJ} H(\mathrm{x}) + \sum_{\substack{K \\ n_K \subset \mathrm{N}^f}} \phi_K(\mathrm{x}) b_{iK} \Psi(\mathrm{x})$$

classical

enriched

$$H(\mathbf{x}) = \begin{cases} +1 & \mathit{if}\ \mathbf{x}\ \mathit{above} \\ -1 & \mathit{if}\ \mathbf{x}\ \mathit{below} \end{cases}$$

Heaviside function

Asymptotic fields

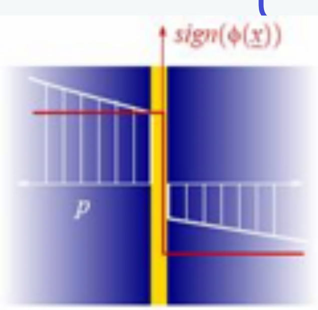

$$\psi(r,\theta) = \sqrt{r}\cos\frac{\theta}{2}, \sqrt{r}\sin\frac{\theta}{2}, \sqrt{r}\sin\theta\sin\frac{\theta}{2}, \sqrt{r}\sin\theta\cos\frac{\theta}{2}$$

Selection of enriched nodes

$$u_i^h(\mathrm{x}) = \sum_{\substack{I \\ n_I \subset \mathrm{N}}} N_I(\mathrm{x}) u_{iI} + \sum_{\substack{J \\ n_J \subset \mathrm{N}^c}} N_J(\mathrm{x}) a_{iJ} H(\mathrm{x}) + \sum_{\substack{K \\ n_K \subset \mathrm{N}^f}} \phi_K(\mathrm{x}) b_{iK} \Psi(\mathrm{x})$$

enriched

Heaviside function

Asymptotic fields

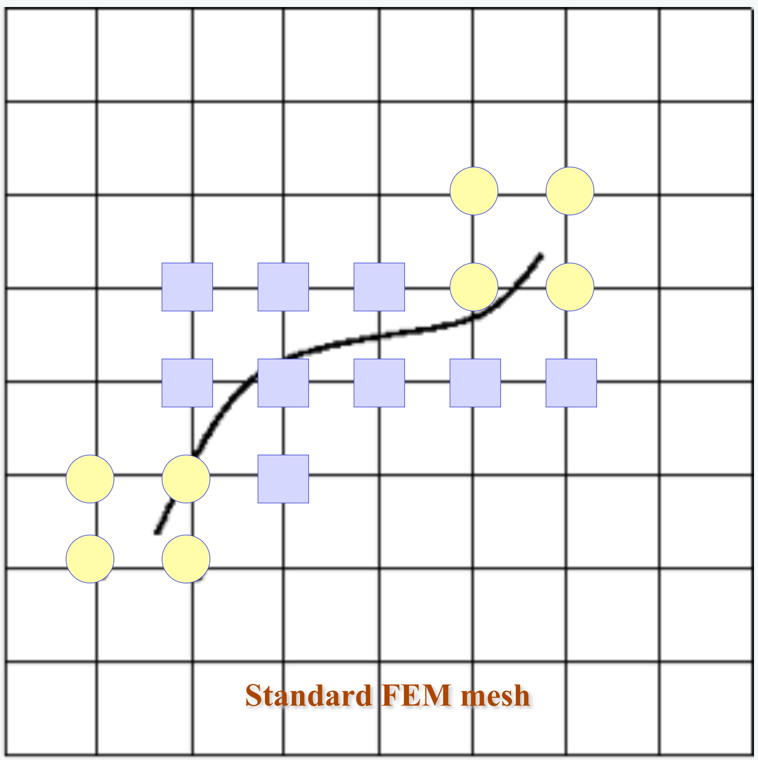

ENRICHED NODES

- Tip (circle)
- Interior (square)

CARDIFF UNIVERSITY

PRIFYS

CAER

uni.lu

SITÉ DU

BOURG

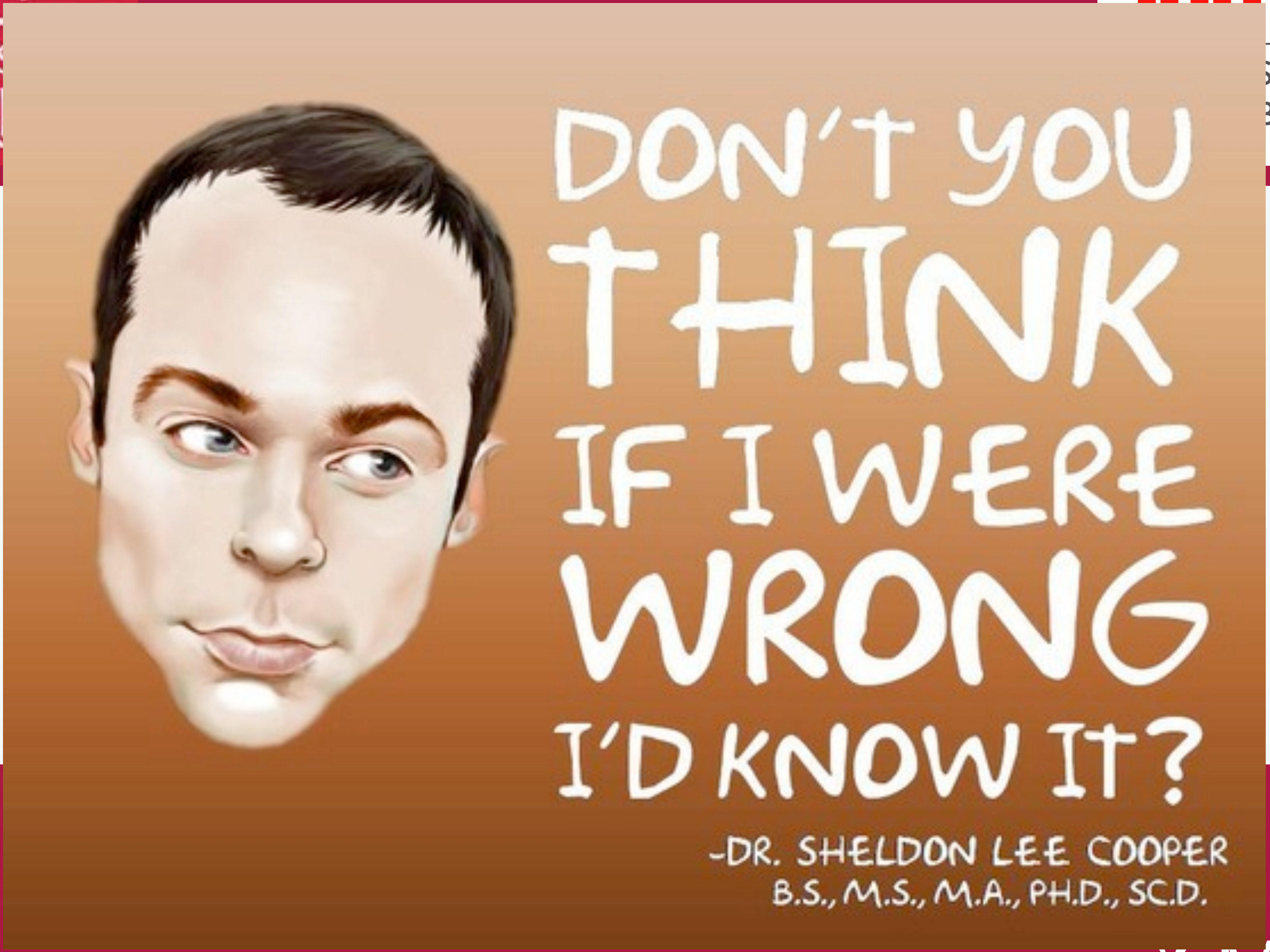

MAM
Institute of Mechanics
& Advanced Materials

CARDIFF UNIVERSITY
PRIFYSGOL CAERDYDD

ITN INSIST

Part I. Streamlining the CAD-analysis transition

Coupling, or decoupling?

IMAM
Institute of Mechanics & Advanced Materials

Reduce the mesh burden

Decouple geometry and analysis
- Meshfree methods (Monaghan, 1977, Belytschko, *et al.* 1994)
- PU enrichment (Melenk & Babuška, 1996; Belytschko, *et al.* 1999)
- Immersed boundary method (Mittal, *et al.* 2005)

Improve element formulations (use simplex elements)
- Smoothed FEM (Liu, *et al.* 2006), smoothed XFEM (Bordas,...)
- Polygonal FEM (Alwood, *et al.* 1969)

Boundary discretisation
- Boundary element method (Rizzo, 1967)
- Scaled boundary FEM (Song, *et al.* 1997)

Couple geometry and analysis: Isogeometric analysis (Hughes, 2005), Isogeometric BEM (Simpson, *et al.* 2012)

Part I.a. *Decoupling CAD and Analysis.*

Separate field and boundary discretisation

- Immersed boundary method (Mittal, *et al.* 2005)
- Fictitious domain (Glowinski, *et al.* 1994)
- Embedded boundary method (Johansen, *et al.* 1998)
- Virtual boundary method (Saiki, *et al.* 1996)
- Cartesian grid method (Ye, *et al.* 1999, Nadal, 2013)

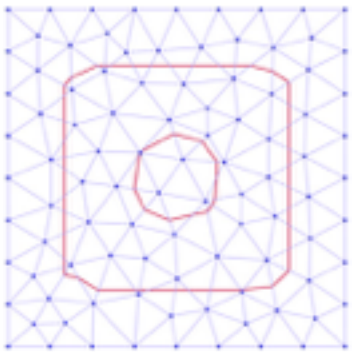

✓ Easy adaptive refinement + error estimation (Nadal, 2013)

✓ Flexibility of choosing basis functions

- Accuracy for complicated geometries? BCs on implicit surfaces?

➡ An accurate and implicitly-defined geometry from arbitrary parametric surfaces including corners and sharp edges (Moumnassi, *et al.* 2011)

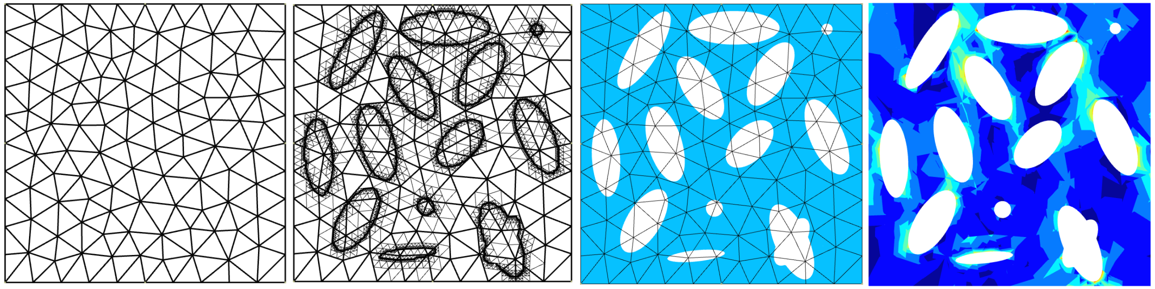

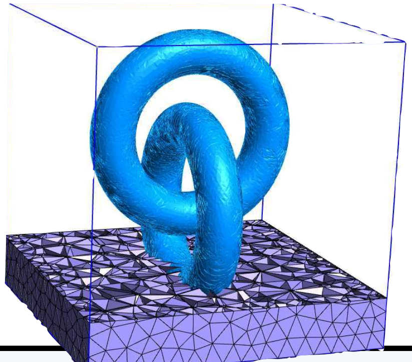

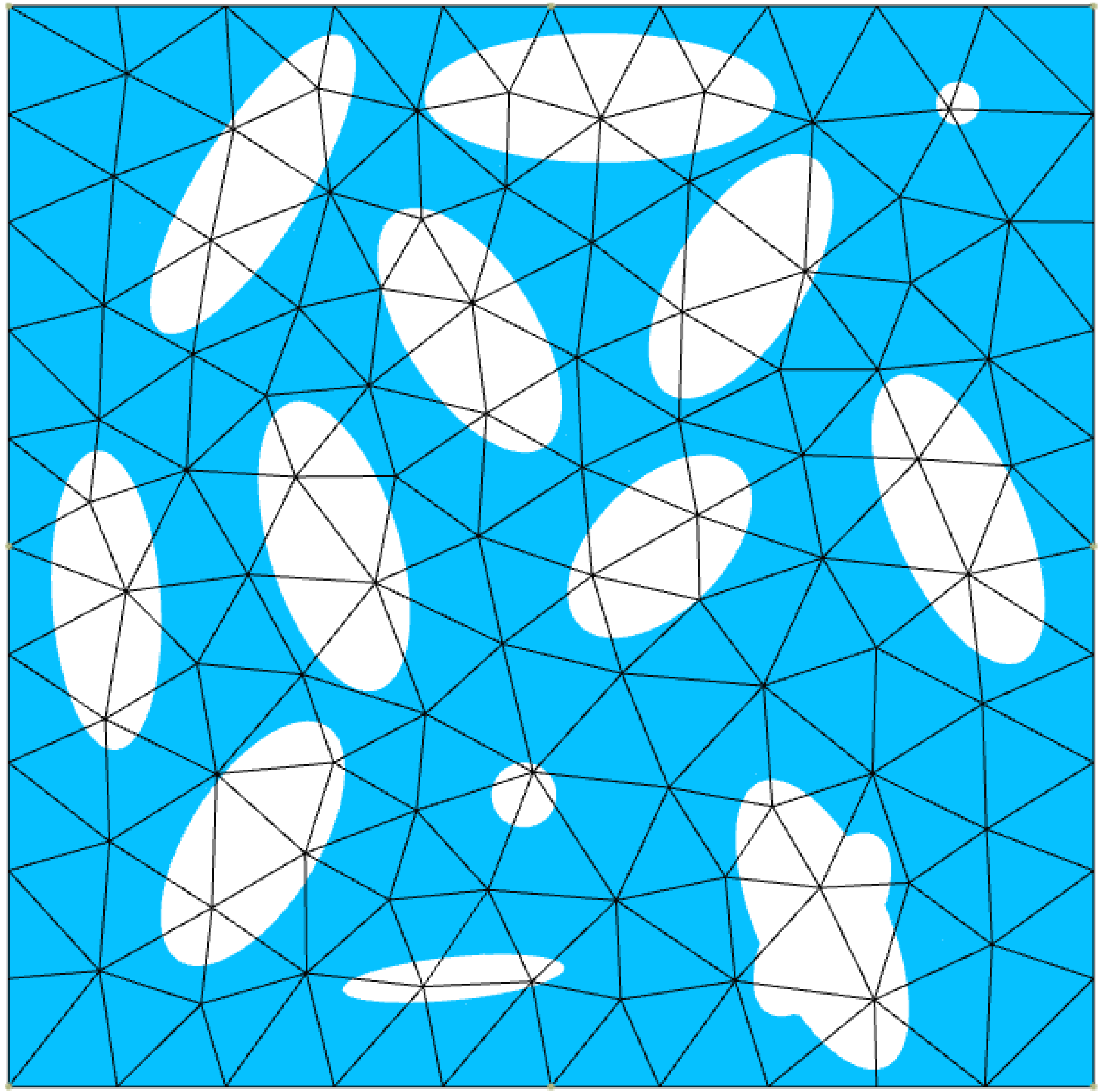

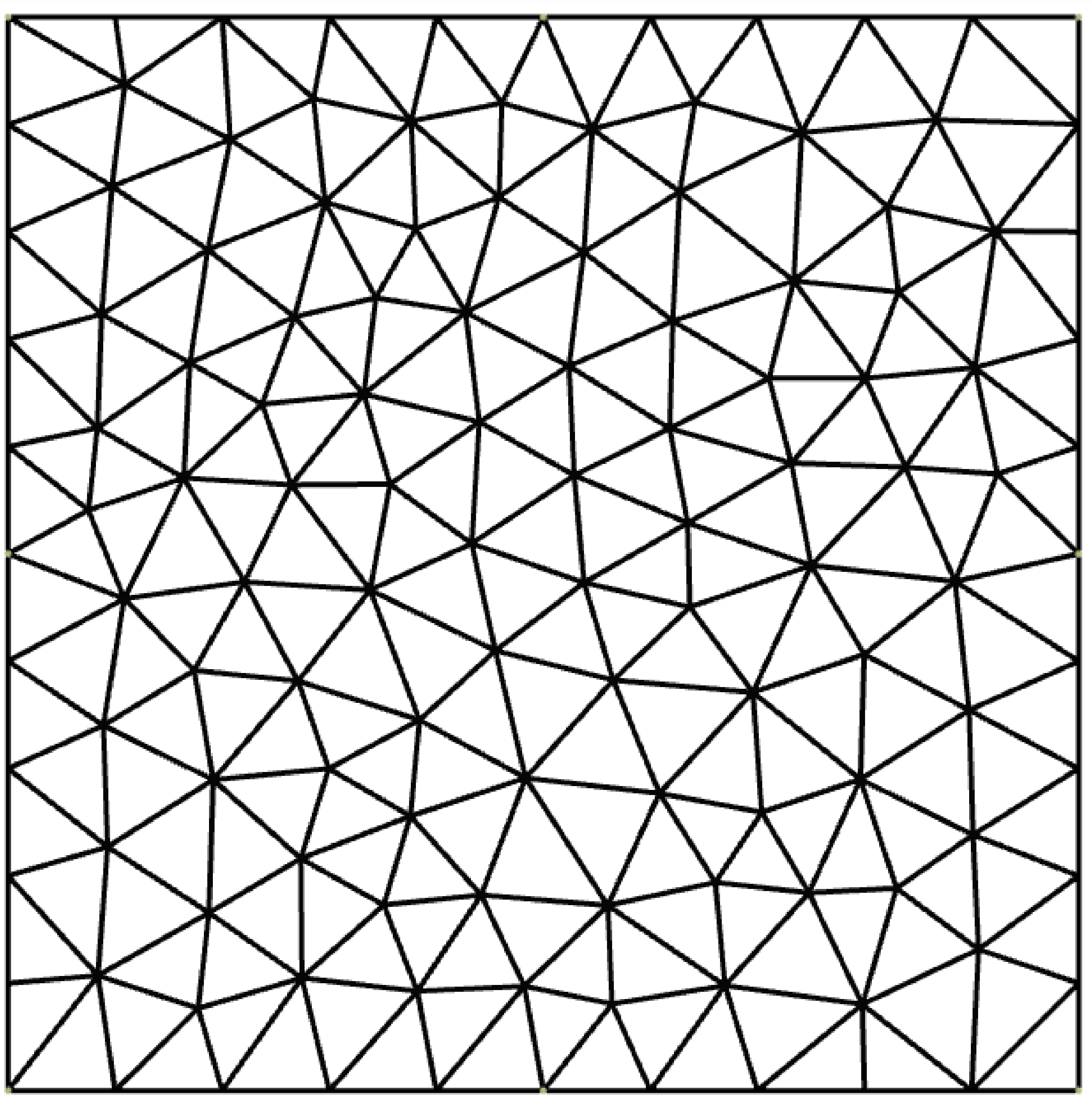

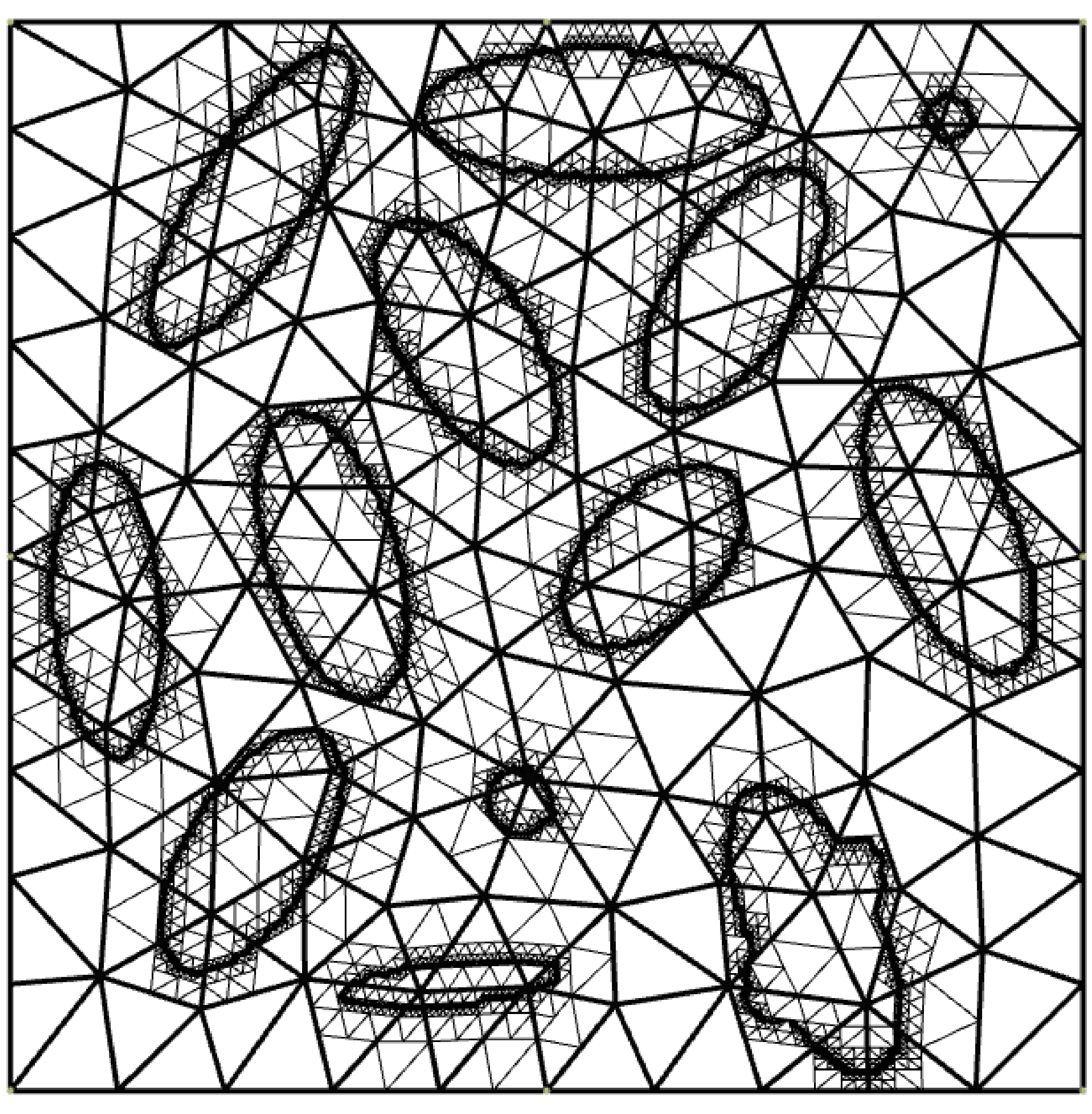

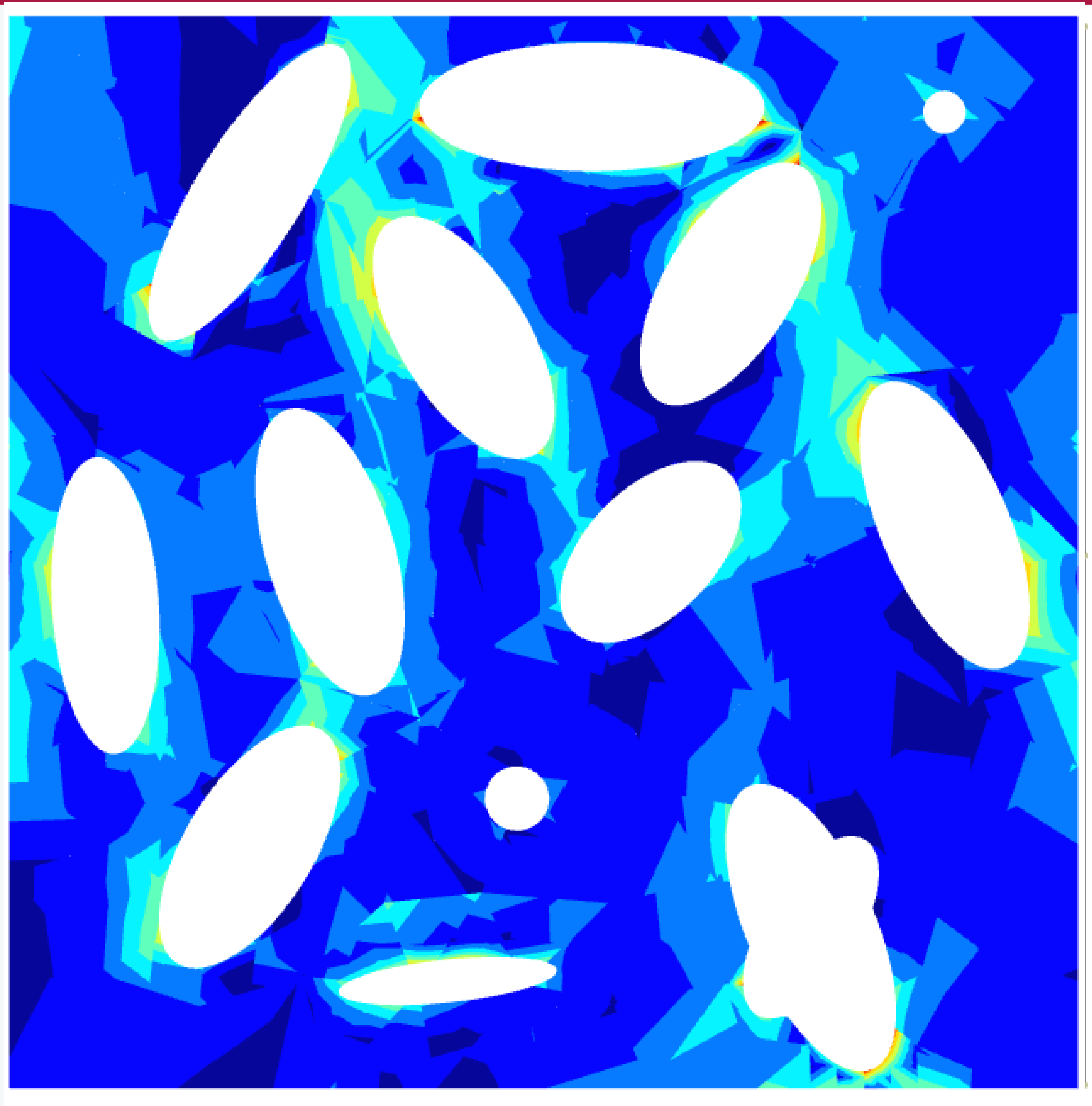

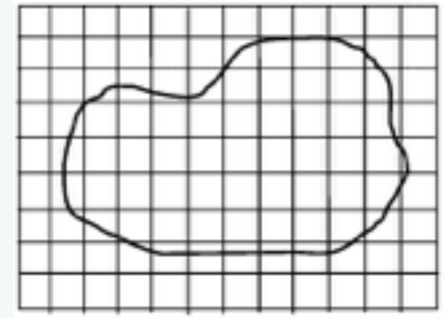

- Objectives
  - insert surfaces in a structured mesh
    - without meshing the surfaces (boundary, cracks, holes, inclusions, etc.)
    - directly from the underlying CAD model
    - model arbitrary solids, including sharp edges and vertices
  - keep as much as possible of the mesh as the CAD model evolves, i.e. reduce mesh dependence of the implicit boundary representation
  - maintain the convergence rates and implementation simplicity of the FEM

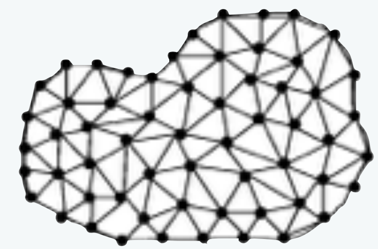

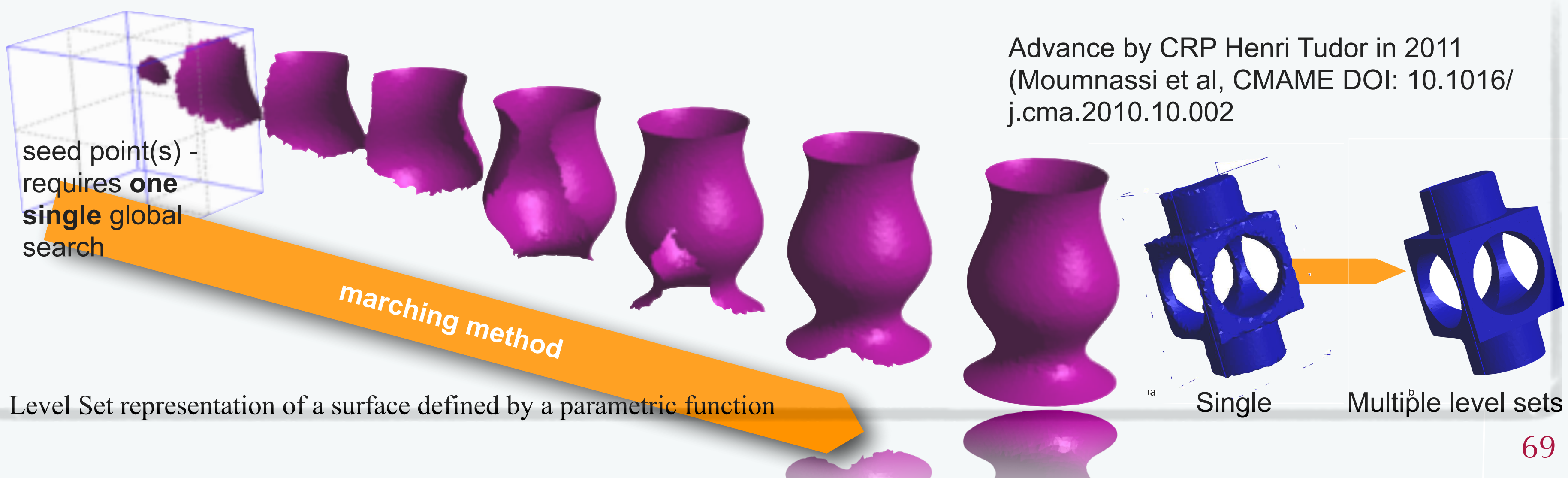

Level Set representation of a surface defined by a parametric function

Examples

- multiple level sets

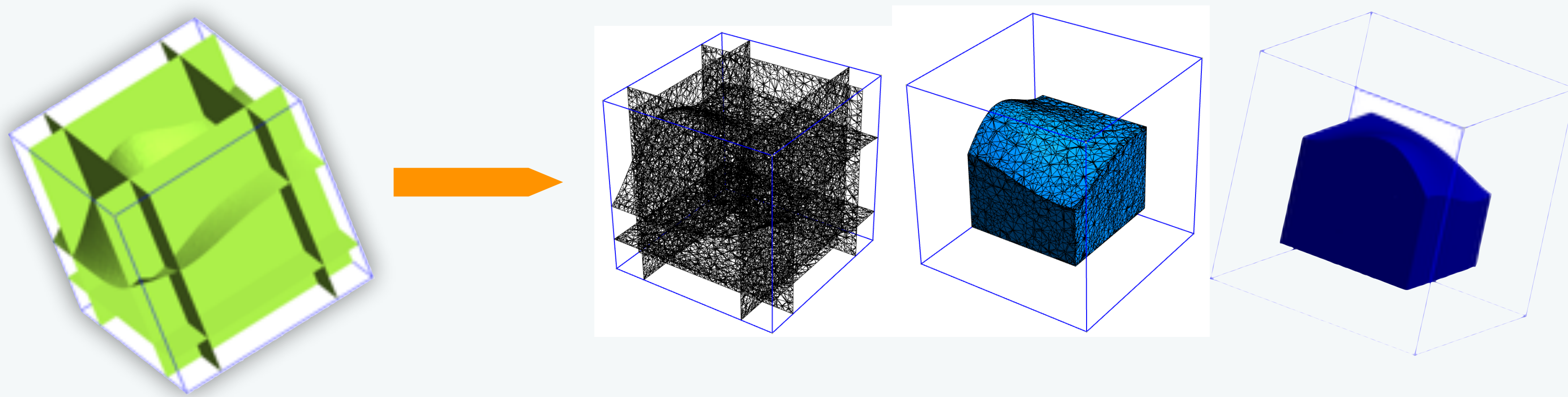

- single (left) versus multiple (right)

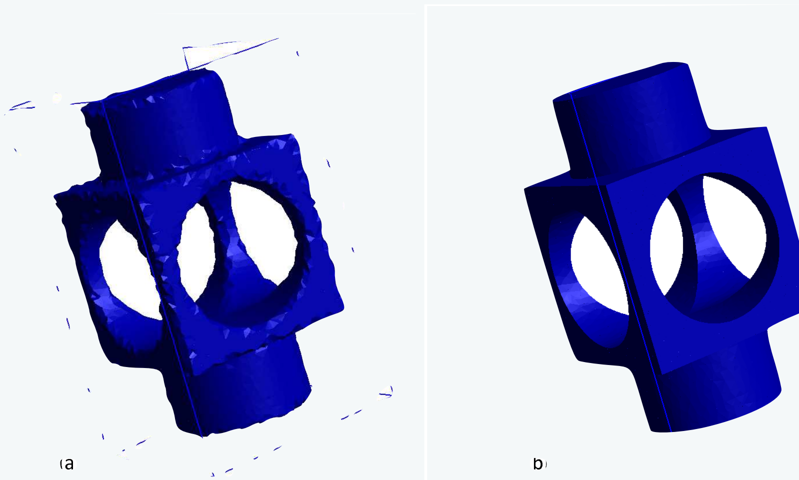

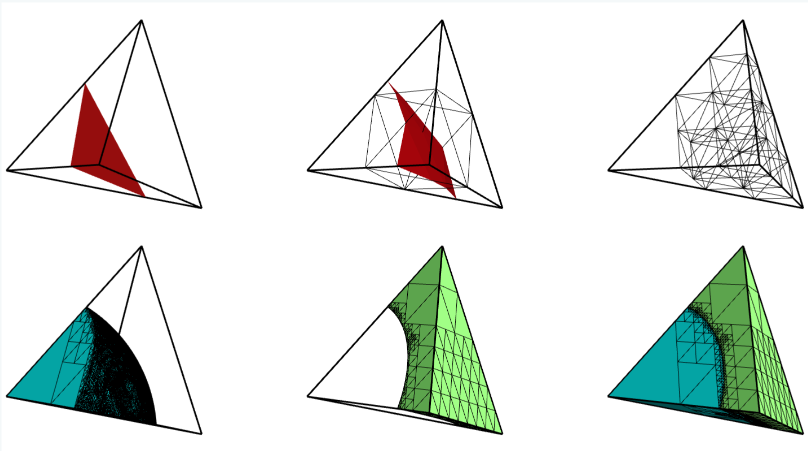

Three-dimensional model problem

- Laplace equation on a cube
- convergence rates
  - optimal
  - requires proper Lagrange multiplier space to eradicate spurious oscillations

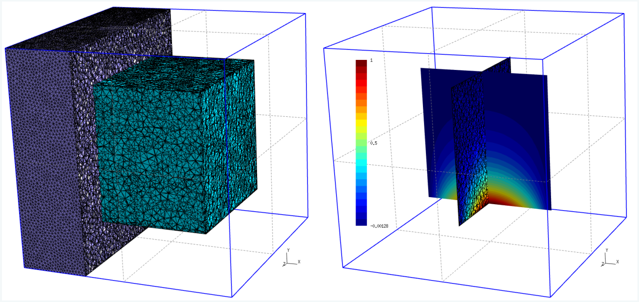

(a) (b)

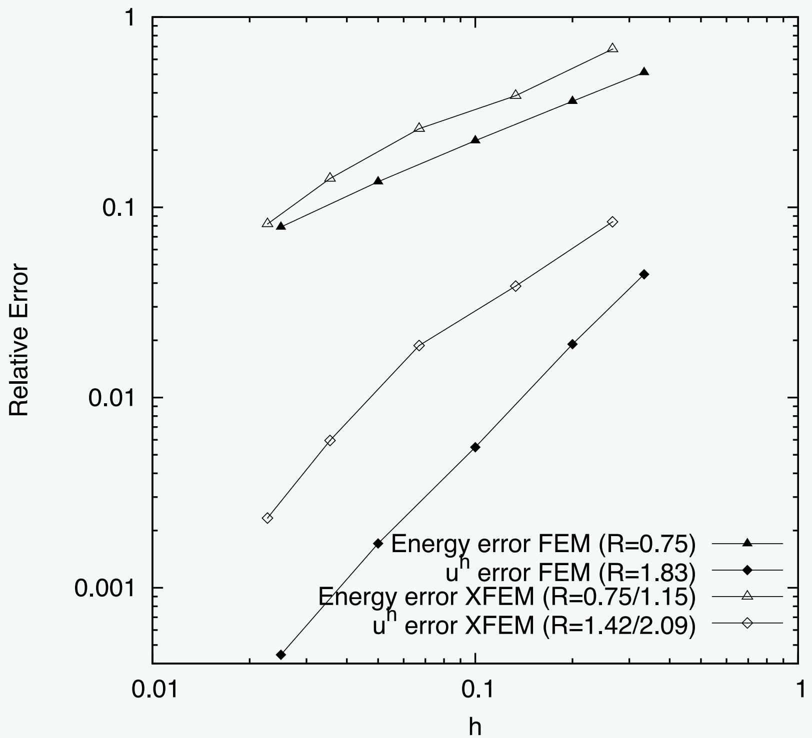

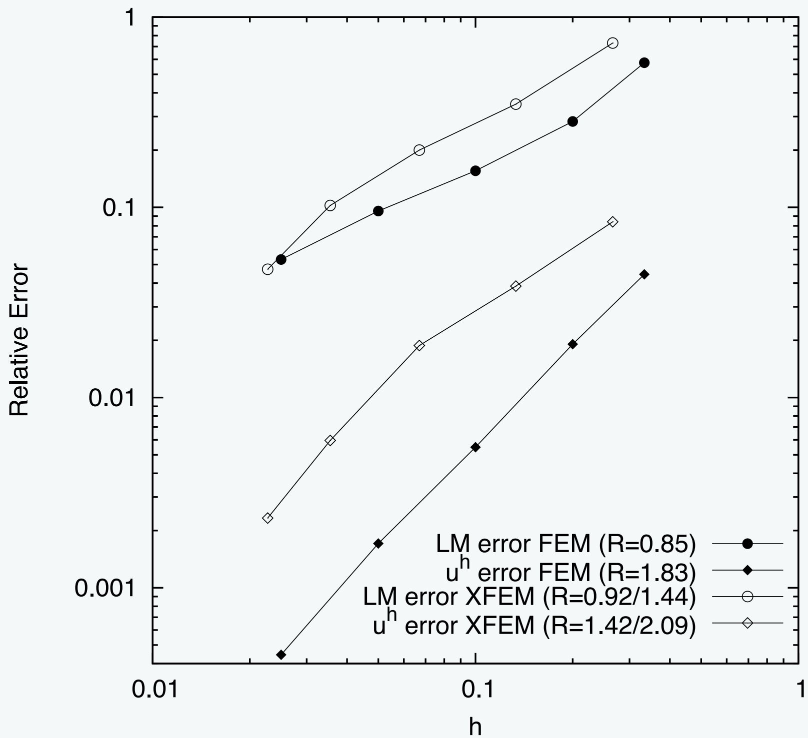

Pixel/Voxel-based FEA on Cartesian grids (Valencia)

I M A M

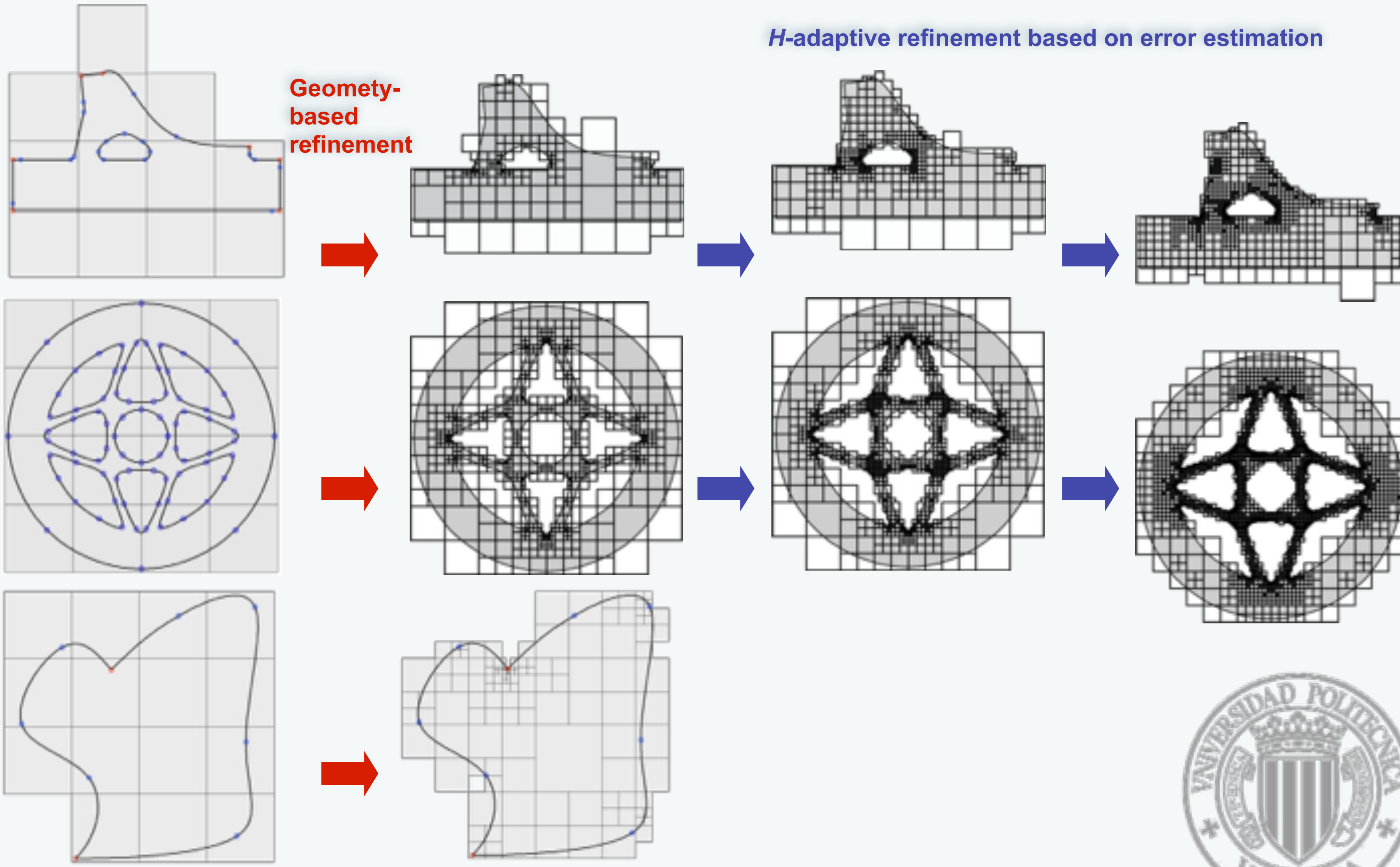

Pixel/Voxel-based FEA on Cartesian grids (Valencia)

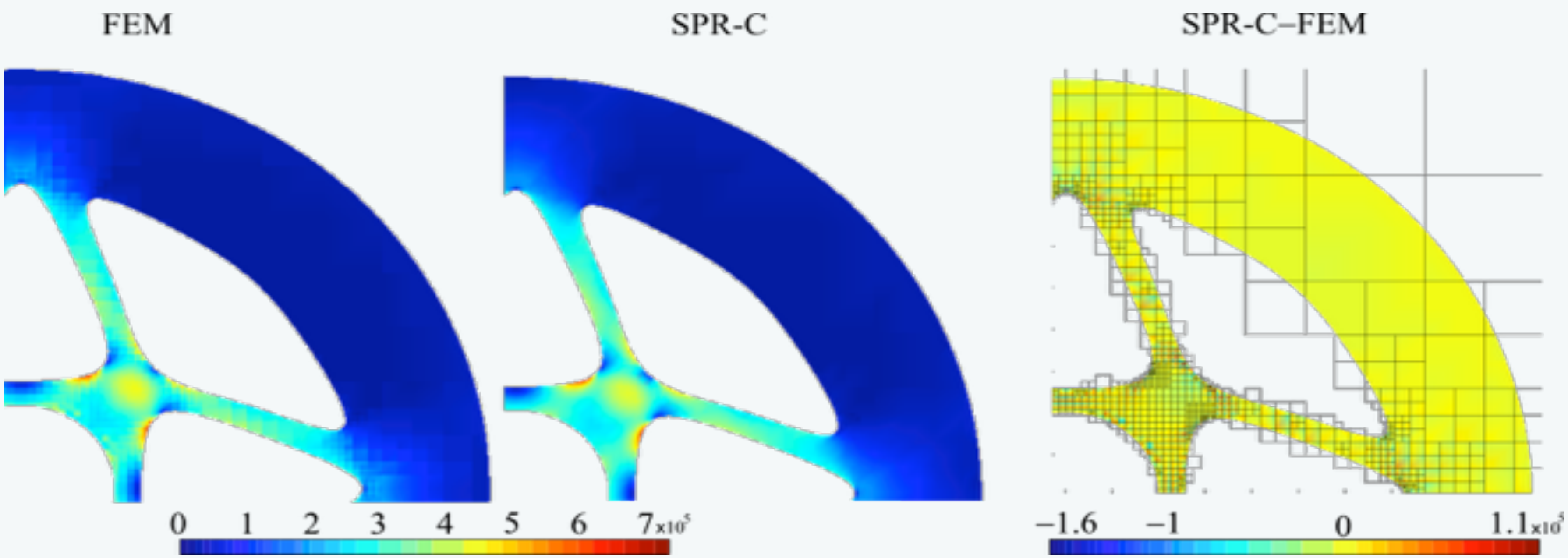

Quad8 uniform refinement

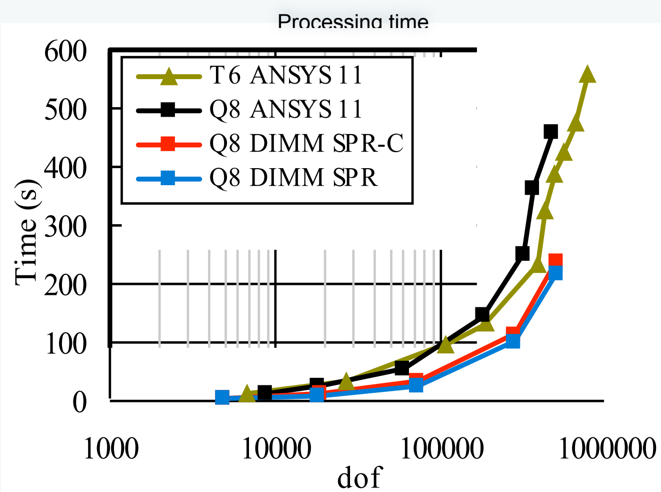

Papers for download

- http://orbilu.uni.lu/handle/10993/17993
- http://orbilu.uni.lu/handle/10993/16606
- http://orbilu.uni.lu/handle/10993/12915

Part I.b. *Coupling CAD and Analysis.*

Isogeometric analysis

- P. Kagan, A. Fischer, and P. Z. Bar-Yoseph. New B-Spline Finite Element approach for geometrical design and mechanical analysis. IJNME, 41(3):435–458, 1998.
- F. Cirak, M. Ortiz, and P. Schröder. Subdivision surfaces: a new paradigm for thin-shell finite-element analysis. IJNME, 47(12): 2039–2072, 2000.
- Constructive solid analysis: a hierarchical, geometry-based meshless analysis procedure for integrated design and analysis. D. Natekar, S. Zhang,and G. Subbarayan. CAD, 36(5): 473--486, 2004.
- T.J.R. Hughes, J.A. Cottrell, and Y. Bazilevs. Isogeometric analysis: CAD, finite elements, NURBS, exact geometry and mesh refinement. CMAME, 194(39-41):4135–4195, 2005.
- J. A. Cottrell, T. J.R. Hughes, and Y. Bazilevs. Isogeometric Analysis: Toward Integration of CAD and FEA. Wiley, 2009.

- P. Kagan, A. Fischer, and P. Z. Bar-Yoseph. New B-Spline Finite Element approach for geometrical design and mechanical analysis. IJNME, 41(3):435–458, 1998.
- F. Cirak, M. Ortiz, and P. Schröder. Subdivision surfaces: a new paradigm for thin-shell finite-element analysis. IJNME, 47(12): 2039–2072, 2000.
- **Constructive solid analysis: a hierarchical, geometry-based meshless analysis procedure for integrated design and analysis. D. Natekar, S. Zhang,and G. Subbarayan. CAD, 36(5): 473--486, 2004.**
- **T.J.R. Hughes, J.A. Cottrell, and Y. Bazilevs. Isogeometric analysis: CAD, finite elements, NURBS, exact geometry and mesh refinement. CMAME, 194(39-41):4135–4195, 2005.**
- J. A. Cottrell, T. J.R. Hughes, and Y. Bazilevs. Isogeometric Analysis: Toward Integration of CAD and FEA. Wiley, 2009.

Knot vector

a non-decreasing set of coordinates in the parametric space.

$$\Xi = \{\xi_1,\ \xi_2,\ \cdots,\ \xi_{n+p+1}\}$$

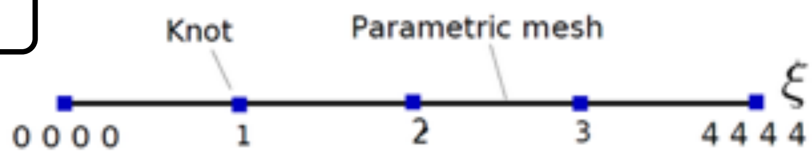

B-spline basis function

$$N_{a,0}(\xi) = \begin{cases} 1, & \text{if } \xi_a \le \xi < \xi_{a+1} \\ 0, & \text{otherwise.} \end{cases}$$

$$N_{a,p}(\xi) = \frac{\xi - \xi_a}{\xi_{a+p} - \xi_a} N_{a,p-1}(\xi) + \frac{\xi_{a+p+1} - \xi}{\xi_{a+p+1} - \xi_{a+1}} N_{a+1,p-1}(\xi).$$

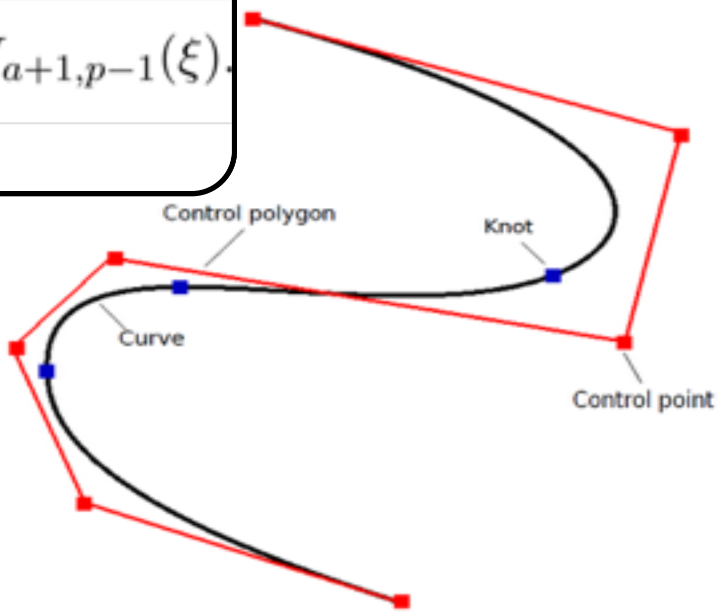

NURBS basis function

$$R_{a,p}(\xi) = \frac{N_{a,p}(\xi) w_a}{W(\xi)} = \frac{N_{a,p}(\xi) w_a}{\sum_{\hat{a}=1}^{n} N_{\hat{a},p} w_{\hat{a}}},$$

Properties of NURBS

- Partition of Unity

$$\sum_{i=1}^{n} R_{i,p}(\xi) = 1$$

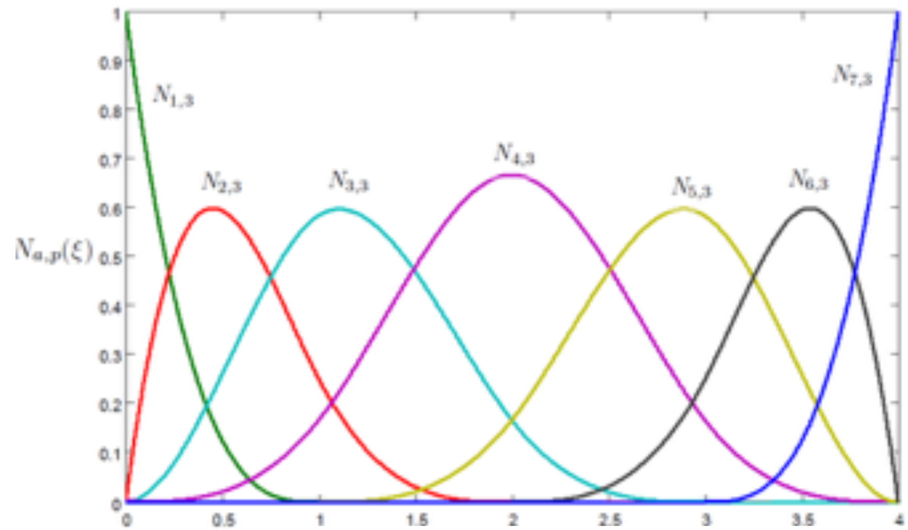

- Non-negative

- *p-1* continuous derivatives

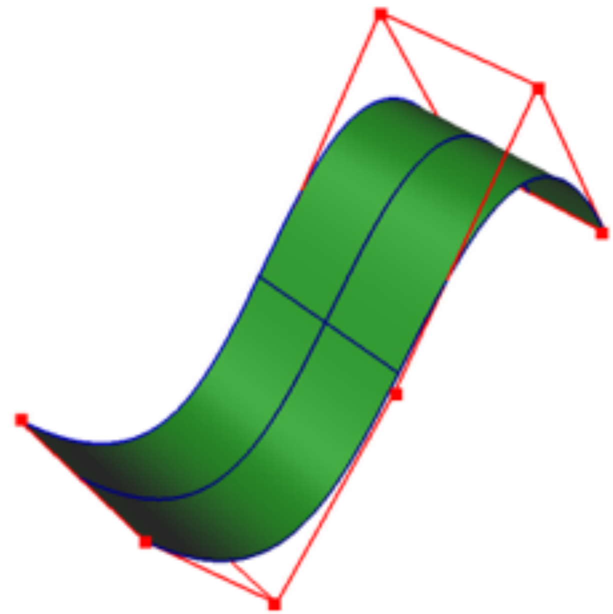

- Tensor product property

$$\mathbf{S}(\xi,\eta) = \sum_{i=1}^{n}\sum_{j=1}^{m} R^{1}{}_{i,p}(\xi) R^{2}{}_{j,q}(\eta) \mathbf{B}_{i,j}$$

$$\sum_{i=1}^{n}\sum_{j=1}^{m} R^{1}{}_{i,p}(\xi) R^{2}{}_{j,q}(\eta) = \left(\sum_{i=1}^{n} R^{1}{}_{i,p}(\xi)\right)\left(\sum_{j=1}^{m} R^{2}{}_{j,q}(\eta)\right)$$

NURBS to T-splines

www.tsplines.com

(NURBS geometry)

www.tsplines.com

(T-splines geometry)

NURBS

- No watertight geometry
- No local refinement scheme

T-splines

- Local knot vector (as Point-based splines)
- Global topology

Y. Bazilevs, V.M. Calo, J.A. Cottrell, J.A. Evans, T.J.R. Hughes, S. Lipton, M.A. Scott, and T.W. Sederberg. Isogeometric analysis using T-splines. CMAME, 199(5-8):229–263, 2010.

Isogeometric Analysis with BEM

Boundary representation

Domain representation

1. IGABEM with NURBS for 2D elastic problems (Simpson, *et al*. CMAME, 2011).

2. IGABEM with T-splines for 3D elastic problems (Scott, *et al.* CMAME, 2012).

3. IGABEM with T-splines for 3D acoustic problems (Simpson, *et al*. 2013 - MAFELAP2013 TH1515).

Difficulties in dealing with nonlinear problems and non-homogeneous materials.

IGABEM formulation

Regularised form of boundary integral equation for 2D linear elasticity

$$\int_\Gamma \mathbf{T}(\mathbf{s},\mathbf{x})[\mathbf{u}(\mathbf{x})-\mathbf{u}(\mathbf{s})]\,\mathrm{d}\Gamma(\mathbf{x}) = \int_\Gamma \mathbf{U}(\mathbf{s},\mathbf{x})\mathbf{t}(\mathbf{x})\,\mathrm{d}\Gamma(\mathbf{x})$$

where $\mathbf{x}$ and $\mathbf{s}$ are field point and source point respectively, $\mathbf{u}$ and $\mathbf{t}$ are displacement and traction around the boundary, $\mathbf{T}$ and $\mathbf{U}$ are fundamental solutions.

Discretise the geometry and solution field using NURBS

$$\mathbf{x} = \sum_{A=1}^{n_A} N_A(\xi)\mathbf{B}_A = N_A(\xi)\mathbf{B}_A$$

$$\mathbf{u} = \sum_{A=1}^{n_A} N_A(\xi)\mathbf{u}_A = N_A(\xi)\mathbf{u}_A$$

$$\mathbf{t} = \sum_{B=1}^{n_B} N_B(\xi)\mathbf{t}_B = N_B(\xi)\mathbf{t}_B$$

Approximate the unknown fields with the same basis functions (NURBS, T-splines …) as that used to generate the CAD model

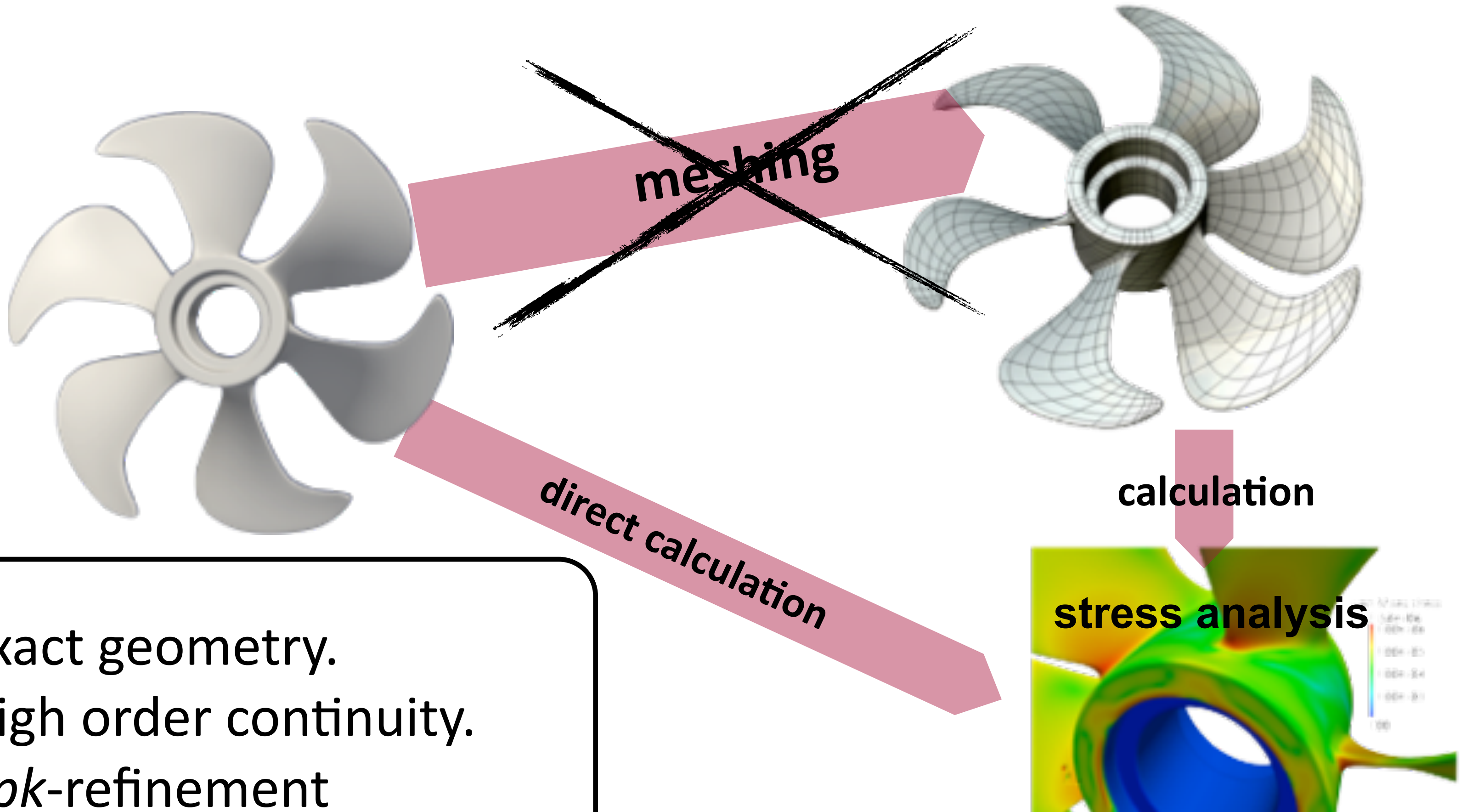

- Exact geometry.
- High order continuity.
- *hpk*-refinement

IGABEM formulation

In Parametric space

$$\int_{\Gamma} \mathbf{T}(\mathbf{s}(\zeta), \mathbf{x}(\xi))[N_A(\xi)\mathbf{u}_A - N_A(\zeta)\mathbf{u}_A] J(\xi) \mathrm{d}\xi$$
$$= \int_{\Gamma} \mathbf{U}(\mathbf{s}(\zeta), \mathbf{x}(\xi)) N_B \mathbf{t}_B(\xi) J(\xi) \mathrm{d}\xi$$

Integration in parent element

$$\left\{ \sum_{e=1}^{N_e} \int_{-1}^{+1} \mathbf{T}(\mathbf{s}(\zeta), \mathbf{x}(\xi))[N_A(\xi) - N_A(\zeta)] J(\xi) \hat{J}^e(\hat{\xi}) \mathrm{d}\hat{\xi} \right\} \mathbf{u}_A$$
$$= \left\{ \sum_{e=1}^{N_e} \int_{-1}^{+1} \mathbf{U}(\mathbf{s}(\zeta), \mathbf{x}(\xi)) N_B(\xi) J(\xi) \hat{J}^e(\hat{\xi}) \mathrm{d}\hat{\xi} \right\} \mathbf{t}_B$$

Matrix equation

$$\mathbf{Hu} = \mathbf{Gt}$$

Special techniques for IGABEM

Collocation point (Greville abscissae)

$$\zeta_a = \frac{\xi_{a+1} + \xi_{a+2} + \ldots + \xi_{a+p}}{p} \qquad a = 1, 2, \ldots, n-1$$

Boundary condition

Collocate on the prescribed boundary

$$\mathbf{N}(\xi)\mathbf{u} = \bar{\mathbf{u}}(\xi)$$
$$\mathbf{N}(\xi)\mathbf{t} = \bar{\mathbf{t}}(\xi)$$

Integration

High order Gauss integration

Nuclear reactor

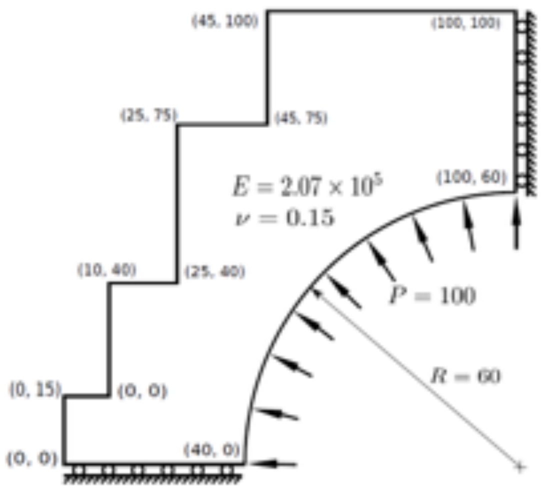

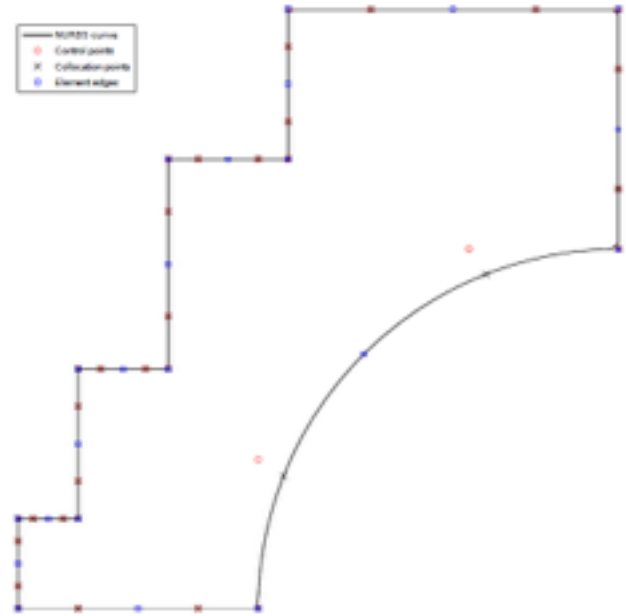

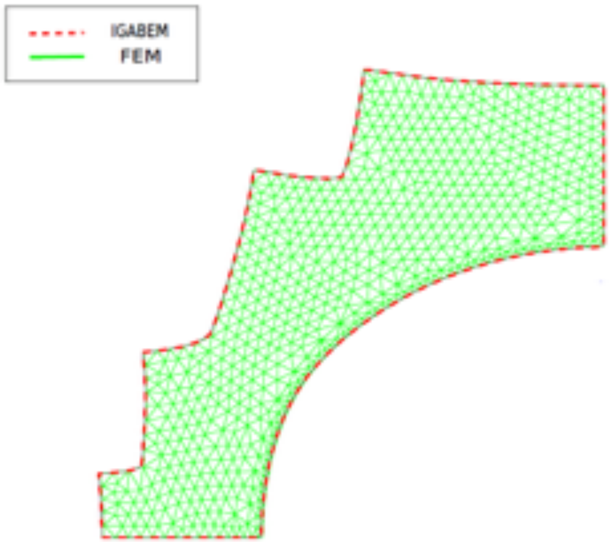

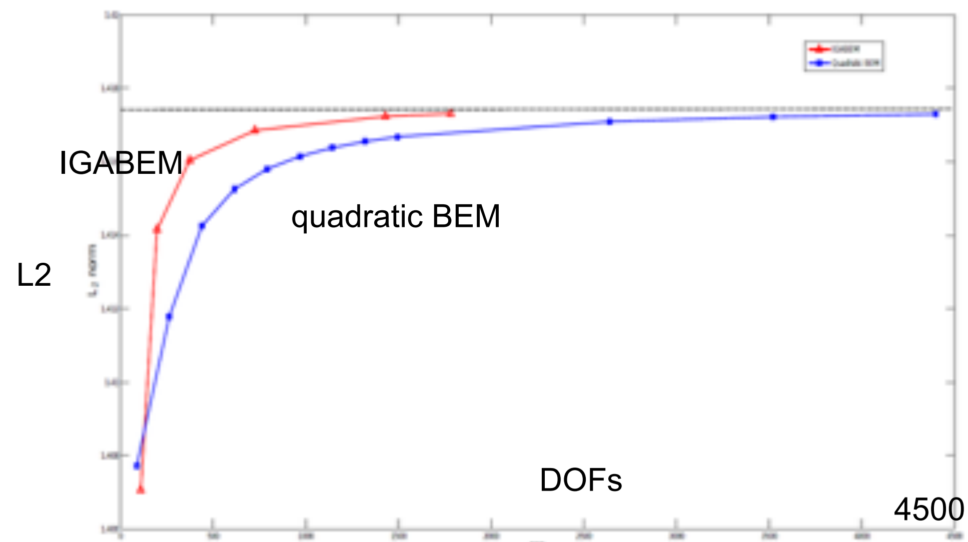

Dam

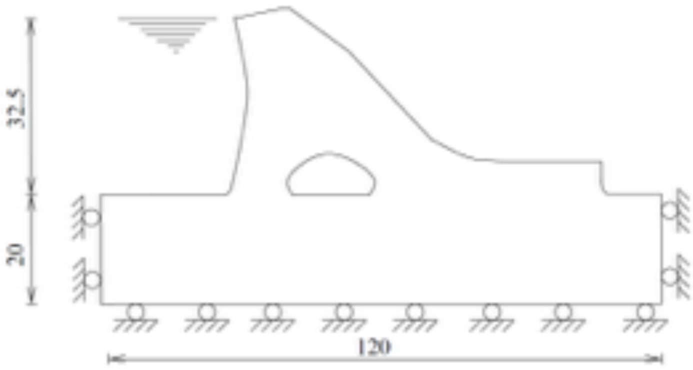

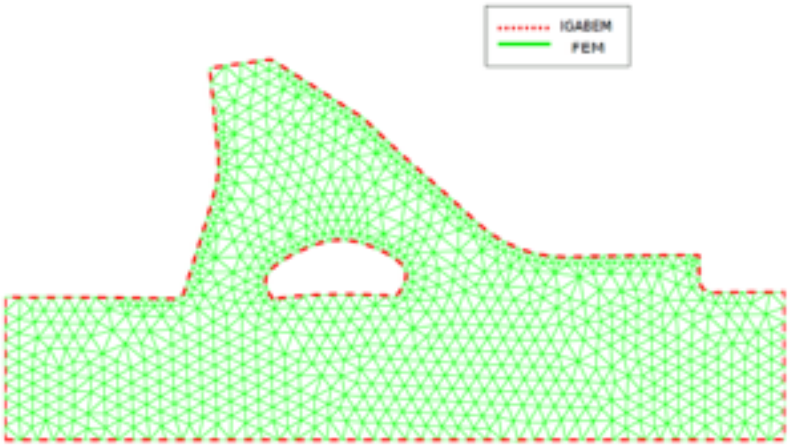

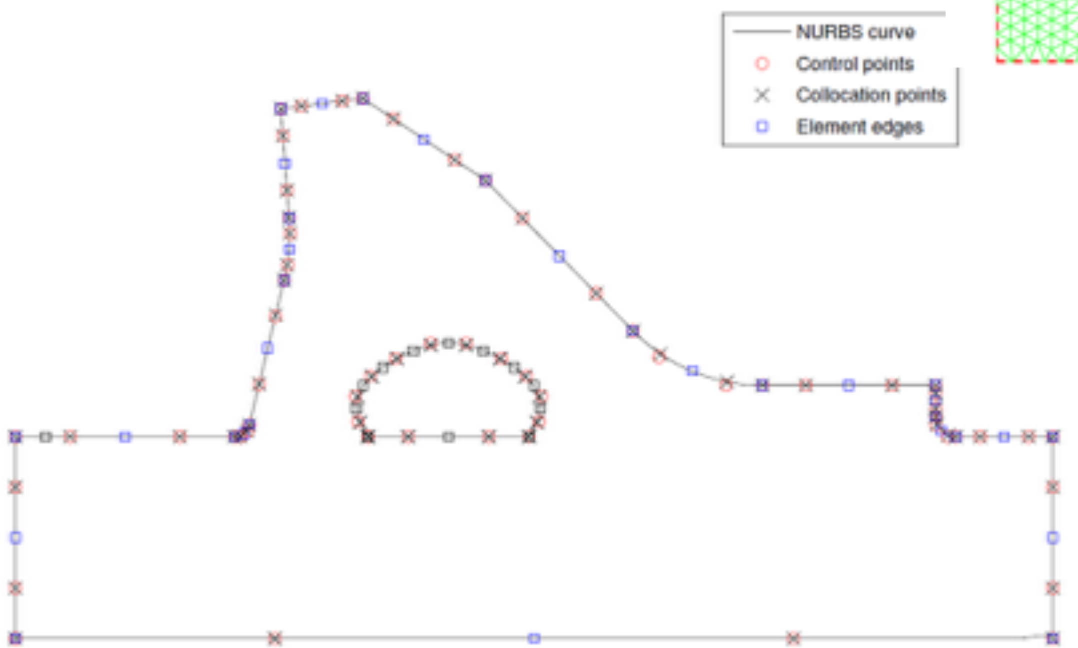

Stress analysis without meshing: isogeometric boundary-element method
ICE Proceeding, 2013, H Lian, RN Simpson, SPA Bordas

Propeller: NURBS would require several patches - single patch T-splines

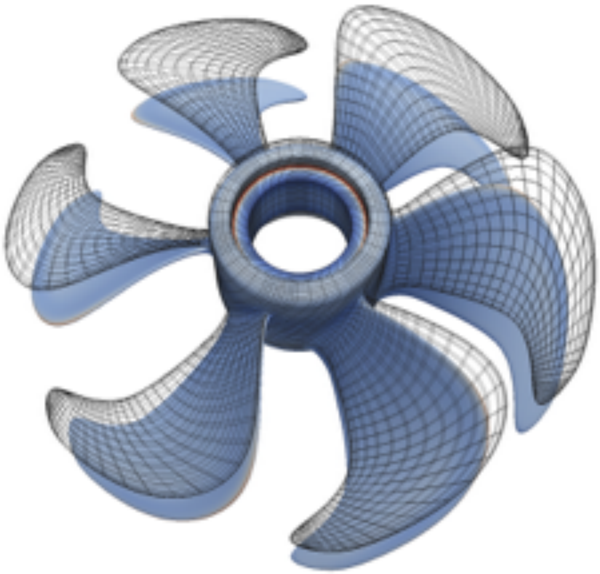

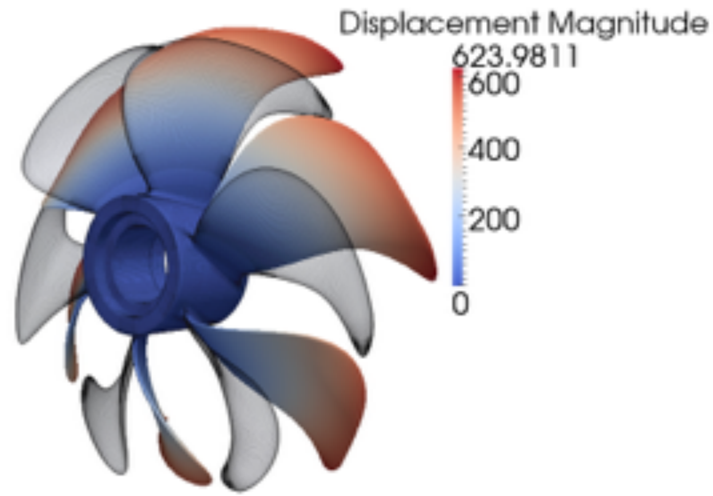

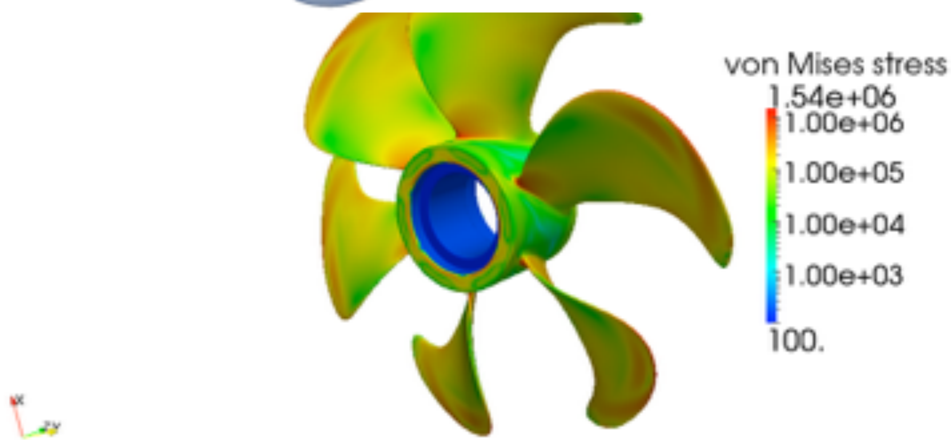

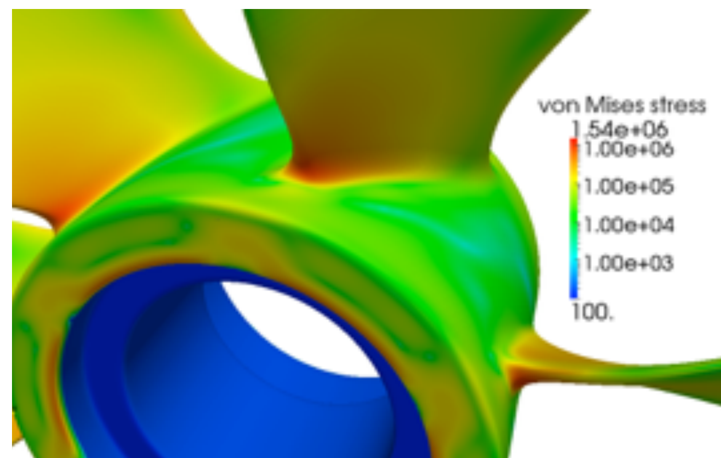

Isogeometric boundary element analysis using unstructured T-splines
MA Scott, RN Simpson, JA Evans, S Lipton, SPA Bordas, TJR Hughes, TW Sederberg
CMAME, 2013.


"What computer do you have?
And please don't say a white one."
BACONWRAPPEDMEDIA.COM

Part I.b.1 Shape optimisation directly from CAD

Stéphane P.A. Bordas, Pierre Kerfriden, Elena Atroshchenko, Xuan Peng, Haojie Lian

IGABEM sensitivity analysis formulation

Governing equations in parametric space, which can be viewed as material coordinate system

$$\int_\Gamma \mathbf{T}(\mathbf{s}(\zeta),\mathbf{x}(\xi))[\mathbf{u}(\mathbf{x}(\xi))-\mathbf{u}(\mathbf{s}(\zeta))]J(\xi)\mathrm{d}\xi = \int_\Gamma \mathbf{U}(\mathbf{s}(\zeta),\mathbf{x}(\xi))\mathbf{t}(\mathbf{x}(\xi))J(\xi)\mathrm{d}\xi$$

Differentiate the equation w.r.t. design variables (implicit differentiation)

$$\int_\Gamma (\mathbf{T}_{,m}J+\mathbf{T}J_{,m})(\mathbf{u}-\mathbf{u}^s)\mathrm{d}\xi + \int_\Gamma (\mathbf{T}J)(\mathbf{u}_{,m}-\mathbf{u}^s_{,m})\mathrm{d}\xi$$
$$= \int_\Gamma (\mathbf{U}_{,m}J+\mathbf{U}J_{,m})\mathbf{t}\mathrm{d}\xi + \int_\Gamma (\mathbf{U}J)\mathbf{t}_{,m}\mathrm{d}\xi$$

Discretise the derivatives of displacement and traction using NURBS basis

$$\mathbf{u}_{,m} = \sum_{A=1}^{n_A} N_A(\xi)\mathbf{u}^A_{,m} = N_A(\xi)\mathbf{u}^A_{,m}$$
$$\mathbf{t}_{,m} = \sum_{B=1}^{n_B} N_B(\xi)\mathbf{t}^B_{,m} = N_B(\xi)\mathbf{t}^B_{,m}$$

Finally $$\mathbf{H}_m\mathbf{u} + \mathbf{H}\mathbf{u}_m = \mathbf{G}_m\mathbf{t} + \mathbf{G}\mathbf{t}_m$$

Pressure cylinder problem

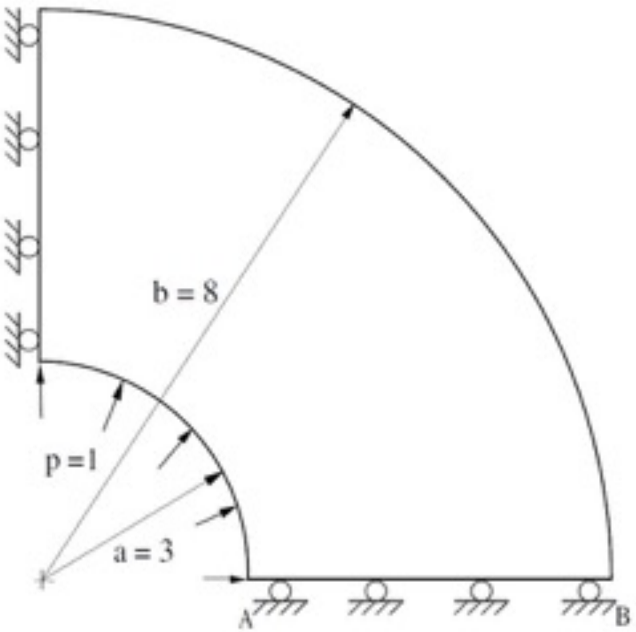

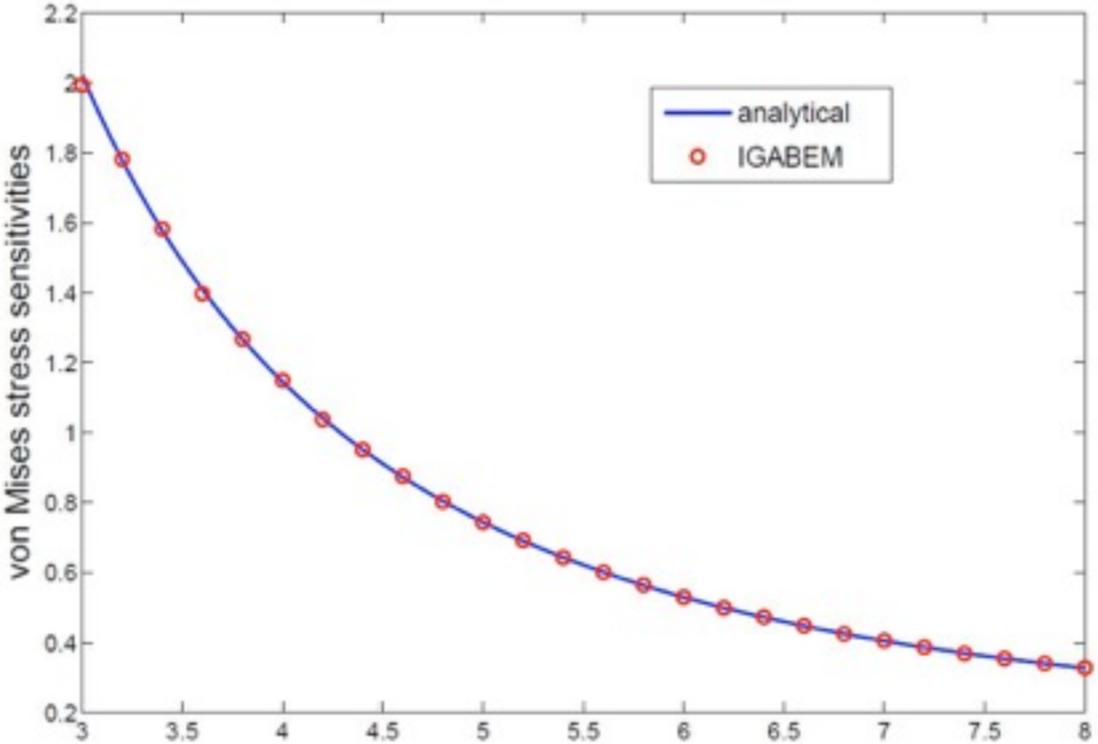

Design variable is outer circle radius *b*

Infinite plate with a hole

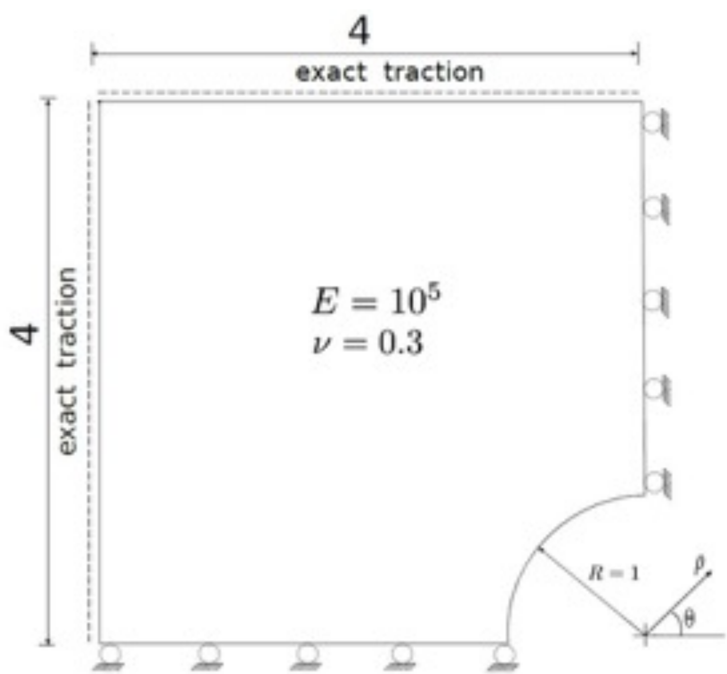

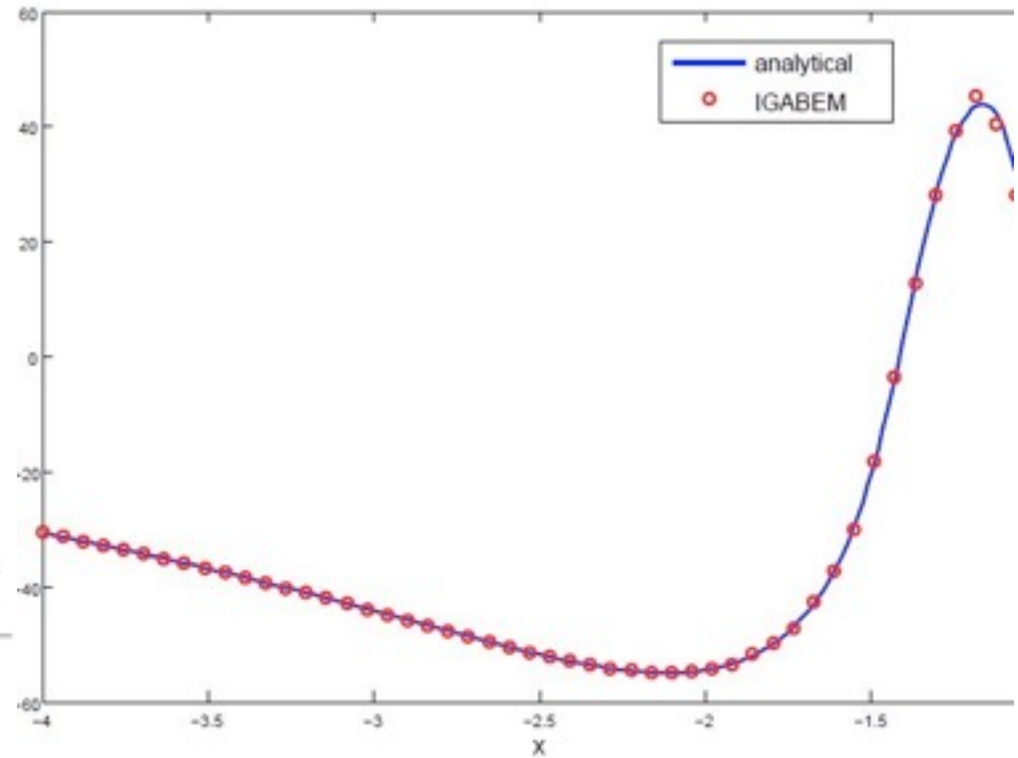

Design variable is radius *R*

3D Lamé problem

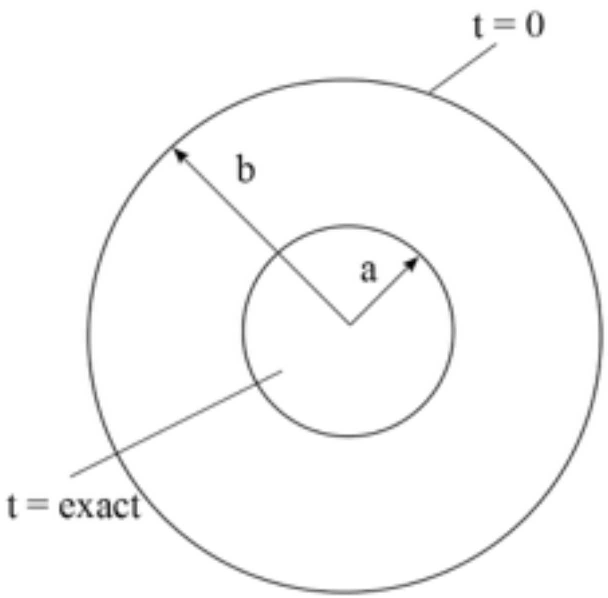

Design parameter: ***b***

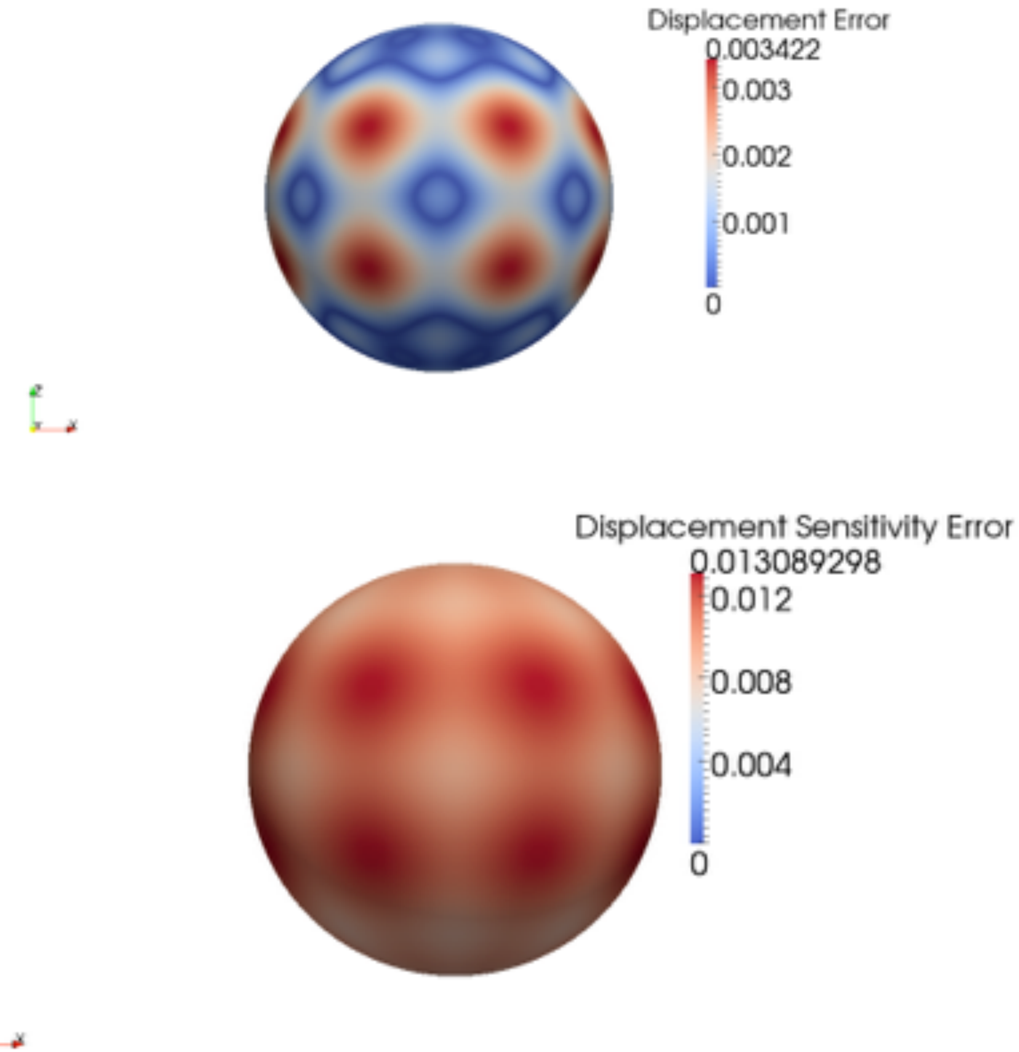

Fillet

Design curve is *ED.*

Minimise the area without violating von Mises stress criterion.

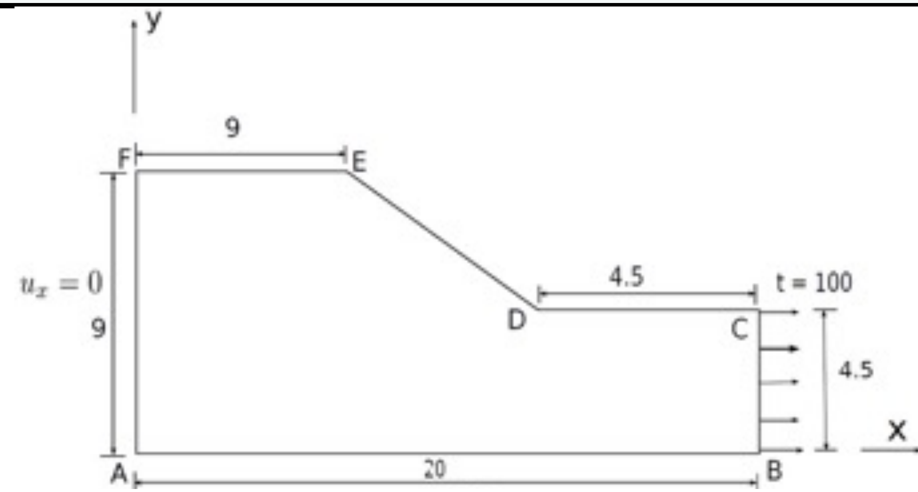

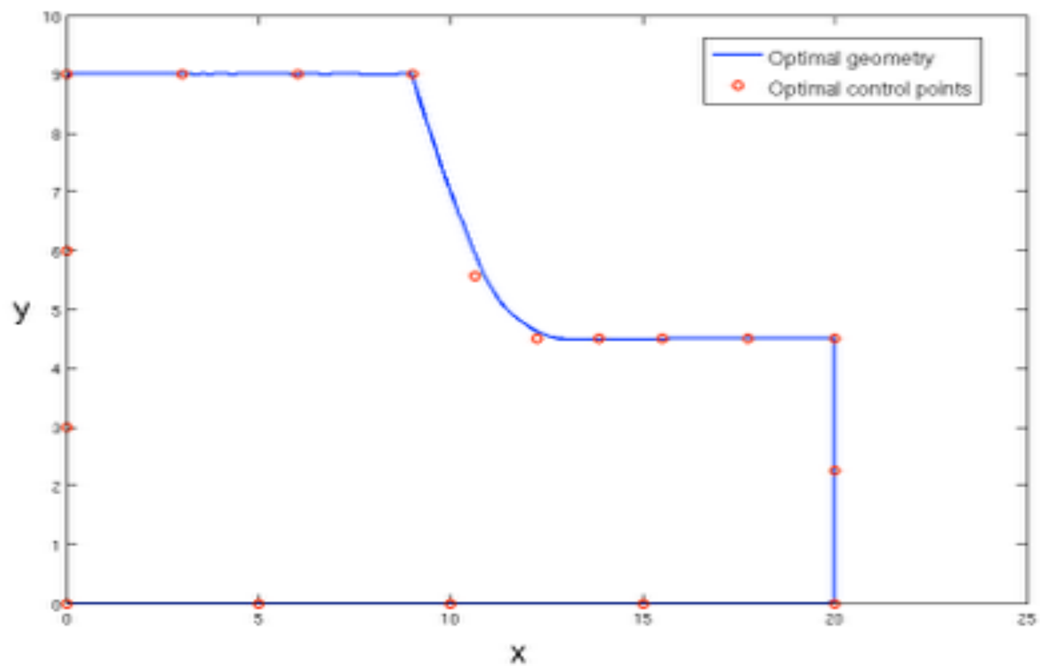

- IGA
- BEM
- T-splines
- Control points and weights as design variables
- Maximize stiffness, minimise volume

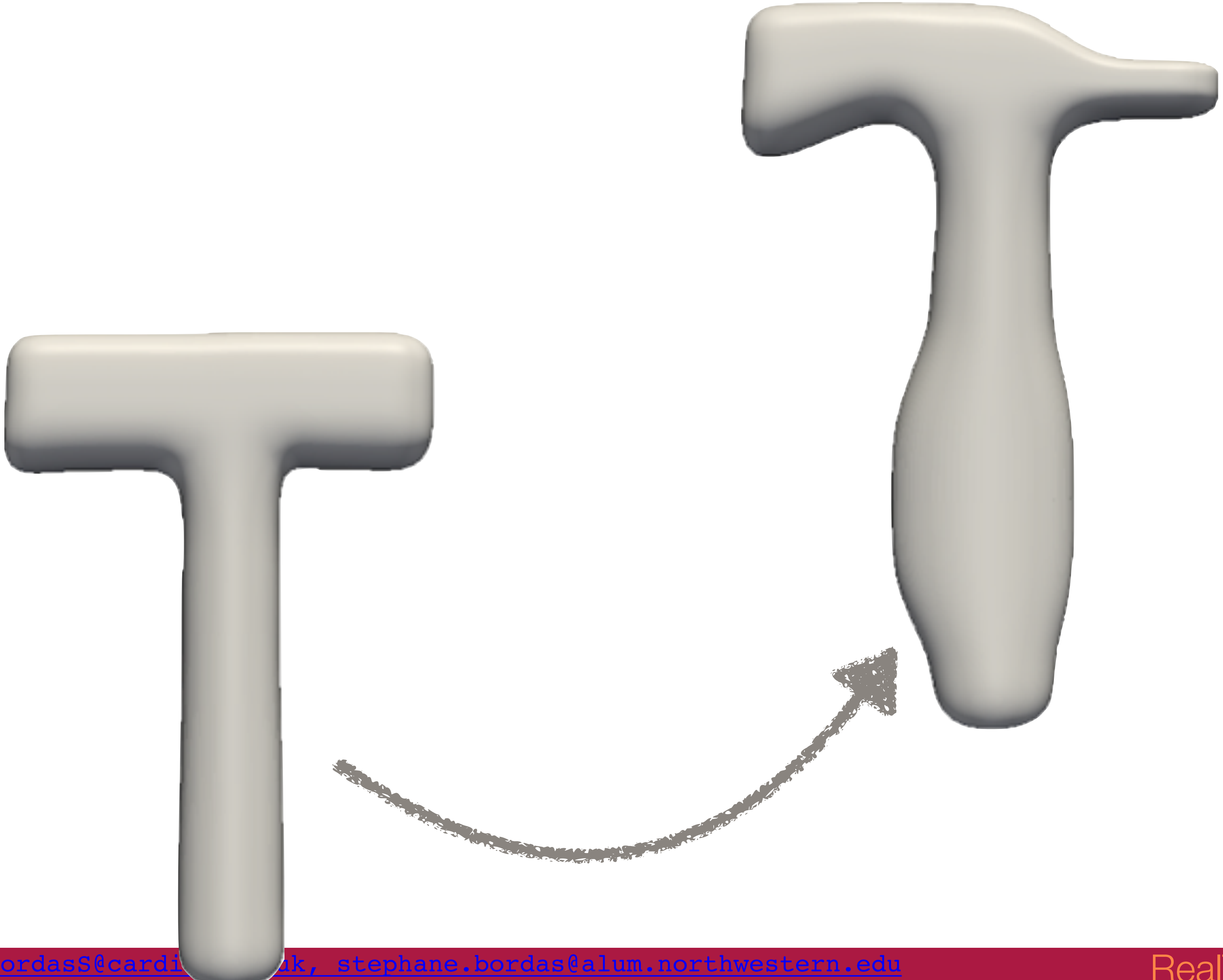

R. Alwood, G. Cornes, “A polygonal finite element for plate bending problems using the assumed stress approach”, International Journal for Numerical Methods in Engineering, 1(2): 135–149, 1969.

T. Belytschko, Y. Lu, L. Gu, “Element-free Galerkin methods”, International Journal for Numerical Methods in Engineering, 37: 229–256, 1994.

T. Belytschko, T. Black, “Elastic crack growth in finite elements with minimal remeshing”, International Journal for Numerical Methods in Engineering, 45: 601–620, 1999.

R. Mittal, G. Iaccarino, “Immersed boundary methods”, Annual Review of Fluid Mechanics, 37: 239–261, 2005.

G.R. Liu, K. Dai, T. Nguyen, “A smoothed finite element method for mechanics problems”, Computational Mechanics, 39: 859–877, 2007.

LB da Veiga, F Brezzi, LD Marini - Virtual Elements for linear elasticity problems SIAM Journal on Numerical Analysis, 2013.

F. Rizzo, “An integral equation approach to boundary value problems of classical elastostatics”, Quart. Appl. Math, 25(1): 83–95, 1967.

R. Glowinski, T. Pan, J. Periaux, “A fictitious domain method for Dirichlet problem and applications”, Computer Methods in Applied Mechanics and Engineering, 111(3-4): 283–303, 1994.

C. Song, J. Wolf, “The scaled boundary finite-element method–alias consistent infinitesimal finite-element cell method–for elastodynamics”, Computer Methods in Applied Mechanics and Engineering, 147(3): 329–355, 1997.

R. Simpson, S. Bordas, J. Trevelyan, T. Rabczuk, “A two-dimensional isogeometric boundary element method for elastostatic analysis”, Computer Methods in Applied Mechanics and Engineering, 209-212: 87–100, 2012.

Isogeometric boundary element analysis using unstructured T-splines
MA Scott, RN Simpson, JA Evans, S Lipton, SPA Bordas, TJR Hughes, TW Sederberg Computer Methods in Applied Mechanics and Engineering, 2013.

Reduce mesh burden

E. Saiki, S. Biringen, “Numerical simulation of a cylinder in uniform flow: application of a virtual boundary method”, Journal of Computational Physics, 123(2): 450–465, 1996.

H. Johansen, P. Colella, “A Cartesian grid embedded boundary method for Poisson’s equation on irregular domains”, Journal of Computational Physics, 147(1): 60–85, 1998.

T. Ye, R. Mittal, H. Udaykumar, W. Shyy, “An accurate Cartesian grid method for viscous incompressible flows with complex immersed boundaries”, Journal of Computational Physics, 156(2): 209–240, 1999.

M. Moumnassi, S. Belouettar, E. Bechet, S. Bordas, D. Quoirin, M. Potier Ferry, “Finite element analysis on implicitly defined domains: An accurate representation based on arbitrary parametric surfaces”, Computer Methods in Applied Mechanics and Engineering, 200(5): 774–796, 2011.

Part I.b.2 Isogeometric Boundary Element Method for Damage Tolerance Assessment directly from CAD

Institute of Mechanics & Advanced Materials

➢**Fatigue Fracture Failure of Structure**

•Initiation: micro defects

•Loading : cyclic stress state (temperature, corrosion)

➢**Numerical methods for crack growth**

•Volume methods:
FEM, XFEM/GFEM, Meshfree

•Boundary methods: BEM

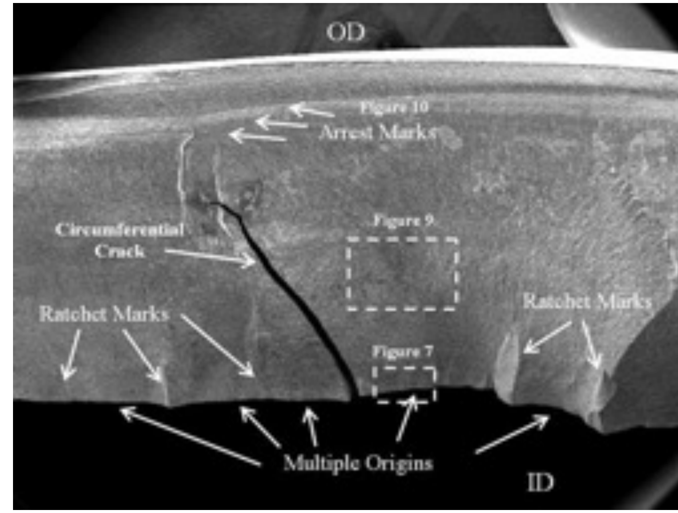

Fatigue cracking of nozzle sleeve
http://met-tech.com/

Bordas & Moran, 2006

XFEM+LEVEL SET

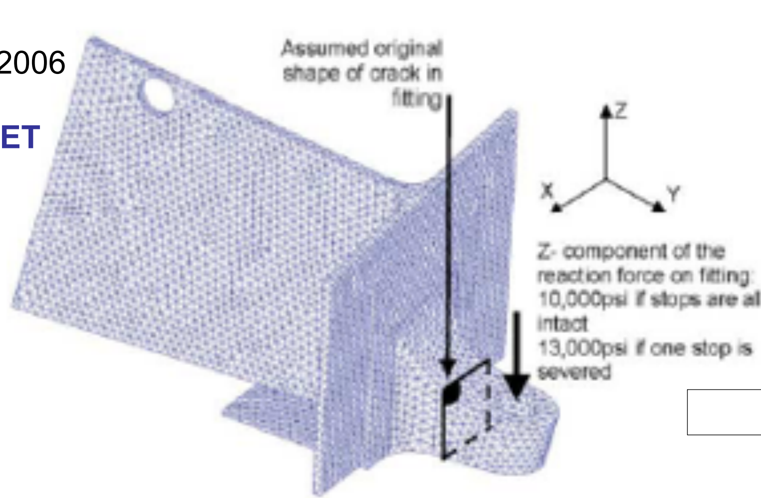

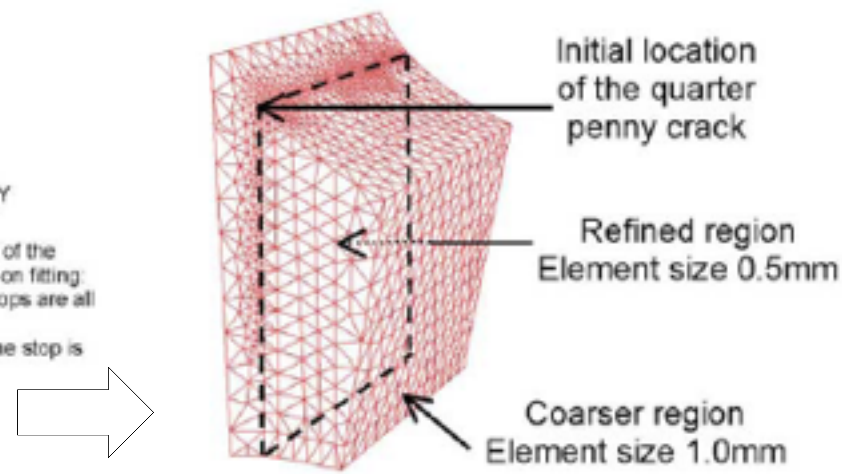

➢ Challenges in volume-based methods

- Remeshing (FEM)
- Local mesh refinement

Efficiency & Accuracy

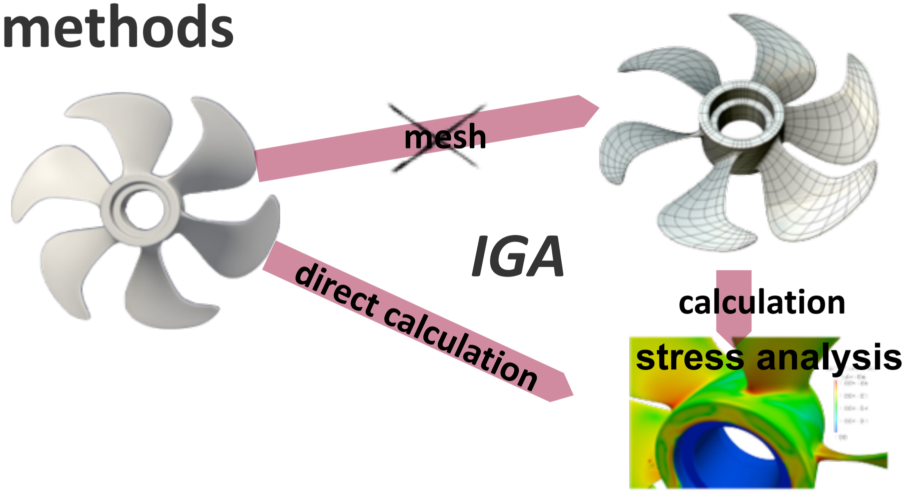

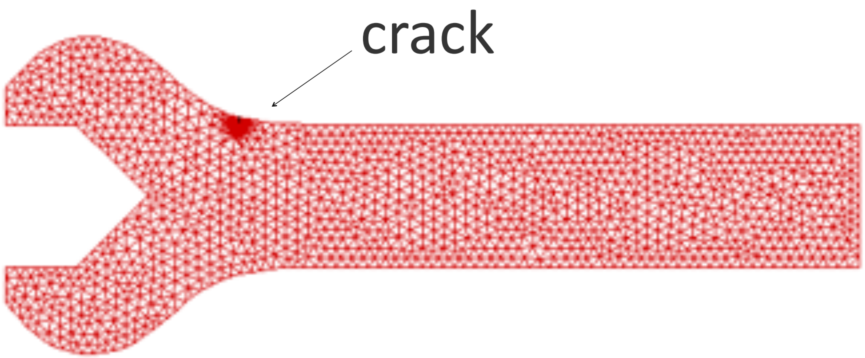

XFEM
adaptive refinement

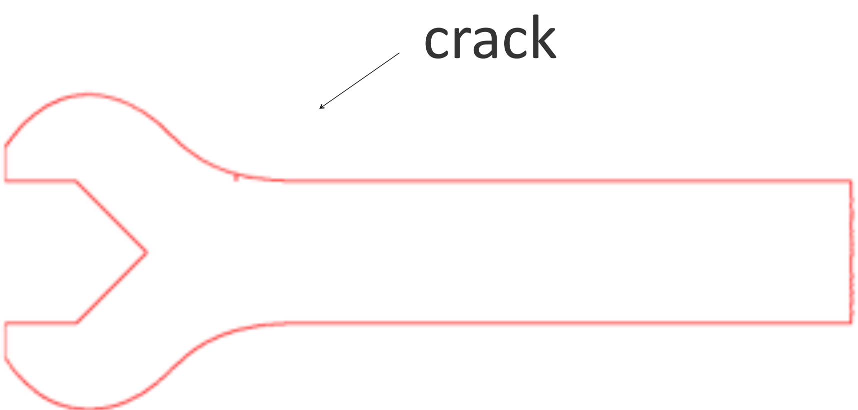

IGABEM
Direct CAD used

Weighted residual method, collocation

Linear elasticity problem:

$$\mathscr{L}(\mathbf{u}) = \nabla \cdot (\mathbf{C}\nabla^s \mathbf{u}) = \mathbf{f}, \quad \text{in } \Omega$$

$$\mathbf{u} = \bar{\mathbf{u}}, \quad \text{on } \Gamma_u$$

$$\mathbf{t} = (\mathbf{C}\nabla^s \mathbf{u}) \cdot \mathbf{n} = \bar{\mathbf{t}}, \quad \text{on } \Gamma_t$$

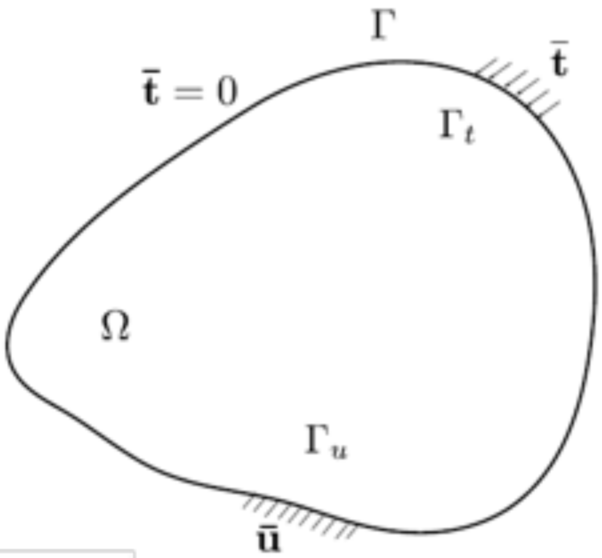

Approximation of $\mathbf{u}$:

$$\mathbf{u}^h = \bar{\mathbf{u}} + \sum_{I=1}^{n} N_I(\mathbf{x})\mathbf{u}^I$$

Weighted residual form:

$$\int_\Omega (\nabla \cdot (\mathbf{C}\nabla^s \mathbf{u}) - \mathbf{f}) \cdot \mathbf{v} \mathrm{d}\Omega + \int_{\Gamma_t} (\mathbf{t} - \bar{\mathbf{t}}) \cdot \mathbf{v} \mathrm{d}\Gamma = 0$$

Collocation method: $\mathbf{v}(\mathbf{z}) = \sum_{I=1}^{k} \mathbf{v}^I \delta(\mathbf{s}_I, \mathbf{z})$

sifting property: $\int_\Omega g(\mathbf{z})\delta(\mathbf{s}, \mathbf{z}) \mathrm{d}\Omega = g(\mathbf{s})$

Galerkin method (variational principle): $\mathbf{v}(\mathbf{z}) = \sum_{I=1}^{k} N_I(\mathbf{z})\mathbf{v}^I$

$$\int_\Omega (\nabla \mathbf{v} : \mathbf{C}\nabla^s \mathbf{u} - \mathbf{f} \cdot \mathbf{v}) \mathrm{d}\Omega + \int_{\Gamma_t} \mathbf{t} \cdot \mathbf{v} \mathrm{d}\Gamma = 0$$

Kelvin fundamental solution

Navier equation: $\mu\nabla^2\mathbf{u} + (\mu+\lambda)\nabla(\nabla\cdot\mathbf{u}) = \mathbf{f}$

Kelvin solution: assuming a unit concentrated force applied on a point $\mathbf{s}$ in the infinite domain $\mathbf{f}(\mathbf{z}) = \mathbf{e}\delta(\mathbf{s},\mathbf{z})$, we seek $\mathbf{u}(\mathbf{z})$ and $\mathbf{t}(\mathbf{z})$ for any point $\mathbf{z}$

$$u_i^* = U_{ij}e_j \qquad t_i^* = T_{ij}e_j$$

for 3D problems, the expressions are:

$$U_{ij}(\mathbf{s},\mathbf{z}) = \frac{1}{16\pi\mu(1-\nu)r}[(3-4\nu)\delta_{ij} + r_{,i}r_{,j}]$$

$$T_{ij}(\mathbf{s},\mathbf{z}) = -\frac{1}{8\pi(1-\nu)}\left[\frac{\partial r}{\partial n}((1-2\nu)\delta_{ij} + 3r_{,i}r_{,j}) - (1-2\nu)(n_j r_{,i} - n_i r_{,j})\right]$$

Boundary integral equations (BIEs) and IGABEM crack modeling

- **Displacement BIE** $c_{ij}(\mathbf{s})u_j(\mathbf{s}) + \fint_\Gamma T_{ij}(\mathbf{s},\mathbf{x})u_j(\mathbf{x})\mathrm{d}\Gamma(\mathbf{x}) = \int_\Gamma U_{ij}(\mathbf{s},\mathbf{x})t_j(\mathbf{x})\mathrm{d}\Gamma(\mathbf{x})$
- **Traction BIE** $c_{ij}(\mathbf{s})t_j(\mathbf{s}) + \fint_\Gamma S_{ij}(\mathbf{s},\mathbf{x})u_j(\mathbf{x})\mathrm{d}\Gamma(\mathbf{x}) = \fint_\Gamma K_{ij}(\mathbf{s},\mathbf{x})t_j(\mathbf{x})\mathrm{d}\Gamma(\mathbf{x})$
- **NURBS approximation**

$$u_i(\xi) = \sum_{A=1}^{n} R_{A,p}(\xi)d_i^A$$

$$t_i(\xi) = \sum_{A=1}^{n} R_{A,p}(\xi)q_i^A$$

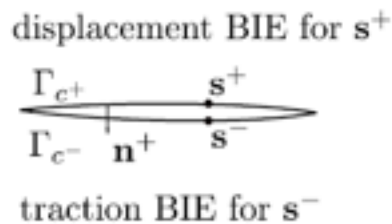

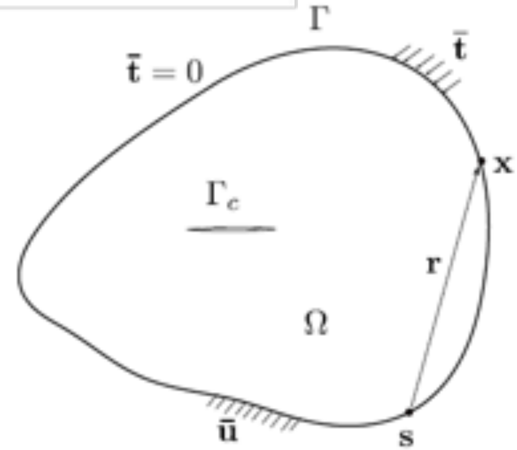

- **Collocation: Greville Abscissae**

$$\xi_s = \frac{\xi_{i+1} + \ldots + \xi_{i+p}}{p}$$

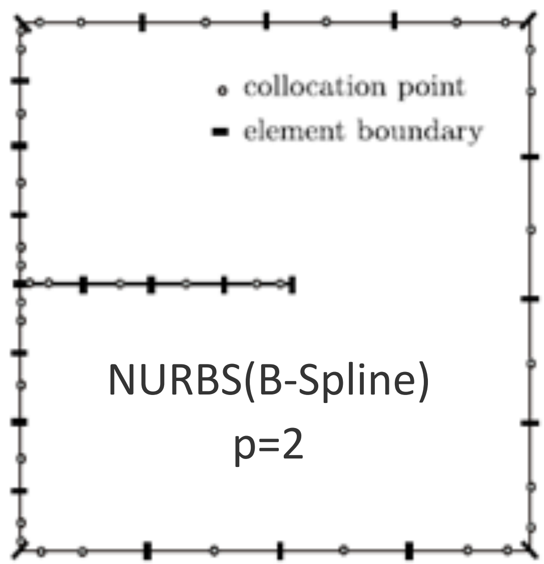

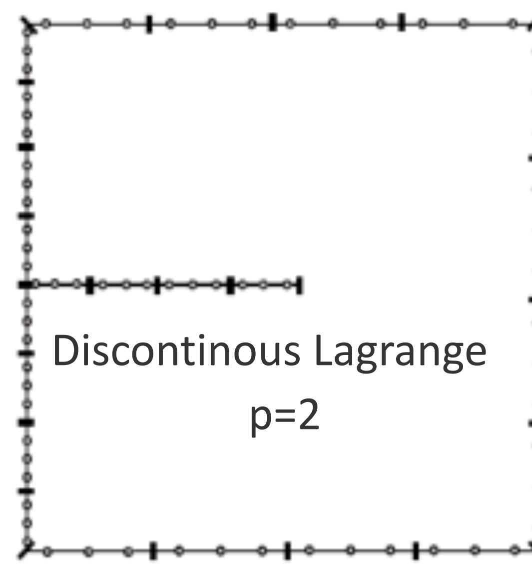

Treatment of crack tip singularity

- Partition of unity enrichment (2D)

$$u_i(\mathbf{x}) = \sum_{I \in \mathcal{N}_I} N_I(\mathbf{x}) d_i^I + \sum_{J \in \mathcal{N}_J} N_J(\mathbf{x}) \phi(\mathbf{x}) a_i^J \qquad \phi = \sqrt{r}$$

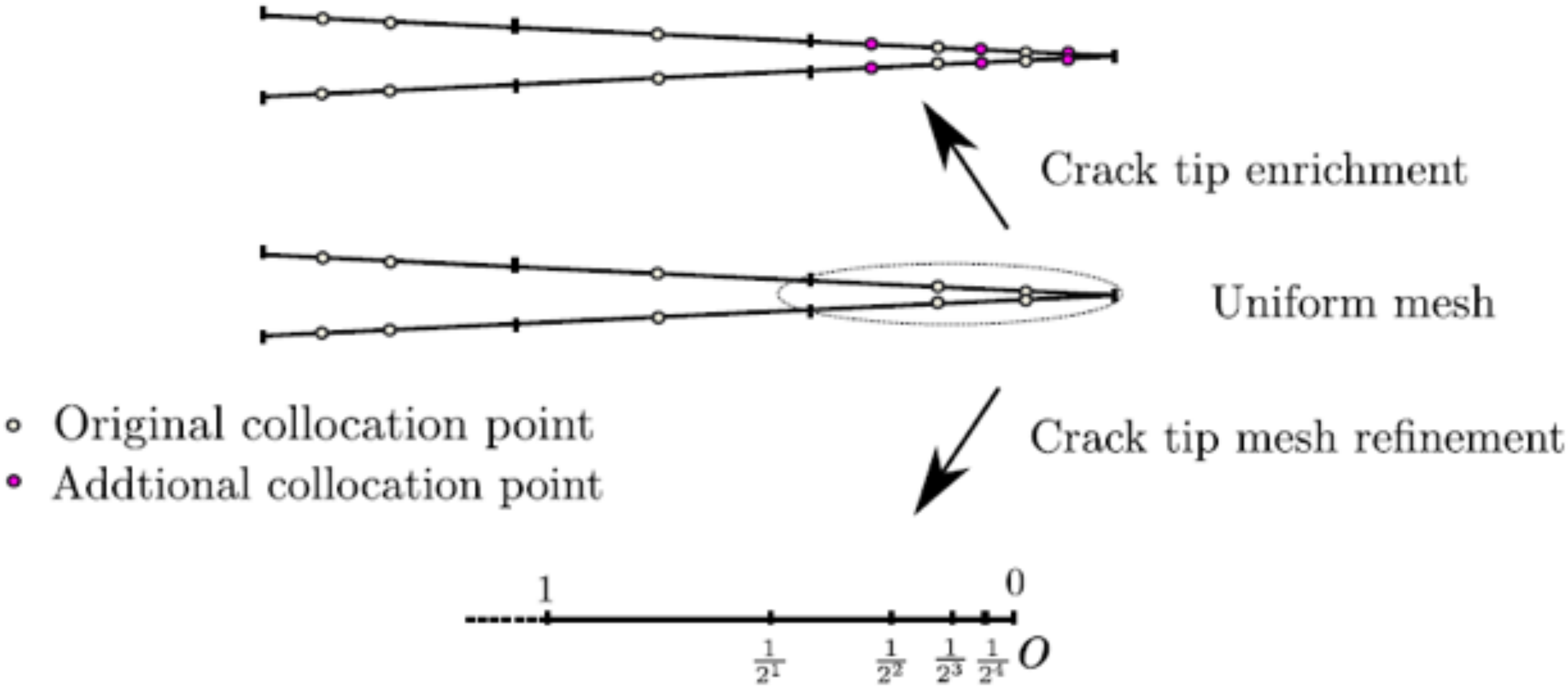

- Consecutive knot insertion at crack tip (2D) or along crack front (3D)

Crack tip refinement VS **enrichment**

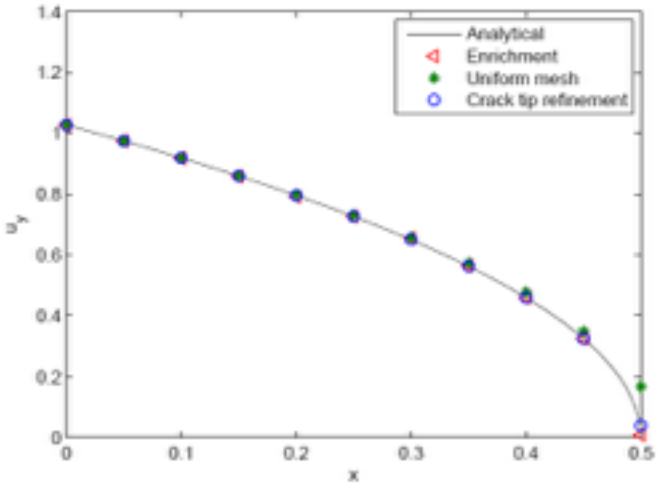

Crack opening displacement

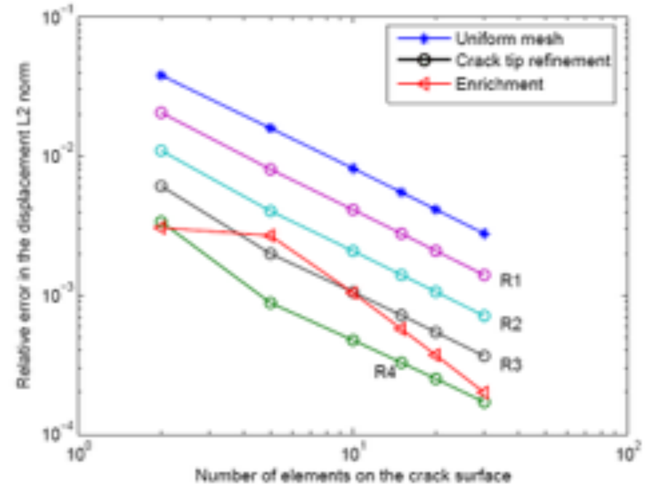

Error in displacement L2 norm

NURBS VS **Lagrange: convergence in SIFs, no crack tip treatment**

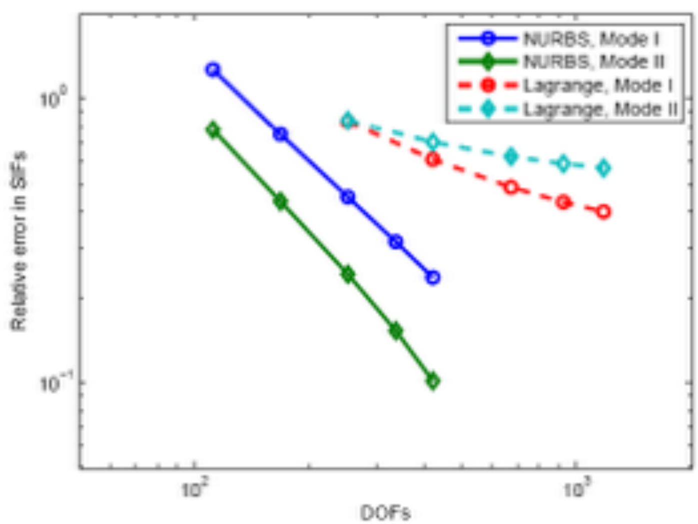

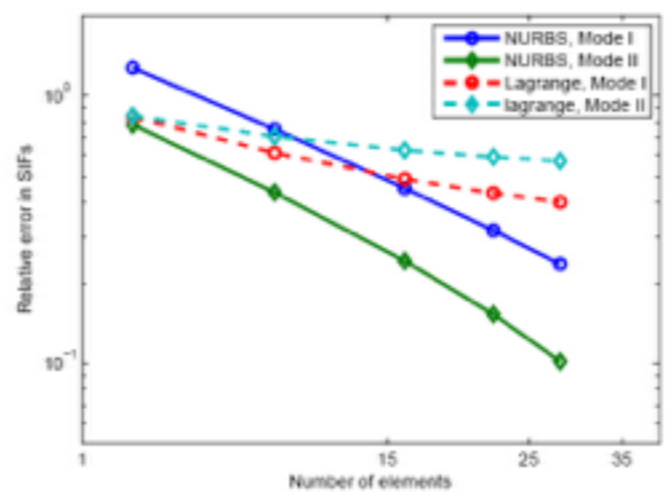

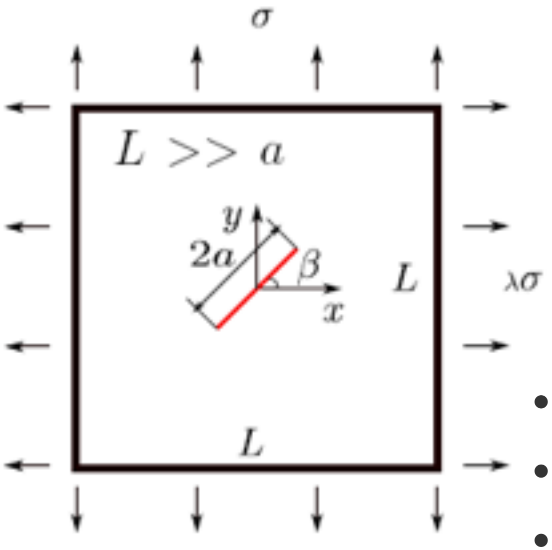

$$K_I = \sigma\sqrt{\pi a}(\cos^2\beta + \lambda\sin^2\beta)$$

$$K_{II} = \sigma\sqrt{\pi a}(1-\lambda)\cos\beta\sin\beta$$

$$\beta = \pi/6, \quad \sigma = 1, \quad \lambda = 0.5$$

- IGABEM(r) :Uniform mesh (refined tip element)
- LBEM: discontinuous Lagrange BEM
- SGBEM: symmetric Galerkin BEM, Sutrahar&Paulino (2004)

m: number of elements in uniform mesh along the crack surface

	K_I/K_I^{exact}			
m	SGBEM	LBEM	IGABEM	IGABEM(r)
3	0.9913	1.00451	1.00982	1.00120
4	1.0002	1.00333	1.00769	1.00105
5	1.0001	1.00268	1.00633	1.00090
6	1.0002	1.00230	1.00539	1.00080
7	1.0003	1.00206	1.00474	1.00074
8	1.0003	1.00190	1.00426	1.00070
9	1.0003	1.00177	1.00389	1.00066
10	1.0003	1.00167	1.00359	1.00064
11	1.0003	1.00159	1.00336	1.00062
12	1.0003	1.00152	1.00316	1.00060
14	1.0003	1.00142	1.00285	1.00058

	K_{II}/K_{II}^{exact}			
m	SGBEM	LBEM	IGABEM	IGABEM(r)
3	1.0075	1.00104	1.00647	1.00146
4	1.0009	1.00129	1.00656	1.00129
5	1.0010	1.00158	1.00607	1.00113
6	1.0009	1.00160	1.00550	1.00102
7	1.0014	1.00153	1.00500	1.00096
8	1.0005	1.00143	1.00458	1.00091
9	0.9997	1.00134	1.00424	1.00087
10	1.0009	1.00126	1.00396	1.00085
11	0.9992	1.00119	1.00373	1.00083
12	1.0013	1.00112	1.00353	1.00081
14	1.0004	1.00102	1.00322	1.00079

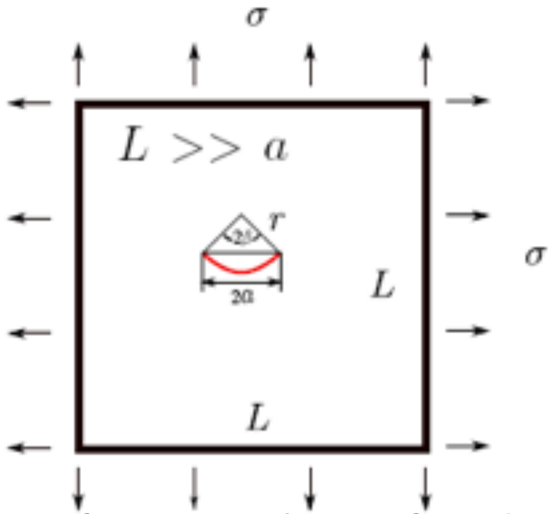

$$K_I = \sigma\sqrt{\pi a}\frac{\cos(\beta/2)}{1+\sin^2(\beta/2)}$$

$$K_{II} = \sigma\sqrt{\pi a}\frac{\sin(\beta/2)}{1+\sin^2(\beta/2)}$$

$$\sigma = 1, \quad \beta = \pi/4$$

- Uniform mesh + refined tip element
- Splitting parameter in **J** integral: $r_{split} = 0.03R_J, 0.04R_J, 0.05R_J, 0.06R_J, 0.07R_J$

m: number of elements in uniform mesh along the crack surface

	K_I/K_I^{exact}		K_{II}/K_{II}^{exact}	
m	M integral	J_k integral	M integral	J_k integral
10	1.00045	0.99972	0.97506	1.00309
14	1.00014	0.99979	0.98621	1.00248
17	1.00011	0.99982	0.98642	1.00217
20	1.00009	0.99985	0.98657	1.00195
23	1.00002	0.99987	0.99407	1.00176
26	1.00002	0.99989	0.99413	1.00163

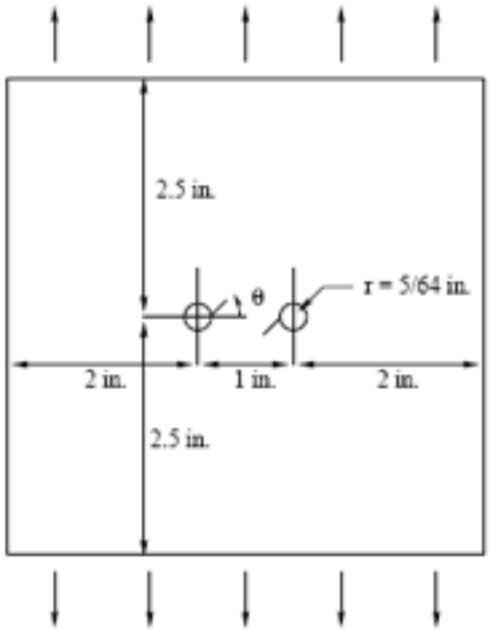

(a) XFEM by Möes et al (1999)

(b) IGABEM

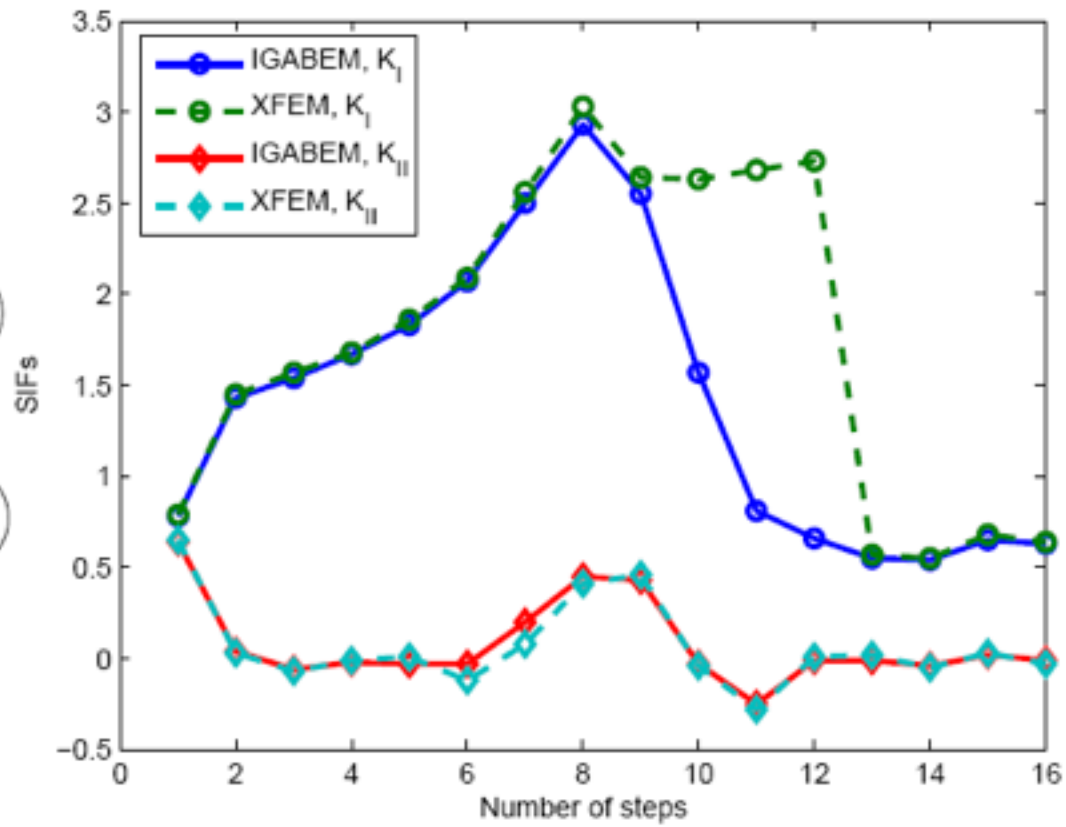

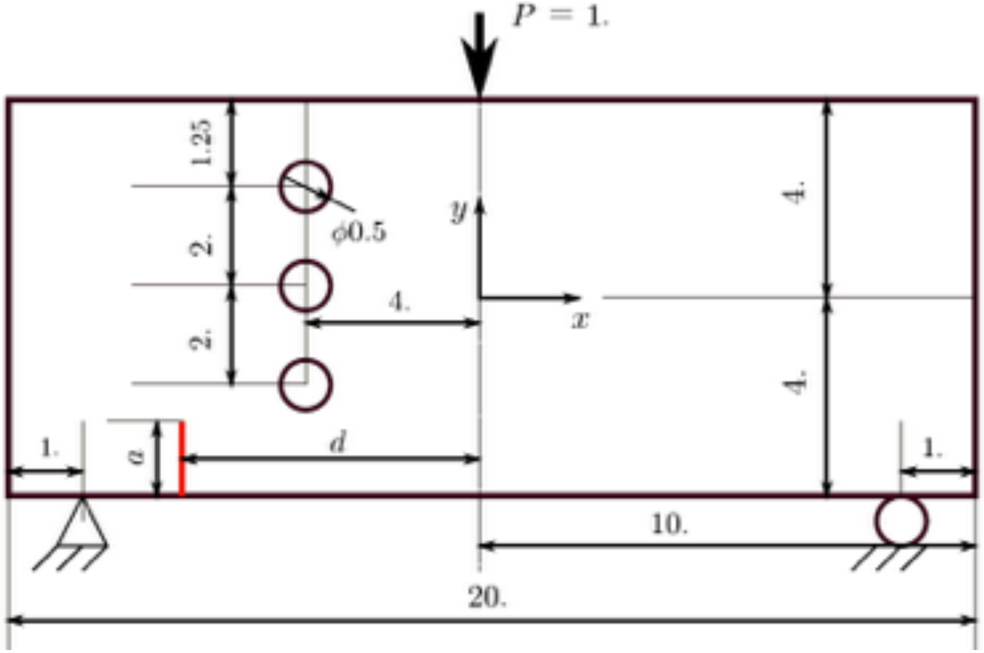
P = 1.
1.25
2.
2.
ϕ0.5
y
x
4.
4.
4.
1.
a
d
1.
10.
20.

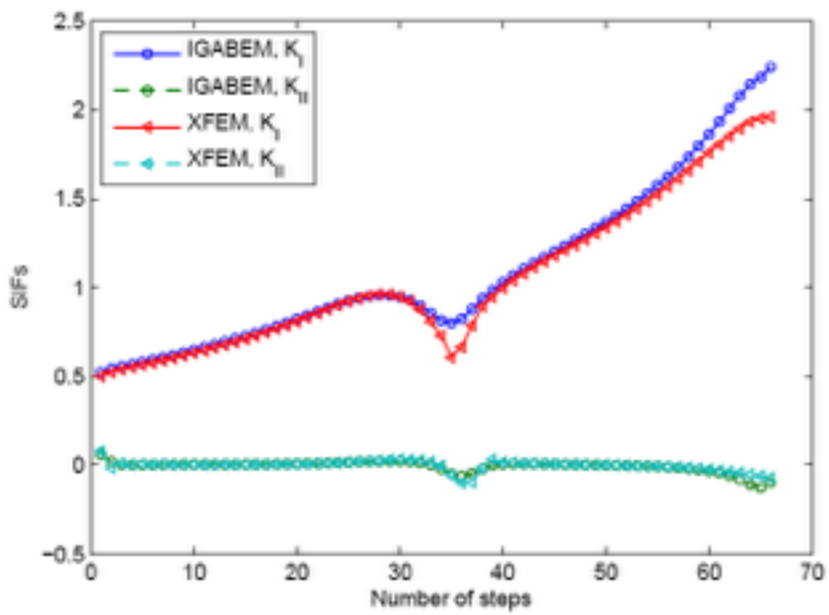
IGABEM, K_I
IGABEM, K_II
XFEM, K_I
XFEM, K_II
SIFs
Number of steps
2.5
2
1.5
1
0.5
0
−0.5
0
10
20
30
40
50
60
70

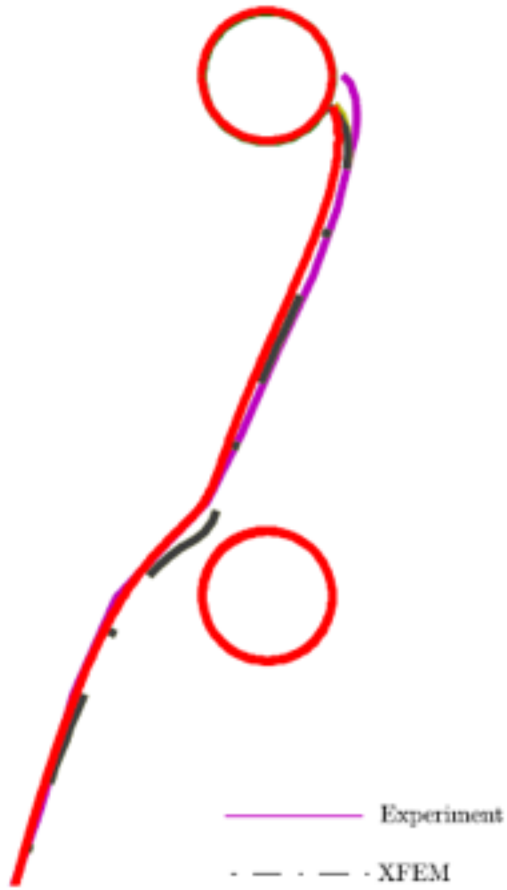
Experiment
XFEM
IGABEM


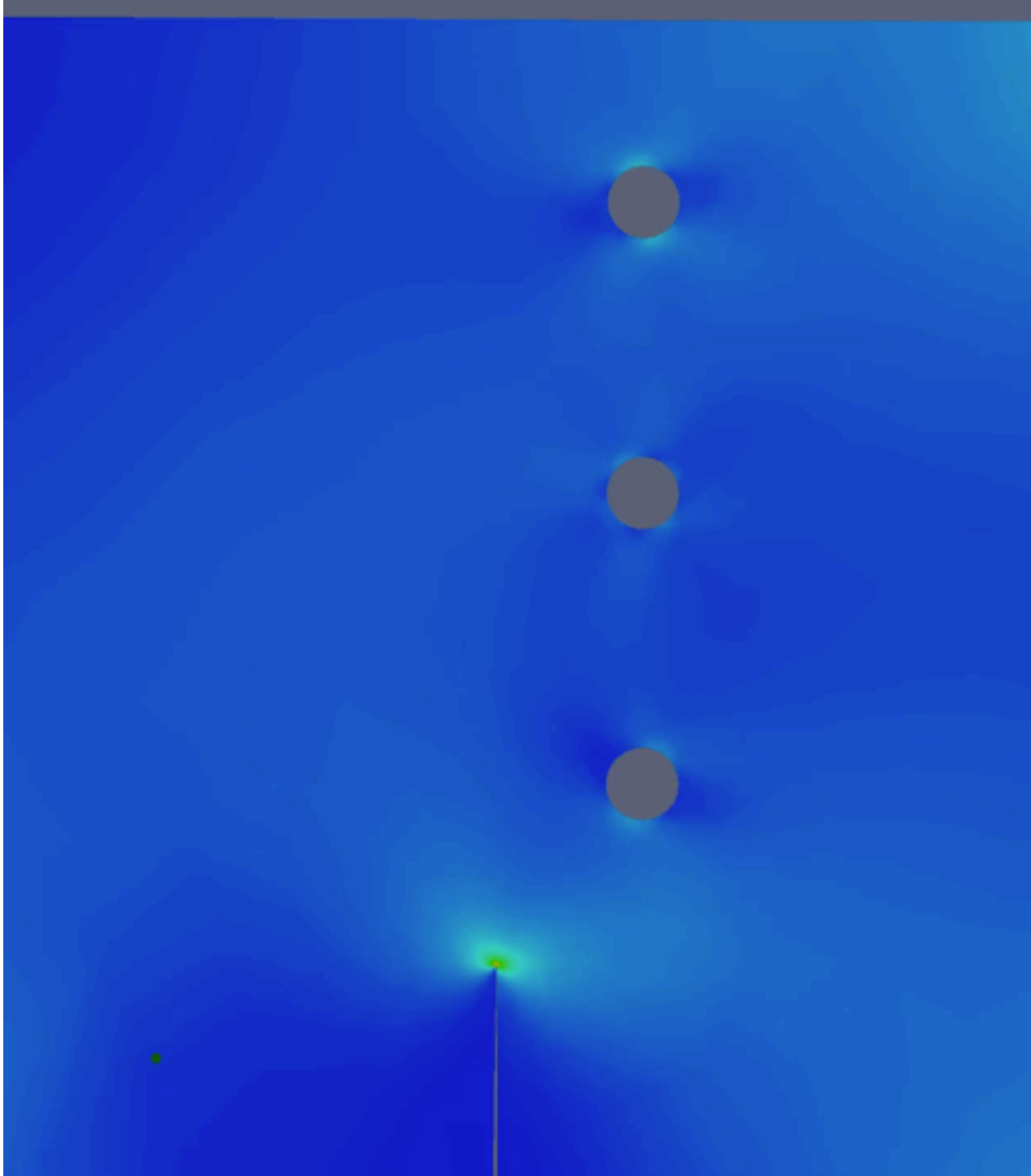

Penny-shaped crack under remote tension

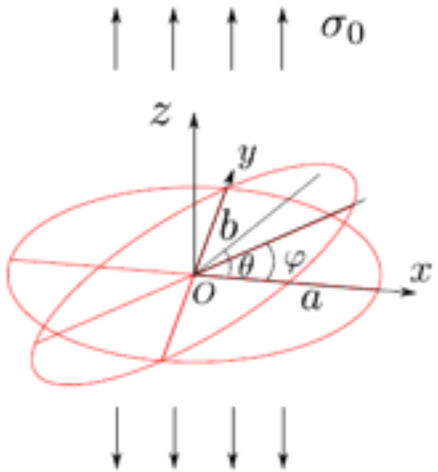

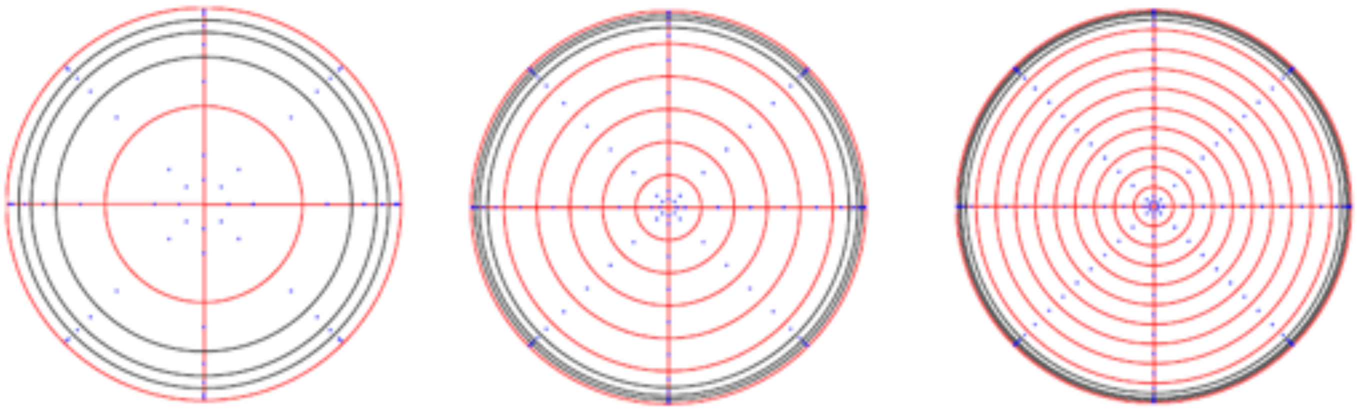

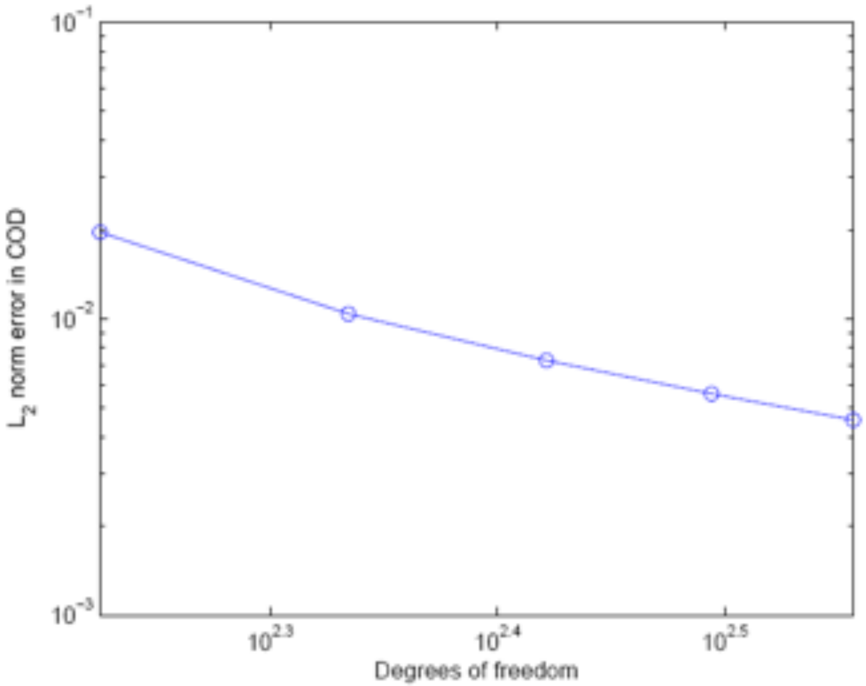

L_2 norm error of COD for penny-shaped crack

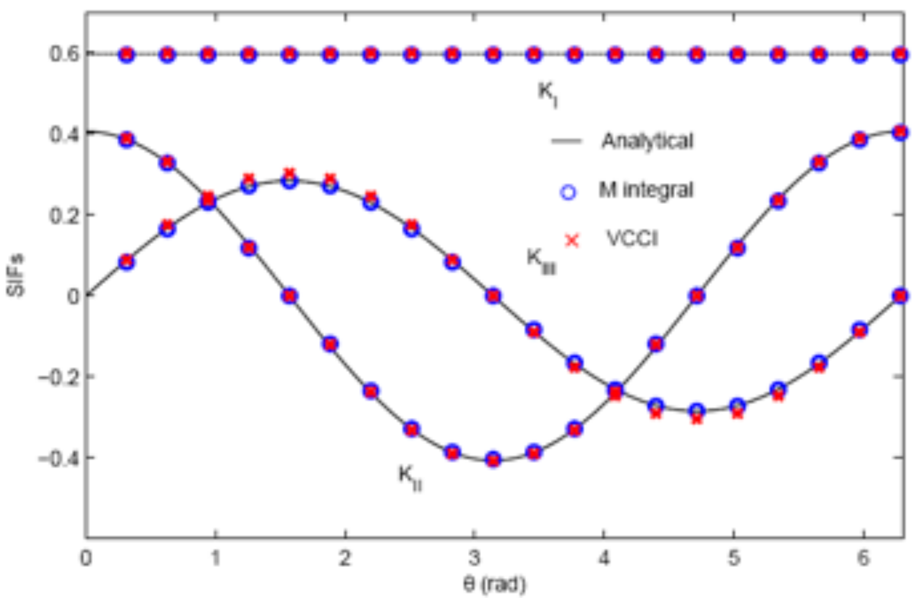

stress intensity factors for penny crack with $\varphi = \pi/6$

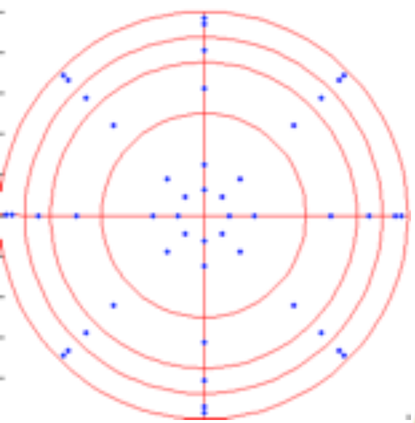

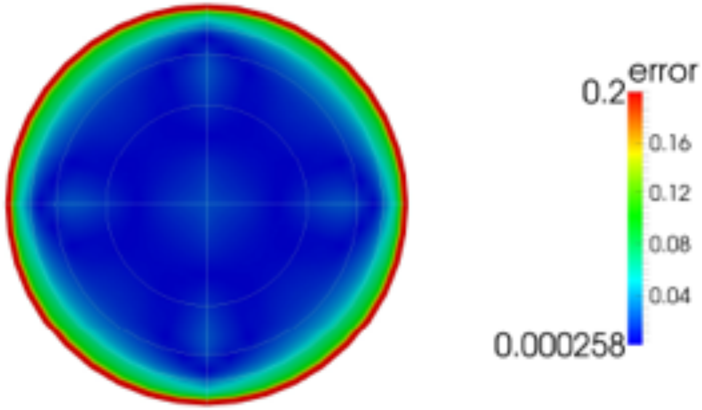

(a) original SST, ngp_s=30, e_{L_2} =3.344418e-2

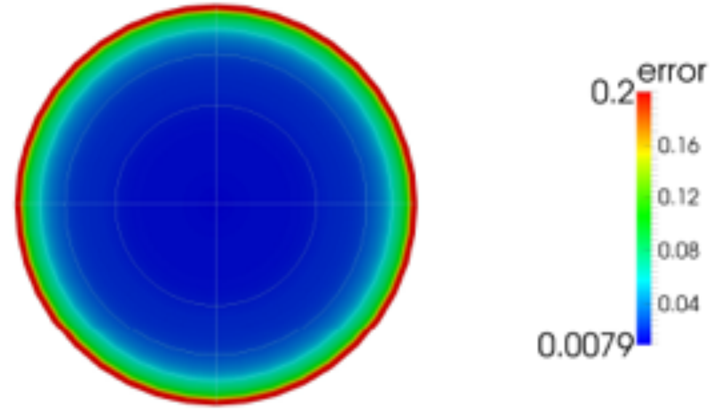

(b) improved SST, ngp_s=30, e_{L_2} =3.844282e-2

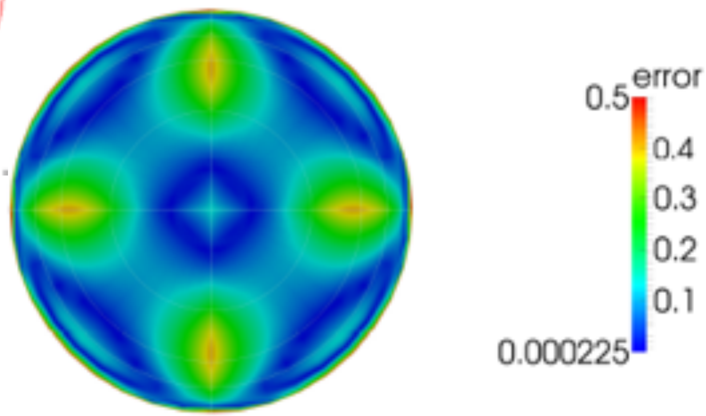

(c) original SST, ngp_s=18, e_{L_2} =1.467716e-1

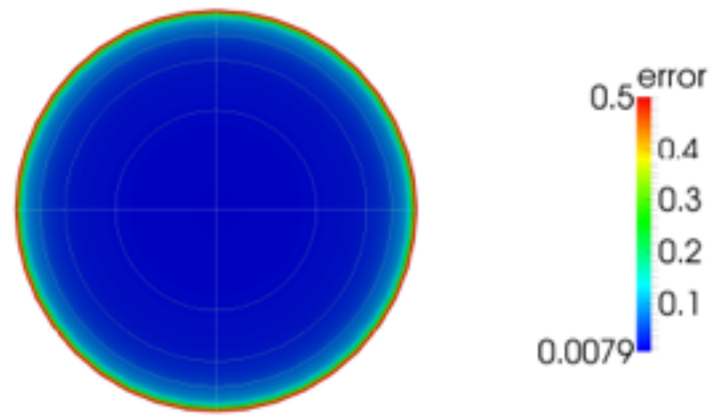

(d) improved SST, ngp_s=18, e_{L_2}=3.844282e-2

Figure 5: Error in crack opening displacement for penny crack

Penny crack under remote tension (embeded crack)

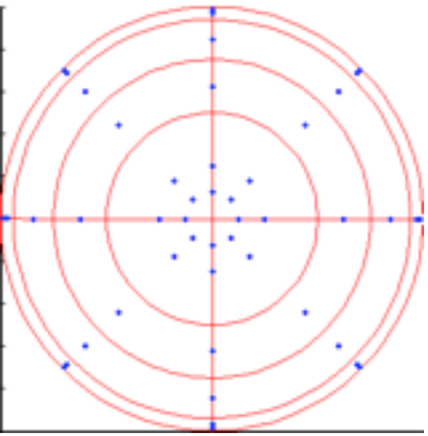

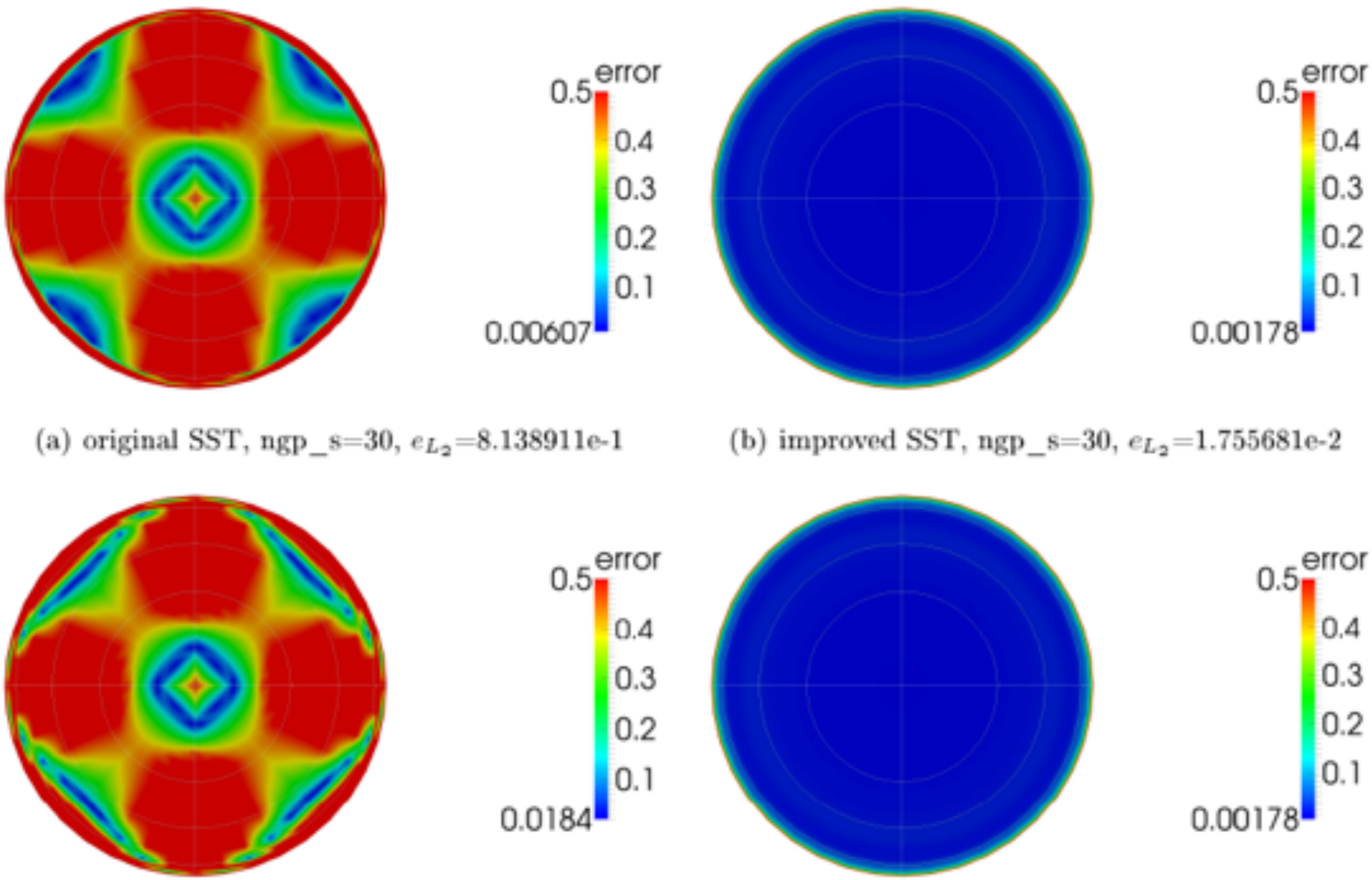

(a) original SST, ngp_s=30, e_{L_2}=8.138911e-1 (b) improved SST, ngp_s=30, e_{L_2}=1.755681e-2

(c) original SST, ngp_s=18, e_{L_2}=7.110011e-1 (d) improved SST, ngp_s=18, e_{L_2}=1.755679e-002

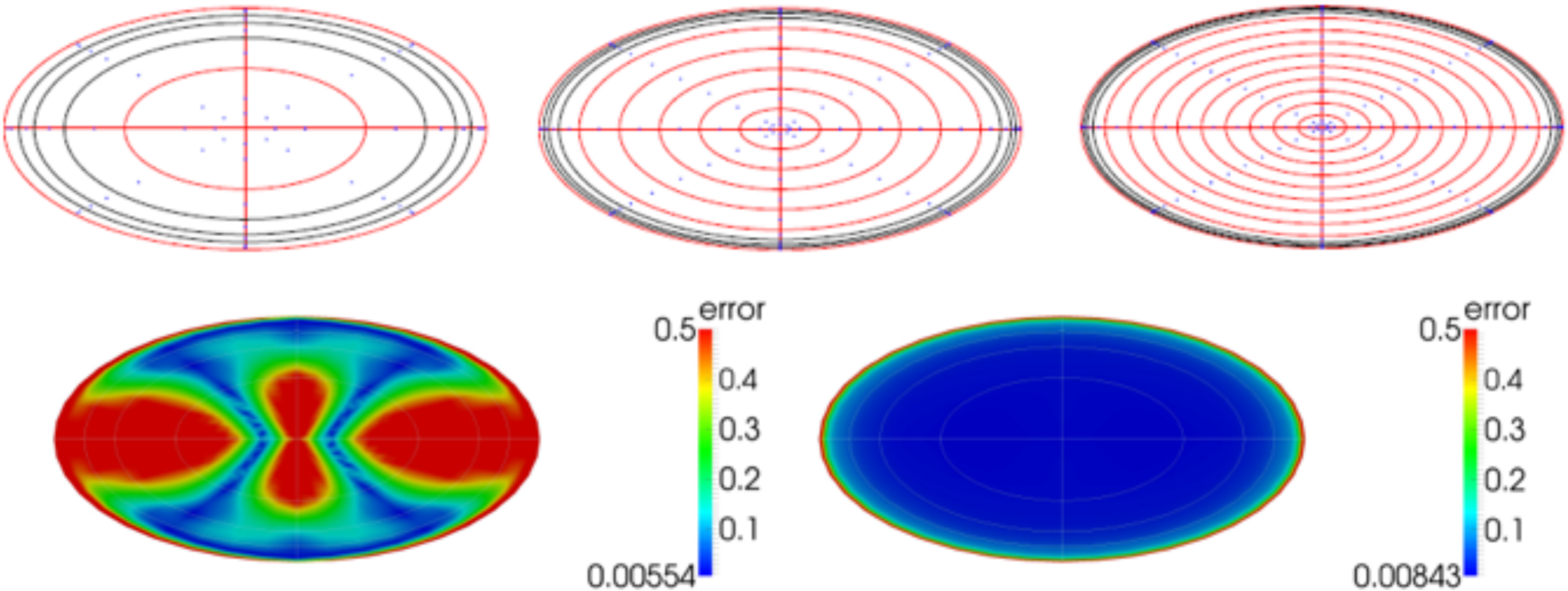

(a) original SST, ngp_s=18, e_{L_2}=4.603473e-1 (b) improved SST, ngp_s=18, e_{L_2}=3.798002e-2

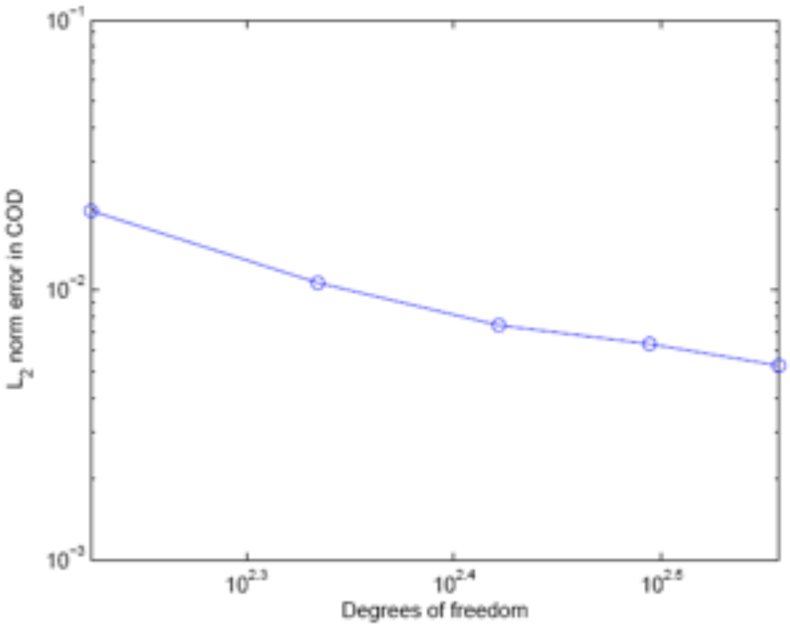

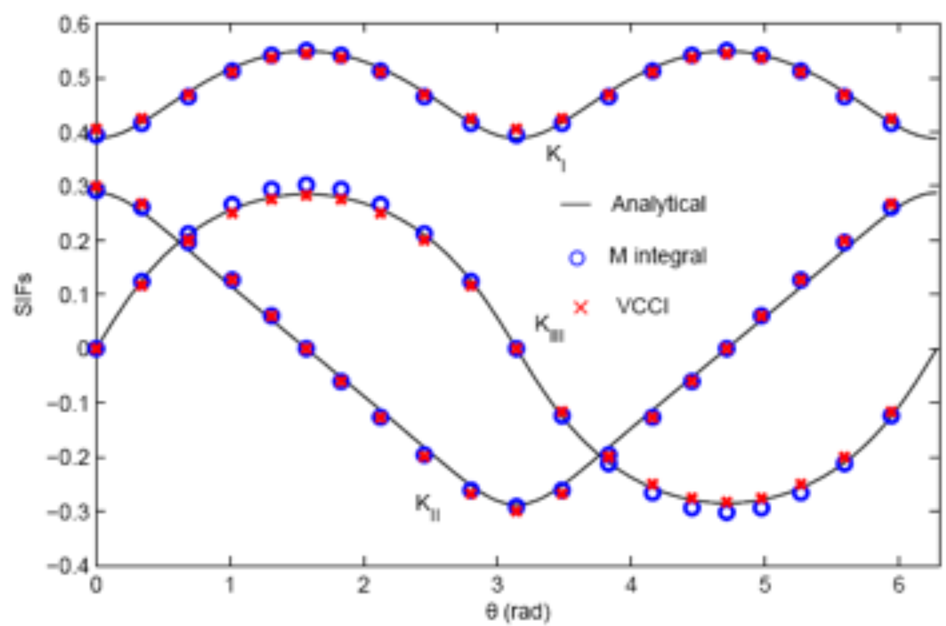

NURBS-represented crack growth algorithm

- **Fatigue fracture: Paris law**

$$\frac{\mathrm{d}a}{\mathrm{d}N} = C(\Delta K)^m$$

$$\Delta a^i = C(\Delta K^i_{eq})^m \frac{\Delta a^{max}}{C(\Delta K^{max}_{eq})} = \Delta a^{max} \left(\frac{\Delta K^i_{eq}}{\Delta^{max}_{eq}}\right)^m$$

Algorithm 1 Crack front updating algorithm

Data: old crack front curve $\mathbb{C}(\xi)$; sample points M_j; new positions of sample points M'_j
Result: new crack front curve that passes through all M'_j

$t = 0$;
$tol = 1.e-4$;
$e_{j,0} = \overrightarrow{M_{j,0}M'_j}$;
while $\|\mathbf{e}_t\| > tol$ **do**
  $t = t + 1$;
  $m_{i,t} = \frac{1}{N}\sum_{j=0}^{N-1} f_{ij} e_{j,t-1}$;
  $P_{i,t} = P_{i,t-1} + m_{i,t}$;
  $e_{j,t} = e_{j,t-1} - \frac{1}{N}\sum_{k=0}^{N-1}\langle \mathbf{R}_j, \mathbf{f}_k\rangle e_{k,t-1}$;
end

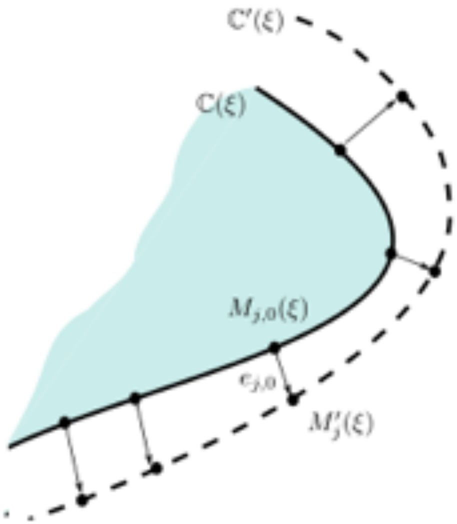

Numerical example of horizontal penny crack growth (first 10 steps)

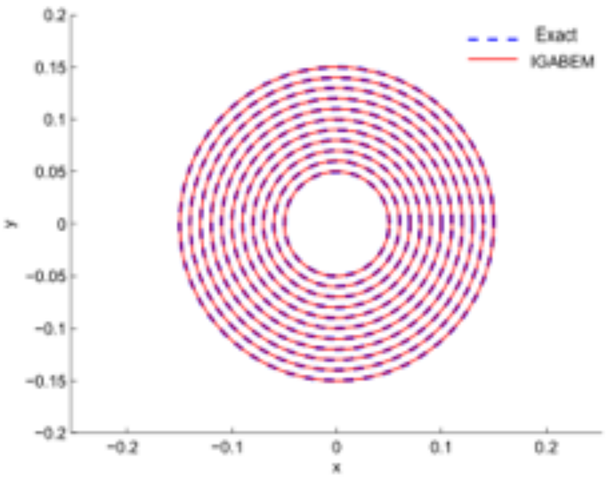

(a) IGABEM, $m = 2.1$

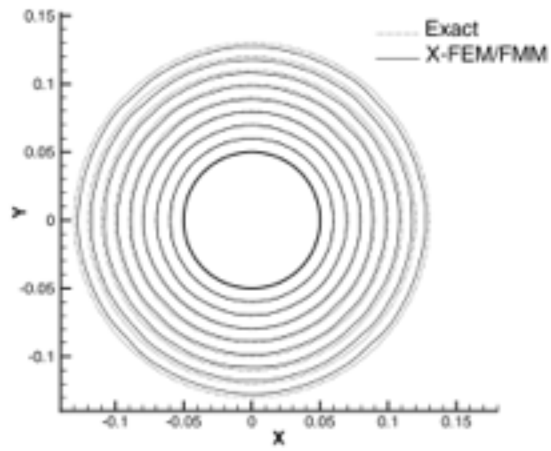

(b) XFEM/FMM, $m = 2.1$, Sukumar *et al* 2003

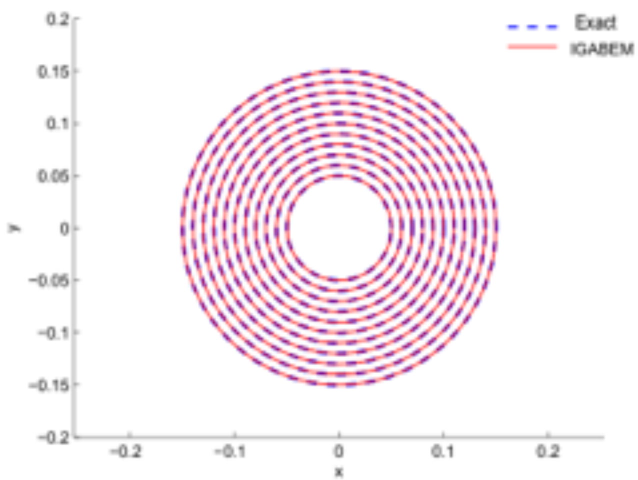

(c) IGABEM, $m = 5$

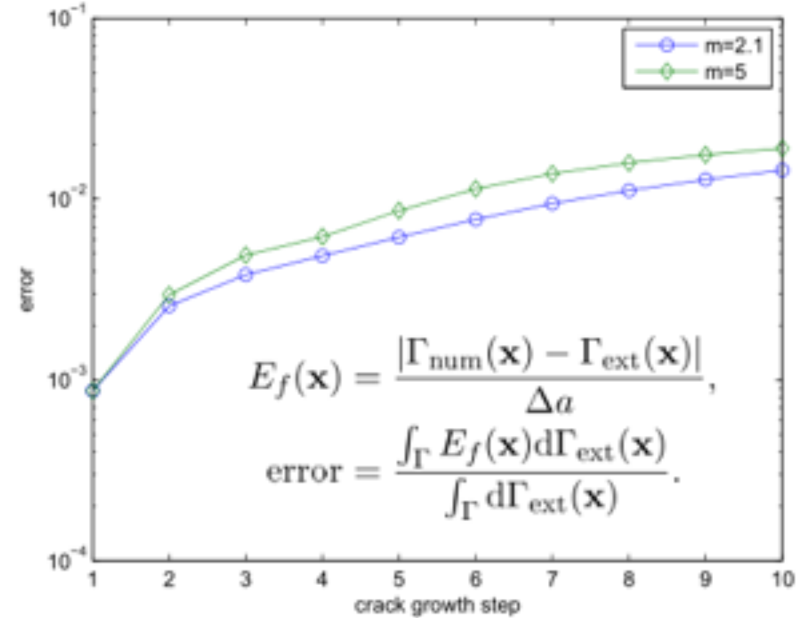

Relative error of the crack front for in each crack growth step by IGABEM

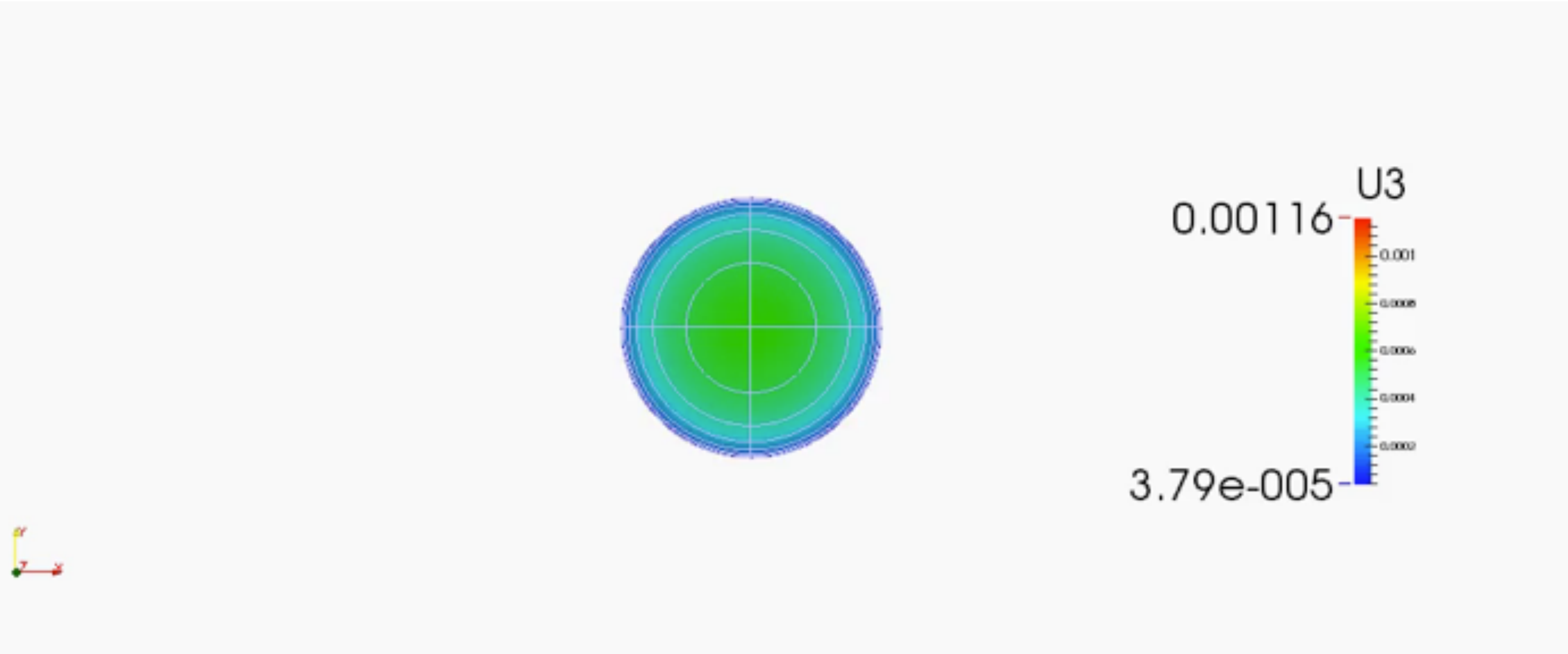
U3
0.00116
0.001
0.0008
0.0006
0.0004
0.0002
3.79e-005

Numerical example of inclined elliptical crack growth (first 10 steps)

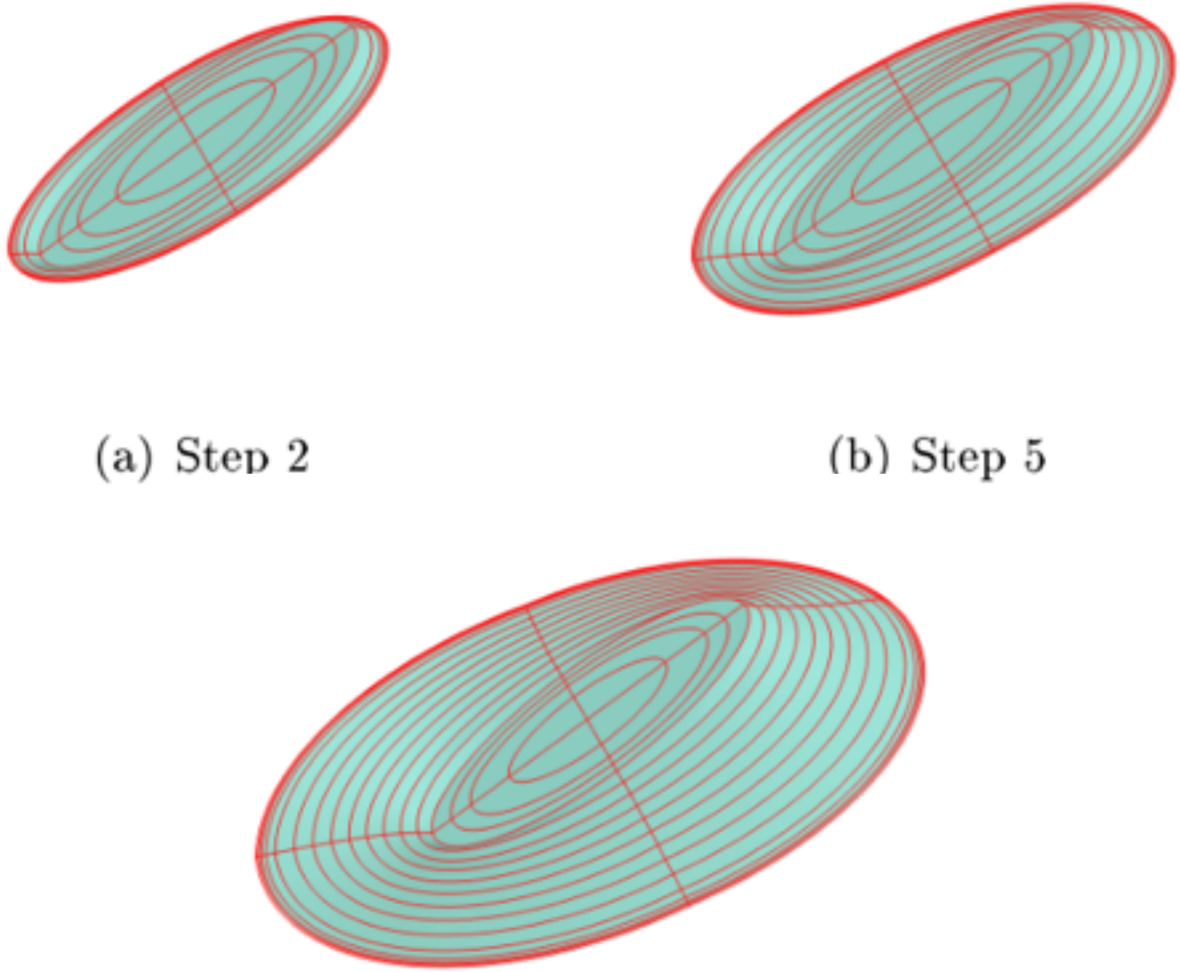

(a) Step 2

(b) Step 5

(c) Step 10

Fatigue crack growth simulation of an elliptical crack

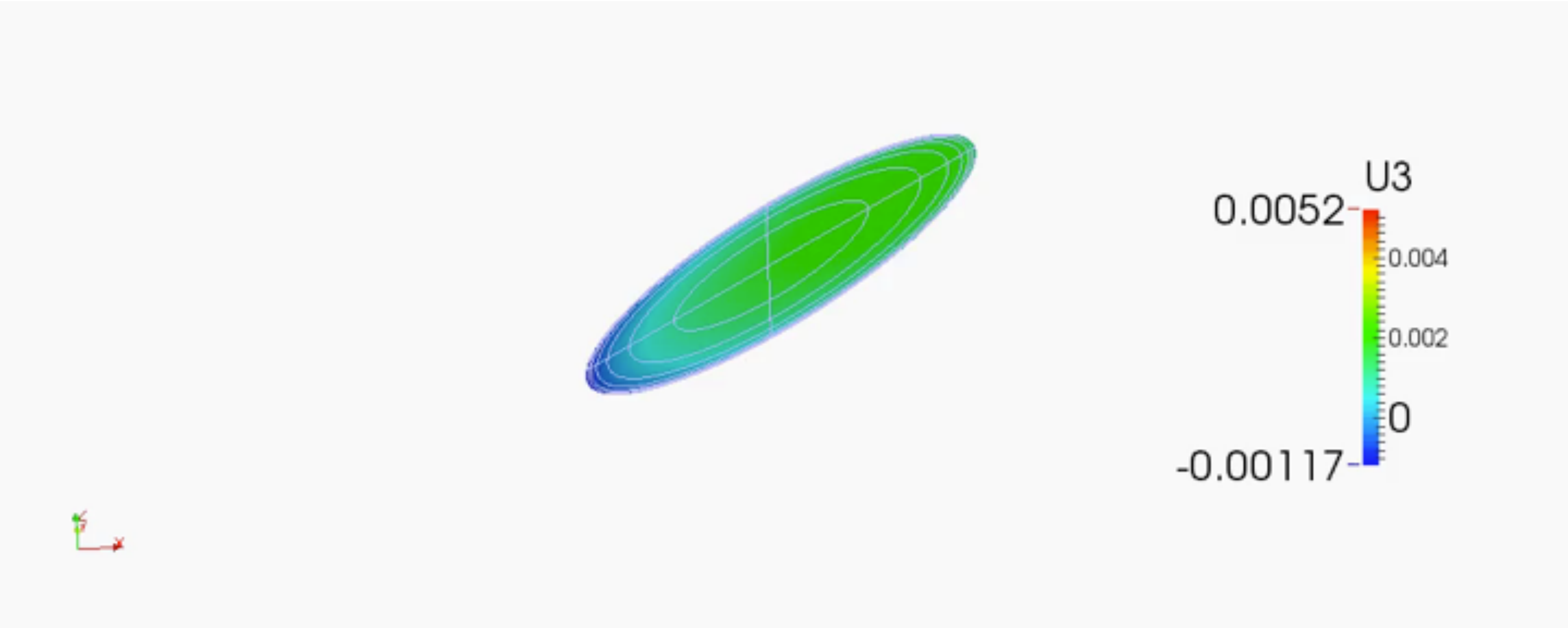
U3
0.0052
0.004
0.002
0
-0.00117

Modeling techniques for surface breaking cracks

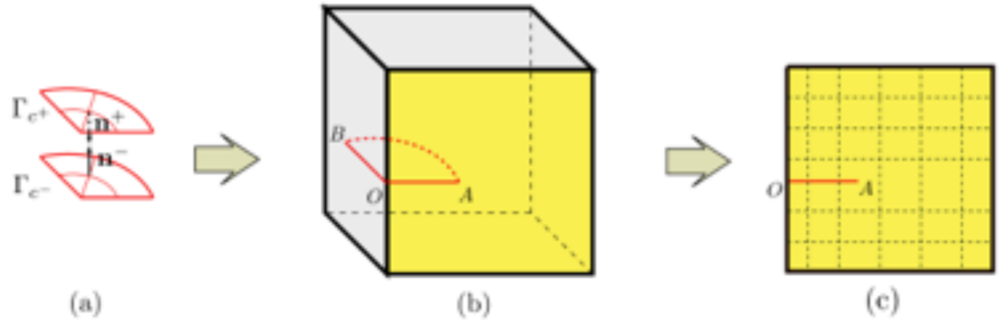

•Surface discontinuity is introduced

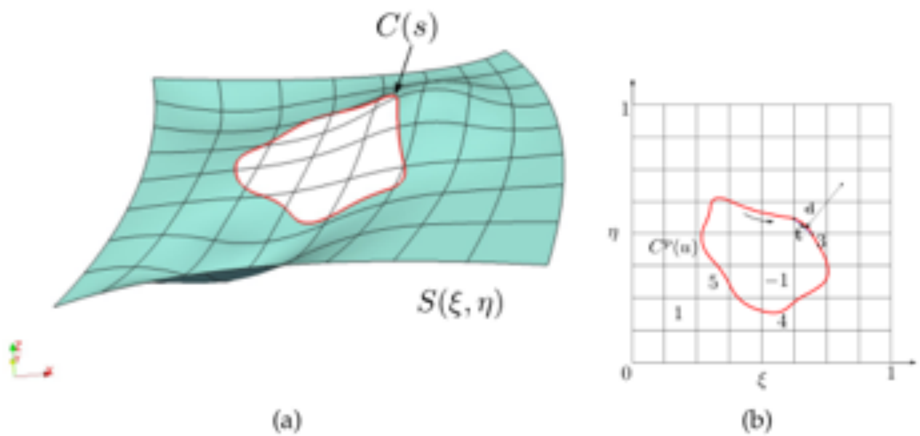

•Trimmed NURBS technique

•Crack → trimming curve

•Phantom node method

$$\mathbf{u}^+(\mathbf{x}) = \sum_{j}^{N^e} \mathbf{R}_j(\mathbf{x})\mathbf{d}_j, \quad \mathbf{x} \in S_e^+,$$

$$\mathbf{u}^-(\mathbf{x}) = \sum_{k}^{N^e} \mathbf{R}_k(\mathbf{x})\mathbf{d}_k, \quad \mathbf{x} \in S_e^-$$

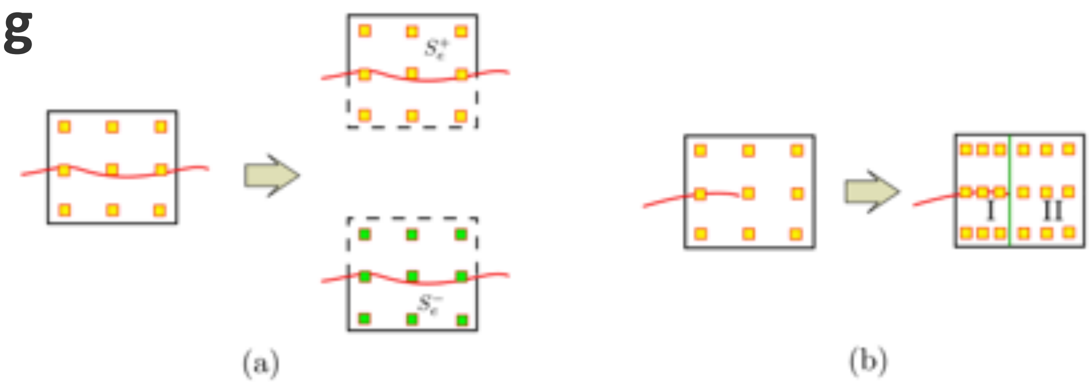

Example of surface breaking cracks: edge crack under uniform tension

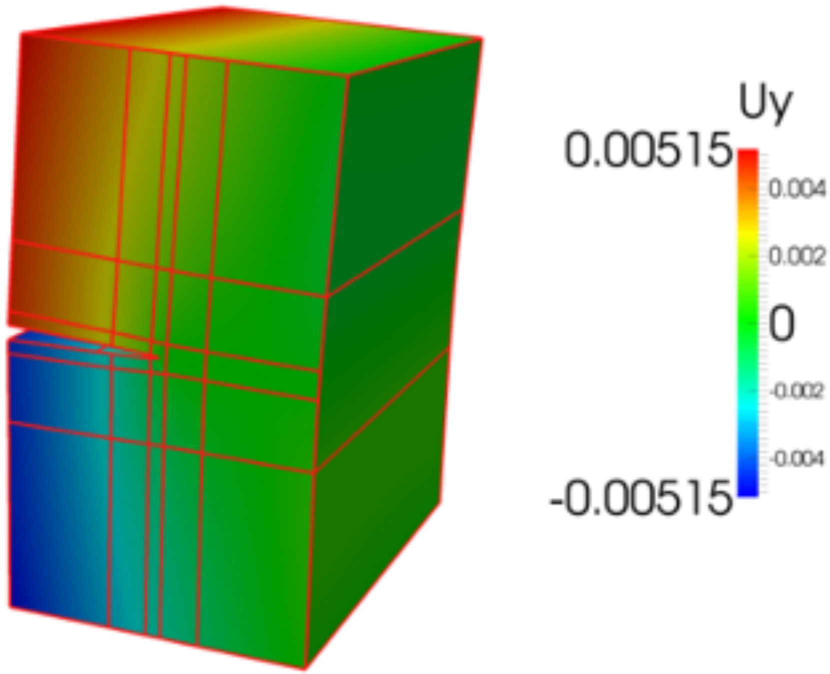

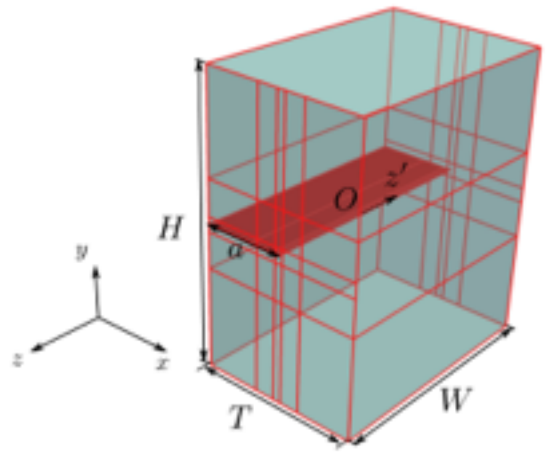

$E = 1.0e3$, $\nu = 0.3$
top face:
$t_x = t_z = 0$, $t_y = 1$
bottom face:
$t_x = t_z = 0, t_y = -1$

$T/a = 2$

$W/a = 3$

$H/a = 3.5$

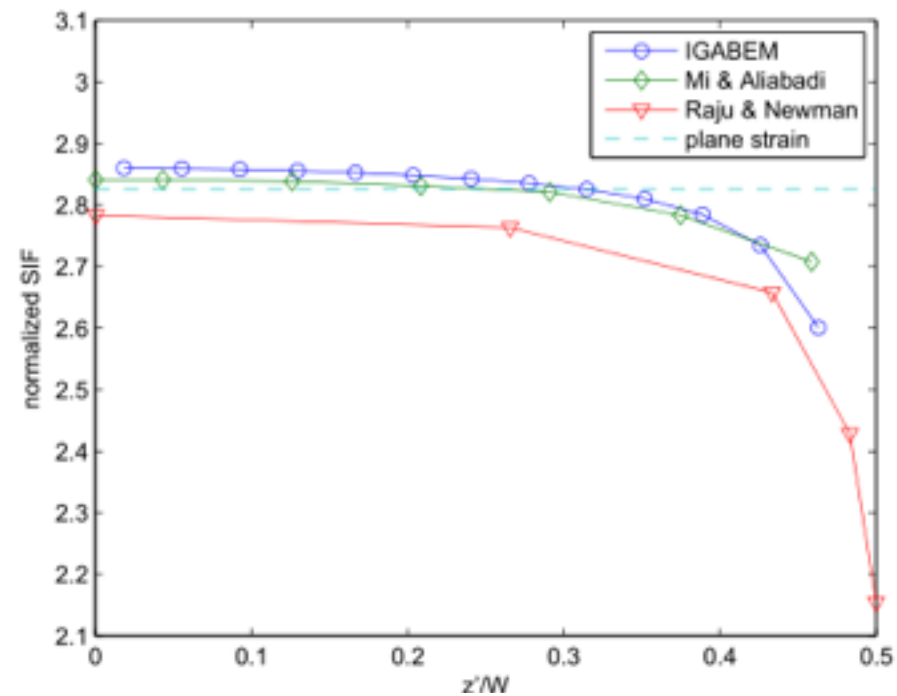

Relative error in $K_I/\sqrt{\pi a}$

- PUBLICATIONS
  - http://www.itn-insist.com/fileadmin/publications/2014/peng2.pdf
  - http://www.itn-insist.com/fileadmin/publications/2014/Peng1.pdf
  - https://orbilu.uni.lu/bitstream/10993/17098/1/dual_igabem5-space.pdf
  - https://publications.uni.lu/bitstream/10993/17100/1/dual_igabem5space.pdf
  - http://orbilu.uni.lu/bitstream/10993/22289/1/igabem3d_01doubleSpace.pdf
  - https://orbilu.uni.lu/handle/10993/26421
  - https://publications.uni.lu/handle/10993/21017
  - https://publications.uni.lu/bitstream/10993/17099/1/abstract_acomen.pdf
  - http://legato-team.eu/category/projects/mesh-burden/
  - http://orbilu.uni.lu/handle/10993/17091

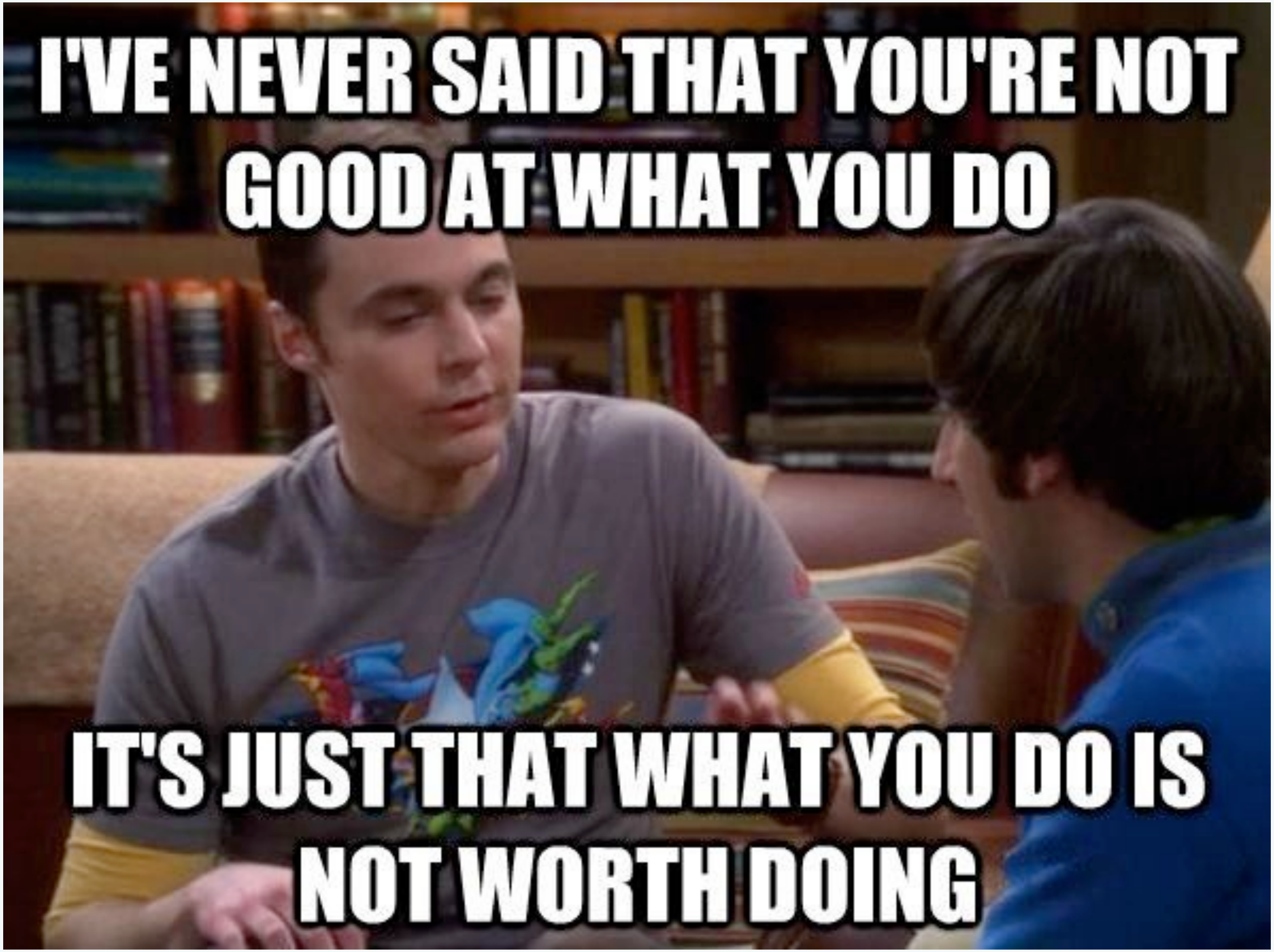
I'VE NEVER SAID THAT YOU'RE NOT GOOD AT WHAT YOU DO
IT'S JUST THAT WHAT YOU DO IS NOT WORTH DOING

Difficulties in 3D application

➢How far we are to non-trivial 3D work pieces

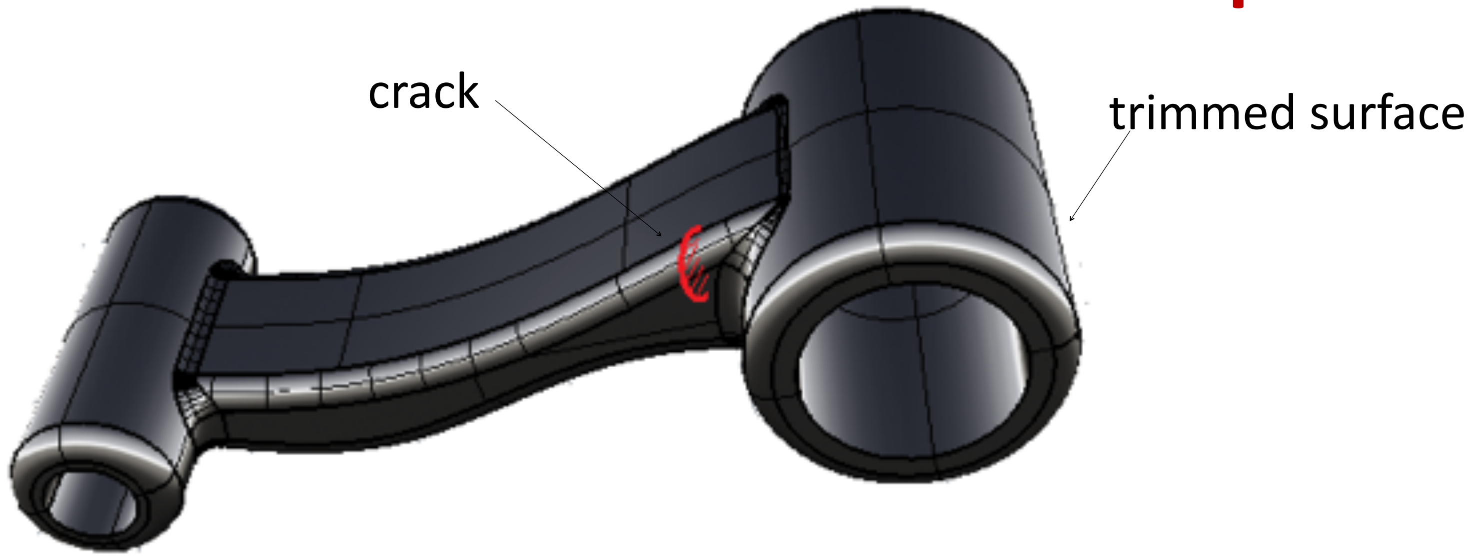

Input from Rhino, ProE, UG,…

CAD model (trimmed NURBS) → Analysis-suitable Splines → Stress analysis

trimmed multiple patches & T-Splines

Analysis-suitable Splines ↓ crack evolution description → fracture analysis

CARDIFF UNIVERSITY
PRIFYSGOL CAERDYDD

Part II. Reducing model complexity

IMAM
Institute of Mechanics & Advanced Materials

Motivation: multiscale fracture of engineering structures and materials

Practical early-stage design simulations (interactive)

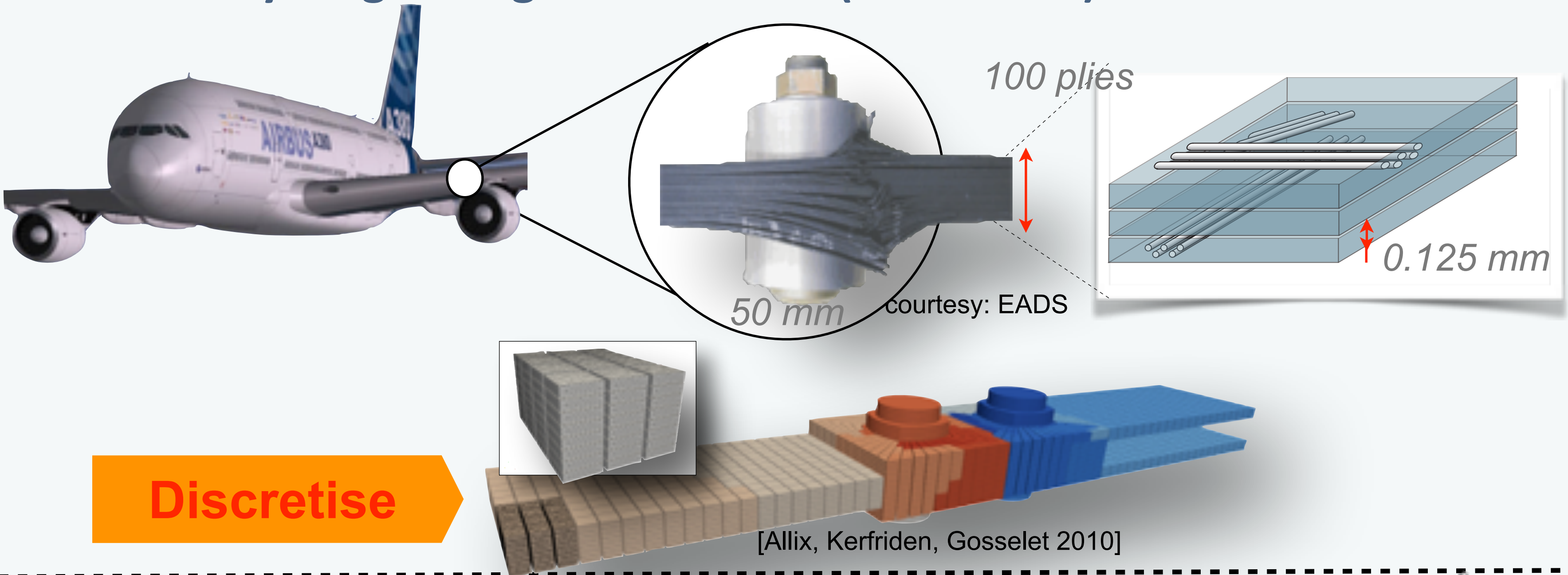

Surgical simulation

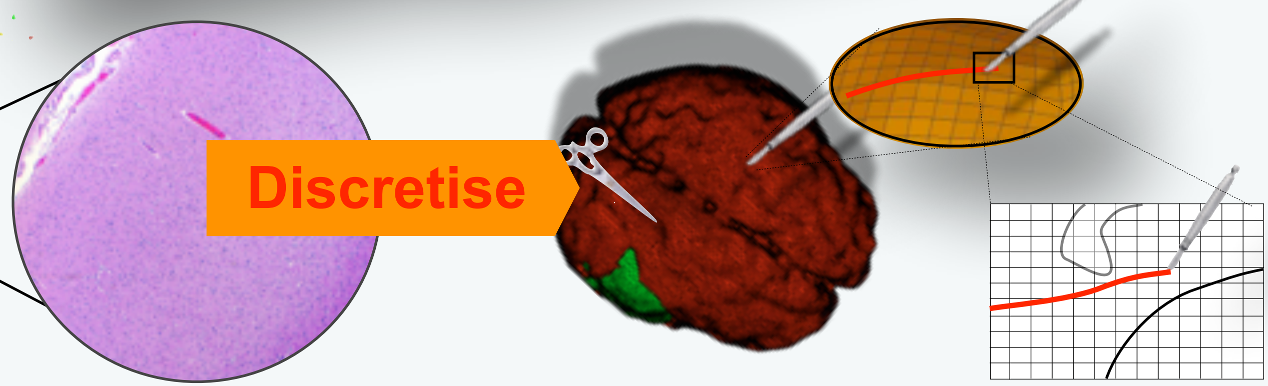

- Reduce the problem size while controlling the error (in QoI) when solving very large (multiscale) mechanics problems

Summary (1/2)

Finite element a priori error analysis

Rough solutions -> increasing polynomial order has no effect

-> enrichment of the basis enables to *capture* the exact solution

-> generalized *reproducing condition*

Interfaces

Lower scales -> higher discontinuities -> interfaces

Model interfaces by **separating** or **linking** geometry and approximation

Implicit boundaries, PUFEM, XFEM, meshfree…

IGA or Geometry-Induced ApproximatioNs (GIAN)

Summary (2/2)

Multiscale approaches to fracture

Enrichment (PUFEM, GFEM, XFEM…)

Concurrent

Information-passing/semi-concurrent

Semi-concurrent methods fail in softening (RVE???)

Hybrid methods enable to post-peak simulations

Today and tomorrow

Algebraic model order reduction

Quasi-continuum method for dissipative systems

Bridging the homogenisation-model order reduction gap

Linearisation of multi-scale problems

Model order reduction to reduce FE^2 problems

Advanced early-stage design simulations

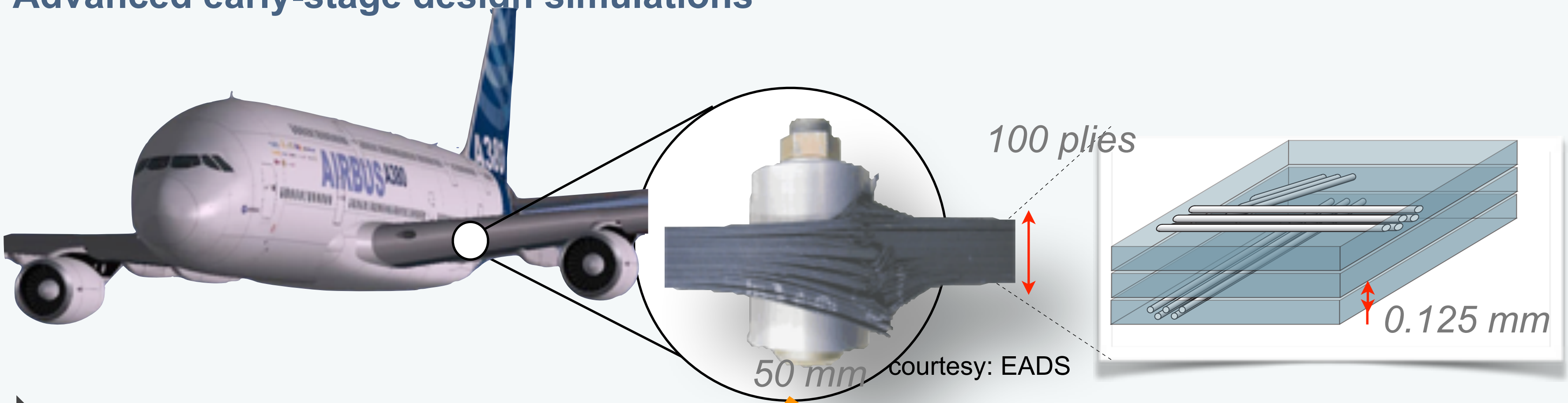

- Large gradients
- Explicit mesostructure description

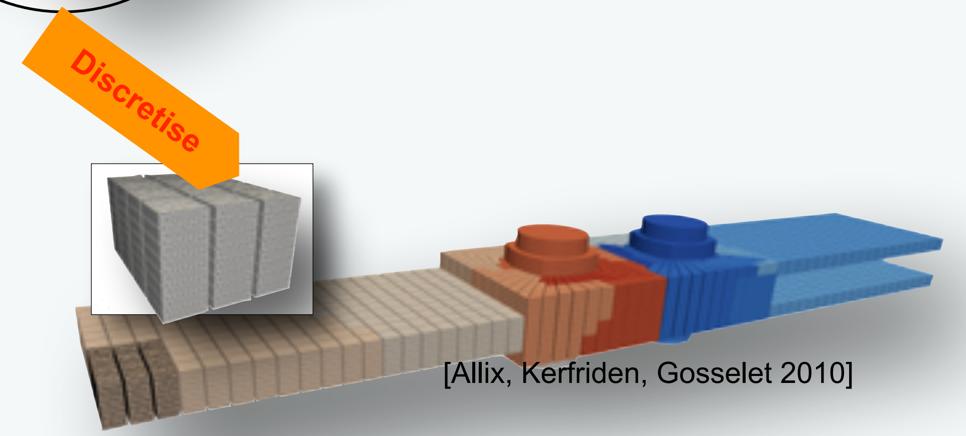

- Large number of parametric studies, e.g. load cases
- Account for the variability of the material

➡ Models and discretisations must be reduced

Ways to reduce the models

- Homogenisation (FE^2, etc.) - Hierarchical
- Concurrent and hybrid (bridging domain, ARLEQUIN, etc.)
- Enrichment (PUFEM, XFEM, GFEM)
- Model reduction (algebraic)

Part II.1. Reduction methods based on homogenisation

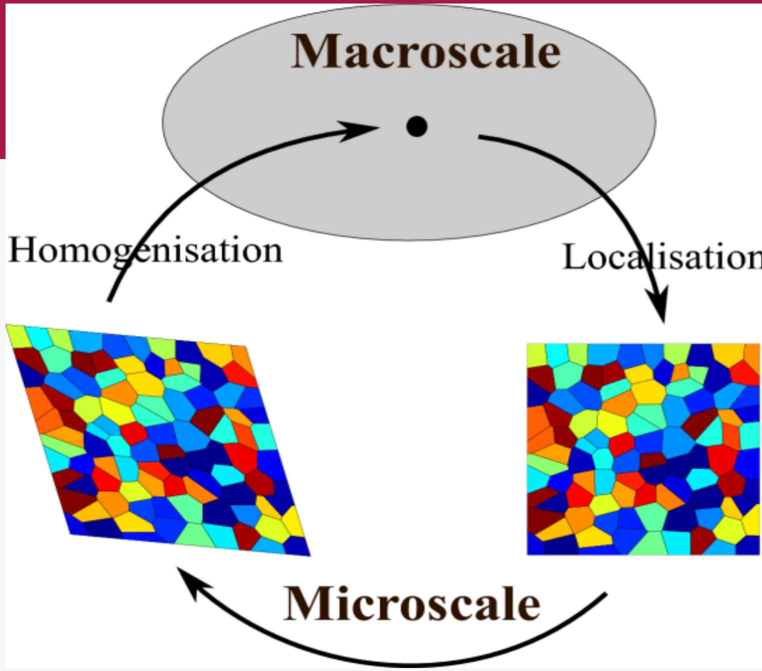

Definition of an RVE

$$l^c \gg l^f \gg l^g$$

Coupling of macroscopic and microscopic levels

The volume averaging theorem is postulated for:

1) Strain tensor:

$$\boldsymbol{\epsilon}^c = \frac{1}{|\Omega(\mathbf{x}^c)|} \int_{\partial\Omega(\mathbf{x}^c)} \mathbf{u}^f \otimes_s \mathbf{n} \, d\Gamma$$

2) Virtual work (Hill-Mandel condition):

$$\boldsymbol{\sigma}^c : \delta\boldsymbol{\epsilon}^c = \frac{1}{|\Omega(\mathbf{x}^c)|} \int_{\partial\Omega(\mathbf{x}^c)} \mathbf{t}^f \cdot \delta\mathbf{u}^f \, d\Gamma$$

3) Stress tensor:

$$\boldsymbol{\sigma}^c = \frac{1}{|\Omega(\mathbf{x}^c)|} \int_{\partial\Omega(\mathbf{x}^c)} \mathbf{t}^f \otimes \mathbf{x}^f \, d\Gamma$$

Hierarchical multi-scale approaches (FE^2)

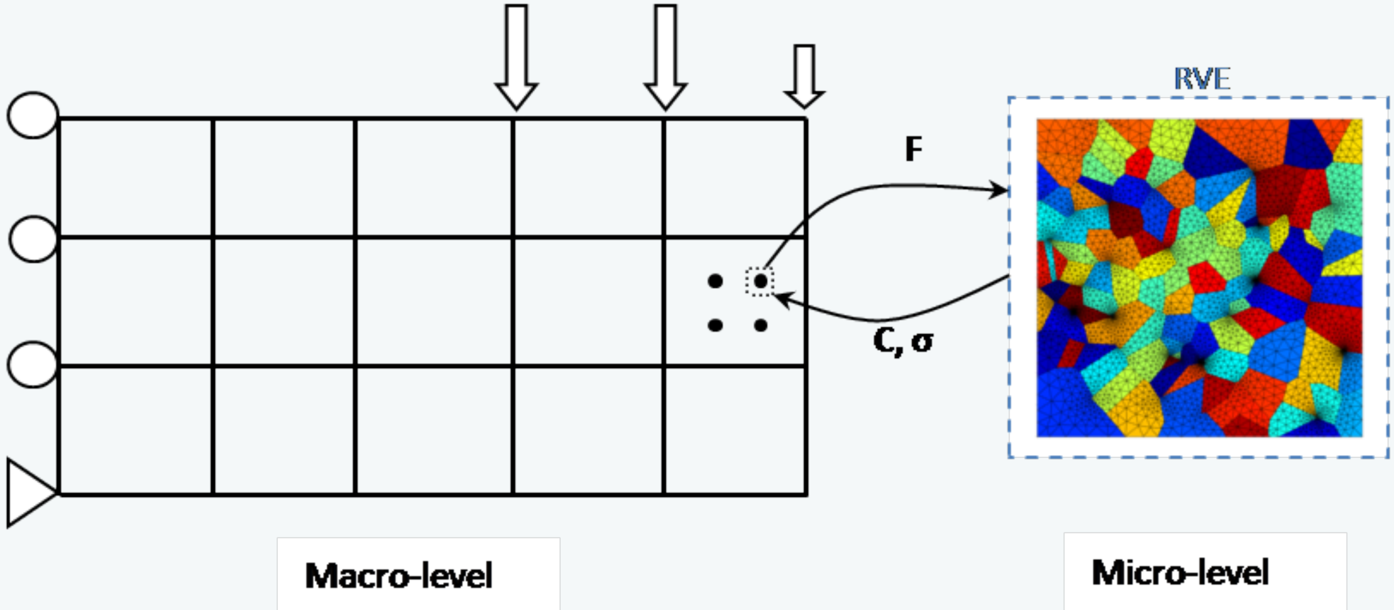

Advantages and abilities:

The macroscopic constitutive law is not required
Non-linear material behaviour can be simulated
Microscale behaviour of material is monitored at each load step

Drawbacks:

In softening regime:

- Lack of scale separation
- Macroscale mesh dependence

bordasS@cardiff.ac.uk, stephane.bordas@alum.northwestern.edu

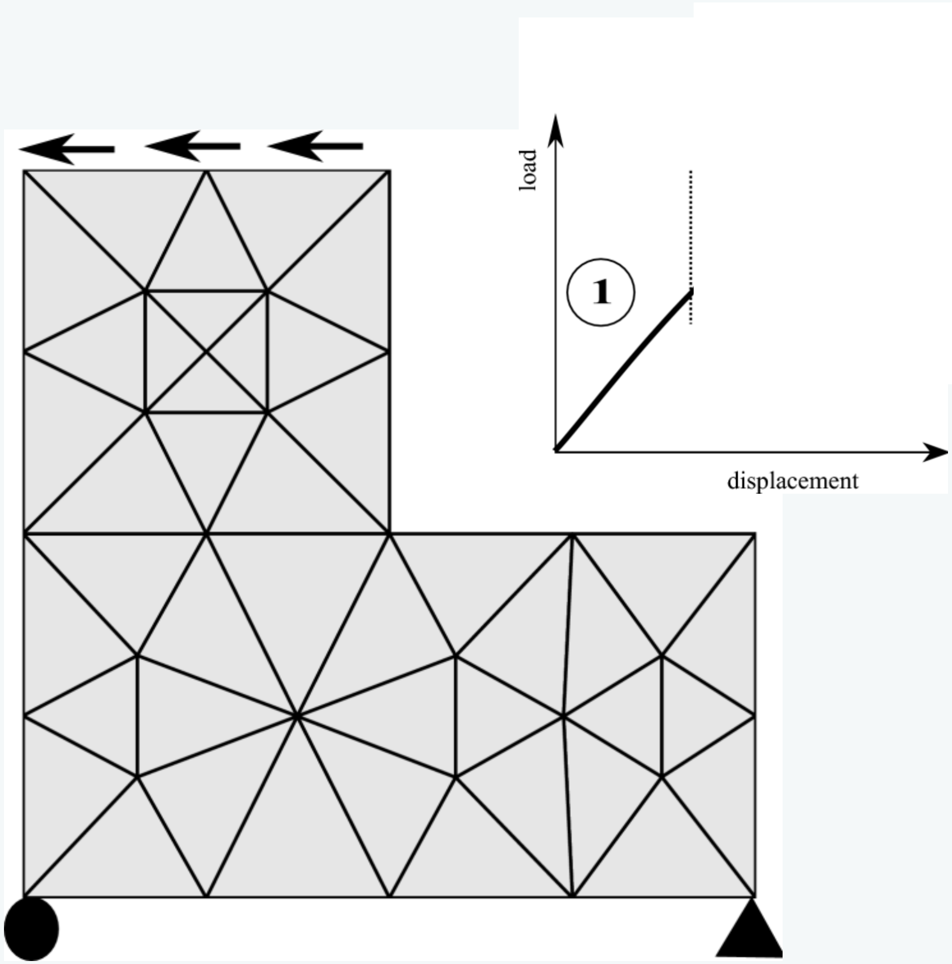
load
1
displacement

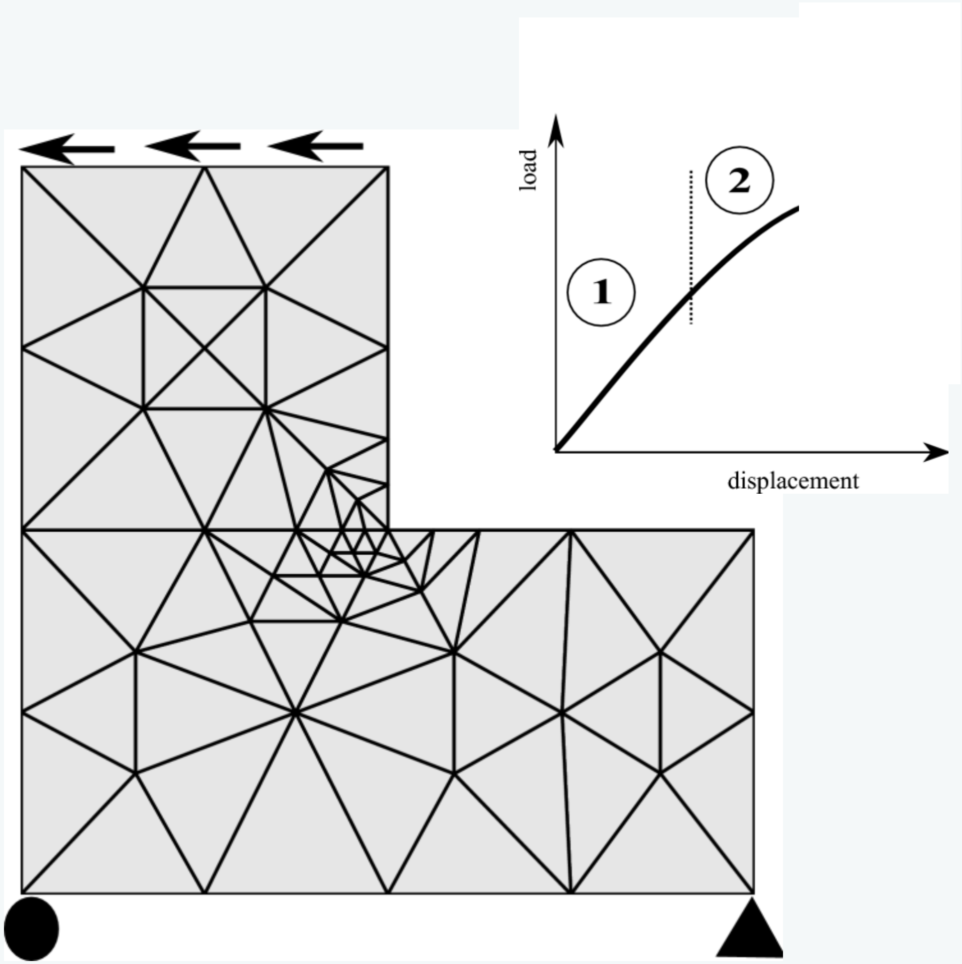
load
2
1
displacement

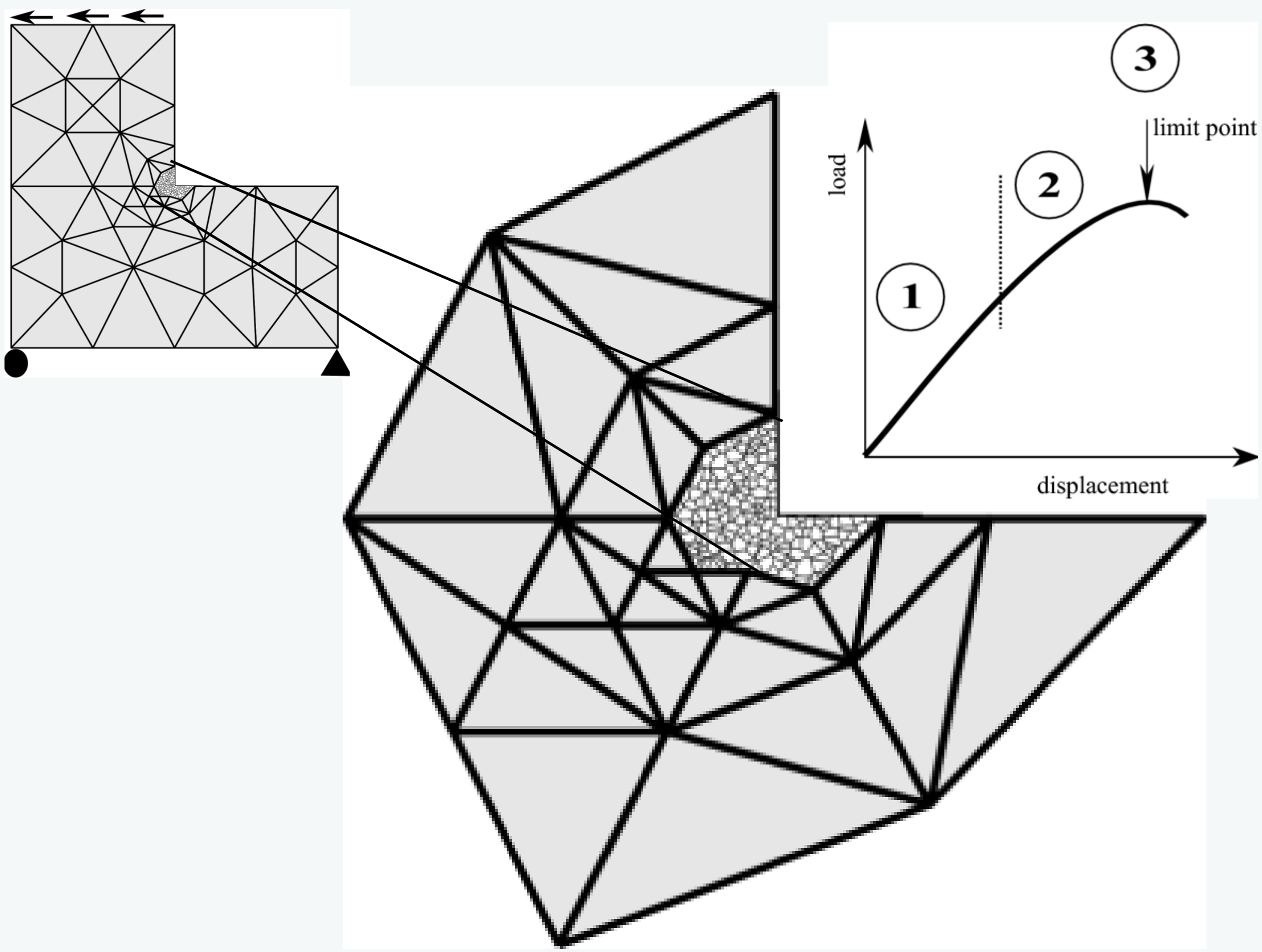

Details in Phil. Magazine, 2015, Akbari, Kerfriden, Bordas

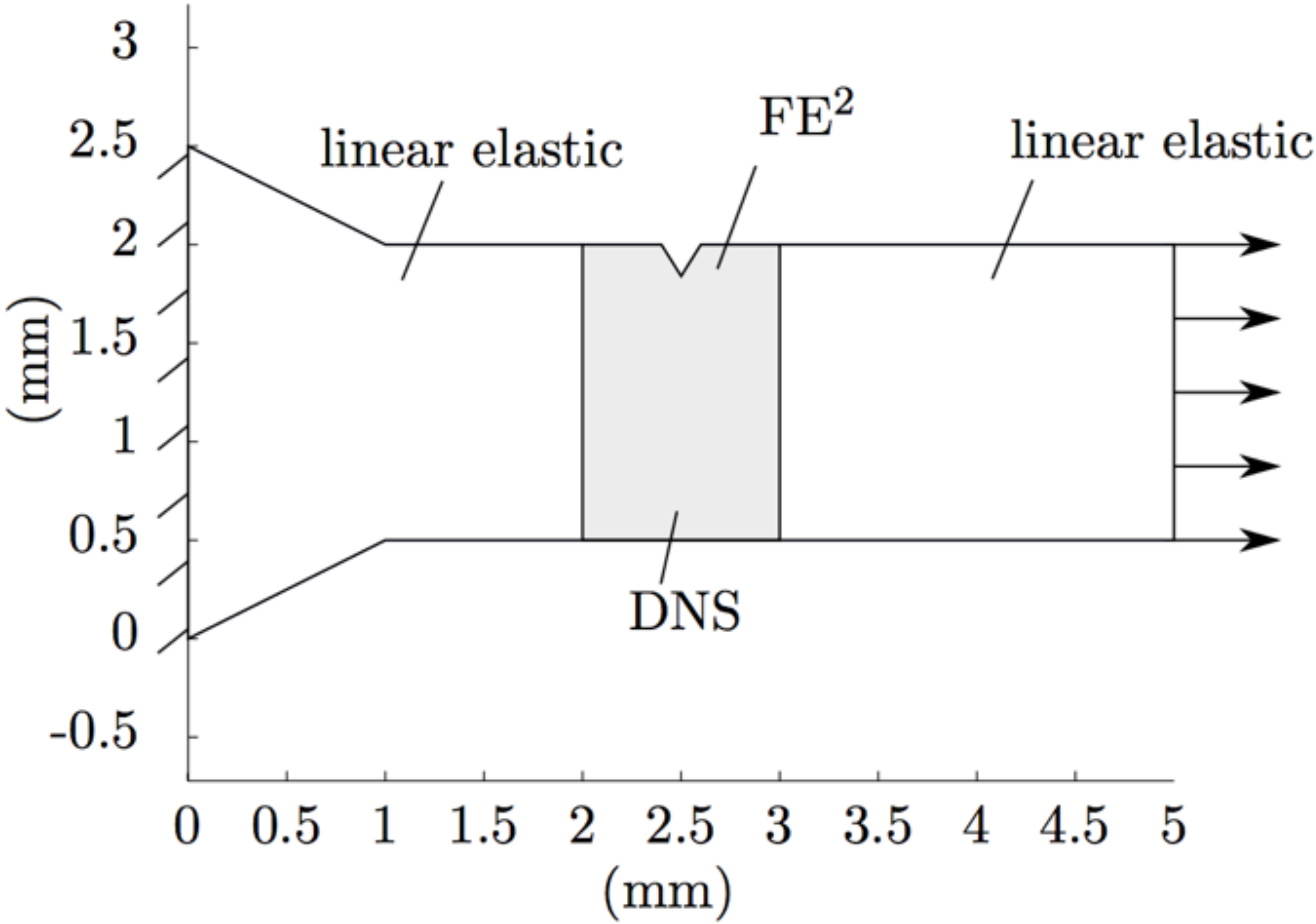

linear elastic
FE^2
linear elastic
DNS
(mm)
(mm)
3
2.5
2
1.5
1
0.5
0
-0.5
0
0.5
1
1.5
2
2.5
3
3.5
4
4.5
5

a)

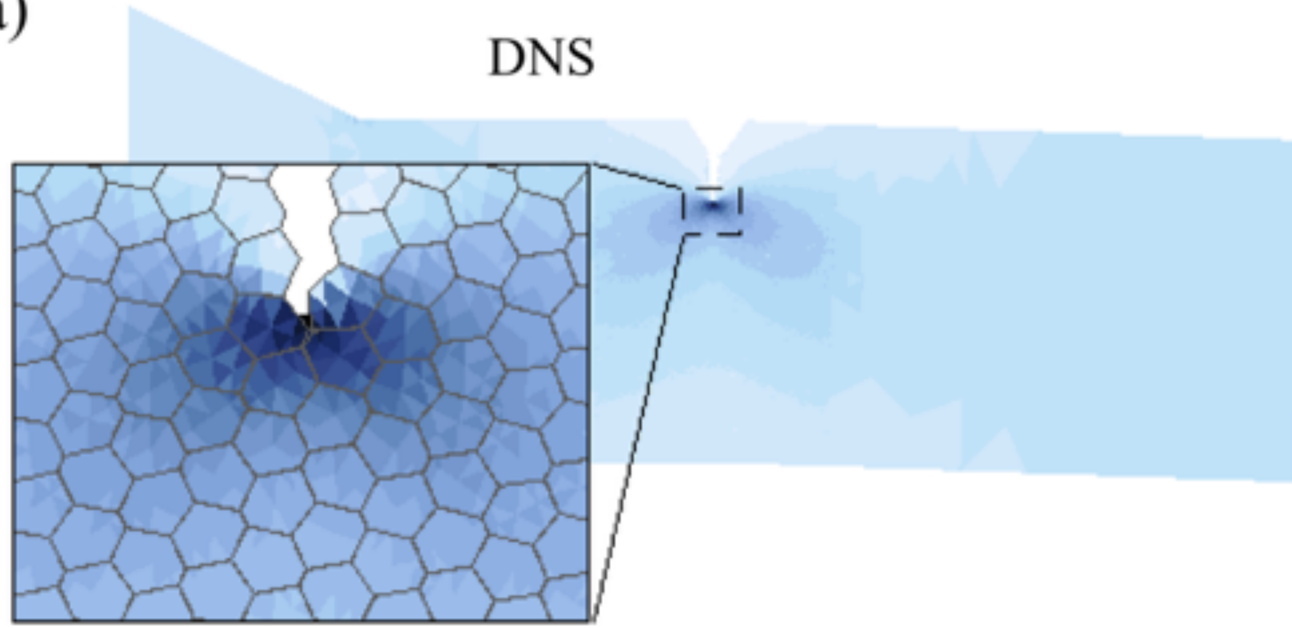

b)

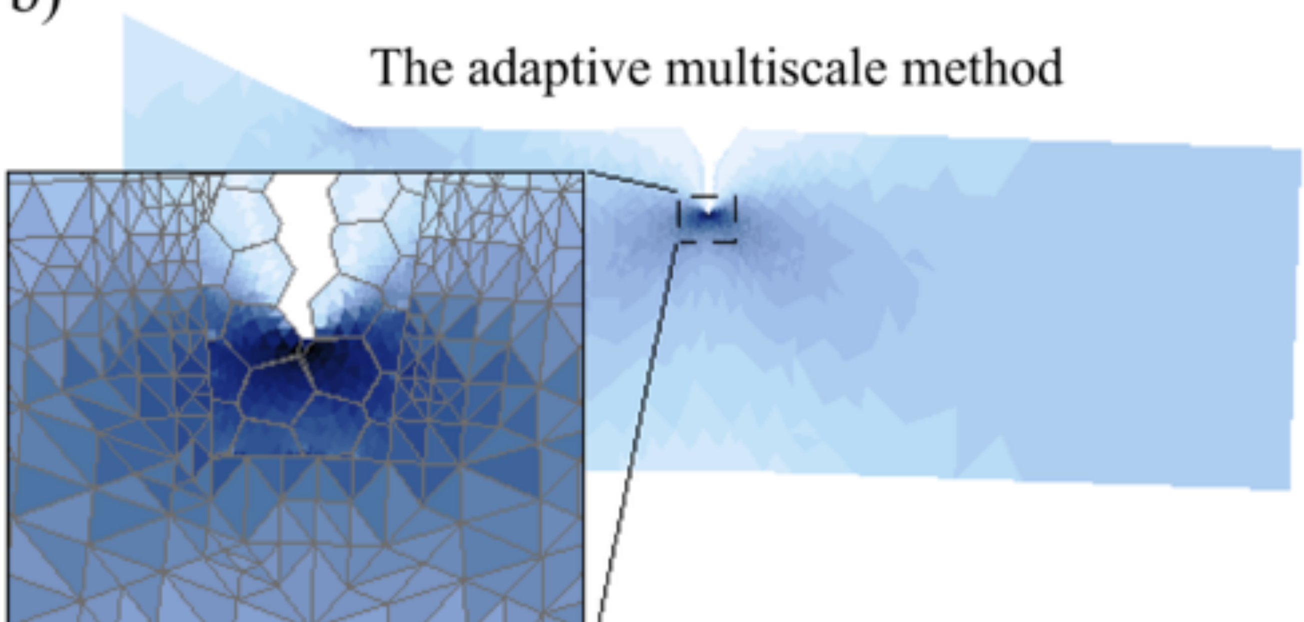

The distribution of strain-gradient sensitivity $L_{\mathcal{V}}||\nabla\nabla\mathbf{u}^c||_e$

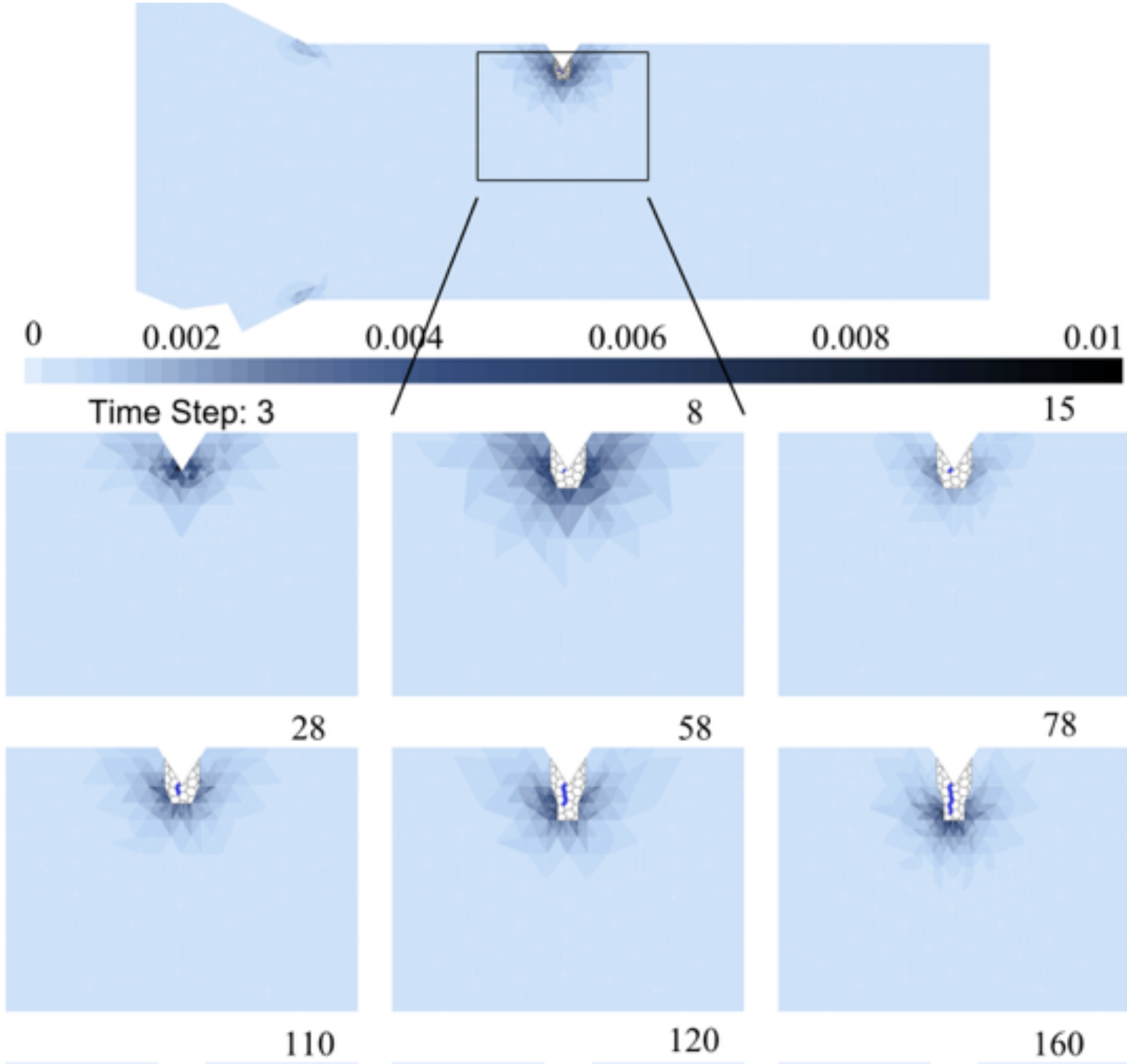

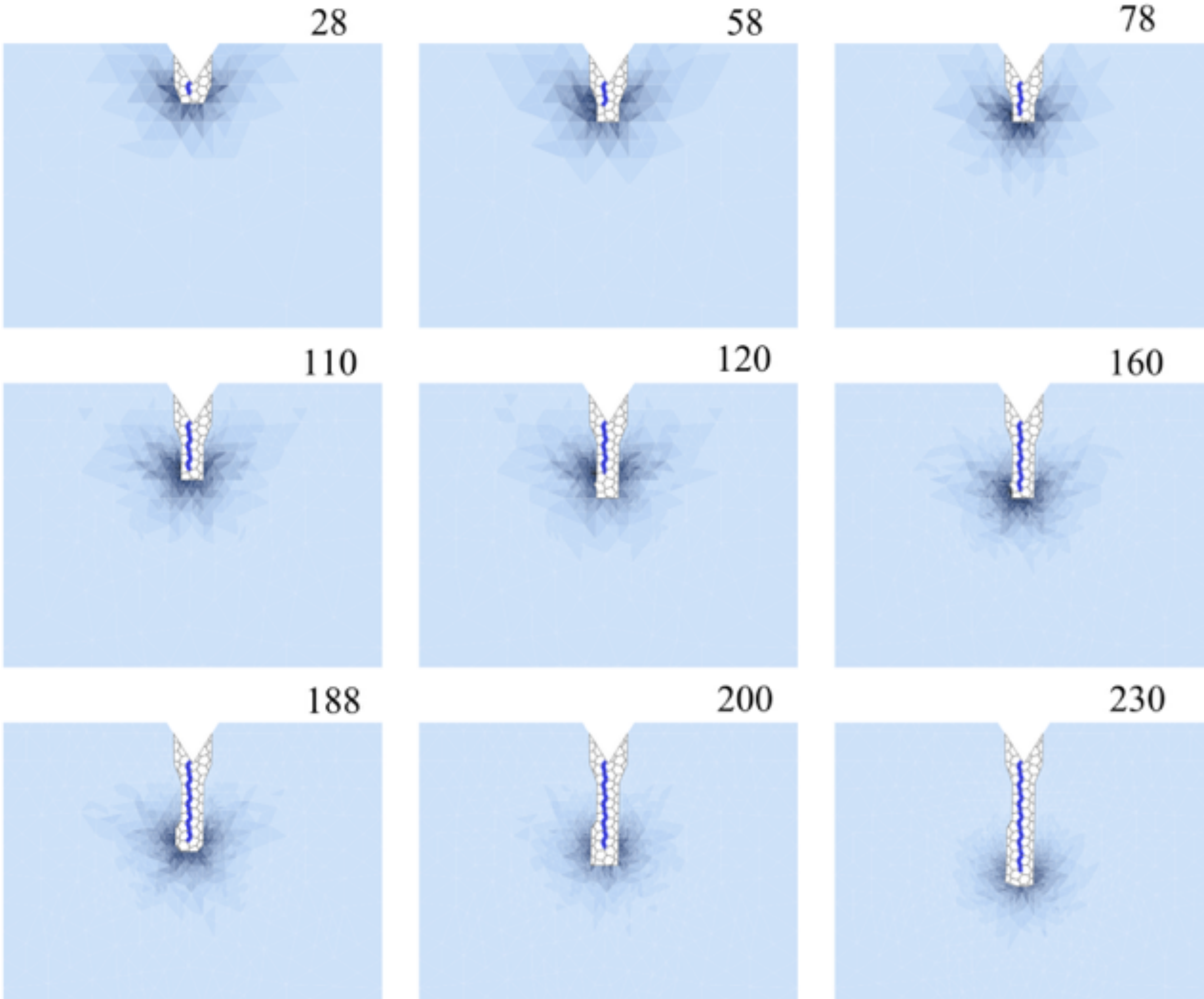

28
58
78
110
120
160
188
200
230

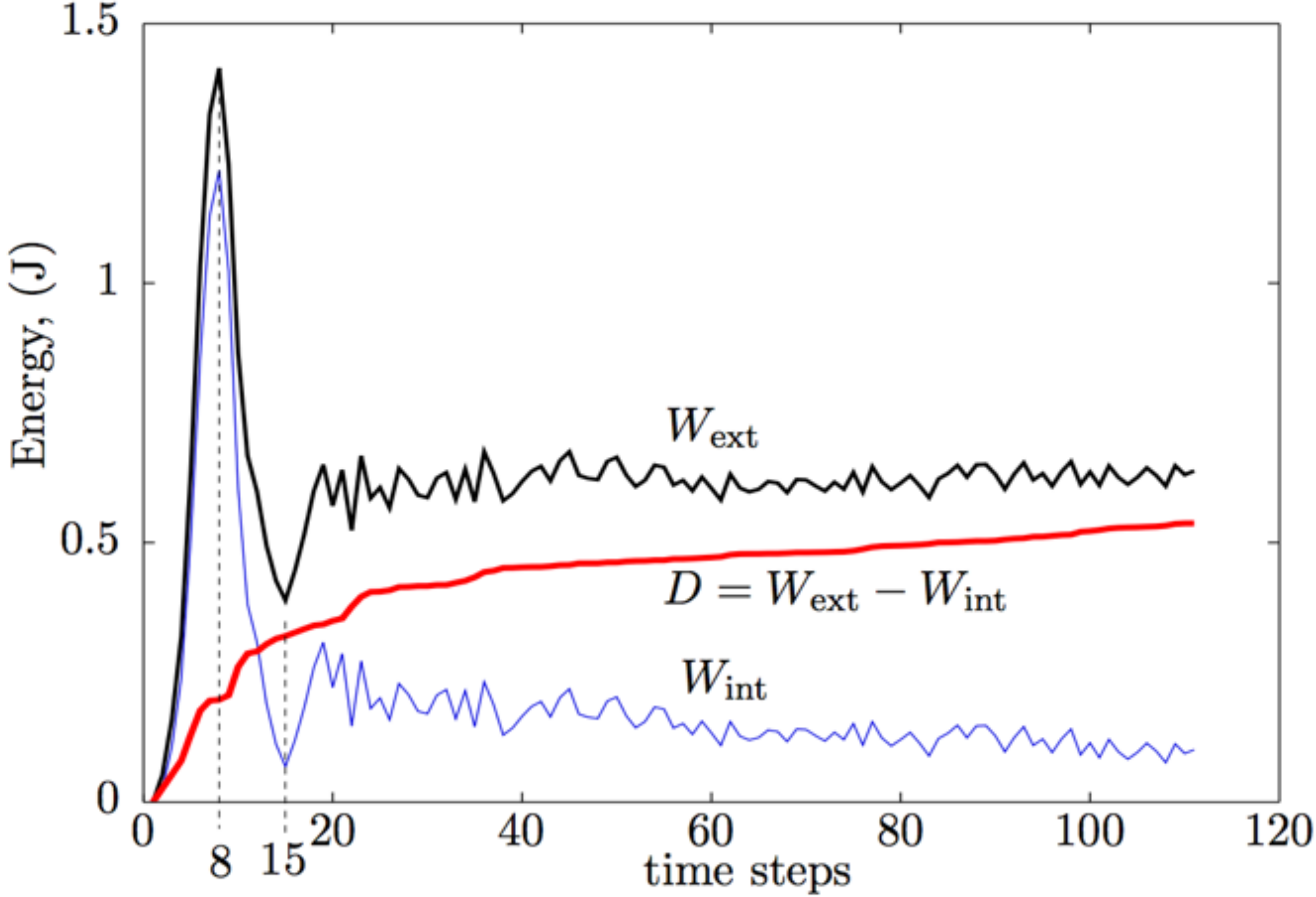

1.5
1
0.5
0
Energy, (J)
$W_{\rm ext}$
$D = W_{\rm ext} - W_{\rm int}$
$W_{\rm int}$
0
20
40
60
80
100
120
8
15
time steps

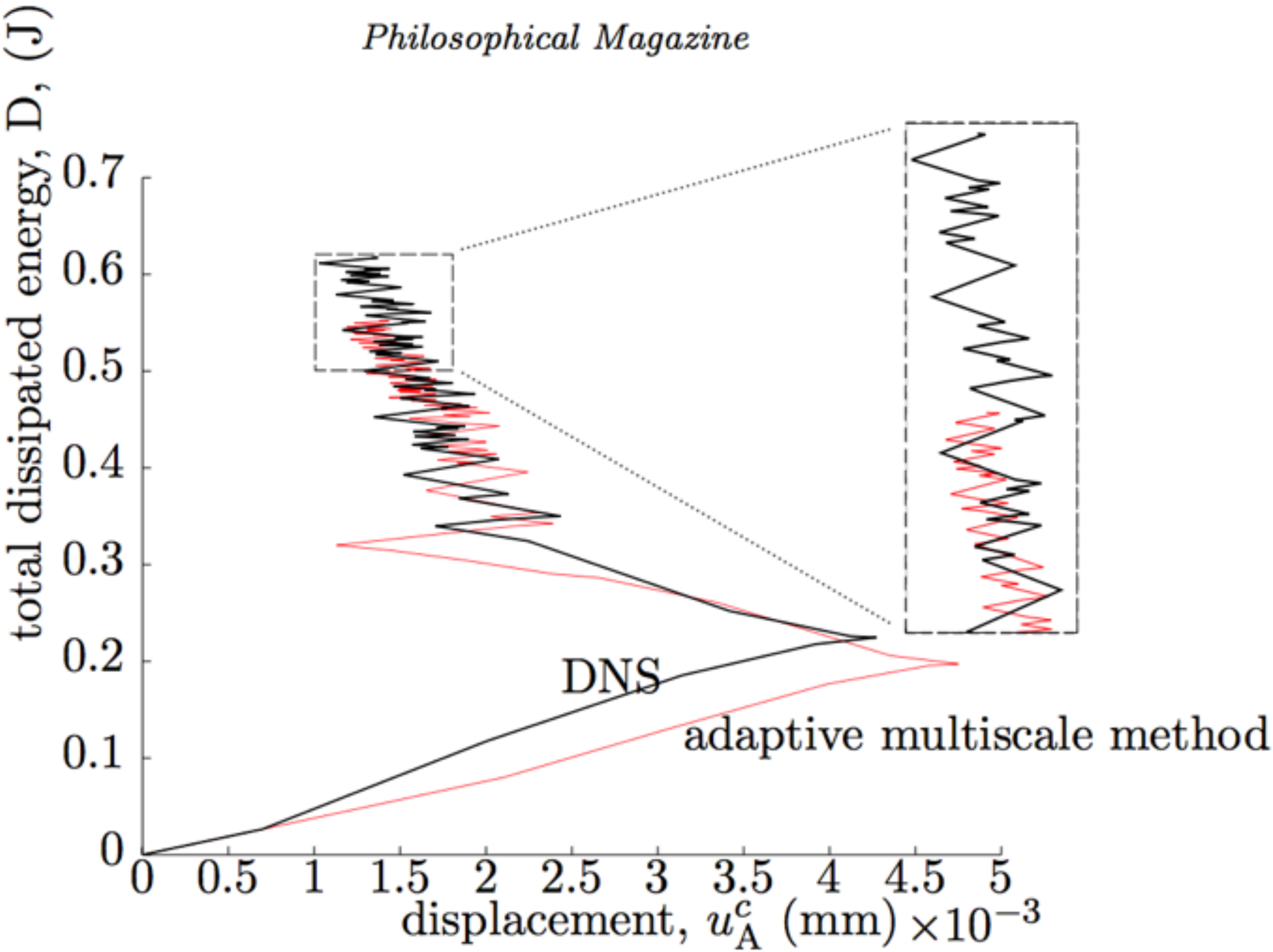
total dissipated energy, D, (J)
0.7
0.6
0.5
0.4
0.3
0.2
0.1
0
0
0.5
1
1.5
2
2.5
3
3.5
4
4.5
5
displacement, u_A^c (mm) $\times 10^{-3}$
DNS
adaptive multiscale method

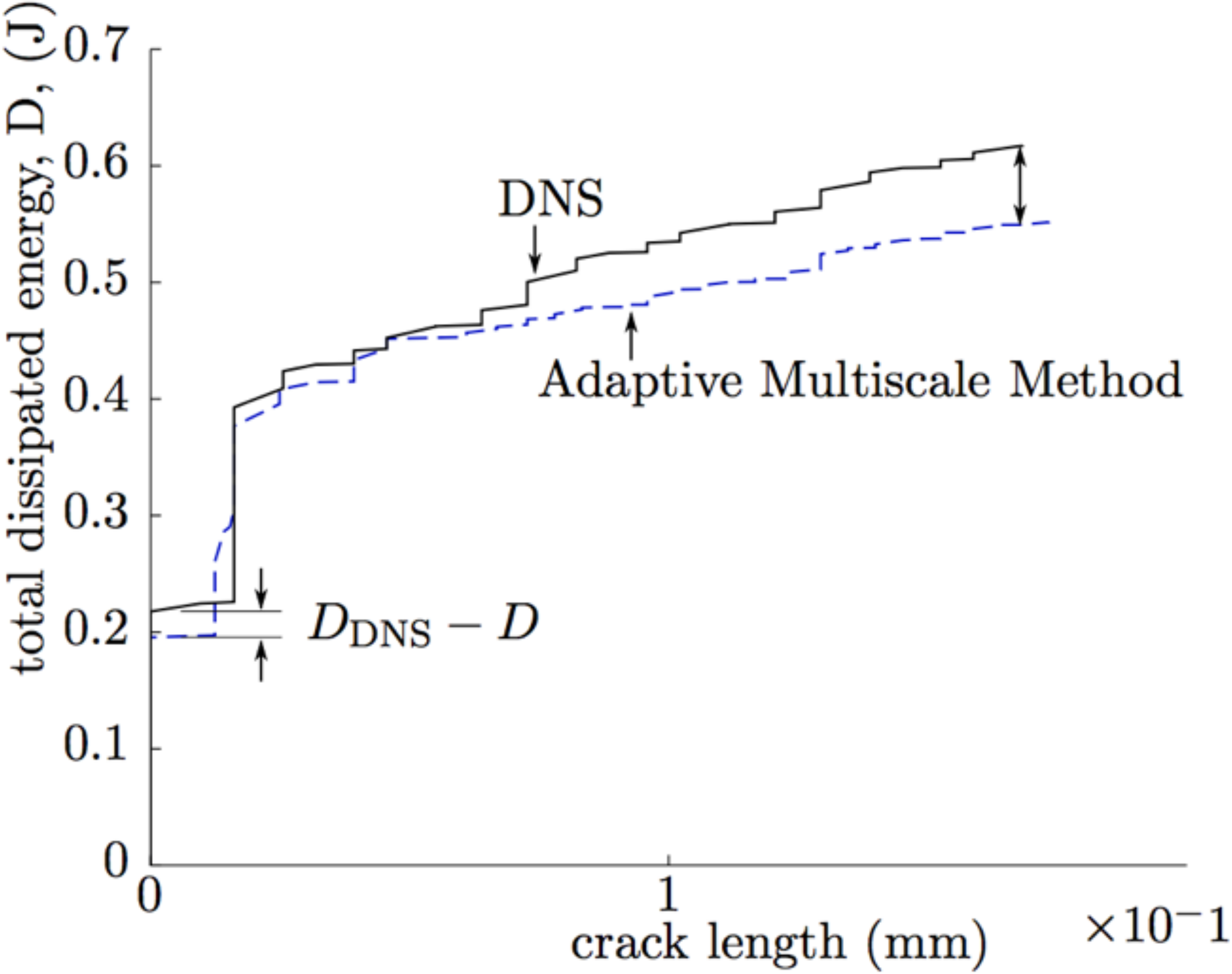

total dissipated energy, D, (J)
0.7
0.6
0.5
0.4
0.3
0.2
0.1
0
DNS
Adaptive Multiscale Method
$D_{\mathrm{DNS}} - D$
0
1
$\times 10^{-1}$
crack length (mm)

Part II.2. Reduction methods based on algebraic reduction

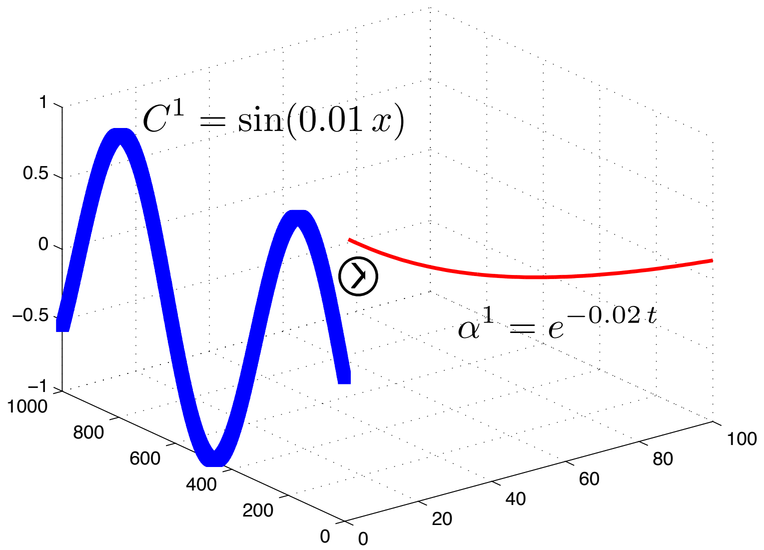
$C^1 = \sin(0.01\,x)$
$\alpha^1 = e^{-0.02\,t}$
1
0.5
0
−0.5
−1
1000
800
600
400
200
0
0
20
40
60
80
100

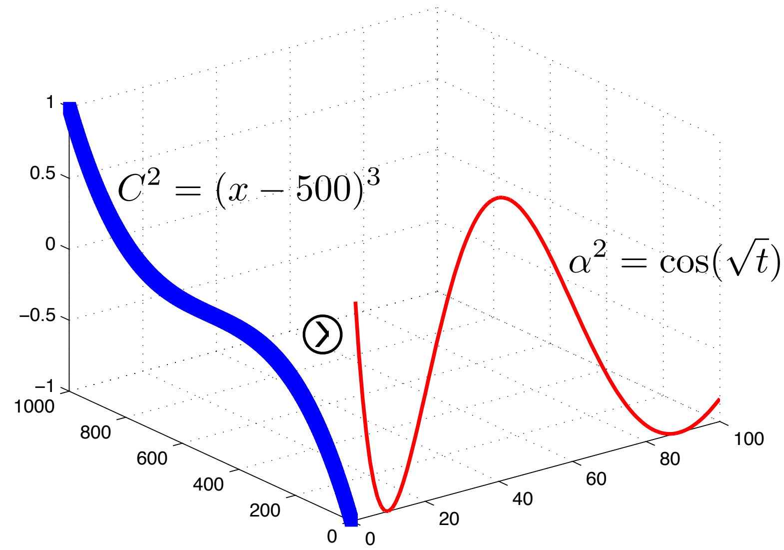
$C^2 = (x - 500)^3$
$\alpha^2 = \cos(\sqrt{t})$
1
0.5
0
−0.5
−1
1000
800
600
400
200
0
0
20
40
60
80
100

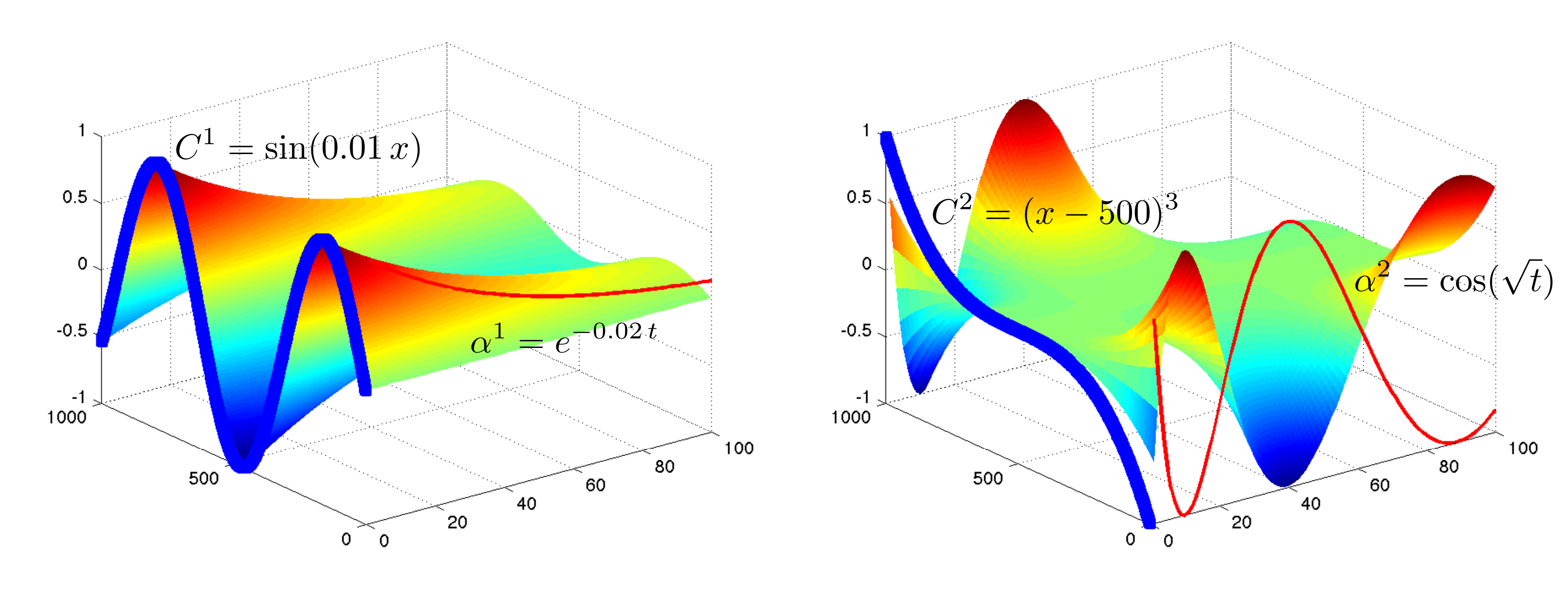

$C^1 = \sin(0.01\,x)$
$\alpha^1 = e^{-0.02\,t}$
1
0.5
0
-0.5
-1
1000
500
0
0
20
40
60
80
100
$C^2 = (x - 500)^3$
$\alpha^2 = \cos(\sqrt{t})$
1
0.5
0
-0.5
-1
1000
500
0
0
20
40
60
80
100

Illustration of the method of separated representation

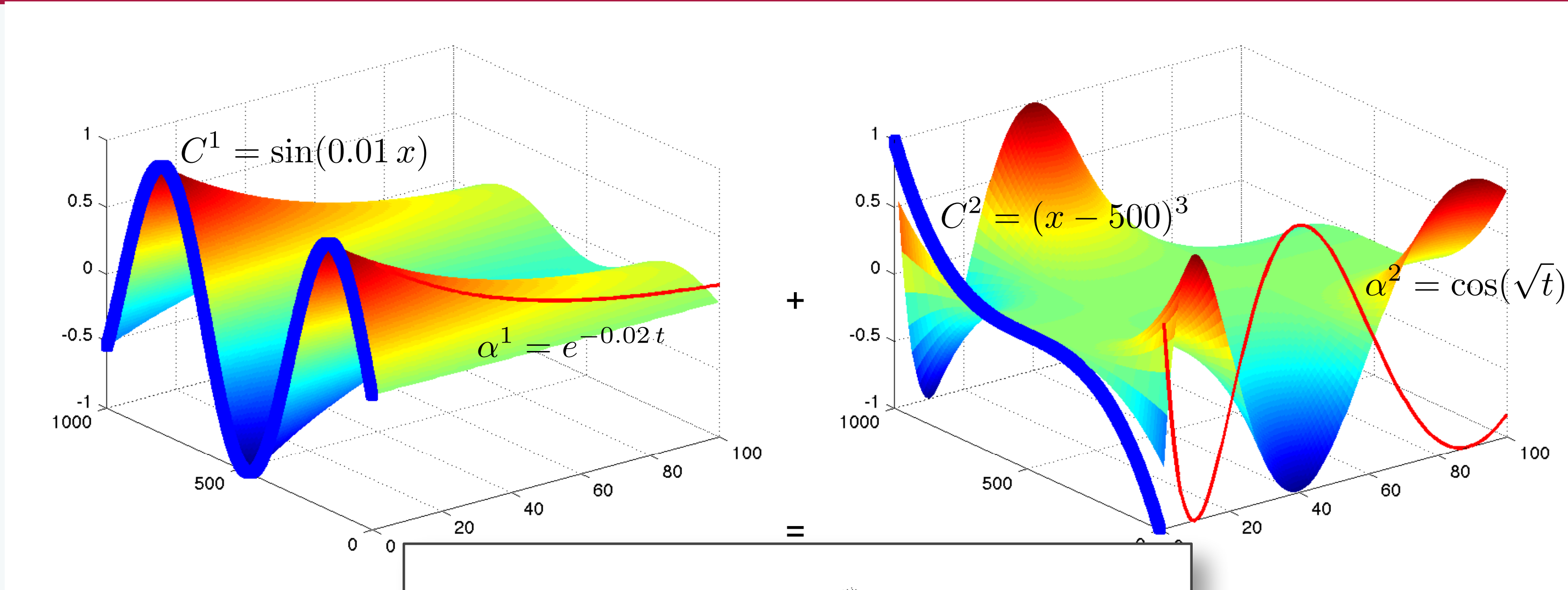

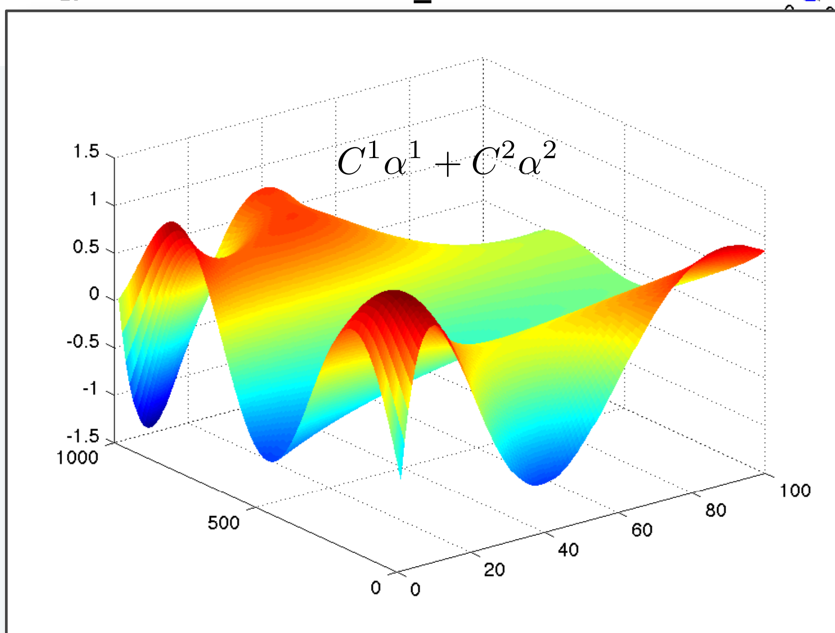

Very rich approximations!

Data compression: get the nose with the POD!

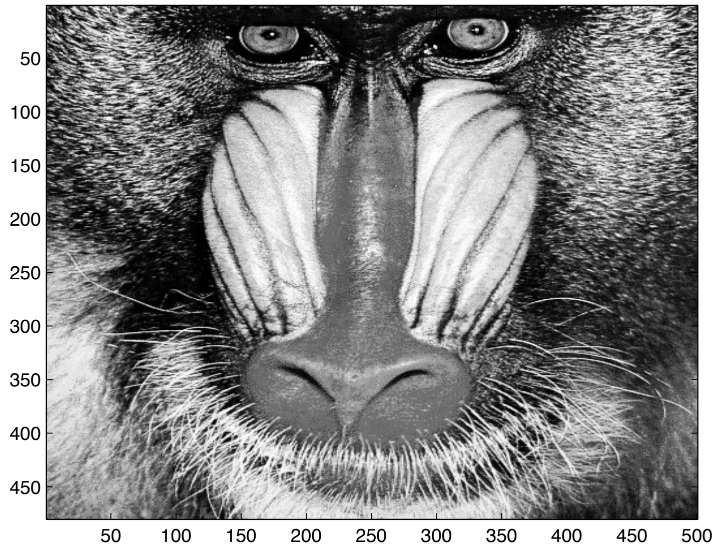

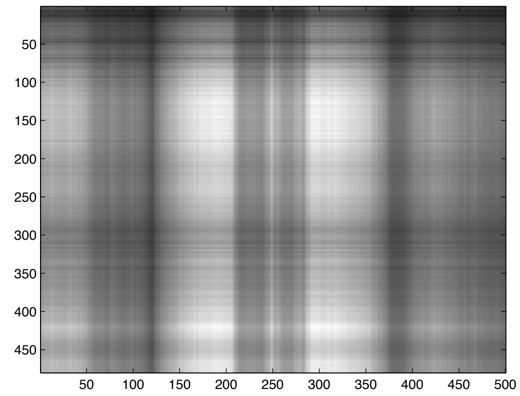

$n_c = 1$

$$\bar{u}(x_i, y_i) = \sum_{i=1}^{n_c} \underline{C_x^i}(x_i)\, \underline{C_y^i}(y_i)$$

$$(C_x^i, C_y^i)_{i \in [\![1, n_c]\!]} = \operatorname{argmin} \sum_{x_i} \sum_{y_j} (u(x_i, y_j) - \bar{u}(x_i, y_j))^2$$

Data compression: get the nose with the POD!

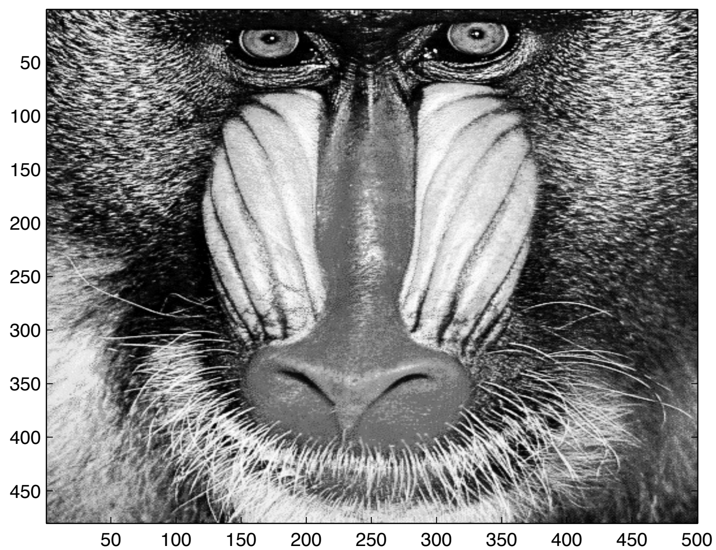

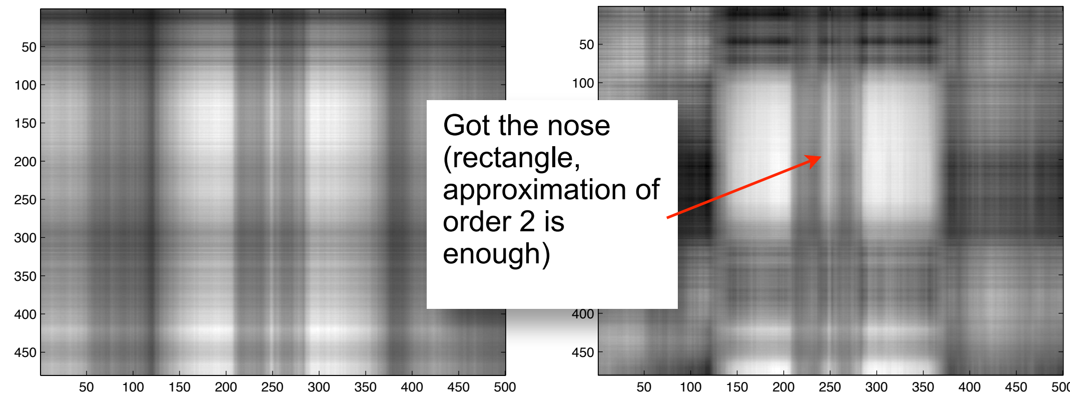

$n_c = 1$ $\qquad$ $n_c = 2$

$$\bar{u}(x_i, y_i) = \sum_{i=1}^{n_c} \underline{C_x^i}(x_i)\, \underline{C_y^i}(y_i)$$

$$(C_x^i, C_y^i)_{i \in [\![1, n_c]\!]} = \operatorname{argmin} \sum_{x_i} \sum_{y_j} (u(x_i, y_j) - \bar{u}(x_i, y_j))^2$$

bordasS@cardiff.ac.uk, stephane.bordas@alum.northwestern.edu

Data compression: get the nose with the POD!

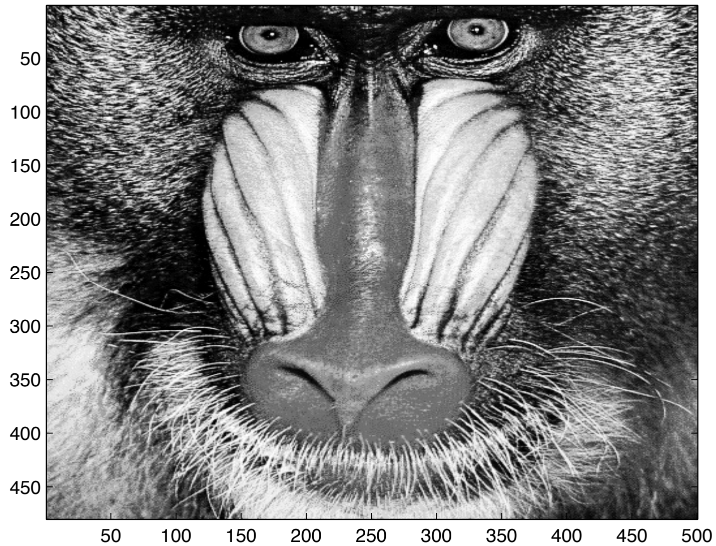

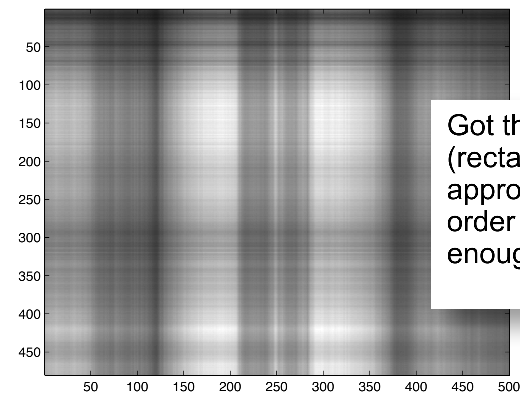

$n_c = 1$

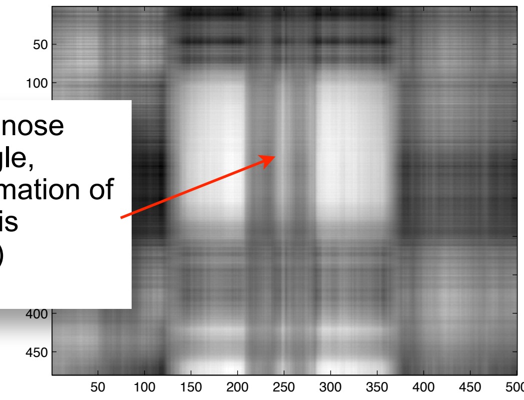

$n_c = 2$

Got the nose (rectangle, approximation of order 2 is enough)

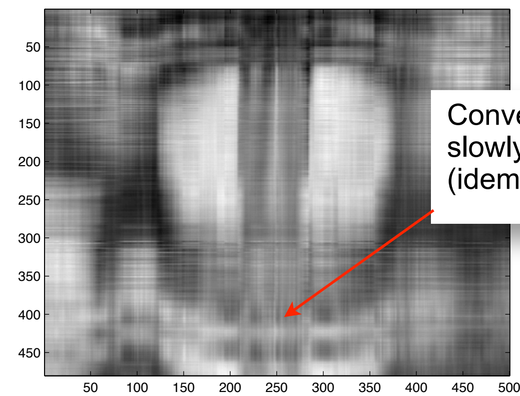

$n_c = 5$

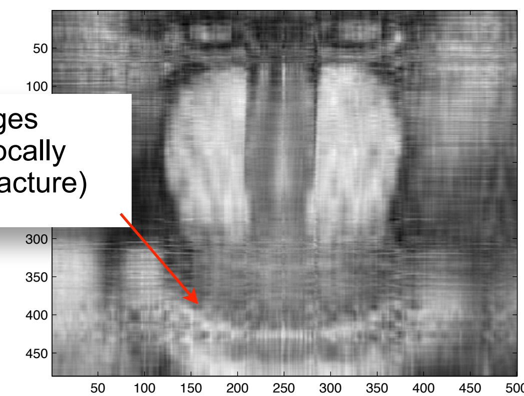

$n_c = 10$

Converges slowly locally (idem fracture)

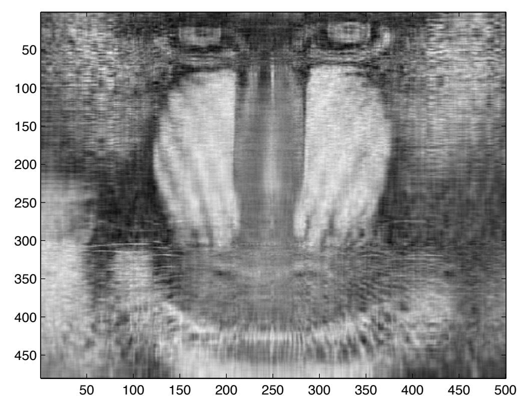

$n_c = 20$

$$\bar{u}(x_i, y_i) = \sum_{i=1}^{n_c} \underline{C_x^i}(x_i)\, \underline{C_y^i}(y_i)$$

$$(C_x^i, C_y^i)_{i \in [\![1, n_c]\!]} = \operatorname{argmin} \sum_{x_i} \sum_{y_j} (u(x_i, y_j) - \bar{u}(x_i, y_j))^2$$

a posteriori model order reduction. **Idea**: search for the **solution as a linear combination** of a set of **pre-calculated representative solutions**

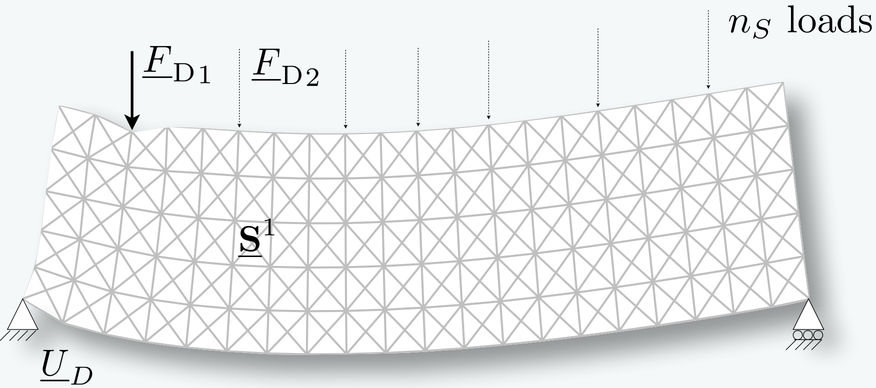

(**1**) Solve FINE for n_S parameters (EXPENSIVE!)

$$\underline{\underline{S}} = \left(\underline{S}^1 \quad \underline{S}^2 \quad \dots \quad \underline{S}^{n_S} \right)$$

(**2**) Singular value decomposition

$$\underline{\underline{S}} = \underline{\underline{U}}\,\underline{\underline{\Sigma}}\,\underline{\underline{V}}^T = \sum_{k=1}^{n_S} \Sigma^k\, \underline{U}^k\, \underline{V}^{k\,T}$$

n_S solutions, sorted by relevance

where $(\Sigma^k)_{k\in[\![1\ n_S]\!]}$ in decreasing order

(**3**) Truncation

Reduced basis: family of representative solutions

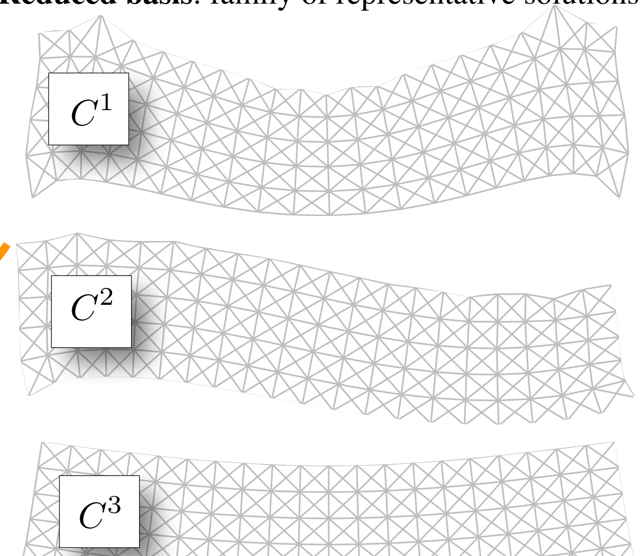

$$\underline{\underline{C}} = \left(\underline{U}^1 \quad \underline{U}^2 \quad \dots \quad \underline{U}^{n_C} \right)$$

Family of representative solutions

$$\underline{U} = \underline{\underline{C}}\,\underline{\alpha}$$

Solution

Coefficients

Initial set of equations

$$\underline{F}_{\mathrm{Int}}(\underline{U}) + \underline{F}_{\mathrm{Ext}} = 0$$

(**4**) Galerkin orthogonality

$$\underline{\underline{C}}^T\, \underline{F}_{\mathrm{int}}(\underline{\underline{C}}\,\underline{\alpha}) + \underline{\underline{C}}^T\, \underline{F}_{\mathrm{ext}} = 0$$

Approximation of the solution in a space of small dimension (n_c)

Limitations: case of highly non-linear fracture mechanics pbs

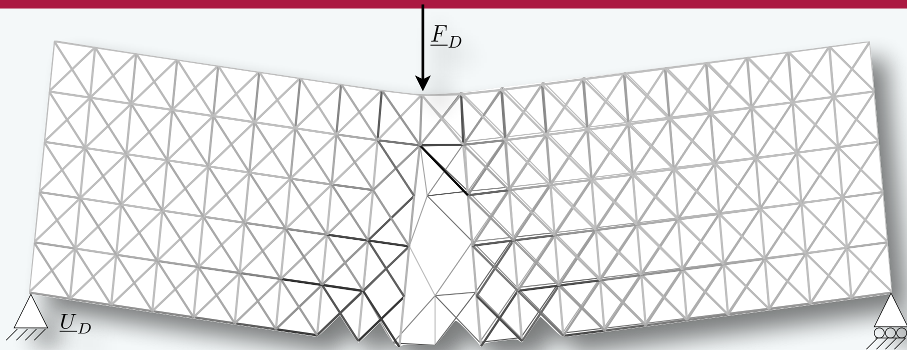

This solution is not in the snapshot !

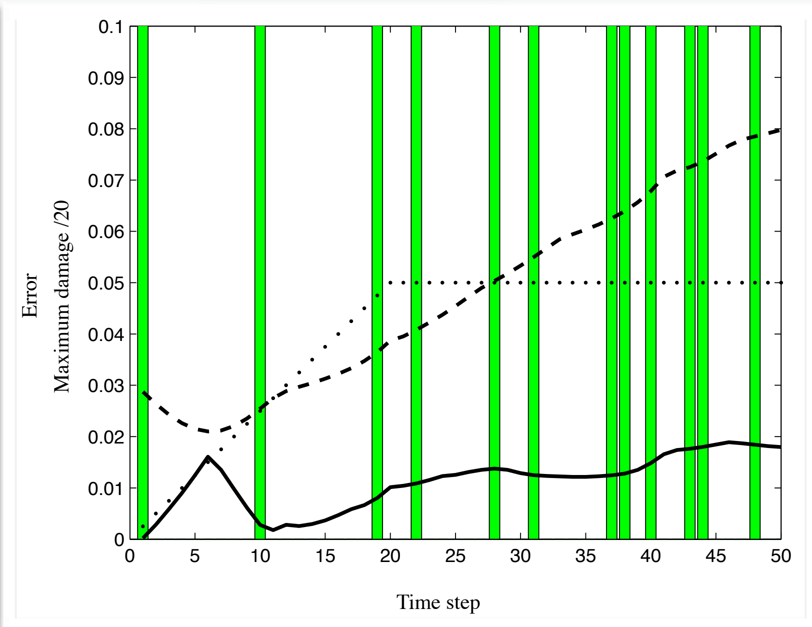

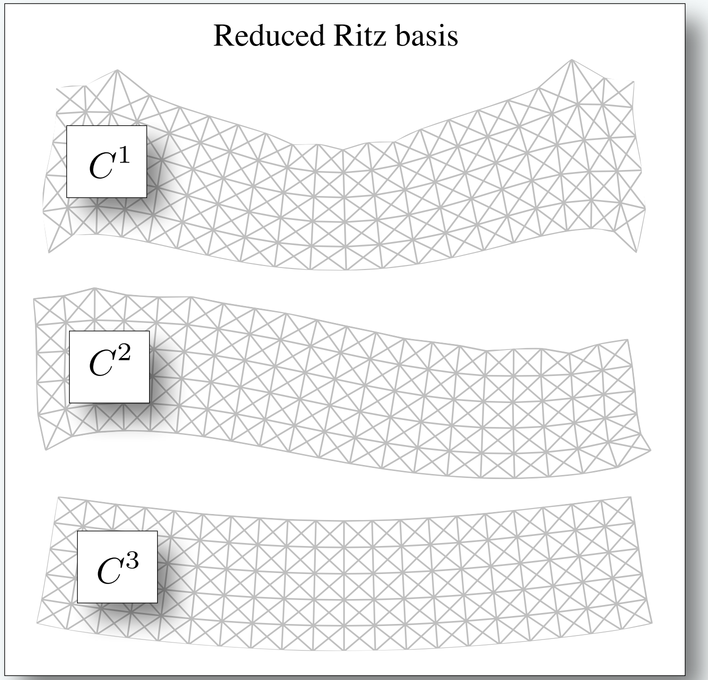

- P. Kerfriden, P. Gosselet, S. Adhikari, and S. Bordas. *Bridging proper orthogonal decomposition methods and augmented Newton-Krylov algorithms: an adaptive model order reduction for highly nonlinear mechanical problems*. Computer Methods in Applied Mechanics and Engineering, 200(5-8):850-866, 2011.

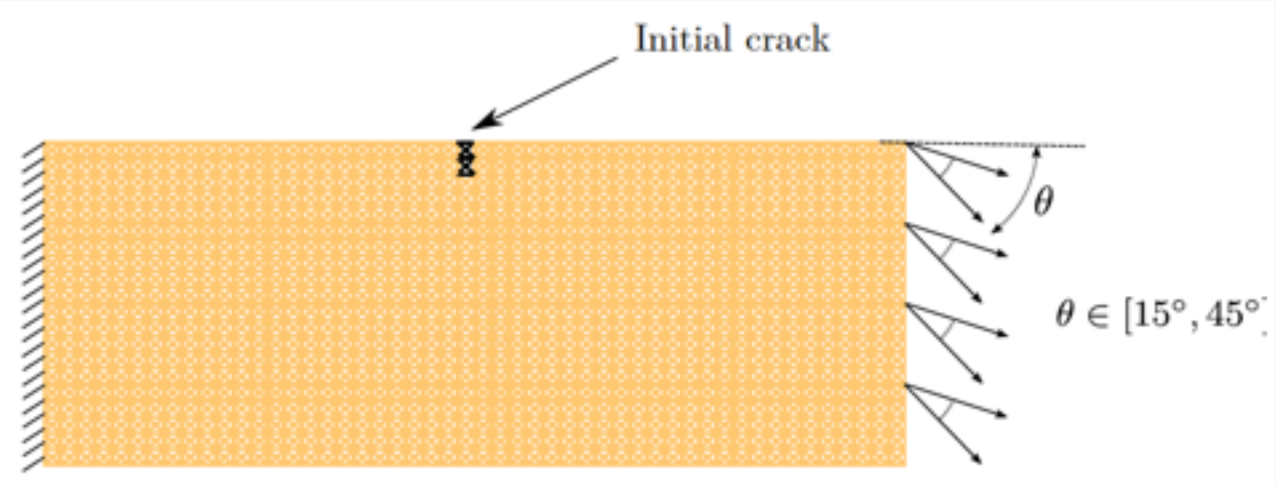
Initial crack
θ
$\theta \in [15°, 45°]$

Application to a parametric fracture problem

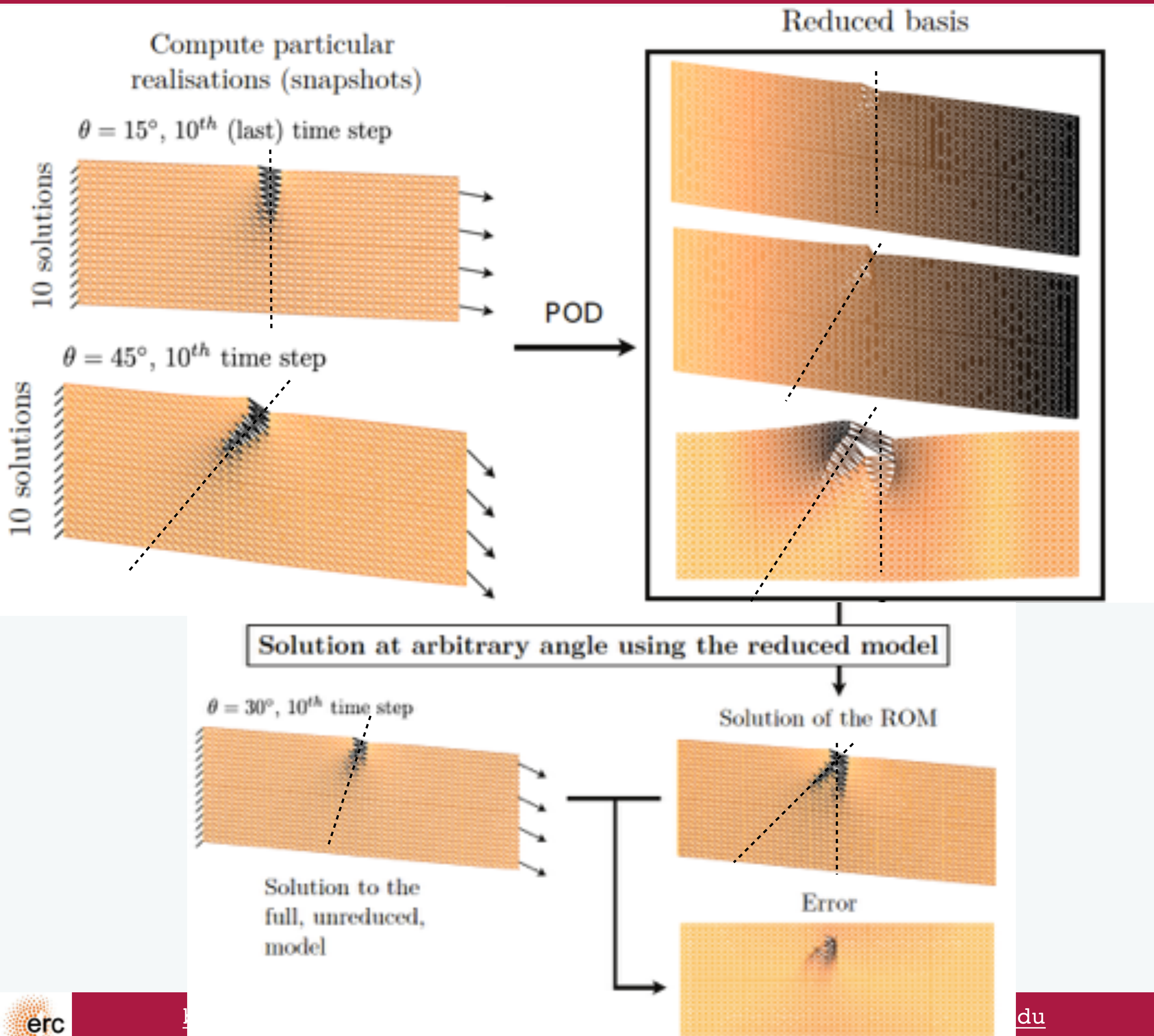

- The POD solution is not able to reproduce the solution in the cracked area
- Due to lack of correlation introduced by crack growth
- Leads to a local projection error

Parametric / stochastic multiscale fracture mechanics

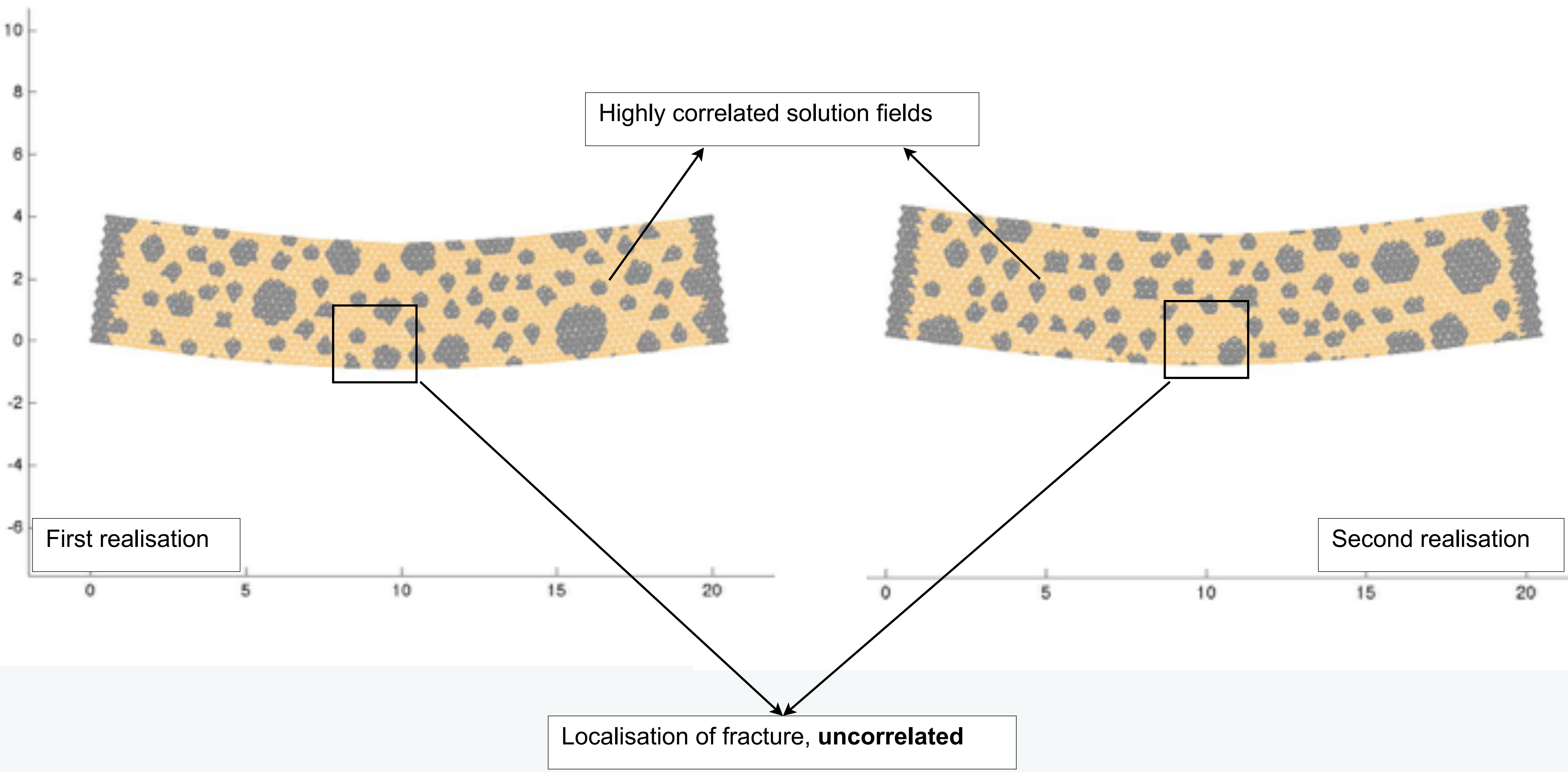

➡ Direct numerical simulation: efficient preconditioner?

➡ Reduced order modelling?

➡ Adaptive coupling?

THE RETURN OF THE MONKEY!

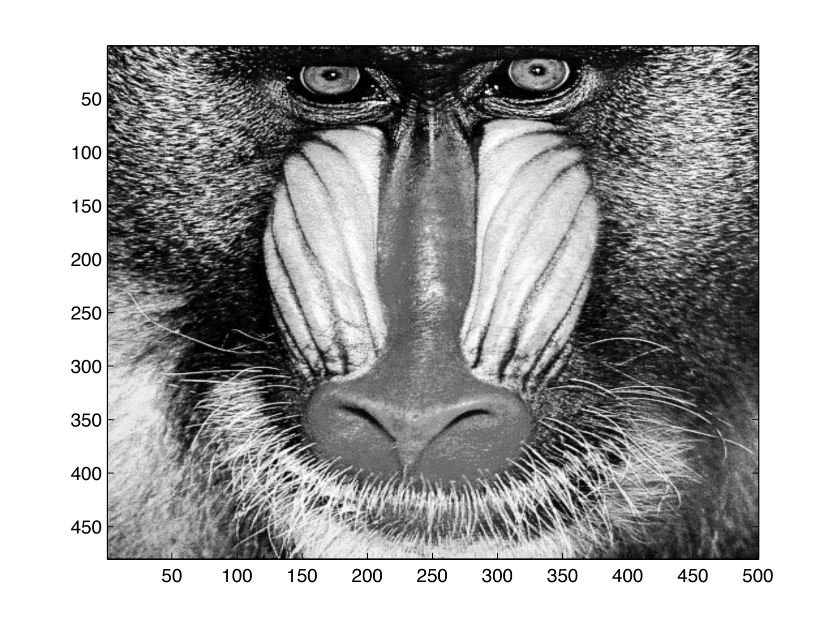

What can we do to address this lack of separation of scales/reducibility?

How we got to this point...

P. Kerfriden, P. Gosselet, S. Adhikari, and S. Bordas. Bridging proper orthogonal decomposition methods and augmented Newton-Krylov algorithms: an adaptive model order reduction for highly nonlinear mechanical problems. *Computer Methods in Applied Mechanics and Engineering*, 200(5-8):850–866, 2011.

P. Kerfriden, J.C. Passieux, and S. Bordas. Local/global model order reduction strategy for the simulation of quasi-brittle fracture. *International Journal for Numerical Methods in Engineering*, 89(2):154–179, 2011.

P. Kerfriden, K.M. Schmidt, T. Rabczuk, and Bordas S.P.A. Statistical extraction of process zones and representative subspaces in fracture of random composites. *Accepted for publication in International Journal for Multiscale Computational Engineering, arXiv:1203.2487v2*, 2012.

http://www.ncbi.nlm.nih.gov/pmc/articles/PMC3672853/

http://orbilu.uni.lu/bitstream/10993/12454/2/presentationUSNCCM

Data compression: fracture

Snapshot POD (snapshot space is spanned by the ensemble of solutions at all time steps)

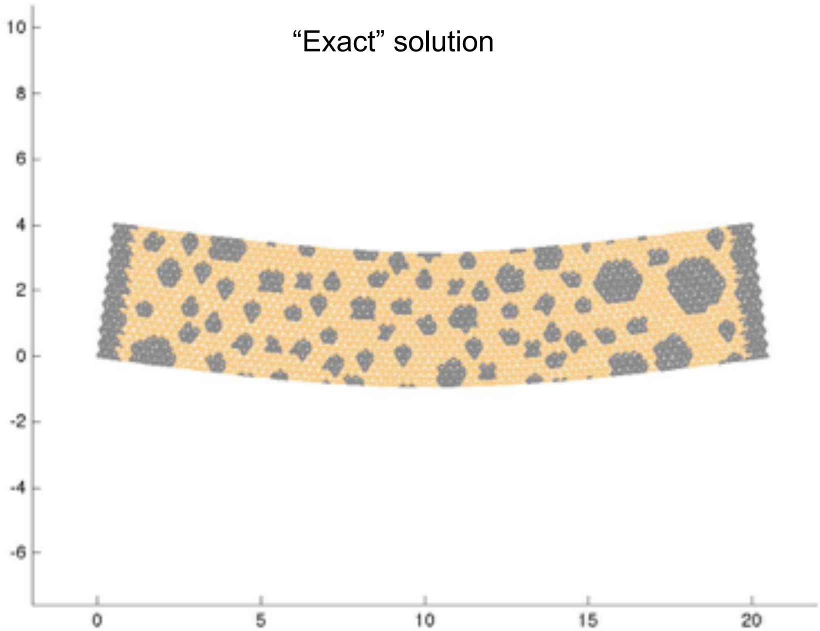

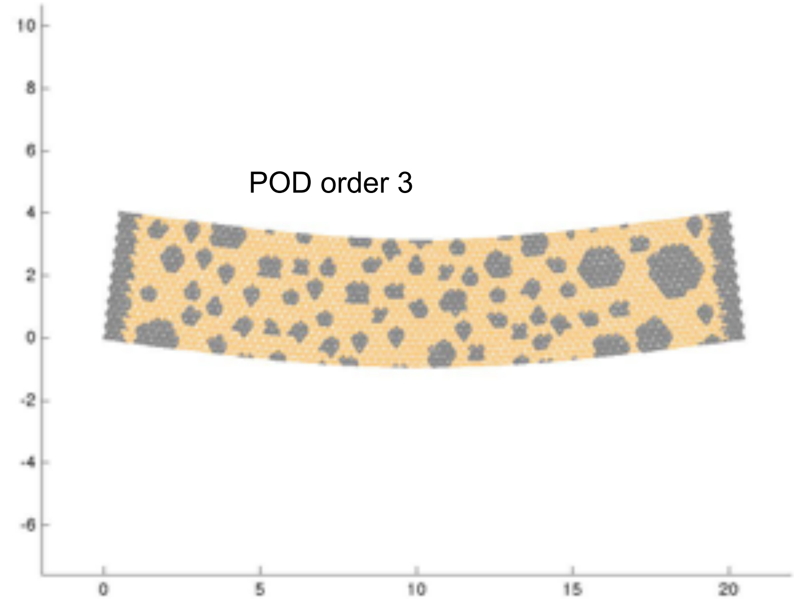

Partitioned POD/DDM

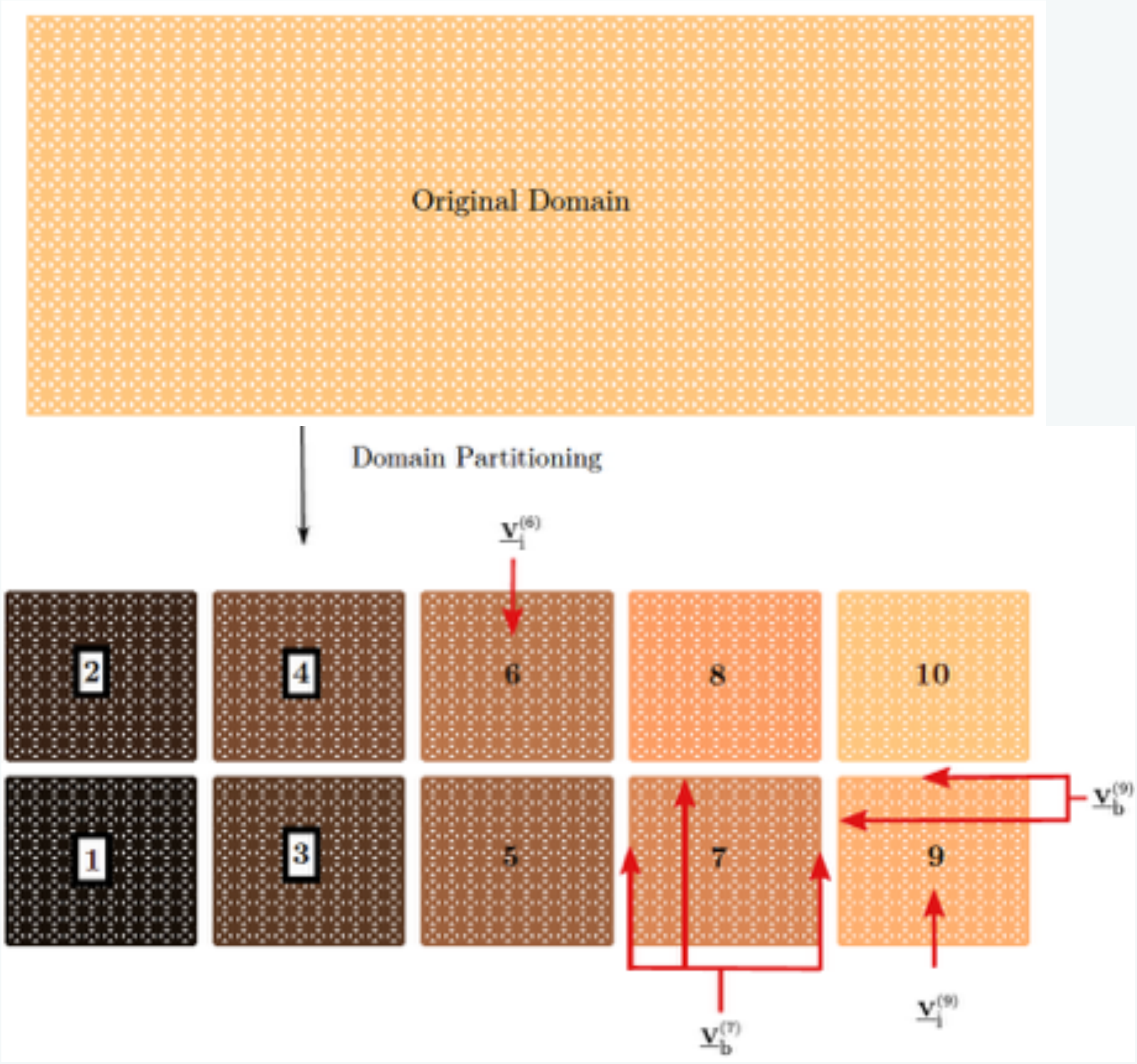

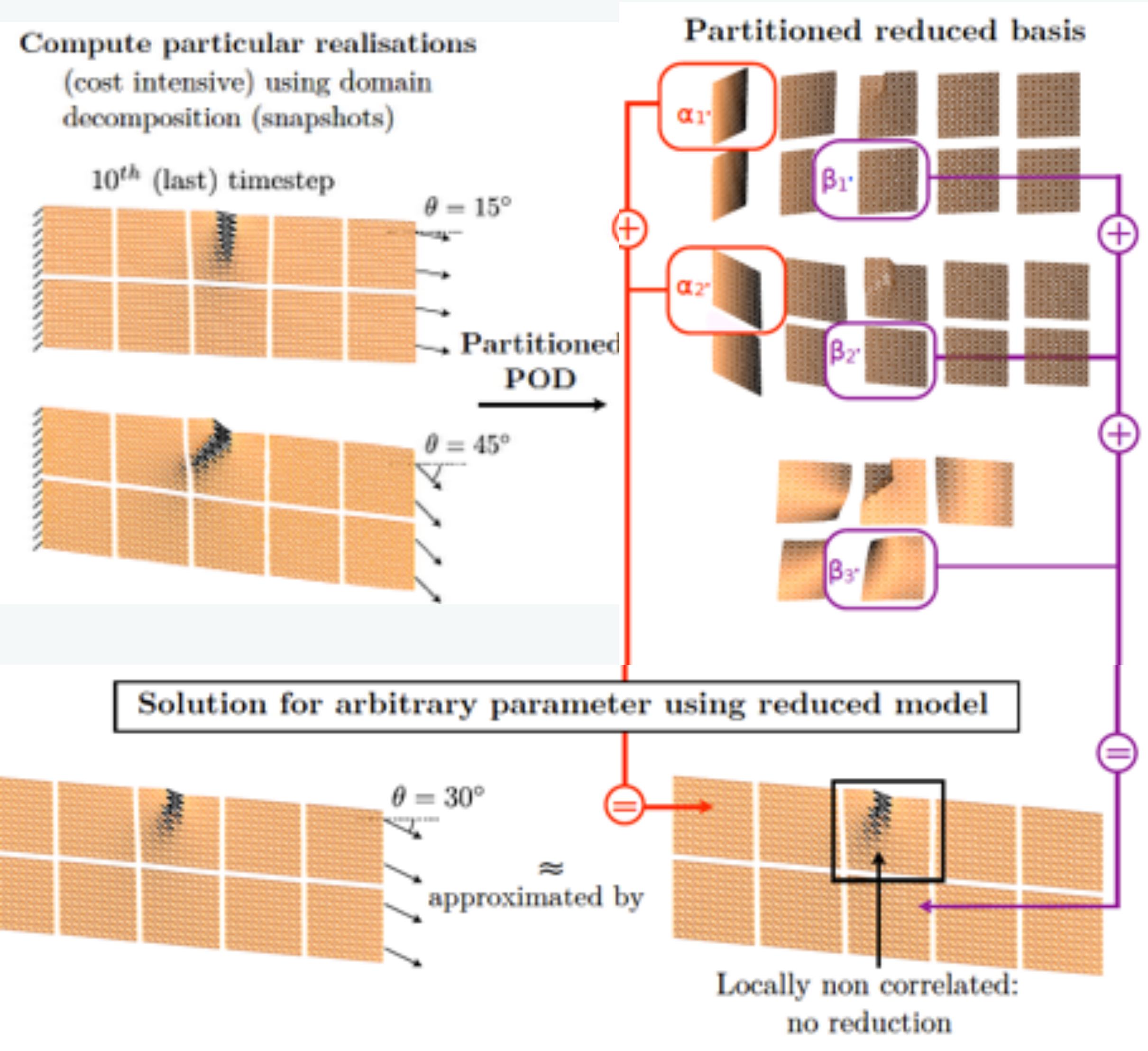

- Decompose the structure into subdomains
- Perform a reduction in the highly correlated region
- Couple the reduced to the non-reduced region by a primal Schur complement

Choice of the reduced subdomains: local error estimation by "leave one out cross-validation" (LOOCV)

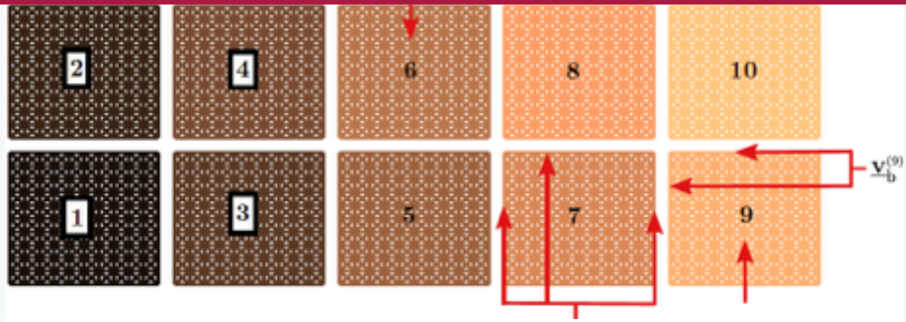

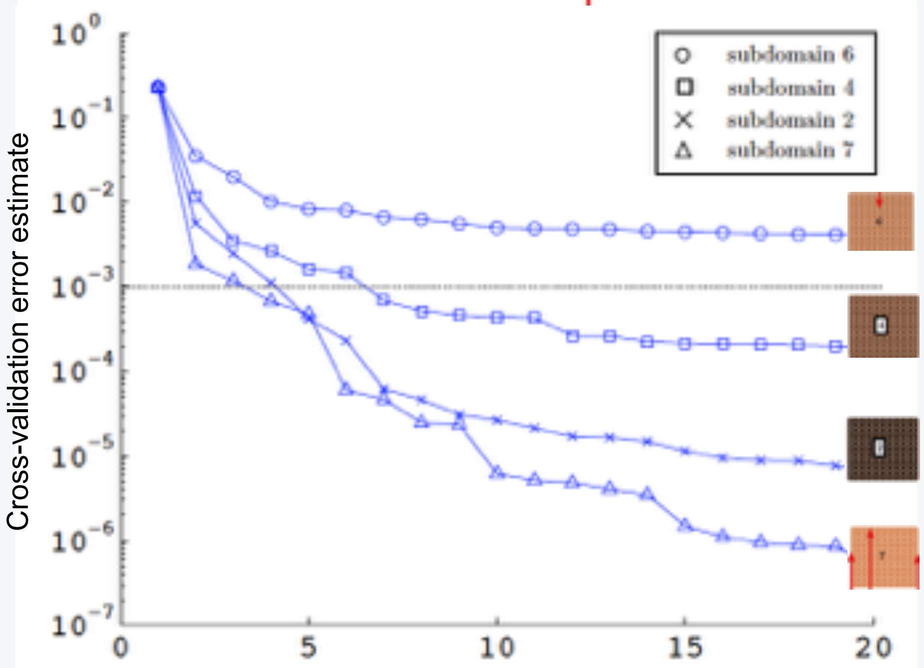

$$\left(\bar{\nu}^{(e)}_{\text{snap}}\right)^2 = \frac{\displaystyle\sum_{\mu\in\mathcal{P}^s}\sum_{t_n\in\mathcal{T}^h}\left\| \underline{\mathbf{U}}_i(t_n,\mu) - \sum_{j=1}^{n_c^{(e)}} \left(\bar{\underline{\mathbf{C}}}_{i,j}^{(e),(\mu)\,T}\,\underline{\mathbf{U}}_i(t_n,\mu)\right)\bar{\underline{\mathbf{C}}}_{i,j}^{(e),(\mu)}\right\|_2^2}{\displaystyle\sum_{t_n\in\mathcal{T}^h}\sum_{\mu\in\mathcal{P}^s}\|\underline{\mathbf{U}}_i(t_n,\mu)\|_2^2}$$

- Reduced subspaces are independent and we assume a snapshot is *a priori* available
  - (1) Dimension of the local space for each subdomain?
  - (2) Is a given subdomain is reducible?
- (1) and (2) will be treated by cross-validation (e.g. W. J. Krzanowski. Cross-validation in principal component analysis. Biometrics, 43(3): 575-584, 1987.)
  - **Training set**: snapshot
  - **Validation set**: set of additional finescale solutions
  - Independent training/validation avoids overfitting
  - Cross validation **emulates independence**. Error calculated using the local reduced basis obtained by a snapshot POD transform of all the available snapshot solutions except the one corresponding to the value of the summation variable.
- **NOTE:** If the snapshot is not assumed *a priori* then
  - Assess whether the snapshot contains sufficient information, and generate additional, suitable, data if required
  - Most analysis (mostly by statisticians) assume the snapshot is known *a priori*. Recent review: Hervé Abdi and Lynne J. Williams. Principal component analysis. Wiley Interdisciplinary Reviews: Computational Statistics, 2(4):433{459, 2010.

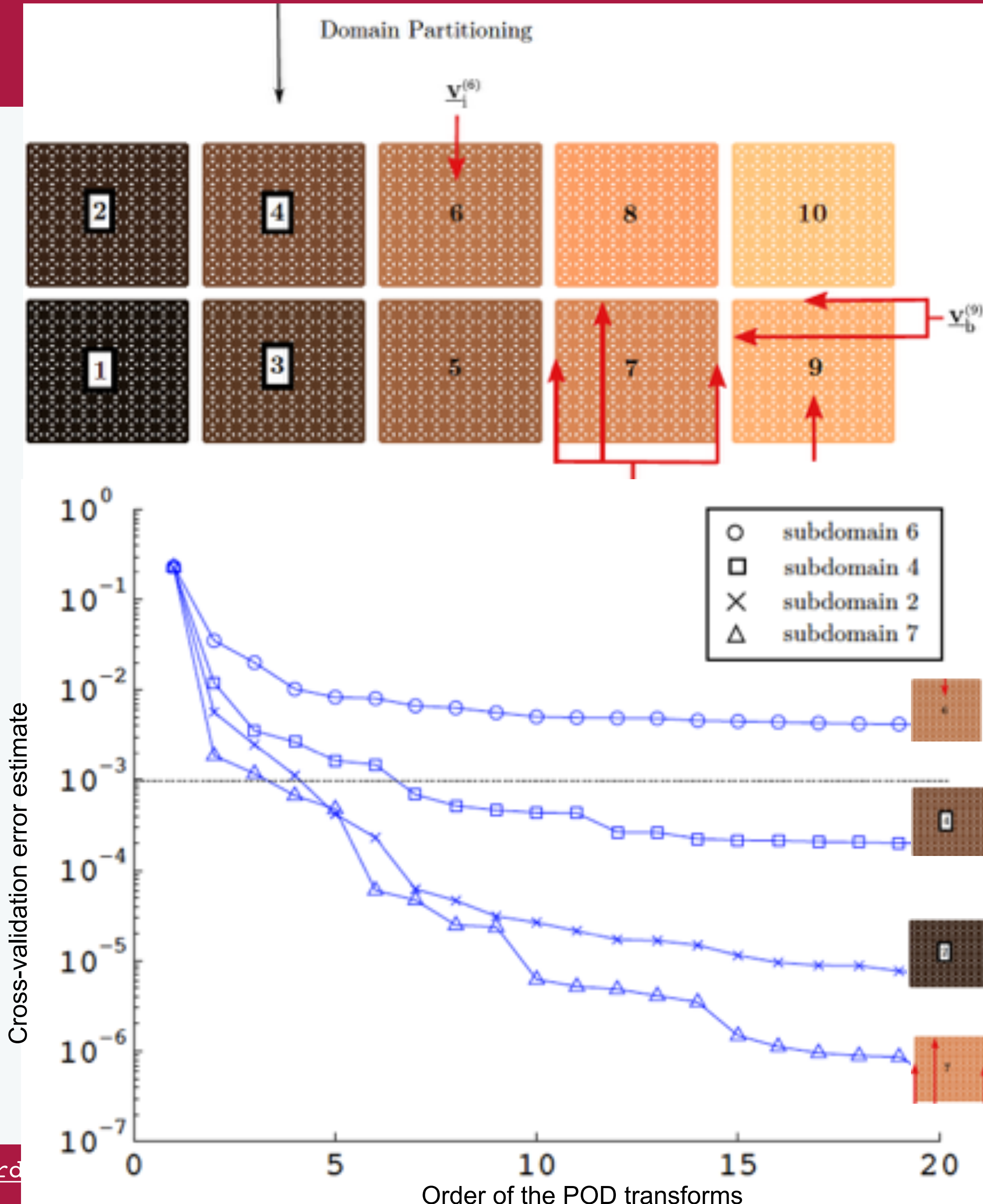

Domain Partitioning
2
4
6
8
10
1
3
5
7
9
subdomain 6
subdomain 4
subdomain 2
subdomain 7
Cross-validation error estimate
Order of the POD transforms

- Relative error

$$\nu^{\mathrm{app},(\mu)}\left(\underline{\mathbf{U}}^{\mathrm{app}}\right)^2 = \frac{\sum_{t_n \in \mathcal{T}^h} \|\underline{\mathbf{U}}^{\mathrm{app}}(t_n,\mu) - \underline{\mathbf{U}}^{\mathrm{ex}}(t_n,\mu)\|_2^2}{\sum_{t_n \in \mathcal{T}^h} \|\underline{\mathbf{U}}^{\mathrm{ex}}(t_n,\mu)\|_2^2}$$

40^o

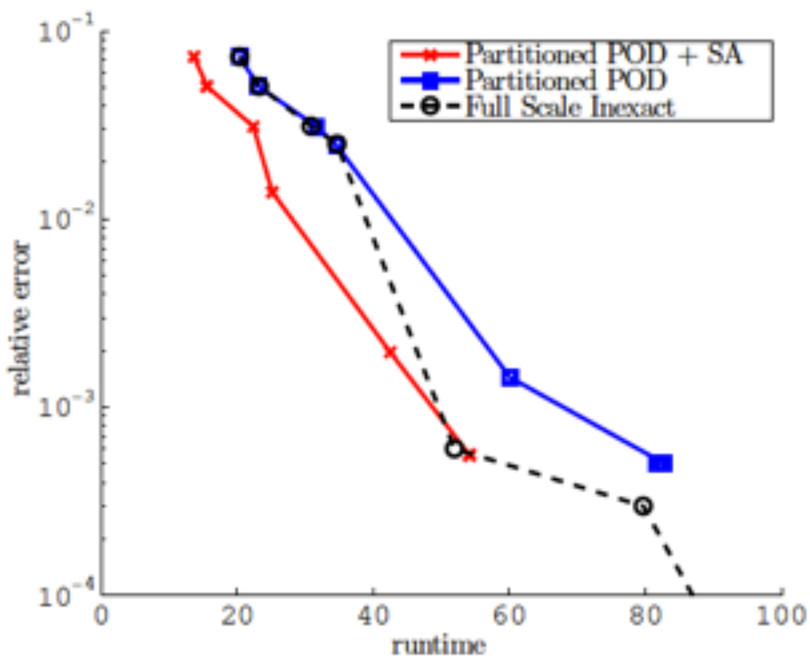

(a) Relative error for the different models using 121 nodes per subdomain

27^o

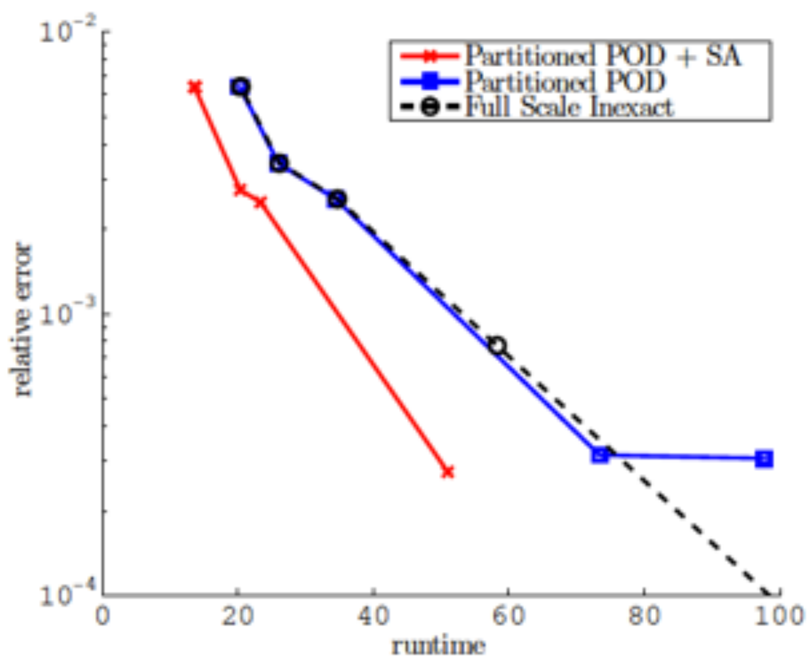

(a) Relative error for the different models using 121 no per subdomain

- Relative error

$$\nu^{\text{app},(\mu)}\left(\underline{\mathbf{U}}^{\text{app}}\right)^2 = \frac{\sum_{t_n \in \mathcal{T}^h} \|\underline{\mathbf{U}}^{\text{app}}(t_n,\mu) - \underline{\mathbf{U}}^{\text{ex}}(t_n,\mu)\|_2^2}{\sum_{t_n \in \mathcal{T}^h} \|\underline{\mathbf{U}}^{\text{ex}}(t_n,\mu)\|_2^2}$$

40^o

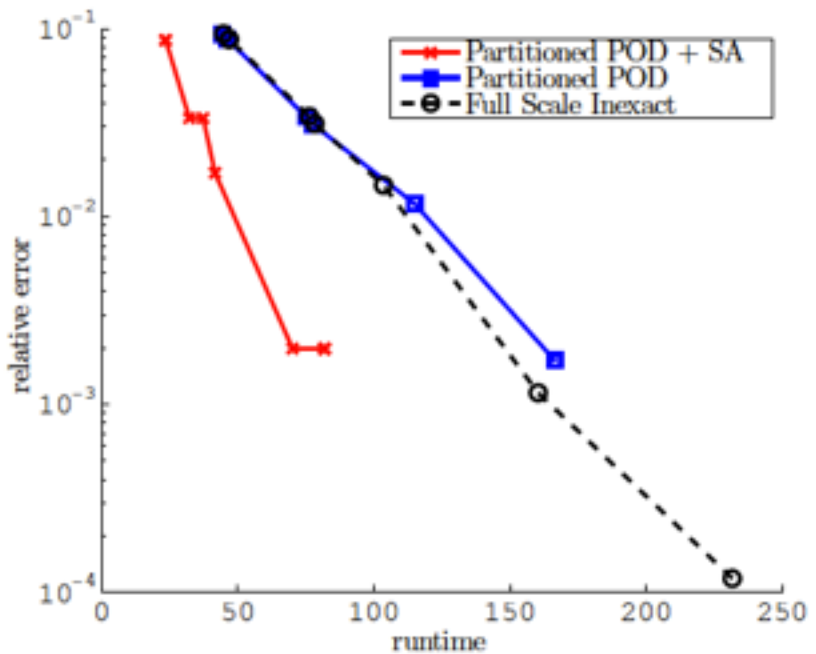

(b) Relative error for the different models using 256 nodes per subdomain

27^o

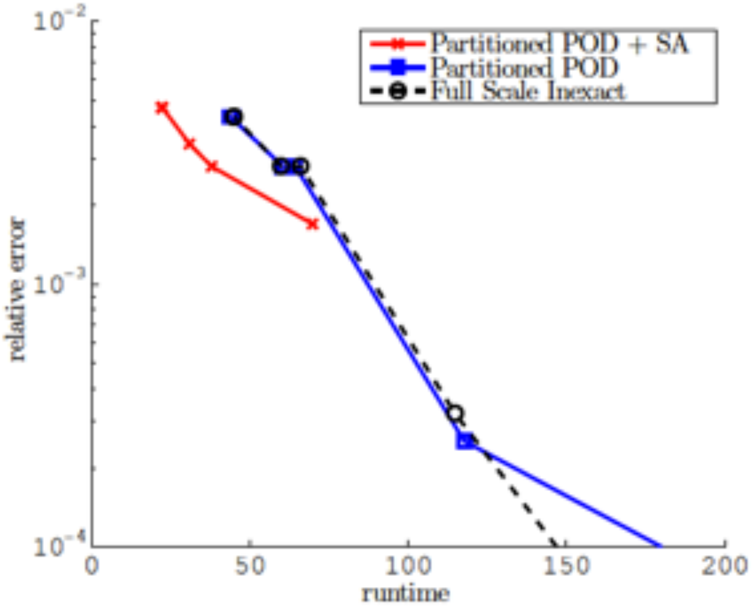

(b) Relative error for the different models using 256 nodes per subdomain

Performance: load angle 40 | 27 - 441 nodes

- Relative error

$$\nu^{\mathrm{app},(\mu)}\left(\underline{\mathbf{U}}^{\mathrm{app}}\right)^2 = \frac{\sum_{t_n \in \mathcal{T}^h} \|\underline{\mathbf{U}}^{\mathrm{app}}(t_n,\mu) - \underline{\mathbf{U}}^{\mathrm{ex}}(t_n,\mu)\|_2^2}{\sum_{t_n \in \mathcal{T}^h} \|\underline{\mathbf{U}}^{\mathrm{ex}}(t_n,\mu)\|_2^2}$$

40^o

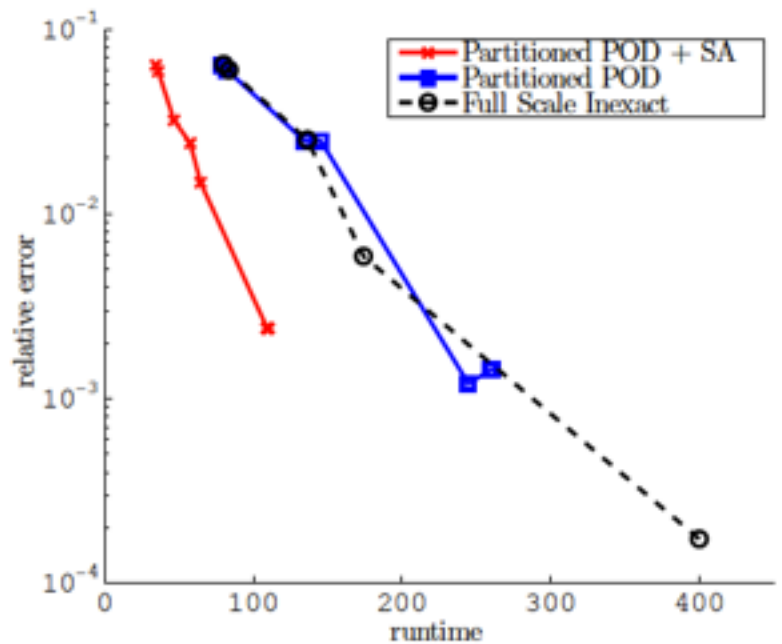

(c) Relative error for the different models using 441 nodes per subdomain

27^o

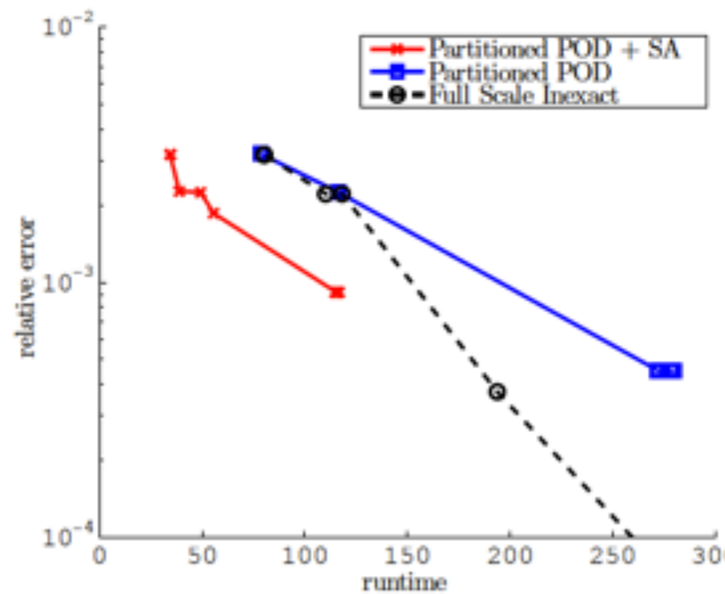

(c) Relative error for the different models using 441 nodes per subdomain

- Relative error

$$\nu^{\mathrm{app},(\mu)}\left(\underline{\mathbf{U}}^{\mathrm{app}}\right)^2 = \frac{\sum_{t_n \in \mathcal{T}^h} \|\underline{\mathbf{U}}^{\mathrm{app}}(t_n,\mu) - \underline{\mathbf{U}}^{\mathrm{ex}}(t_n,\mu)\|_2^2}{\sum_{t_n \in \mathcal{T}^h} \|\underline{\mathbf{U}}^{\mathrm{ex}}(t_n,\mu)\|_2^2}$$

40^o

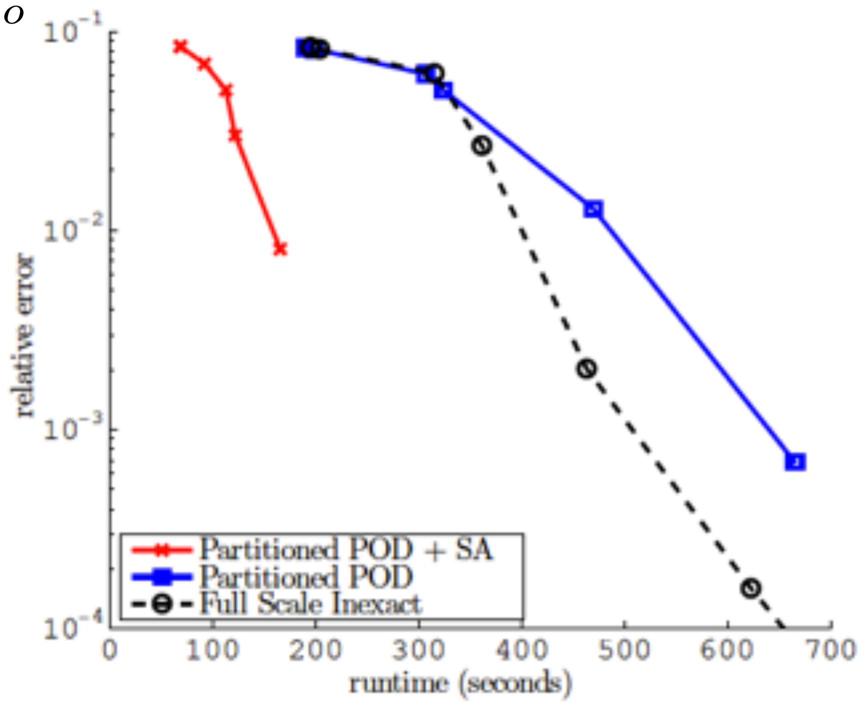

(d) Relative error for the different models using 961 nodes per subdomain

27^o

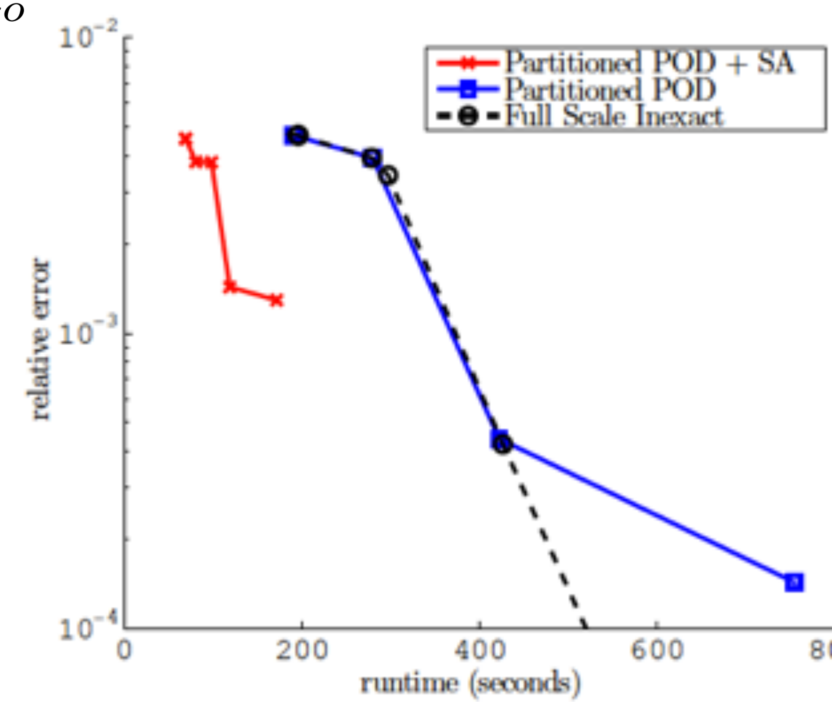

(d) Relative error for the different models using 961 per subdomain

Conclusion

- Dual boundary integral equations combined with isogeometric analysis are used to model fracture (2D & 3D) and crack growth (2D)

- Partition of unity enrichment (2D) and graded mesh refinement (2D & 3D) are used to improve accuracy near the crack tip or crack front

- Stable quadrature scheme is proposed for singular integration in 3D. This makes the method non-sensitive to mesh distortion

- Different ways to extract stress intensity factors based on the framework of IGABEM

- Surface breaking crack can be modeled via phantom node method with help of trimmed NURBS technique

- Dual boundary integral equations combined with isogeometric analysis are used to model fracture (2D & 3D) and crack growth (2D)
- Partition of unity enrichment (2D) and graded mesh refinement (2D & 3D) are used to improve accuracy near the crack tip or crack front
- Stable quadrature scheme is proposed for singular integration in 3D. This makes the method non-sensitive to mesh distortion
- Different ways to extract stress intensity factors based on the framework of IGABEM

➡ **Questions**

- Geometry-independent field approximation (GIFT)
- Independent displacement and traction approximations
- Independent geometry and field approximations
- Contact (BETI)
- BEM Acceleration

Part II. Some recent advances in enriched FEM

CARDIFF UNIVERSITY
PRIFYSGOL CAERDYDD

Handling discontinuities in isogeometric formulations

with Nguyen Vinh Phu, Marie Curie Fellow

IMAM
Institute of Mechanics & Advanced Materials

Discontinuities modeling

PUM enriched methods

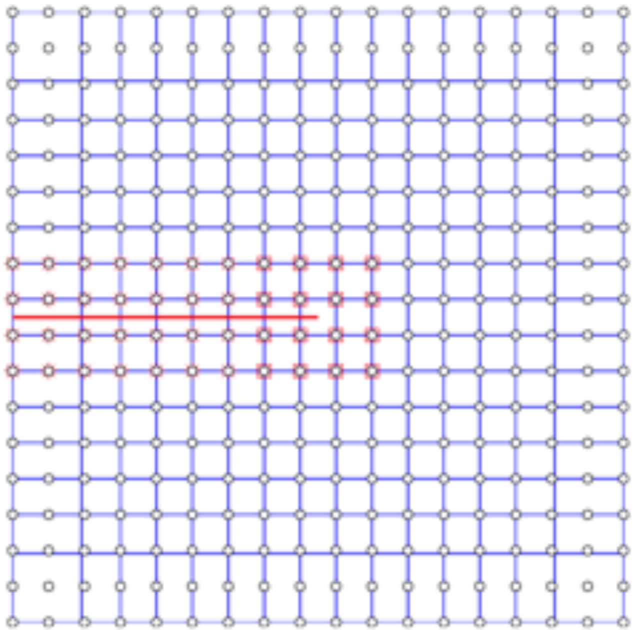

- IGA: link to CAD and accurate stress fields
- XFEM: no remeshing

Mesh conforming methods

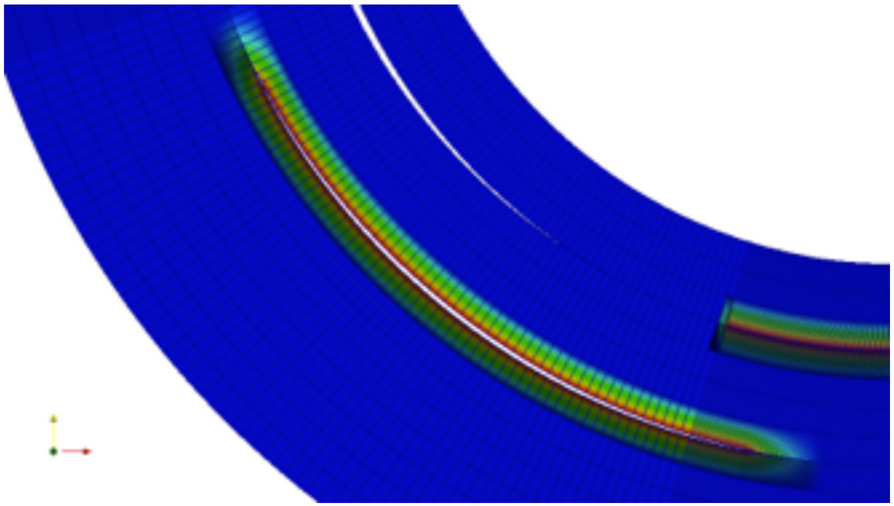

- IGA: link to CAD and accurate stress fields
- Apps: delamination

PUM enriched methods (XIGA)

$$\mathbf{u}^h(\mathbf{x}) = \sum_{I \in \mathcal{S}} R_I(\mathbf{x})\mathbf{u}_I + \sum_{J \in \mathcal{S}^c} R_J(\mathbf{x})\Phi(\mathbf{x})\mathbf{a}_J$$

NURBS basis functions   enrichment functions

1. E. De Luycker, D. J. Benson, T. Belytschko, Y. Bazilevs, and M. C. Hsu. X-FEM in isogeometric analysis for linear fracture mechanics. IJNME, 87(6):541–565, 2011.
2. S. S. Ghorashi, N. Valizadeh, and S. Mohammadi. Extended isogeometric analysis for simulation of stationary and propagating cracks. IJNME, 89(9): 1069–1101, 2012.
3. D. J. Benson, Y. Bazilevs, E. De Luycker, M.-C. Hsu, M. Scott, T. J. R. Hughes, and T. Belytschko. A generalized finite element formulation for arbitrary basis functions: From isogeometric analysis to XFEM. IJNME, 83(6):765–785, 2010.
4. A. Tambat and G. Subbarayan. Isogeometric enriched field approximations. CMAME, 245–246:1 – 21, 2012.

Delamination analysis with cohesive elements (standard approach)

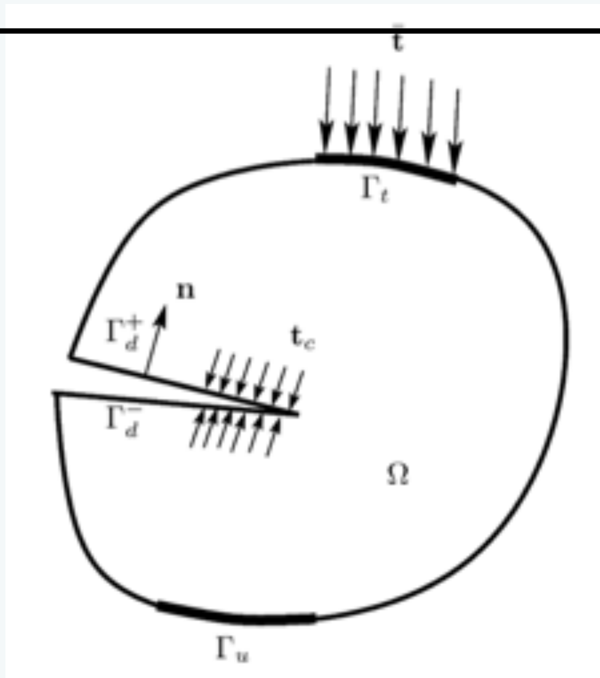

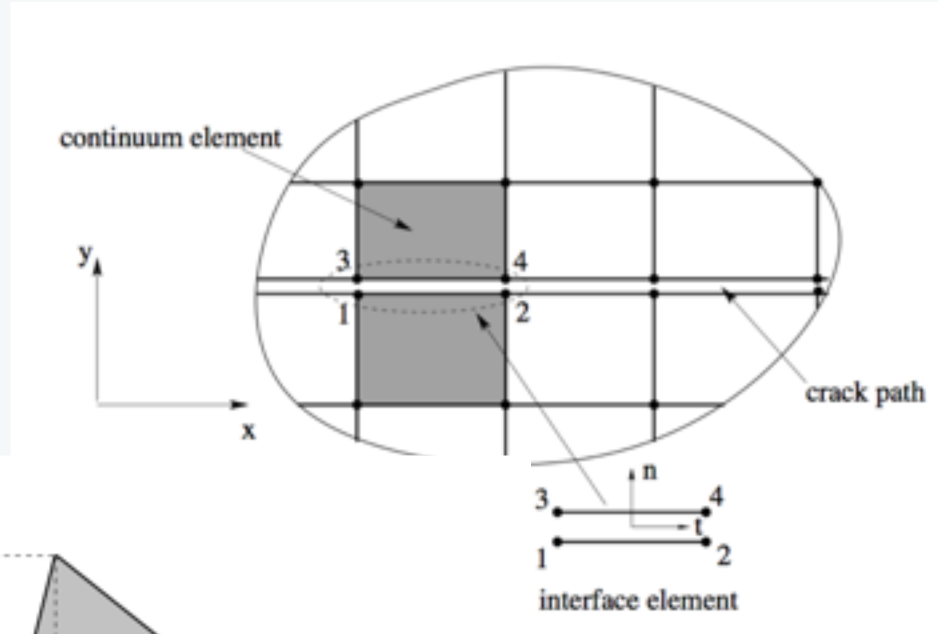

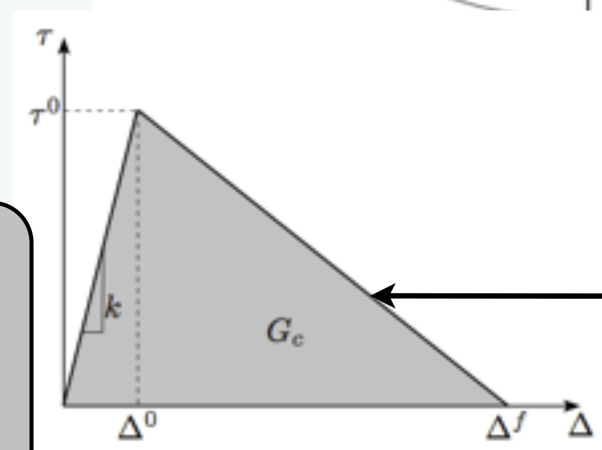

- No link to CAD
- Long preprocessing
- Refined meshes

$$\int_\Omega \delta\mathbf{u}\cdot\mathbf{b}\,\mathrm{d}\Omega + \int_{\Gamma_t}\delta\mathbf{u}\cdot\bar{\mathbf{t}}\,\mathrm{d}\Gamma_t = \int_\Omega \delta\boldsymbol{\epsilon}:\boldsymbol{\sigma}(\mathbf{u})\,\mathrm{d}\Omega + \int_{\Gamma_d}\delta[\![\mathbf{u}]\!]\cdot\mathbf{t}^c([\![\mathbf{u}]\!])\,\mathrm{d}\Gamma_d$$

Isogeometric cohesive elements

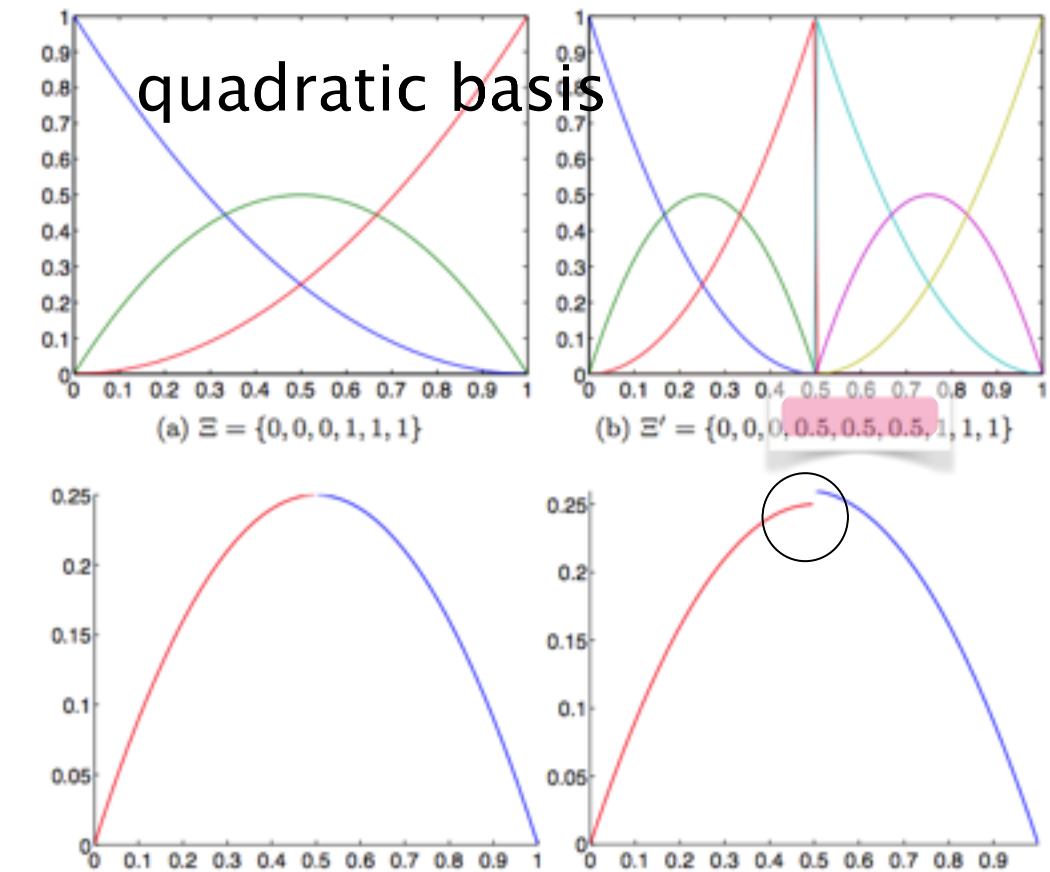

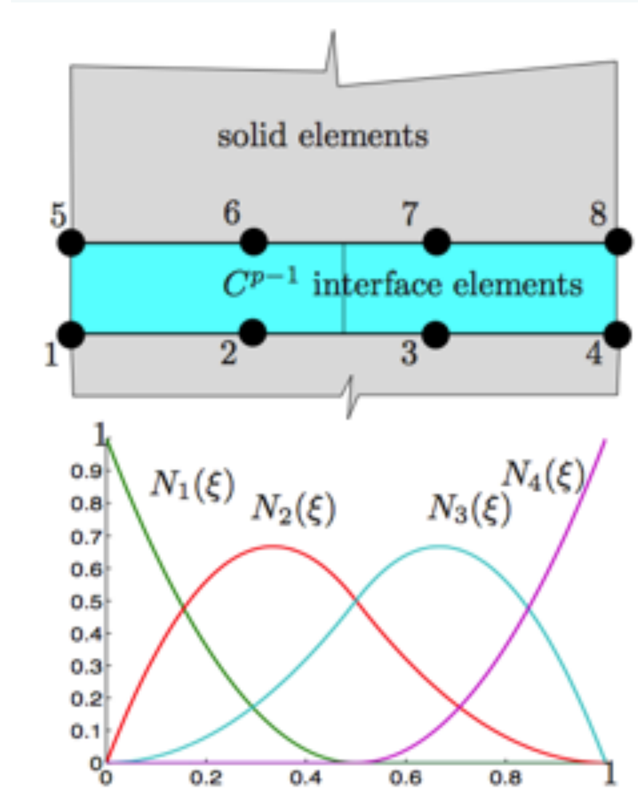

Knot insertion

1. C. V. Verhoosel, M. A. Scott, R. de Borst, and T. J. R. Hughes. An isogeometric approach to cohesive zone modeling. IJNME, 87(15):336–360, 2011.
2. V.P. Nguyen, P. Kerfriden, S. Bordas. Isogeometric cohesive elements for two and three dimensional composite delamination analysis, 2013, Arxiv.

Isogeometric cohesive elements: advantages

- Direct link to CAD
- Exact geometry
- Fast/straightforward generation of interface elements
- Accurate stress field
- Computationally cheaper

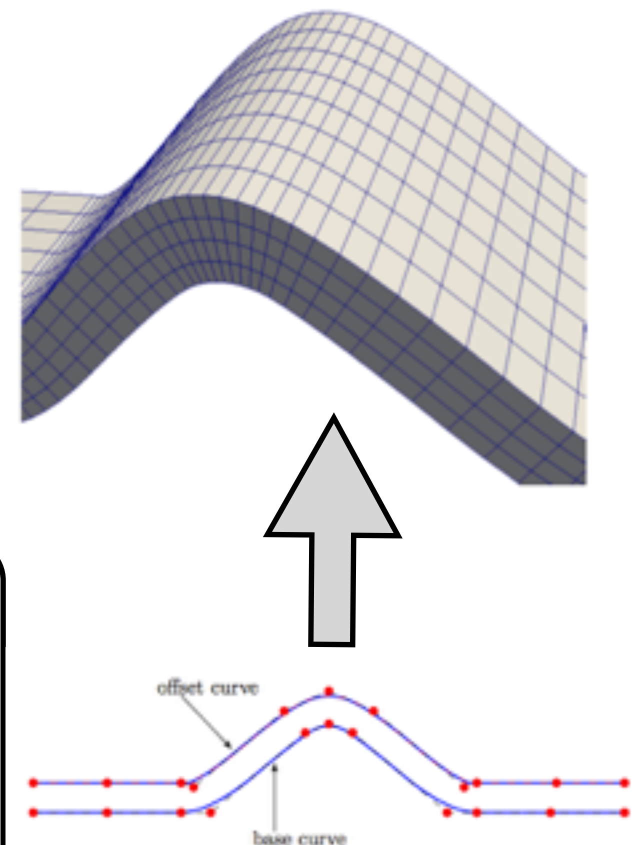

- 2D Mixed mode bending test (MMB)
- 2 x 70 quartic-linear B-spline elements
- Run time on a laptop 4GBi7: 6 s
- Energy arc-length control

V. P. Nguyen and H. Nguyen-Xuan. High-order B-splines based finite elements for delamination analysis of laminated composites. Composite Structures, 102:261–275, 2013.

Isogeometric cohesive elements: 2D example

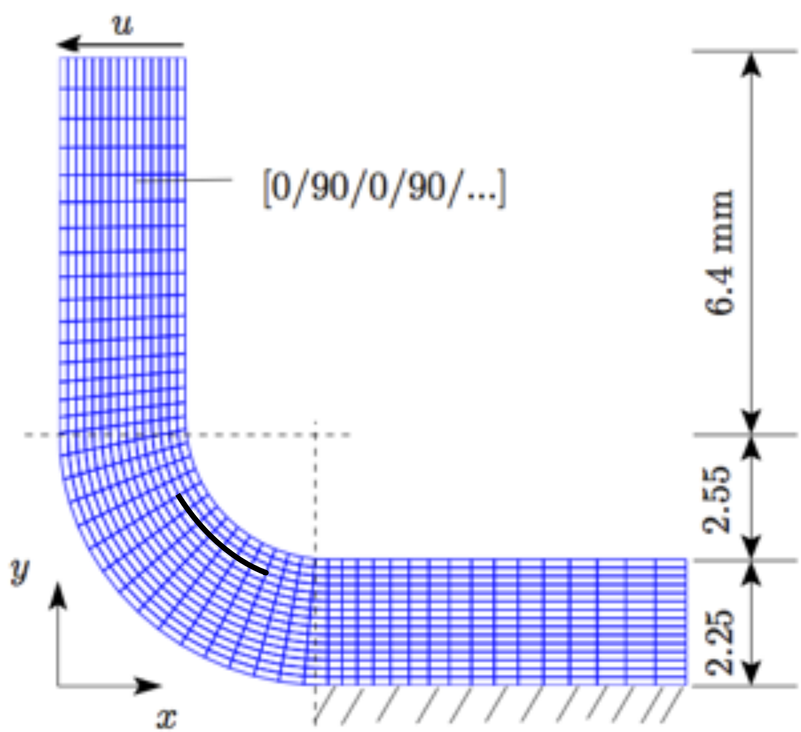

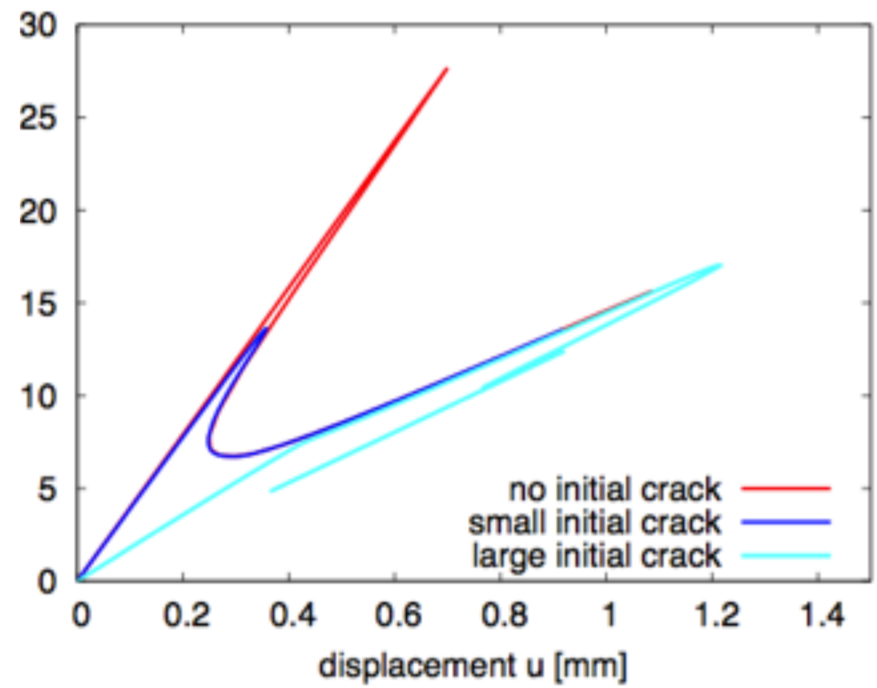

- Exact geometry by NURBS + direct link to CAD
- It is straightforward to vary
  (1) the number of plies and
  (2) # of interface elements:
- Suitable for parameter studies/design
- Solver: energy-based arc-length method (Gutierrez, 2007)

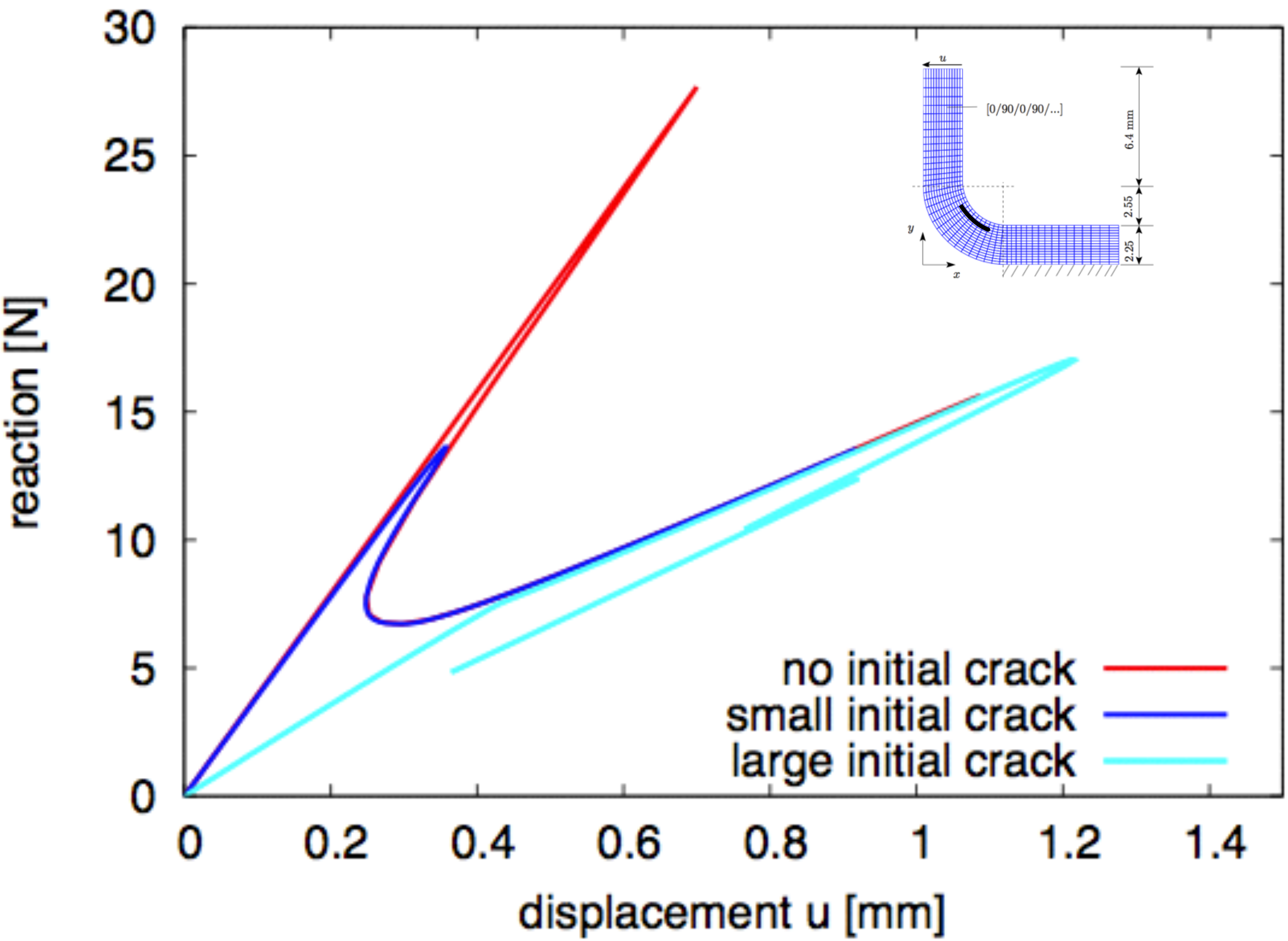
reaction [N]
30
25
20
15
10
5
0
0
0.2
0.4
0.6
0.8
1
1.2
1.4
displacement u [mm]
u
[0/90/0/90/...]
6.4 mm
2.55
2.25
y
x
no initial crack
small initial crack
large initial crack

Isogeometric cohesive elements: 2D example

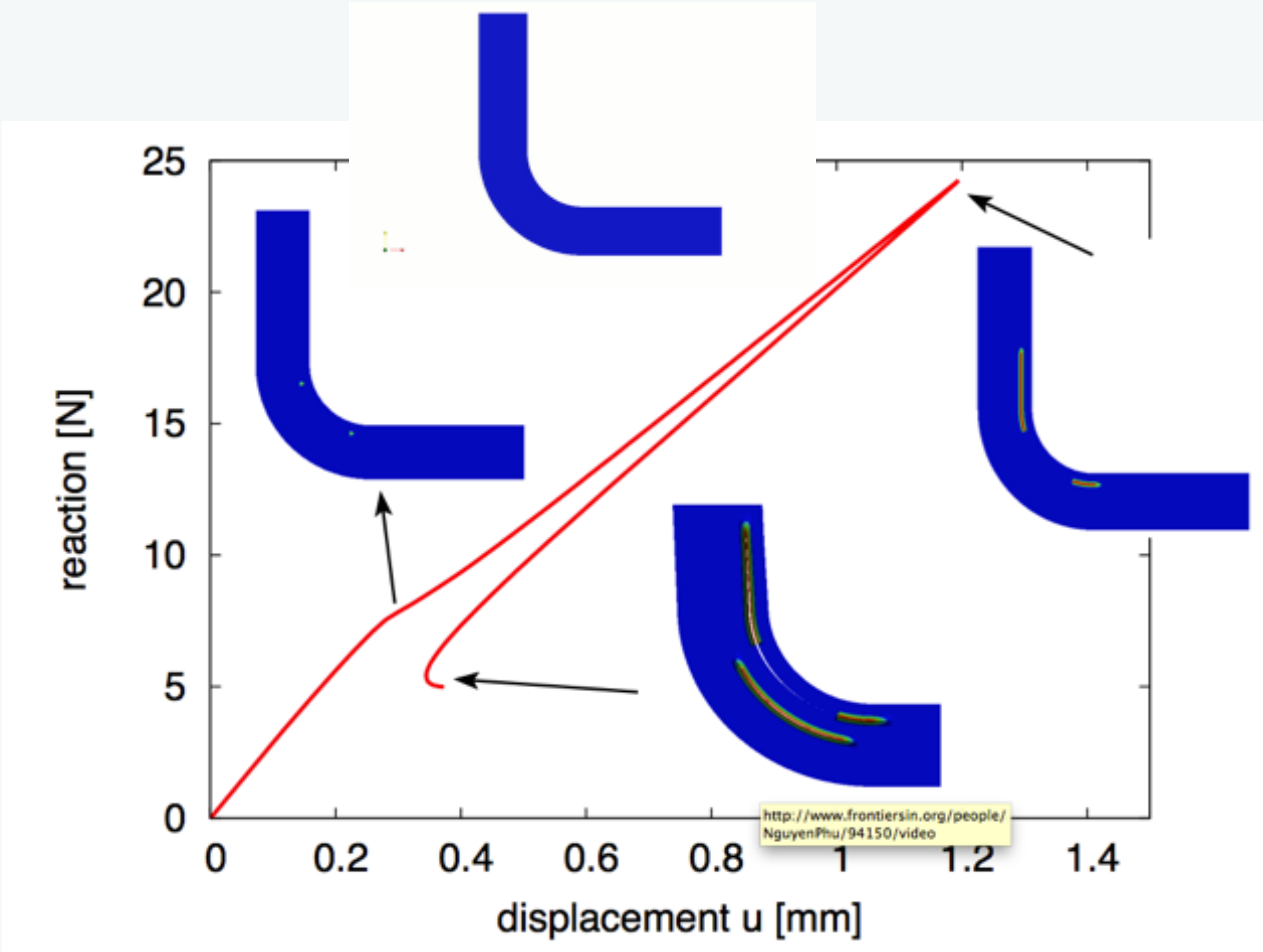

Isogeometric cohesive elements: 3D example with shells

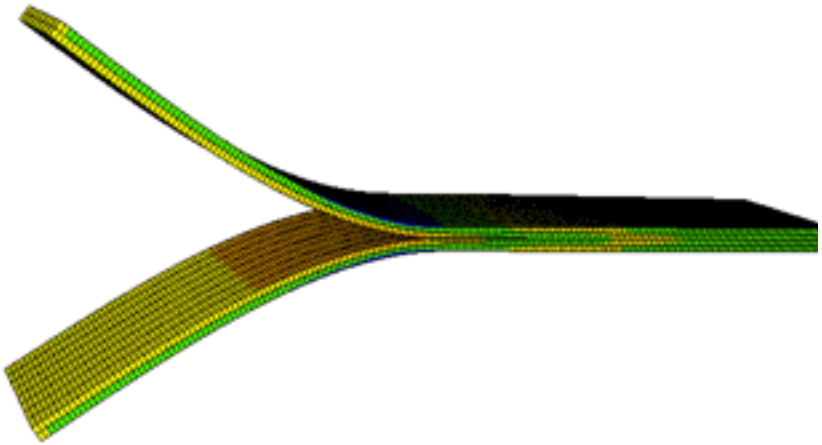

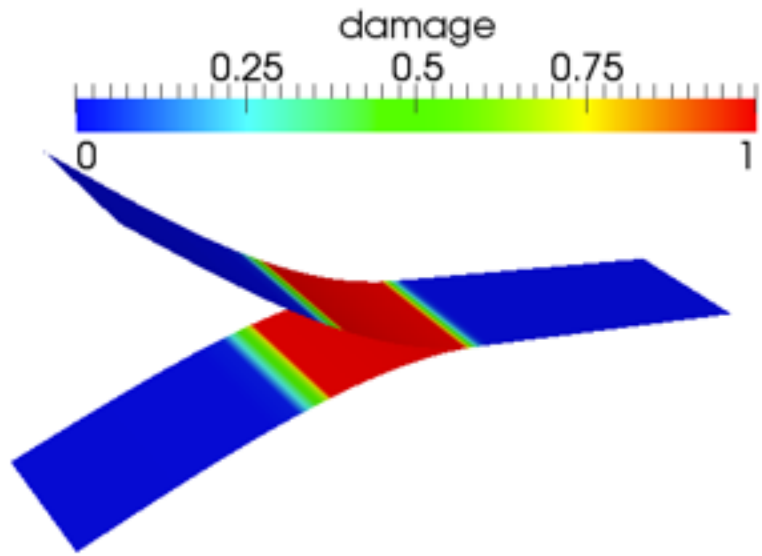

- Rotation free B-splines shell elements (Kiendl et al. CMAME)
- Two shells, one for each lamina
- Bivariate B-splines cohesive interface elements in between

Isogeometric cohesive elements: 3D examples

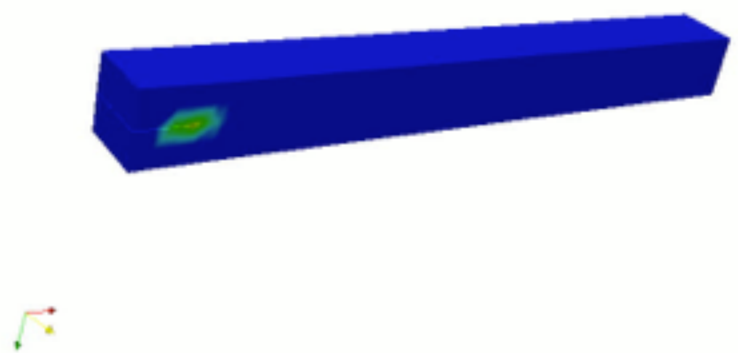

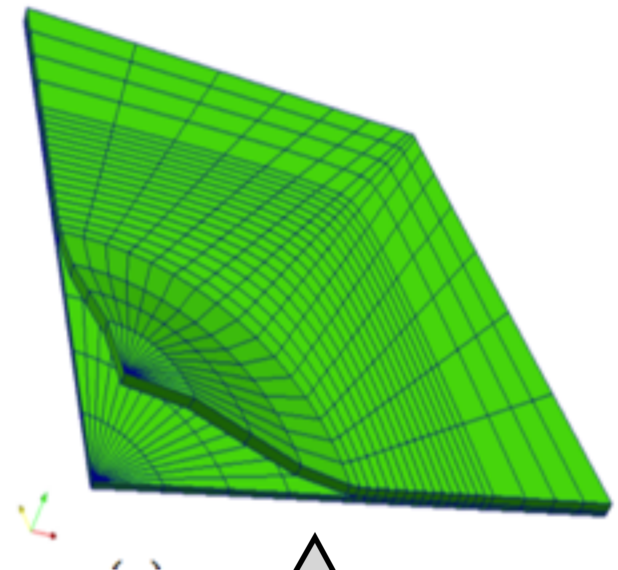

- cohesive elements for 3D meshes the same as 2D
- large deformations

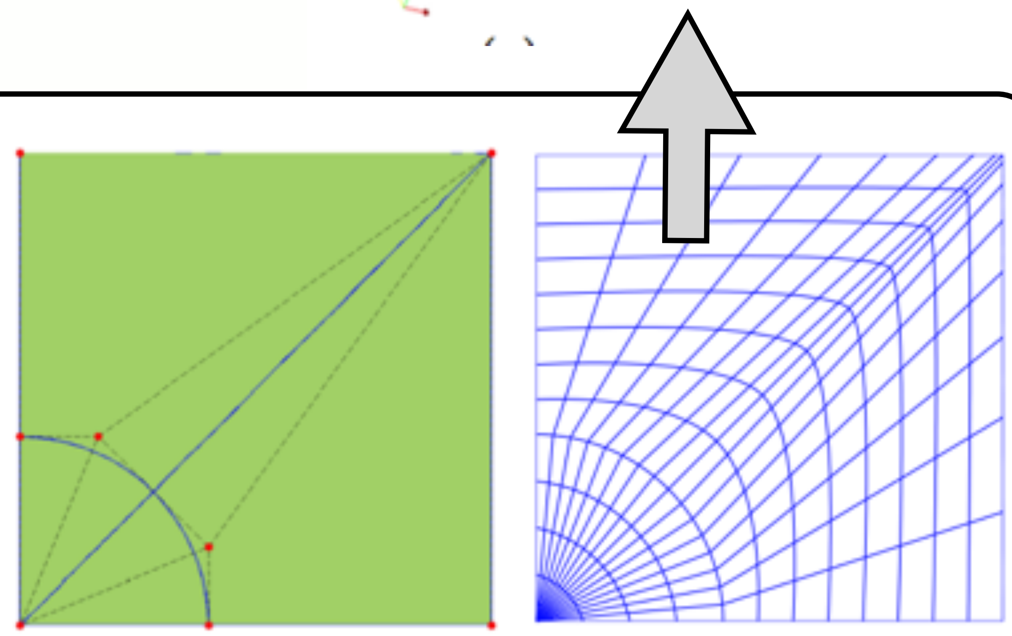

Isogeometric cohesive elements

- singly curved thick-wall laminates
- geometry/displacements: NURBS
- trivariate NURBS from NURBS surface(*)
- cohesive surface interface elements

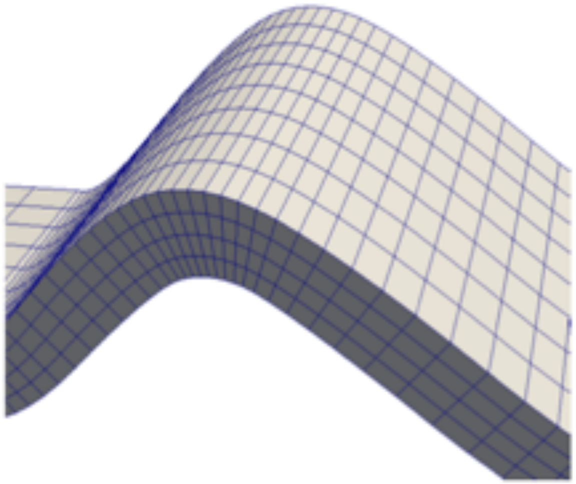

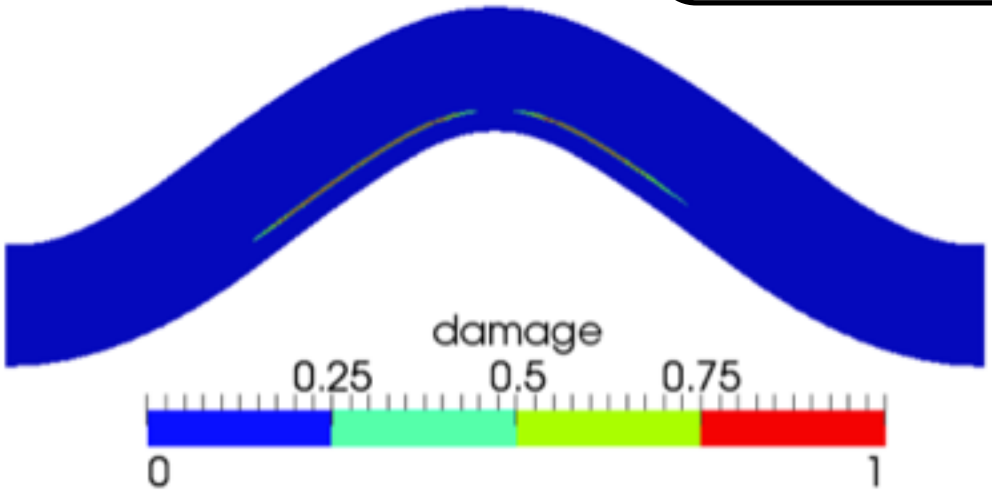

(*)V. P. Nguyen, P. Kerfriden, S.P.A. Bordas, and T. Rabczuk. An integrated design-analysis framework for three dimensional composite panels. Computer Aided Design, 2013. submitted.

Non-matching interface elements for delamination and contact

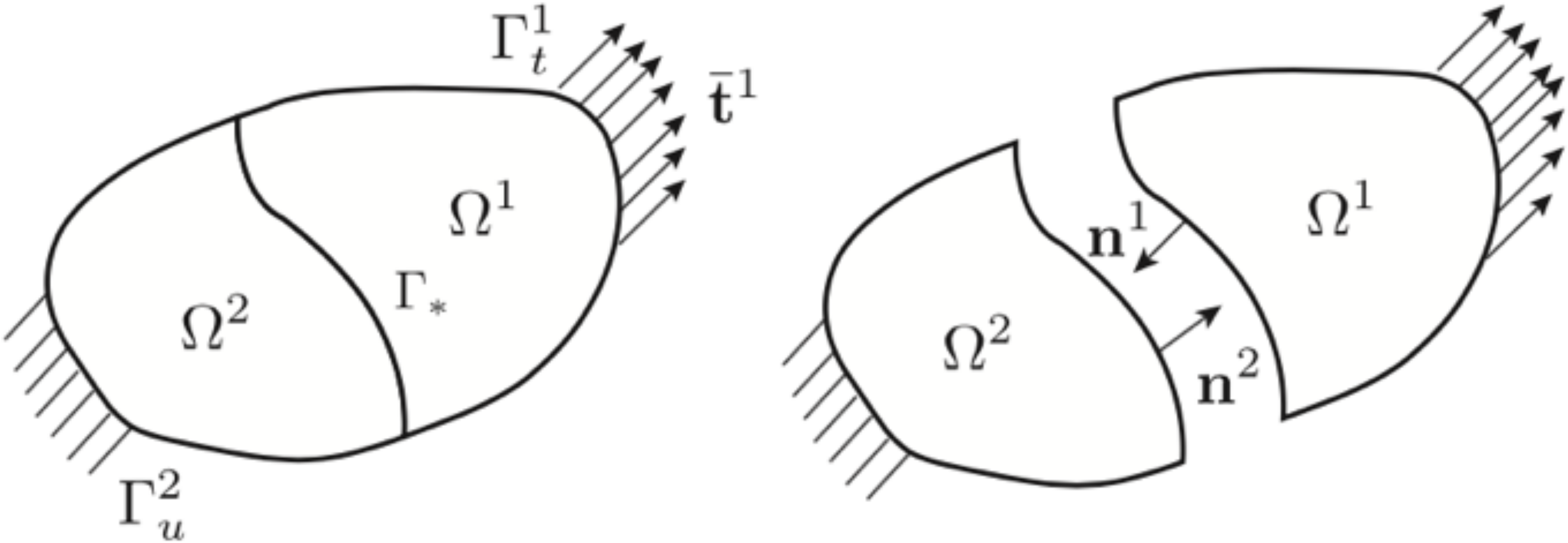

Non-matching interface elements for delamination and contact

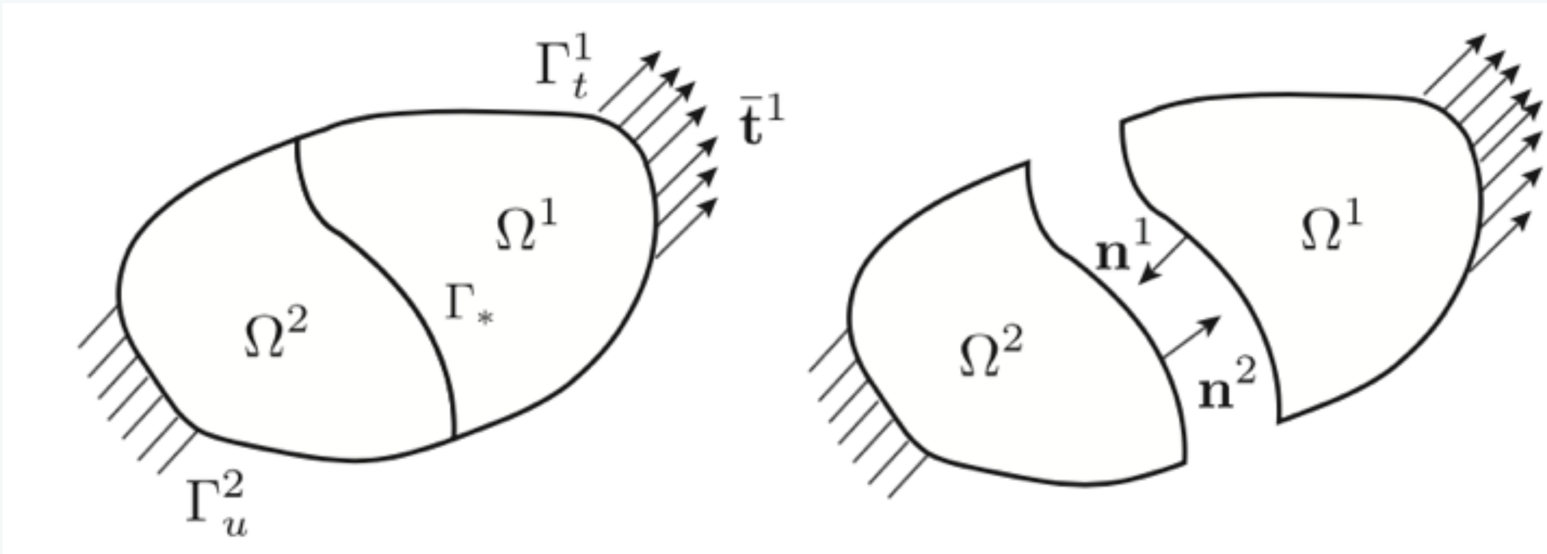

$$
\begin{aligned}
-\nabla \cdot \boldsymbol{\sigma}^m &= \mathbf{b}^m && \text{on} \quad \Omega^m \\
\mathbf{u}^m &= \bar{\mathbf{u}}^m && \text{on} \quad \Gamma_u^m \\
\boldsymbol{\sigma}^m \cdot \mathbf{n}^m &= \bar{\mathbf{t}}^m && \text{on} \quad \Gamma_t^m \\
\mathbf{u}^1 &= \mathbf{u}^2 && \text{on} \quad \Gamma_* \\
\boldsymbol{\sigma}^1 \cdot \mathbf{n}^1 &= -\boldsymbol{\sigma}^2 \cdot \mathbf{n}^2 && \text{on} \quad \Gamma_*
\end{aligned}
$$

$$
\begin{aligned}
-\nabla\, \boldsymbol{\sigma}^m &= \mathbf{b}^m && \text{on} \quad \Omega^m \\
\mathbf{u}^m &= \bar{\mathbf{u}}^m && \text{on} \quad \Gamma_u^m \\
\boldsymbol{\sigma}^m \cdot \mathbf{n}^m &= \bar{\mathbf{t}}^m && \text{on} \quad \Gamma_t^m \\
-\boldsymbol{\sigma}^1 \cdot \mathbf{n}^1 = \boldsymbol{\sigma}^2 \cdot \mathbf{n}^2 &= \mathbf{t} && \text{on} \quad \Gamma_* \\
\mathbf{t} &= \mathbf{t}([\![\mathbf{u}]\!], \zeta) && \text{on} \quad \Gamma_*
\end{aligned}
$$

Non-matching interface elements for delamination and contact

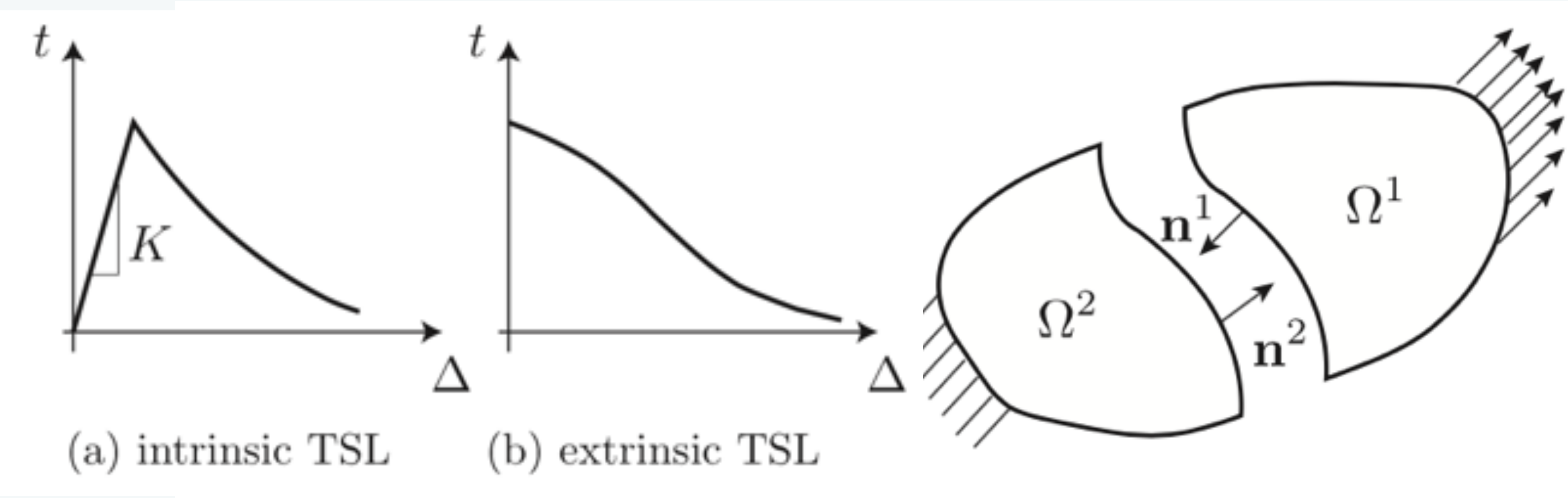

$$
\begin{aligned}
-\nabla \cdot \boldsymbol{\sigma}^m &= \mathbf{b}^m && \text{on} \quad \Omega^m \\
\mathbf{u}^m &= \bar{\mathbf{u}}^m && \text{on} \quad \Gamma_u^m \\
\boldsymbol{\sigma}^m \cdot \mathbf{n}^m &= \bar{\mathbf{t}}^m && \text{on} \quad \Gamma_t^m \\
\mathbf{u}^1 &= \mathbf{u}^2 && \text{on} \quad \Gamma_* \\
\boldsymbol{\sigma}^1 \cdot \mathbf{n}^1 &= -\boldsymbol{\sigma}^2 \cdot \mathbf{n}^2 && \text{on} \quad \Gamma_*
\end{aligned}
$$

$$
\begin{aligned}
-\nabla \, \boldsymbol{\sigma}^m &= \mathbf{b}^m && \text{on} \quad \Omega^m \\
\mathbf{u}^m &= \bar{\mathbf{u}}^m && \text{on} \quad \Gamma_u^m \\
\boldsymbol{\sigma}^m \cdot \mathbf{n}^m &= \bar{\mathbf{t}}^m && \text{on} \quad \Gamma_t^m \\
-\boldsymbol{\sigma}^1 \cdot \mathbf{n}^1 = \boldsymbol{\sigma}^2 \cdot \mathbf{n}^2 &= \mathbf{t} && \text{on} \quad \Gamma_* \\
\mathbf{t} &= \mathbf{t}([\![\mathbf{u}]\!], \zeta) && \text{on} \quad \Gamma_*
\end{aligned}
$$

Weak form

$$\boldsymbol{S}^m = \{\mathbf{u}^m(\mathbf{x}) | \mathbf{u}^m(\mathbf{x}) \in \boldsymbol{H}^1(\Omega^m), \mathbf{u}^m = \bar{\mathbf{u}}^m \text{ on } \Gamma_u^m\}$$

$$\boldsymbol{V}^m = \{\mathbf{w}^m(\mathbf{x}) | \mathbf{w}^m(\mathbf{x}) \in \boldsymbol{H}^1(\Omega^m), \mathbf{w}^m = \mathbf{0} \text{ on } \Gamma_u^m\}$$

Find $(\mathbf{u}^1, \mathbf{u}^2) \in \boldsymbol{S}^1 \times \boldsymbol{S}^2$ such that

$$\sum_{m=1}^{2} \int_{\Omega^m} (\boldsymbol{\epsilon}(\mathbf{w}^m))^{\mathrm{T}} \boldsymbol{\sigma}^m \mathrm{d}\Omega + (1-\beta)\left[-\int_{\Gamma_*} [\![\mathbf{w}]\!]^{\mathrm{T}} \mathbf{n}\{\boldsymbol{\sigma}\} \mathrm{d}\Gamma - \int_{\Gamma_*} \{\boldsymbol{\sigma}(\mathbf{w})\}^{\mathrm{T}} \mathbf{n}^{\mathrm{T}} [\![\mathbf{u}]\!] \mathrm{d}\Gamma + \int_{\Gamma_*} \alpha [\![\mathbf{w}]\!]^{\mathrm{T}} [\![\mathbf{u}]\!] \mathrm{d}\Gamma\right]$$
$$+\beta \int_{\Gamma_*} [\![\mathbf{w}]\!]^{\mathrm{T}} \mathbf{t}([\![\mathbf{u}]\!]) \mathrm{d}\Gamma = \sum_{m=1}^{2} \int_{\Gamma_t^m} (\mathbf{w}^m)^{\mathrm{T}} \bar{\mathbf{t}}^m \mathrm{d}\Gamma + \sum_{m=1}^{2} \int_{\Omega^m} (\mathbf{w}^m)^{\mathrm{T}} \mathbf{b}^m \mathrm{d}\Omega \quad \text{for all } (\mathbf{w}^1, \mathbf{w}^2) \in \boldsymbol{V}^1 \times \boldsymbol{V}^2$$

$$[\![\mathbf{u}]\!] = \mathbf{u}^1 - \mathbf{u}^2, \quad \{\boldsymbol{\sigma}\} = \gamma \boldsymbol{\sigma}^1 + (1-\gamma)\boldsymbol{\sigma}^2$$

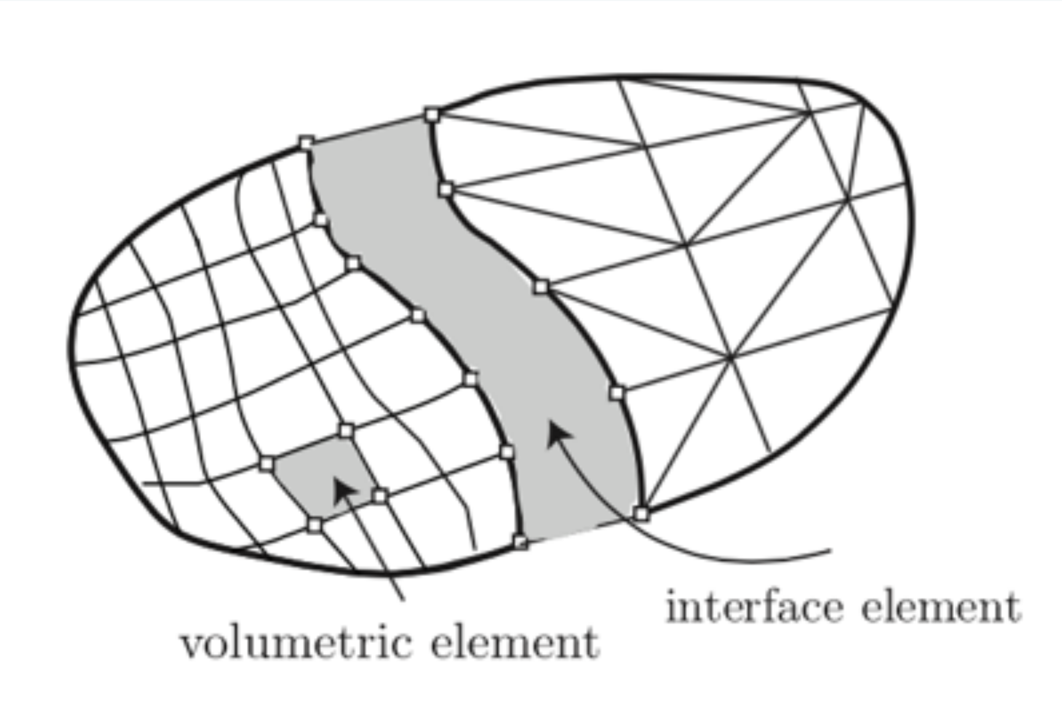

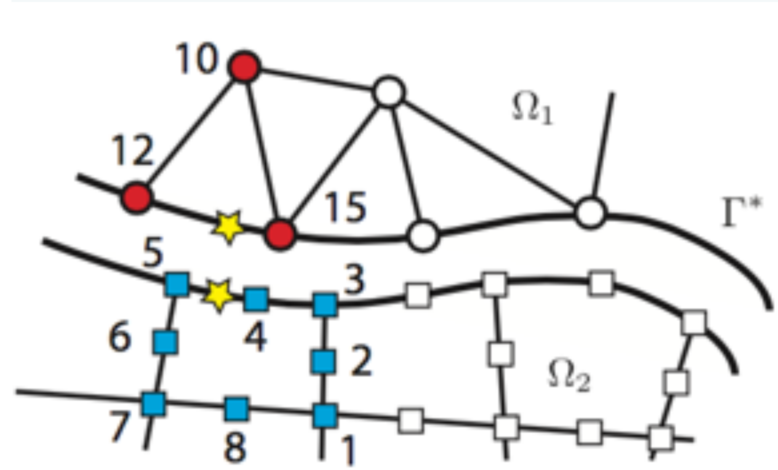

The interface elements are of zero thickness.

2D uniaxial tension test

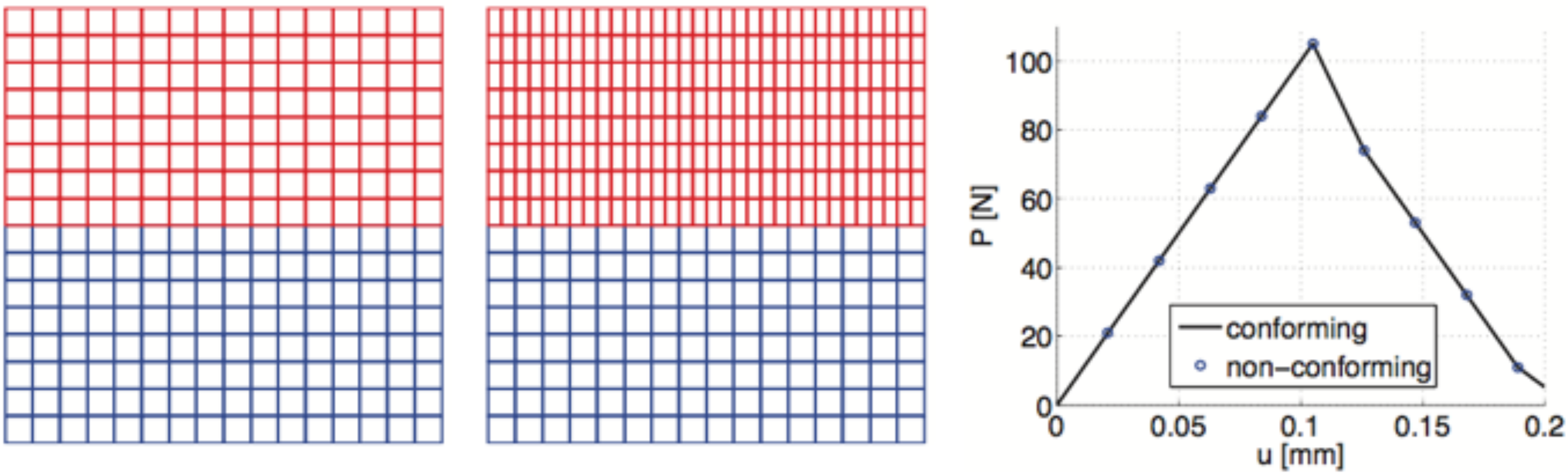

(a) conforming mesh (b) nonconforming mesh (c) load-displacement

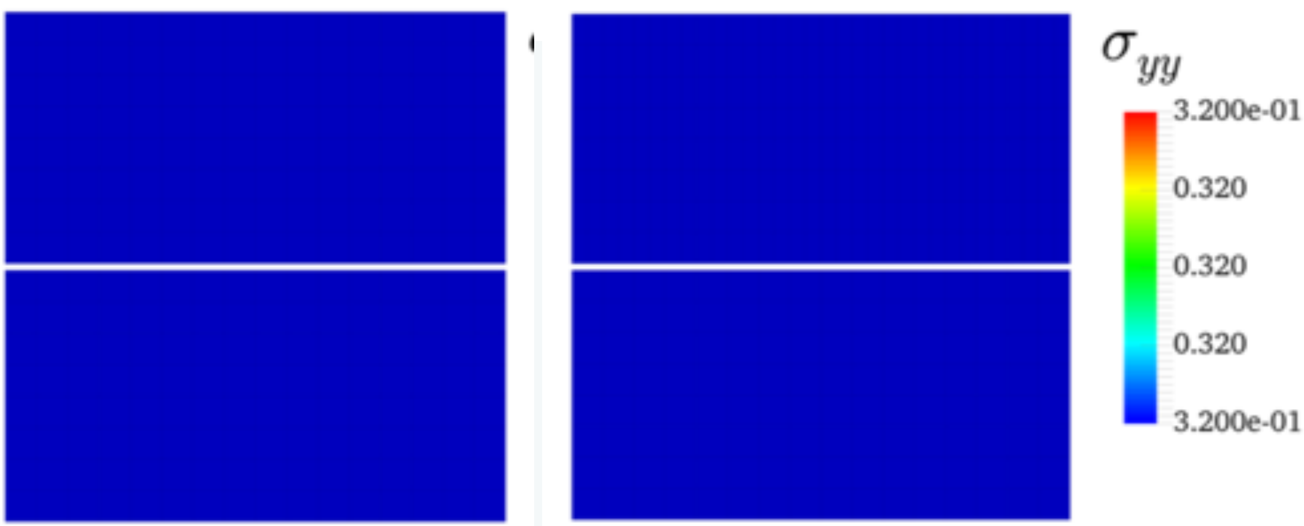

(a) matching mesh (b) non-matching mesh

3D uniaxial tension

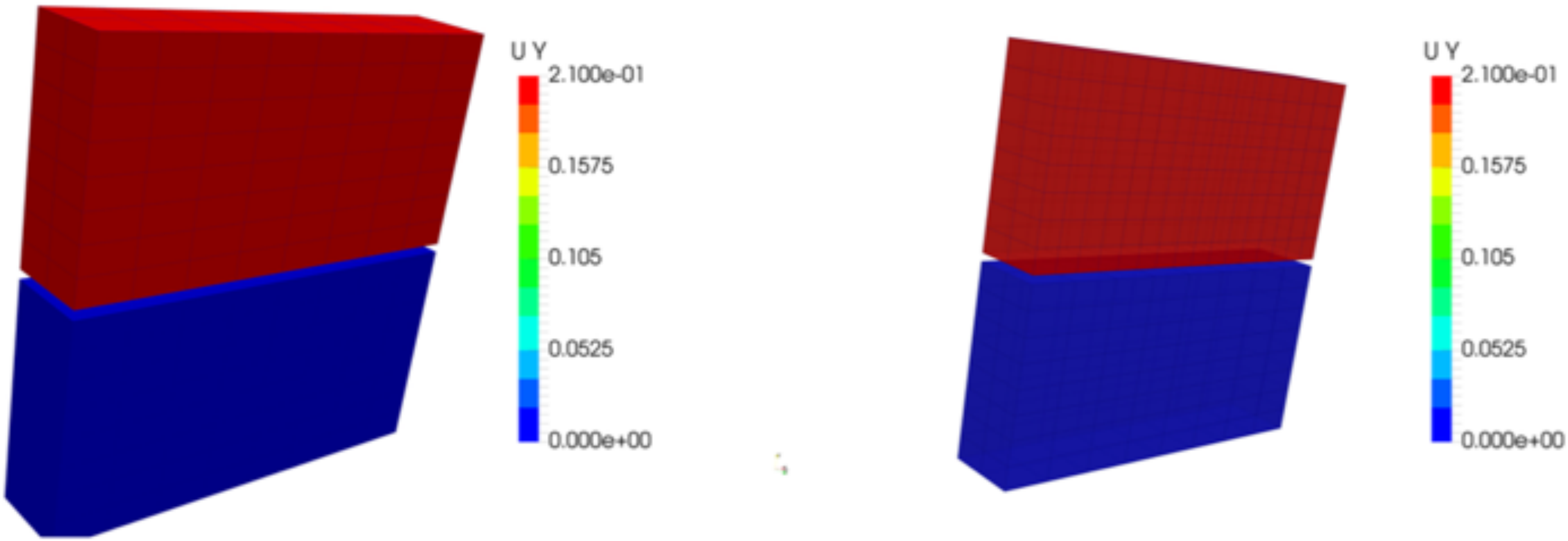

(a) matching mesh (b) non-matching mesh

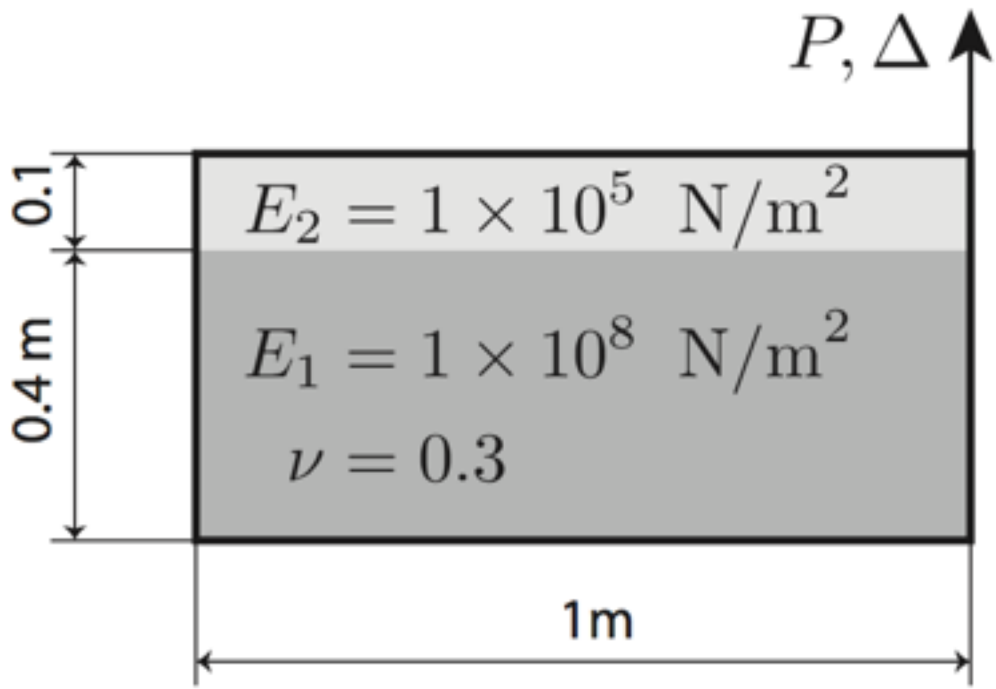

Figure 12: Peeling test: problem configuration.

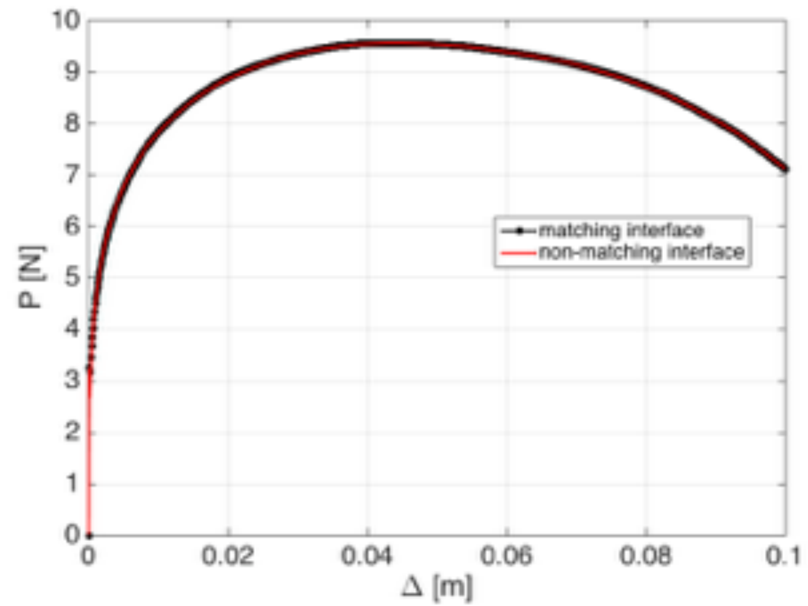

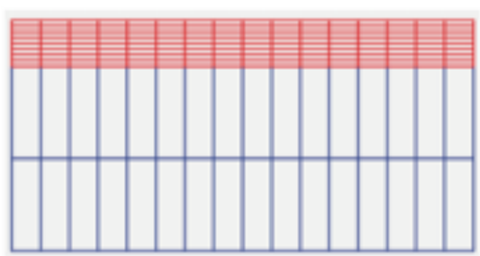

(a) matching mesh

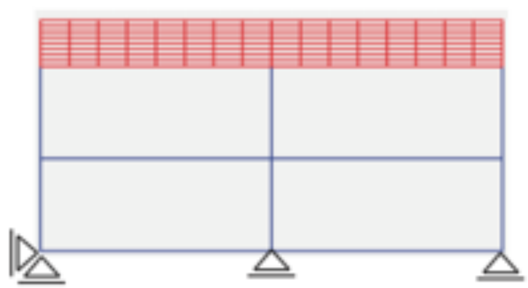

(b) non-matching mesh

2D peeling test

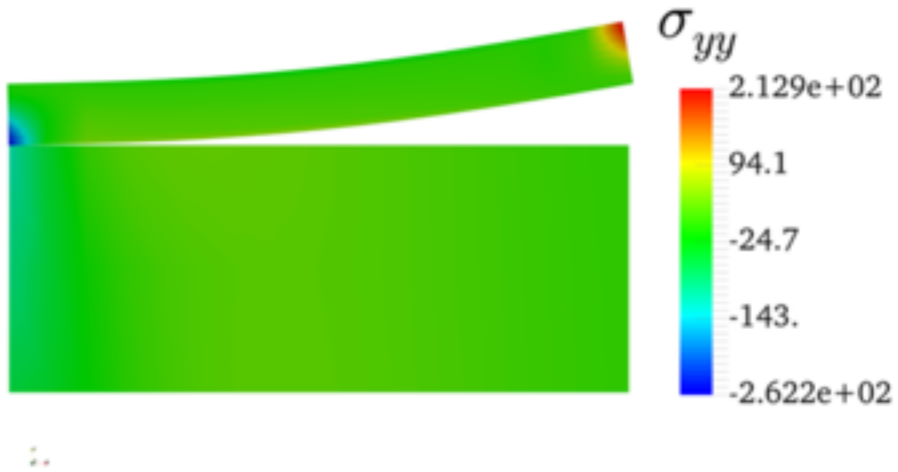

(a) matching mesh

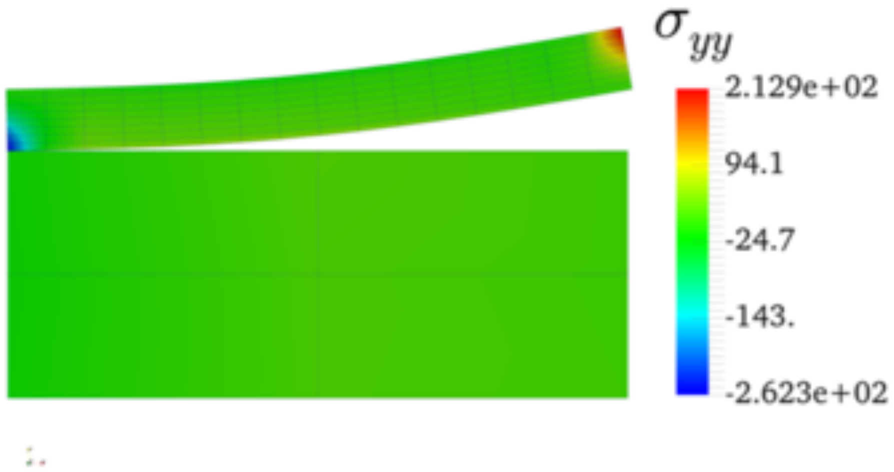

(b) non-matching mesh

2D peeling test

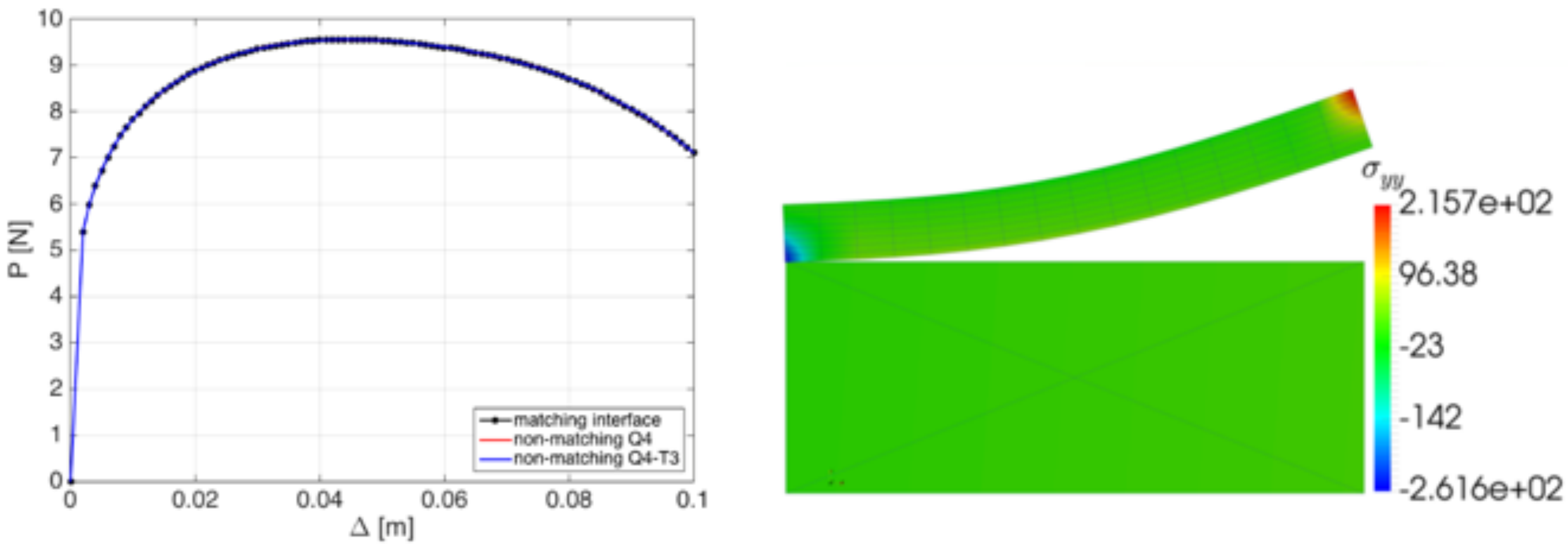

(a) load-displacement (b) stress contour

Figure 17: Peeling test: substrate discretised by three-node triangular elements whereas layer is meshed by Q4 elements. Note that there is a slight difference with the $P - \Delta$ curves in Fig. 14 as displacement increments that are ten times larger were used.

2D peeling test F(D) curves

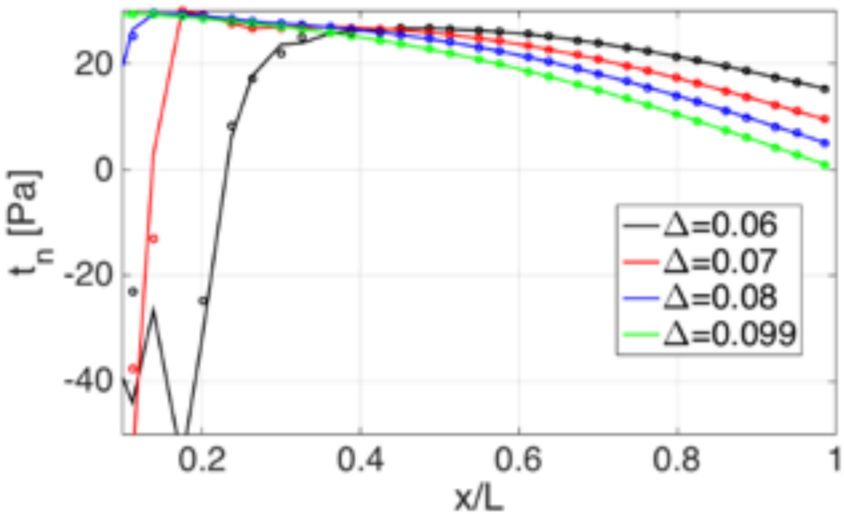

(a) normal cohesive traction

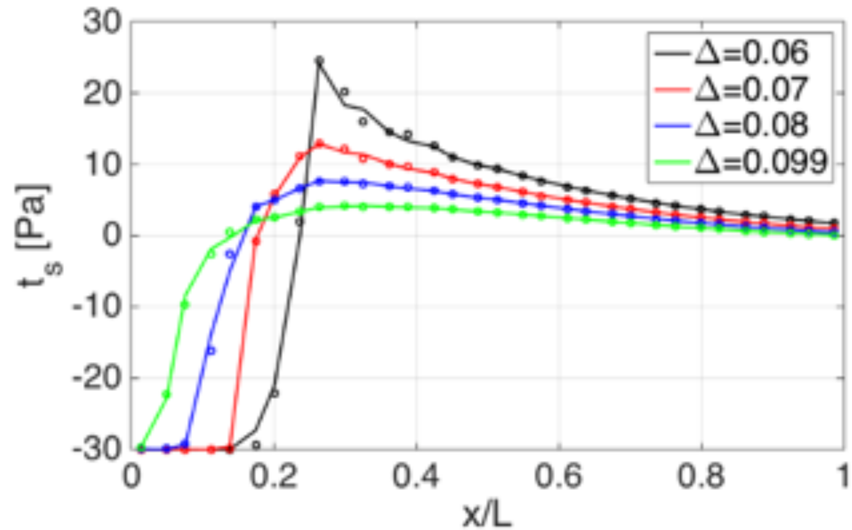

(b) tangential cohesive traction

Figure 18: Peeling test: local response of the proposed interface element (solid lines) vs. standard interface element (circles) for different imposed displacements Δ.

2D peeling test - role of integration

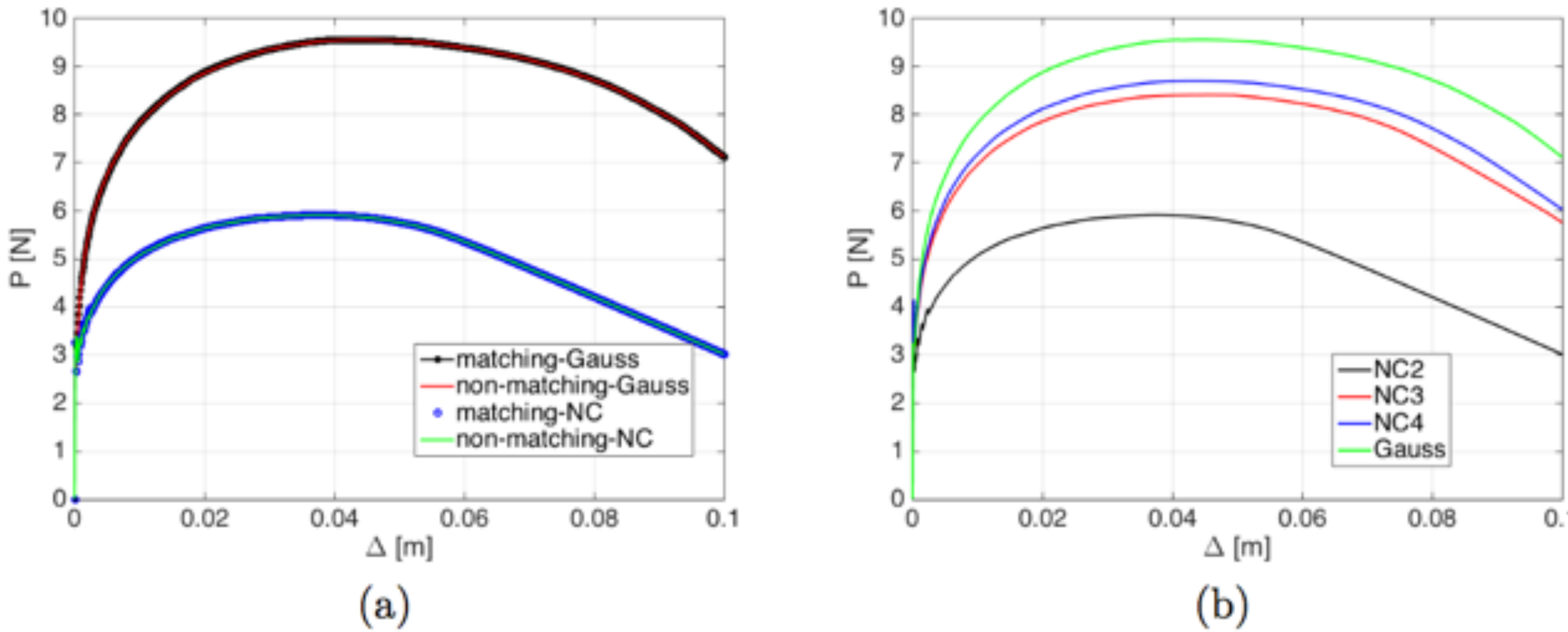

Figure 19: Peeling test: $P - \Delta$ curves obtained with matching and non-matching FE meshes with Gausss and Newton-Cotes (NC) quadrature rules. Increasing the number of NC integration points shift the $P - \Delta$ curves to the Gauss-based curve (right).

3D peeling test

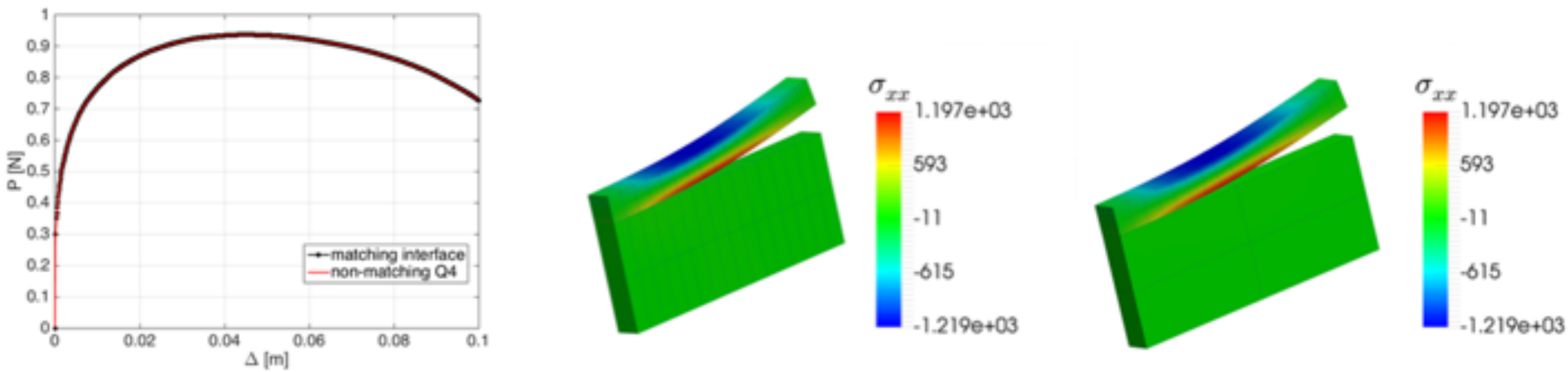

(a) load-displacement (b) matching mesh (c) non-matching

Figure 20: Three dimensional peeling test: $P - \Delta$ curves and stress distribution.

Fibre-reinforced composite - debonding

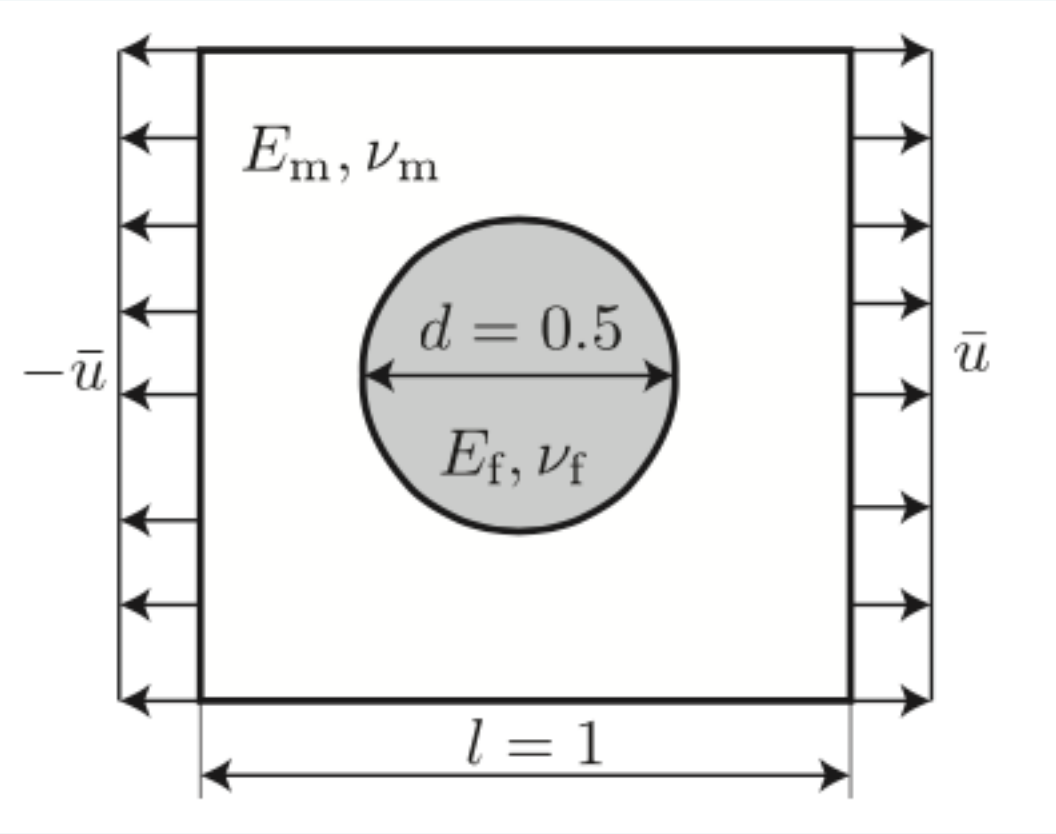

Non-matching interfaces

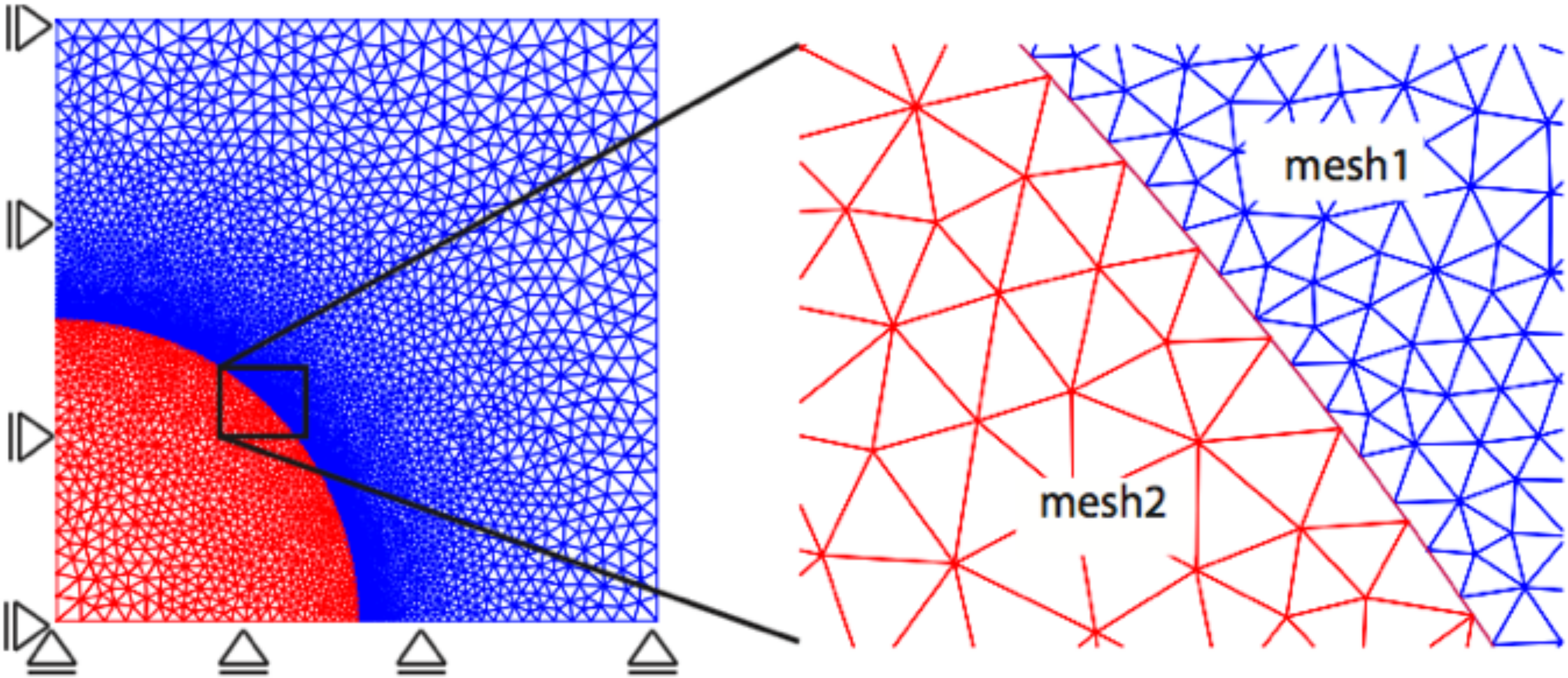

Fibre-debonding

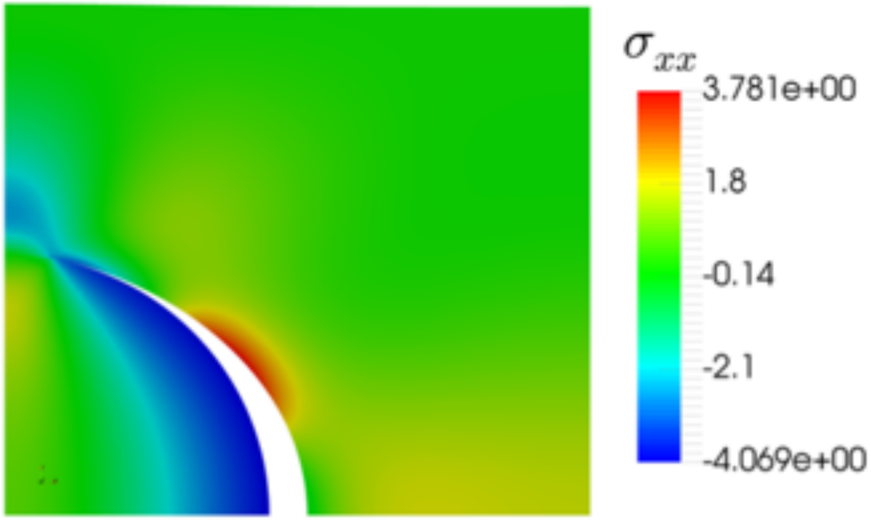

(a) matching mesh

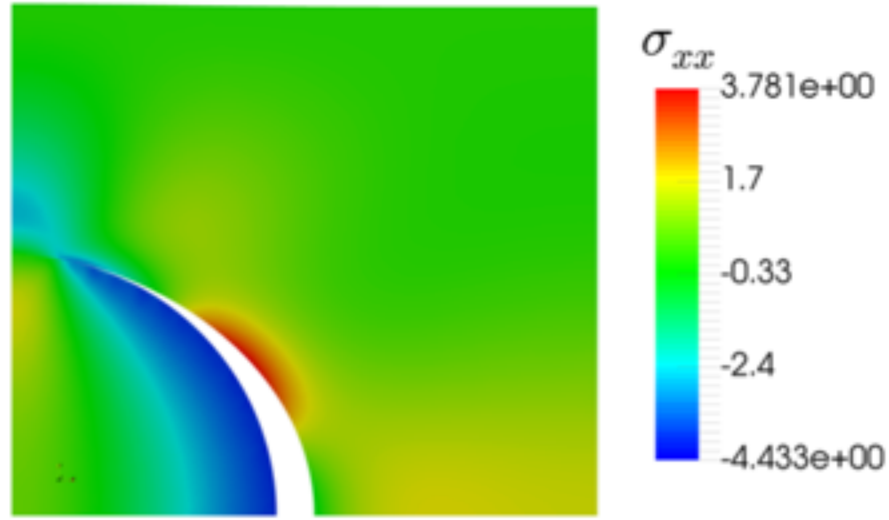

(b) non-matching mesh

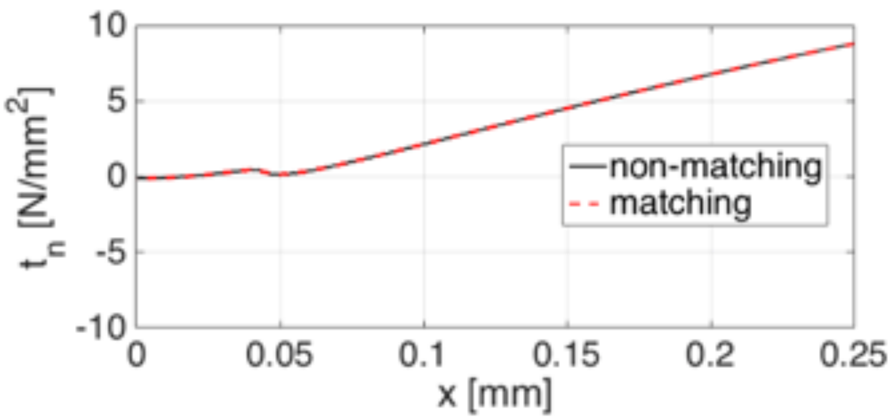

(a) normal stress

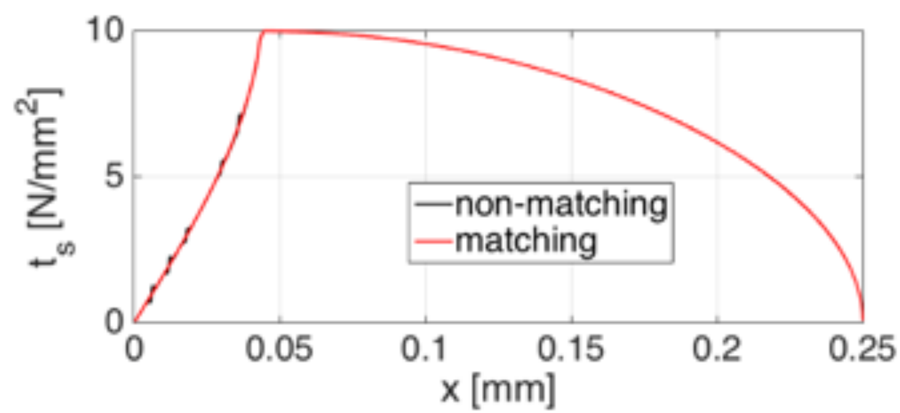

(b) tangential stress

Conclusions

- Incompatible/non-matching elements
- Small strain interfacial fracture
  - No need for conforming meshes along the interface
  - non-matching interface
  - no high-dummy stiffness
  - fewer elements (up to twice as fast)
  - Newton-Cotes integration leads to premature failure

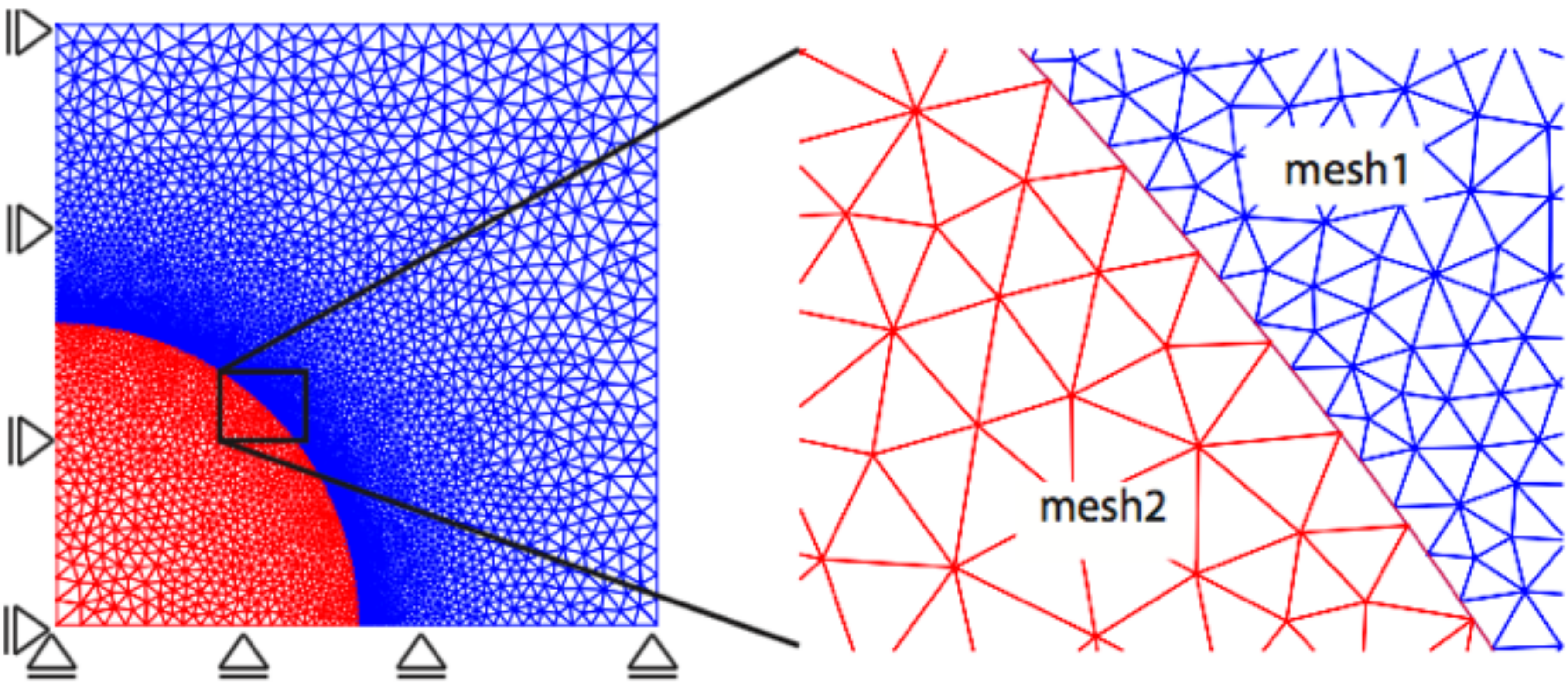

Third medium contact formulation, Wriggers

A finite element method for contact using a third medium P. Wriggers · J. Schröder · A. Schwarz Comput Mech (2013) 52:837–847

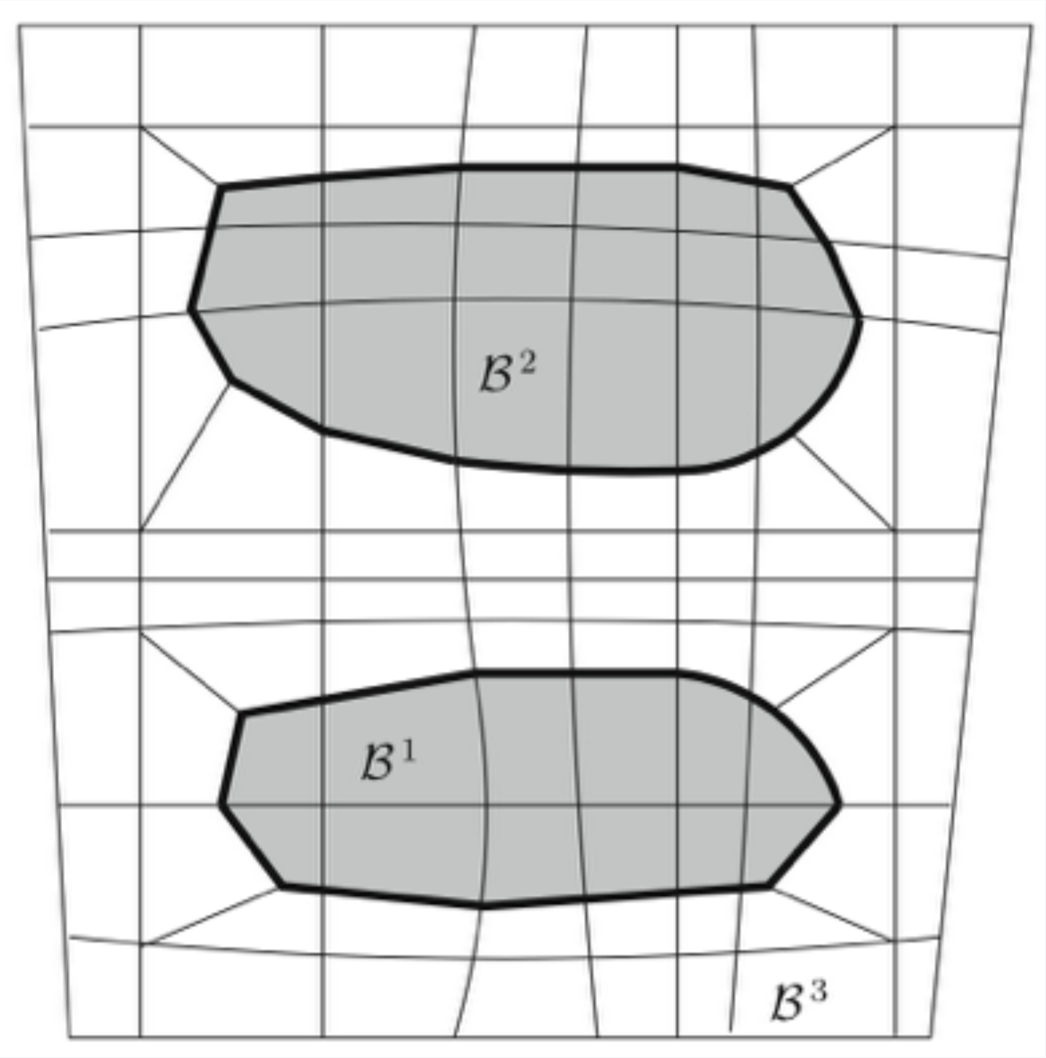

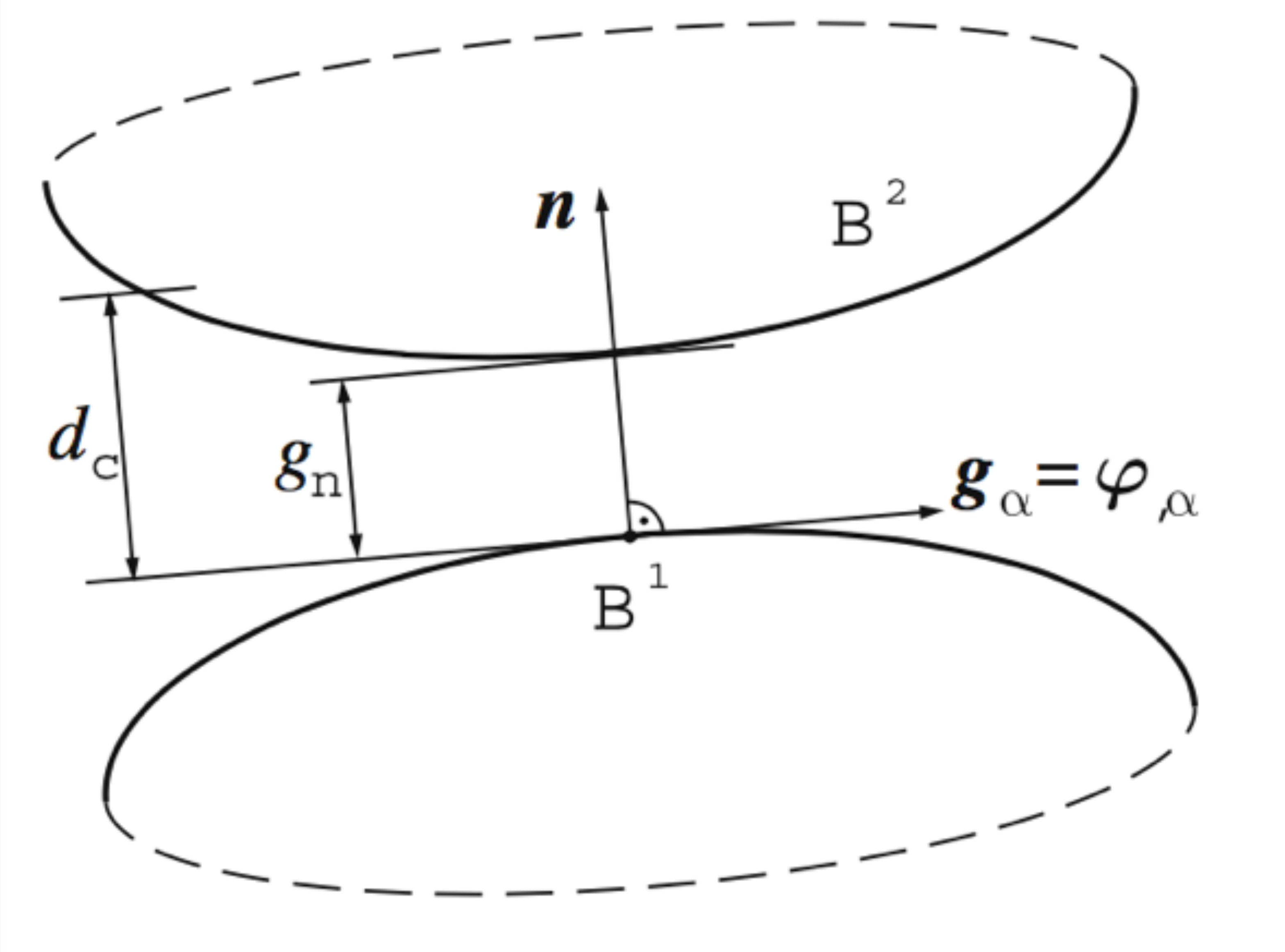

n
B²
d_c
g_n
g_α = φ_,α
B¹

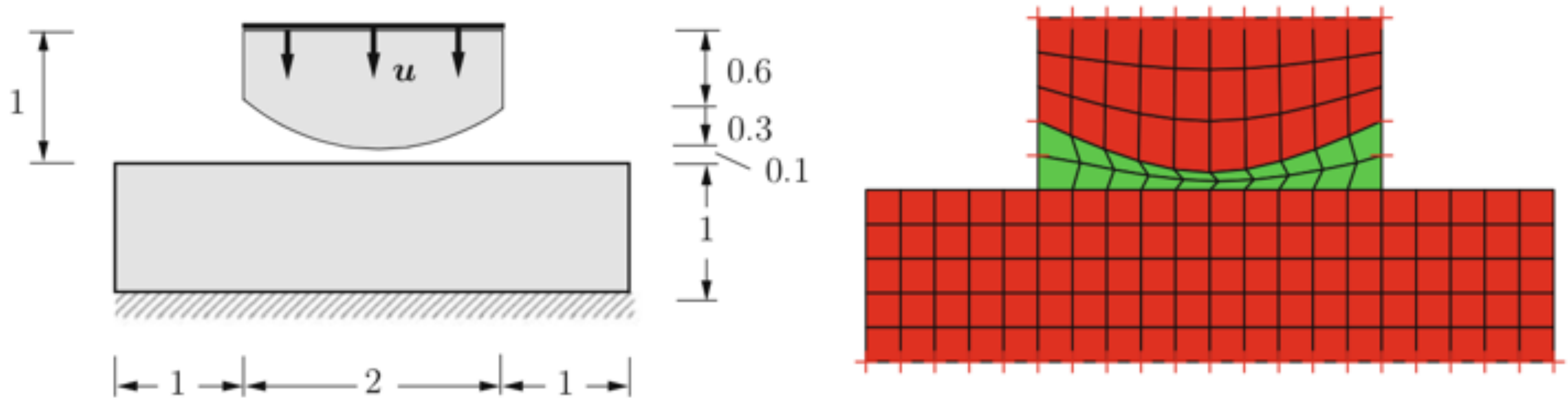
1
u
0.6
0.3
0.1
1
1
2
1

Future work: model selection (continuum, plate, beam, shell?)

Model selection

- Model with shells
- Identify “hot spots” - dual
- Couple with continuum
- Coarse-grain

- Nitsche coupling - NURBS-NURBS

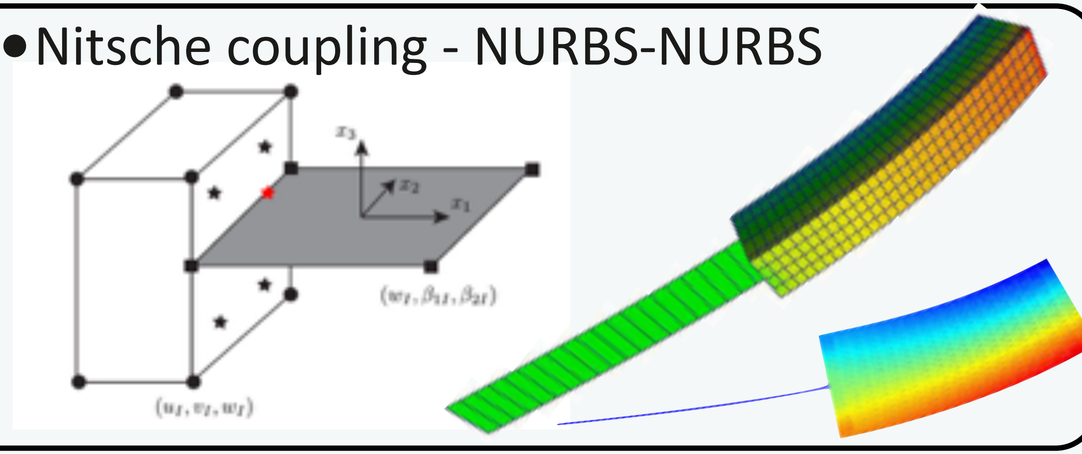

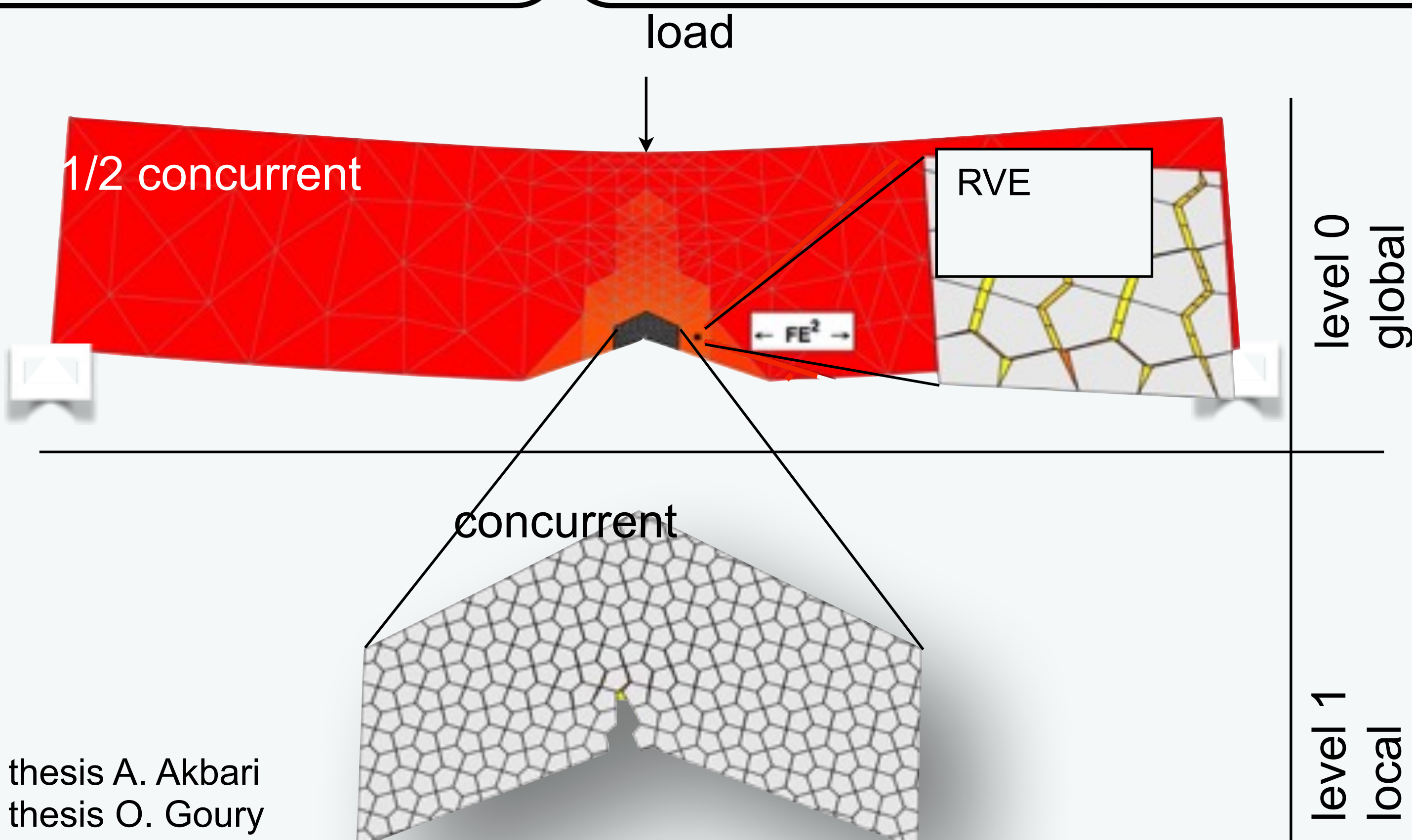

thesis A. Akbari
thesis O. Goury

CARDIFF UNIVERSITY
PRIFYSGOL CAERDYDD

Extended finite element method with smooth nodal stress for linear elastic crack growth

with Xuan Peng, PhD student

IMAM
Institute of Mechanics & Advanced Materials

Double-interpolation finite element method (DFEM)

➢The construction of DFEM in 1D

Discretization

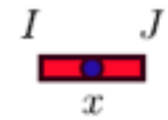

Support domain of FEM

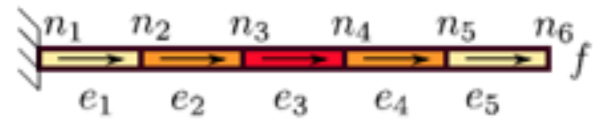

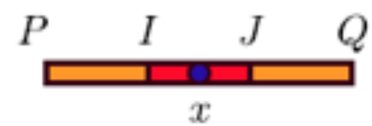

Support domain of DFEM

The ***first stage*** of interpolation: traditional FEM

$$u^h(x) = N_I(x_I)u^I + N_J(x_I)u^J$$

Provide $u, \bar{u}_{,x}$ at each node

The ***second stage*** of interpolation: reproducing from previous result

$$u^h(x) = \phi_I(x)u^I + \psi_I(x)\bar{u}^I_{,x} + \phi_J(x)u^J + \psi_J(x)\bar{u}^J_{,x}$$

$\phi_I, \psi_I, \phi_J, \psi_J$ are Hermitian basis functions

Double-interpolation finite element method (DFEM)

➢ Calculation of average nodal derivatives

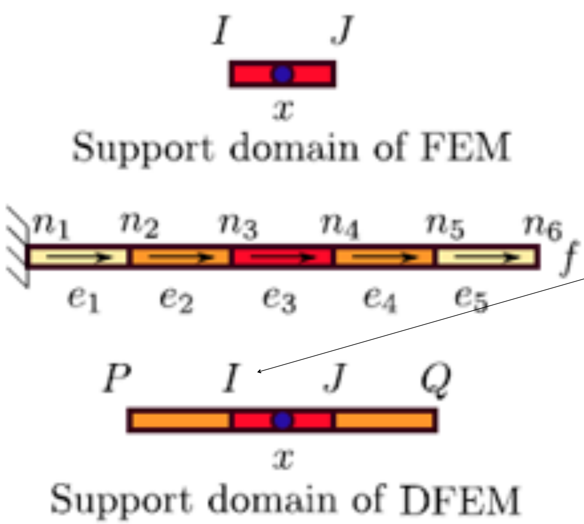

For node I, the support elements are: e_2, e_3

In element 2, we use linear Lagrange interpolation:

$$u_{,x}^{e_2}(x_I) = N_{P,x}^{e_2}(x_I)u^P + N_{I,x}^{e_2}(x_I)u^I$$

Weight function of e_2:

$$\omega_{e_{2,I}} = \frac{meas(e_{2,I})}{meas(e_{2,I}) + meas(e_{3,I})}$$

Element length

$$\bar{u}_{,x}^{I} = \bar{u}_{,x}(x_I) = \omega_{e_{2,I}} u_{,x}^{e_2}(x_I) + \omega_{e_{3,I}} u_{,x}^{e_3}(x_I)$$

Double-interpolation finite element method (DFEM)

The $\bar{u}^I_{,x}$ can be further rewritten as:

$$\bar{u}^I_{,x} = \begin{bmatrix} \omega_{e_{2,I}} N^{e2}_{P,x} & \omega_{e_{2,I}} N^{e2}_{I,x} + \omega_{e_{3,I}} N^{e3}_{I,x} & \omega_{e_{3,I}} N^{e3}_{J,x} \end{bmatrix} \begin{bmatrix} u^P \\ u^I \\ u^J \end{bmatrix}$$

$$= \bar{N}_{P,x}(x_I)u^P + \bar{N}_{I,x}(x_I)u^I + \bar{N}_{J,x}(x_I)u^J$$

Substituting $\bar{u}^I_{,x}$ and $\bar{u}^J_{,x}$ into the second stage of interpolation leads to:

$$u^h(x) = \sum_{L \in N_S} \hat{N}_L(x) u^L$$

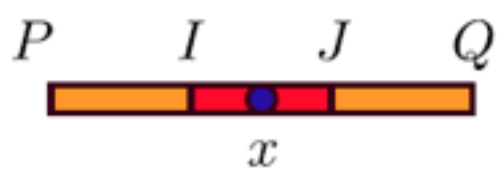

Support domain of DFEM

$$\hat{N}_L(x) = \phi_I(x)N_L(x_I) + \psi_I(x)\bar{N}_{L,x}(x_I) + \phi_J(x)N_L(x_J) + \psi_J(x)\bar{N}_{L,x}(x_J)$$

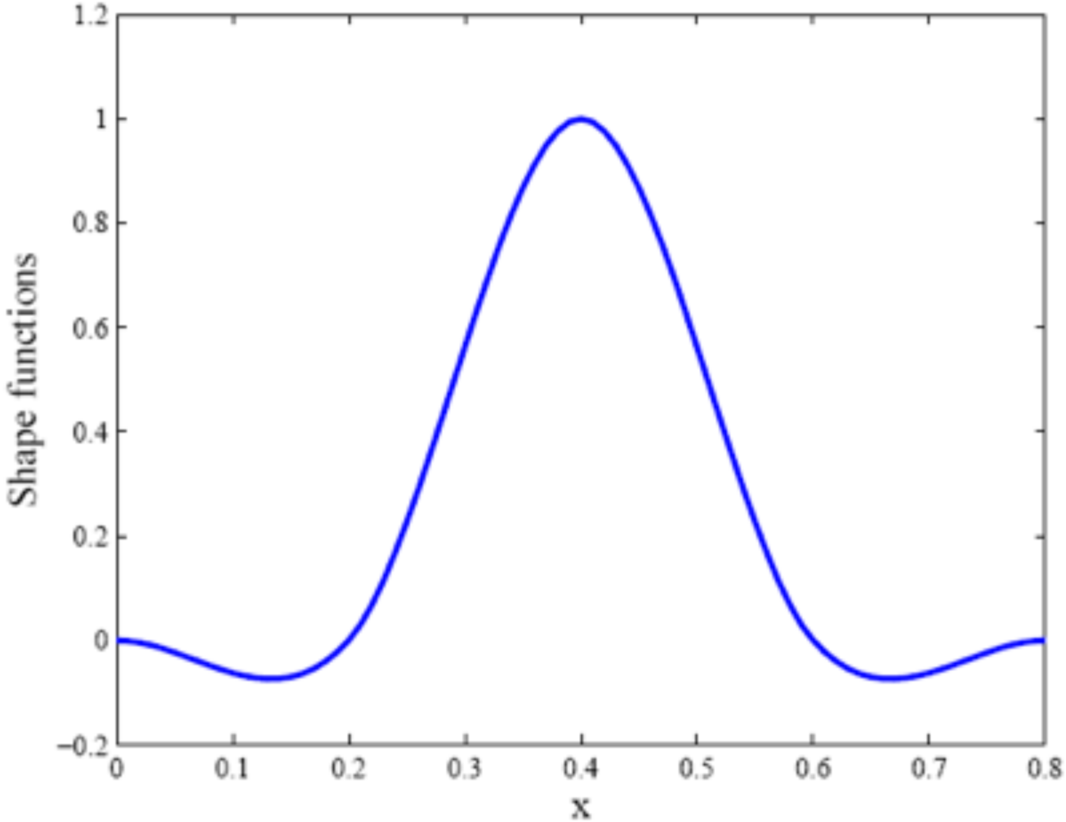

Shape function of DFEM 1D

Derivative of Shape function

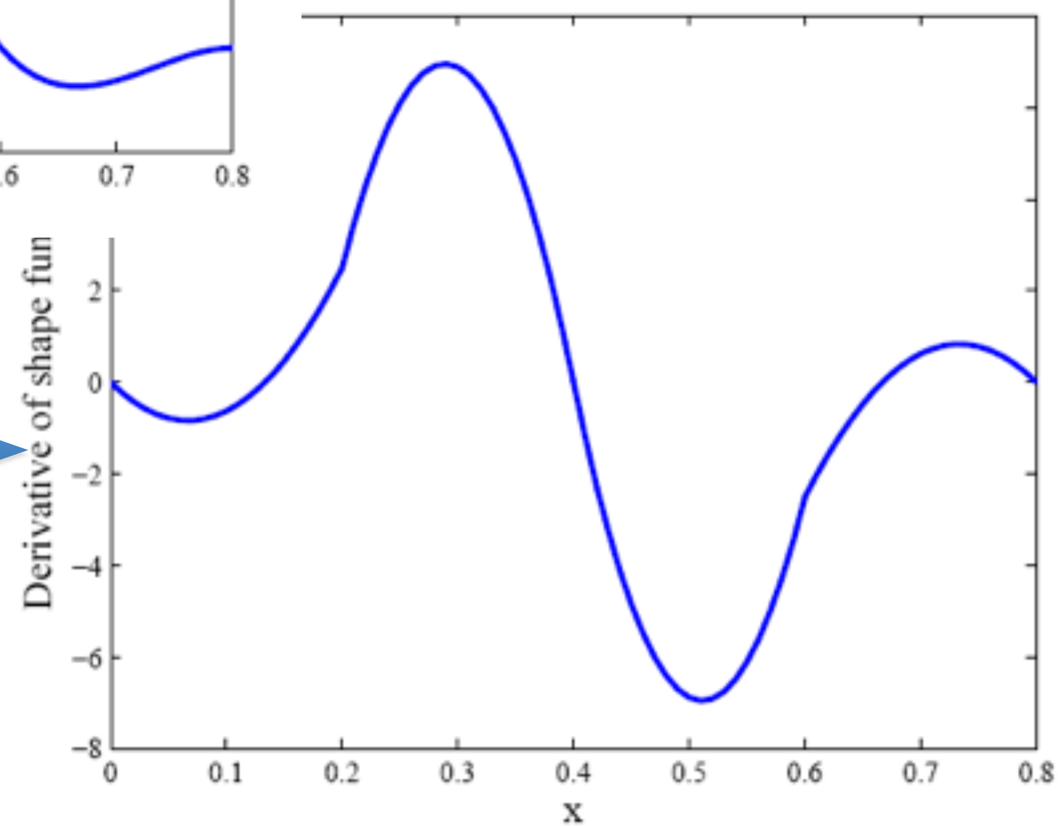

Double-interpolation finite element method (DFEM)

Same procedure for 2D ***triangular*** elements

First stage of interpolation (traditional FEM):

$$u^h(\mathbf{x}) = L_I(\mathbf{x})u^I + L_J(\mathbf{x})u^J + L_K(\mathbf{x})u^K$$

Second stage of interpolation :

$$\begin{aligned} u^h(\mathbf{x}) = &\phi_I(\mathbf{x})u^I + \psi_I(\mathbf{x})\bar{u}^I_{,x} + \varphi_I(\mathbf{x})\bar{u}^I_{,y} + \\ &\phi_J(\mathbf{x})\bar{u}^J + \psi_J(\mathbf{x})\bar{u}^J_{,x} + \varphi_J(\mathbf{x})\bar{u}^J_{,y} + \\ &\phi_K(\mathbf{x})\bar{u}^K + \psi_K(\mathbf{x})\bar{u}^K_{,x} + \varphi_K(\mathbf{x})\bar{u}^K_{,y} \end{aligned}$$

$\phi_I, \psi_I, \varphi_I, \phi_J, \psi_J, \varphi_J, \phi_K, \psi_K, \varphi_K$ are the basis functions with regard to $L_I(\mathbf{x}), L_J(\mathbf{x}), L_K(\mathbf{x})$

Double-interpolation finite element method (DFEM)

Calculation of Nodal derivatives:

$$\bar{N}_{L,x}(\mathbf{x}_I) = \sum_{e_{i,I}\in\Lambda_I} \omega_{e_{i,I}} N^{e_i}_{L,x}(\mathbf{x}_I)$$

$$\bar{N}_{L,y}(\mathbf{x}_I) = \sum_{e_{i,I}\in\Lambda_I} \omega_{e_{i,I}} N^{e_i}_{L,y}(\mathbf{x}_I)$$

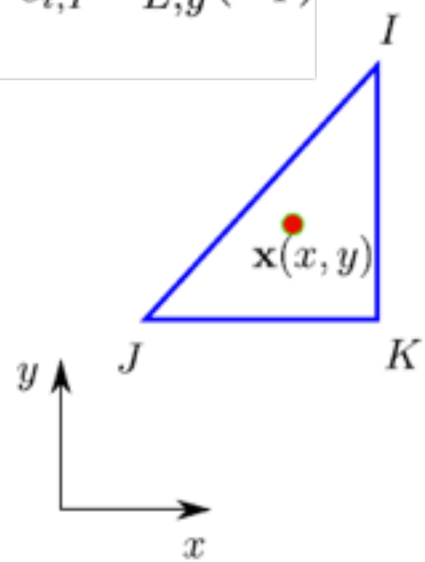

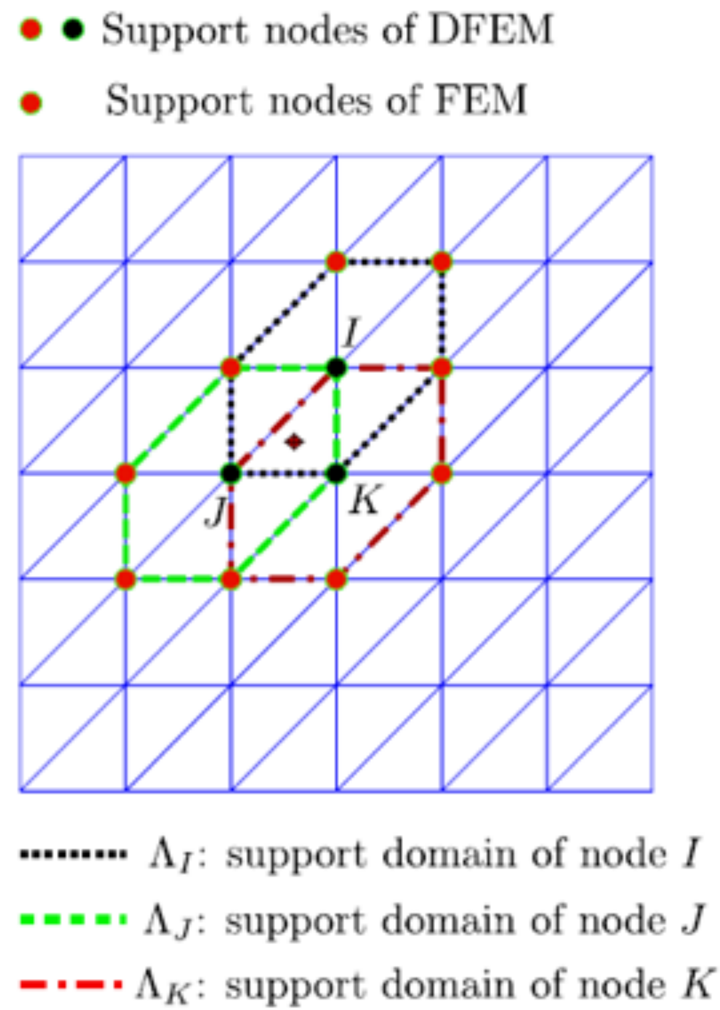

Calculation of weights:

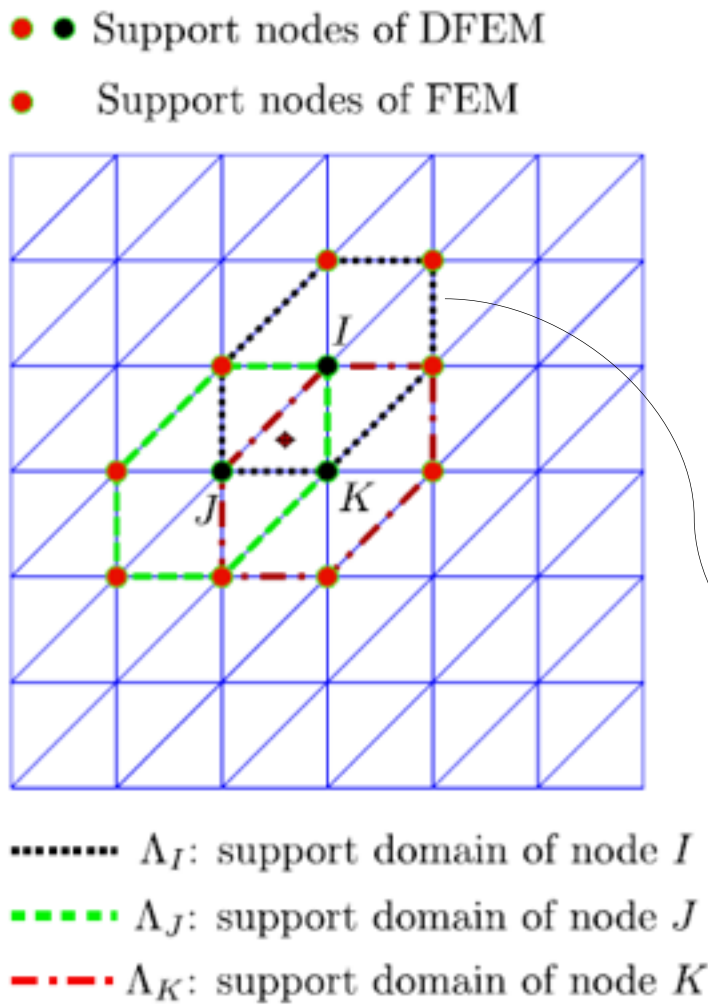

The weight of triangle *i* in support domain of *I* is:

$$\omega_{e_{i,I}} = \frac{\triangle_{e_{i,I}}}{\sum_{e_{j,I}\in\Lambda_I} \triangle_{e_{j,I}}}$$

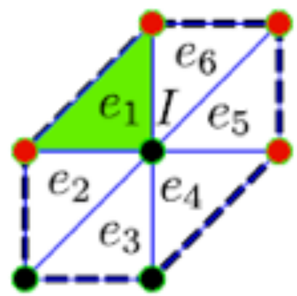

$$\omega_{e_1} = S_{e_1}/(\textstyle\sum_{e_i\in\Lambda_I} S_{e_i})$$

The basis functions are given as (node *I*):

$$\phi_I(\mathbf{x}) = L_I + L_I^2 L_J + L_I^2 L_K - L_I L_J^2 - L_I L_K^2$$

$$\psi_I(\mathbf{x}) = -c_J\left(L_K L_I^2 + \frac{1}{2} L_I L_J L_K\right) + c_K\left(L_I^2 L_J + \frac{1}{2} L_I L_J L_K\right)$$

$$\varphi_I(\mathbf{x}) = b_J\left(L_K L_I^2 + \frac{1}{2} L_I L_J L_K\right) - b_K\left(L_I^2 L_J + \frac{1}{2} L_I L_J L_K\right)$$

L_I, L_J, L_K are functions w.r.t $\mathbf{x}$

$$L_I(\mathbf{x}) = \frac{1}{2\triangle}(a_I + b_I x + c_I y)$$

Area of triangle

$$a_I = x_J y_K - x_K y_J$$
$$b_I = y_J - y_K$$
$$c_I = x_K - x_J$$

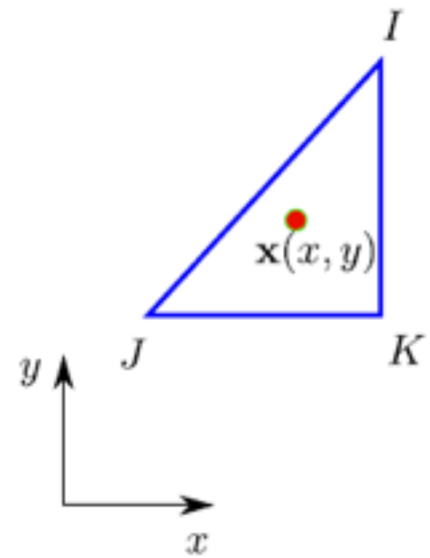

Shape functions

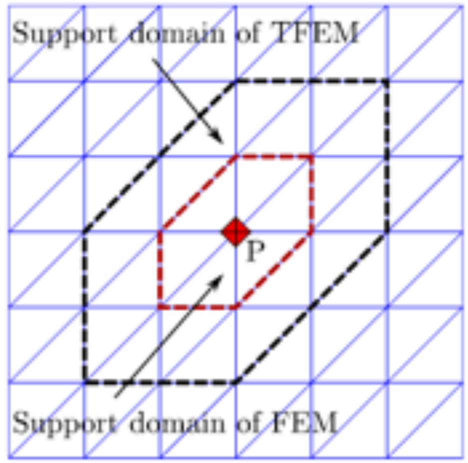

(a) Interior of the 2D domain

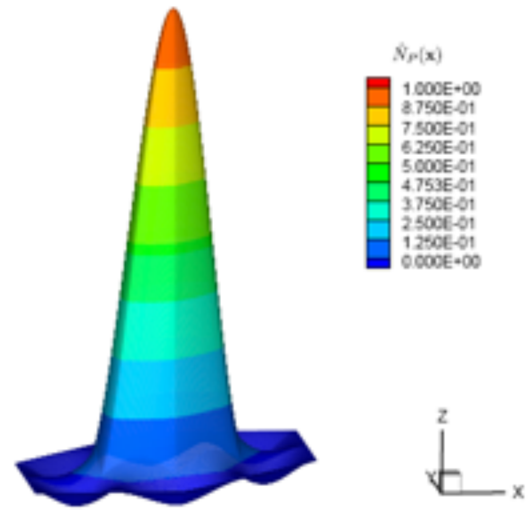

(b) 3D plot

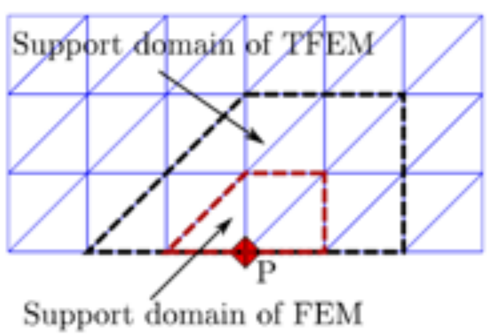

(c) Boundary of the 2D domain

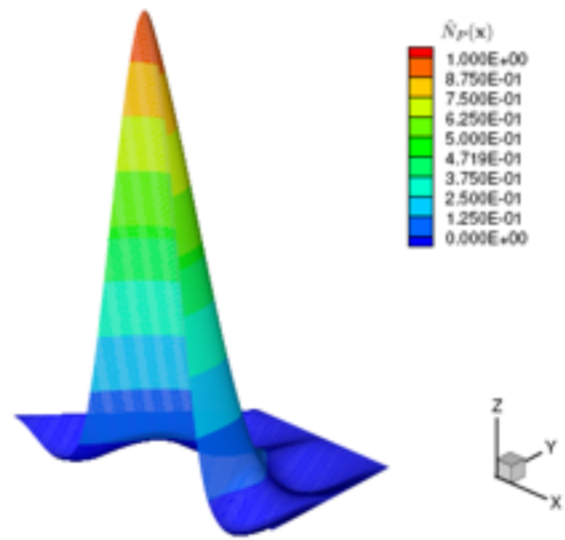

(d) 3D plot

DFEM shape function

$$\mathbf{u}^h(\mathbf{x}) = \sum_{I \in \mathcal{N}_I} \hat{N}_I(\mathbf{x})\mathbf{u}^I + \sum_{J \in \mathcal{N}_J} \hat{N}_J(\mathbf{x})H(\mathbf{x})\mathbf{a}^J + \sum_{K \in \mathcal{N}_K} \hat{N}_K(\mathbf{x}) \sum_{\alpha=1}^{4} f_\alpha(\mathbf{x})\mathbf{b}^{K\alpha}$$

$$\{f_\alpha(r,\theta), \alpha = 1,4\} = \left\{\sqrt{r}\sin\frac{\theta}{2}, \sqrt{r}\cos\frac{\theta}{2}, \sqrt{r}\sin\frac{\theta}{2}\sin\theta, \sqrt{r}\cos\frac{\theta}{2}\sin\theta\right\}$$

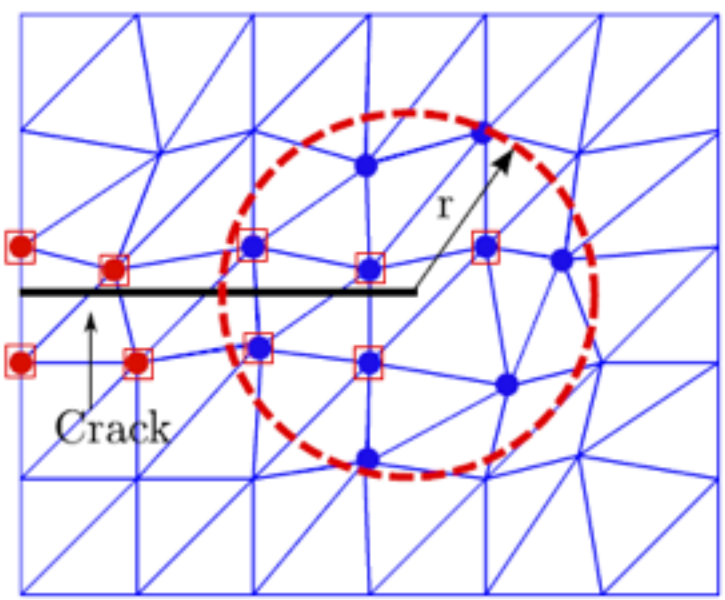

● Crack tip enriched node

● Heaviside enriched node

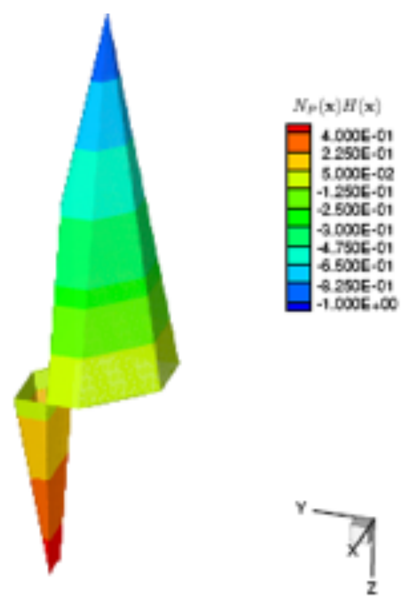

(d) XFEM

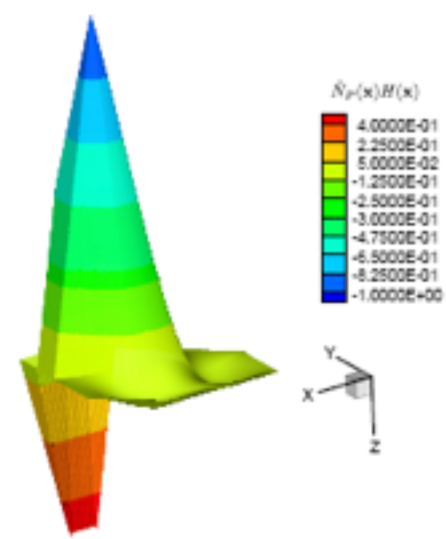

(b) XDFEM

Numerical example of 1D bar

Problem definition:

$$EA\frac{\mathrm{d}^2u}{\mathrm{d}x^2} + f = 0$$

$$u|_{x=0} = 0$$

Analytical solutions:

$$u(x) = \frac{fL^2}{EA}\left(\frac{x}{L} - \frac{1}{2}\left(\frac{x}{L}\right)^2\right)$$

$$\sigma(x) = \frac{fL}{A}\left(1 - \frac{x}{L}\right)$$

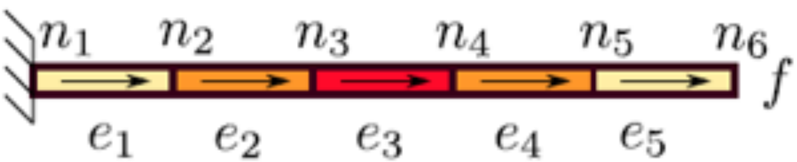

E: Young's Modulus

A: Area of cross section

L:Length

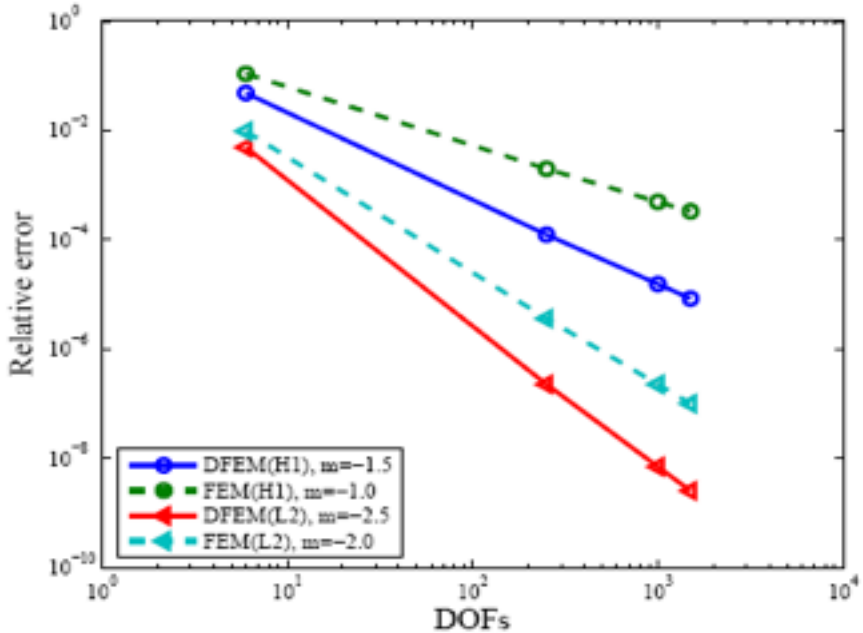

Displacement(L2) and energy(H1) norm

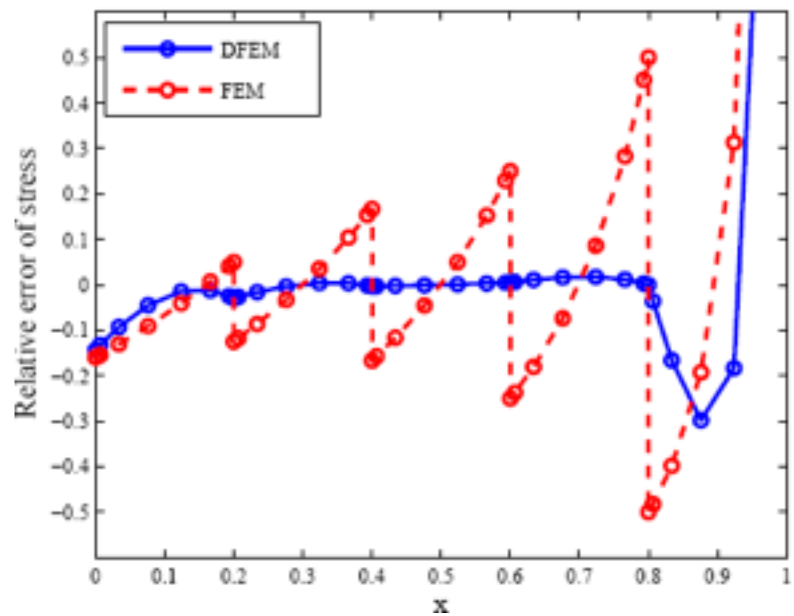

Relative error of stress distribution

Numerical example of Cantilever beam

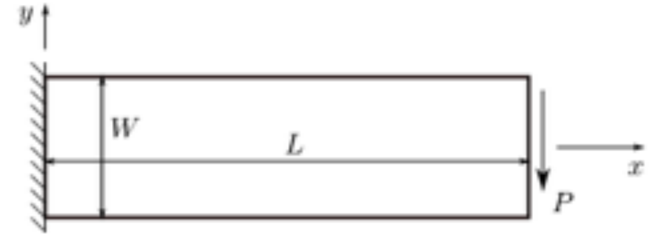

Analytical solutions

$$u_x(x,y) = \frac{Py}{6EI}\left[(6L-3x)x + (2+\nu)(y^2 - \frac{W^2}{4})\right]$$

$$u_y(x,y) = -\frac{P}{6EI}\left[3\nu y^2(L-x) + (4+5\nu)\frac{W^2 x}{4} + (3L-x)x\right.$$

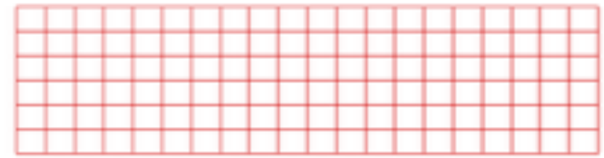

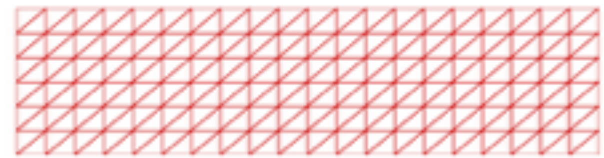

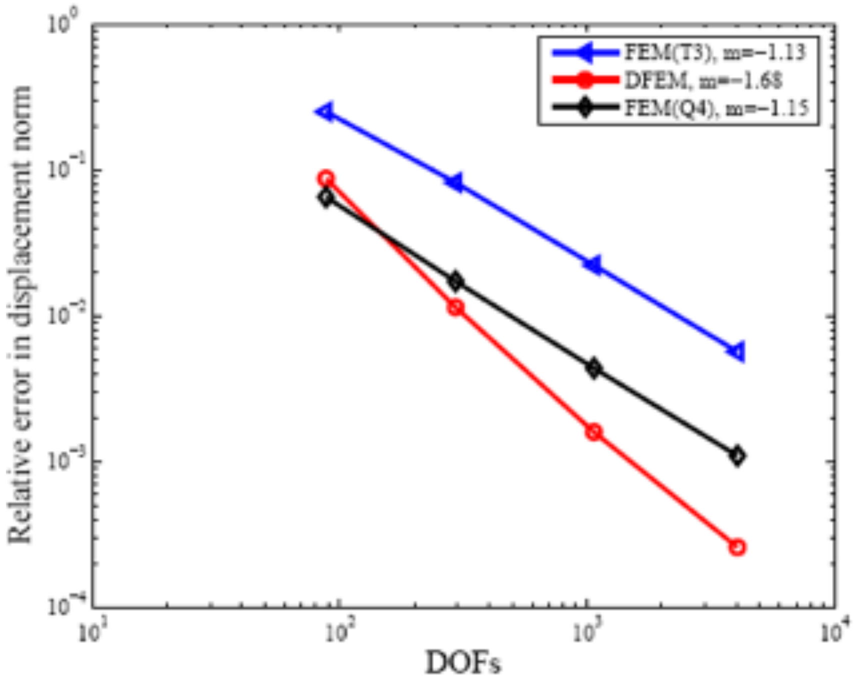

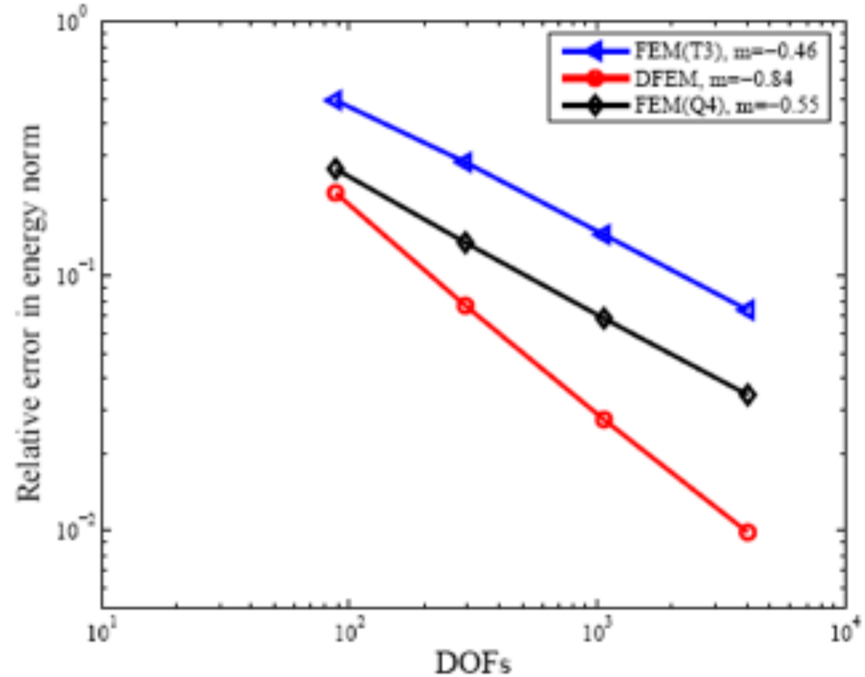

Numerical example of Cantilever beam

Mode-I crack results:

a) explicit crack (FEM);
b) only Heaviside enrichment;
c) full enrichment

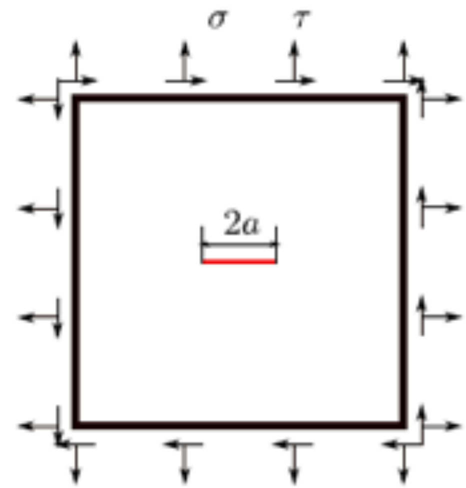

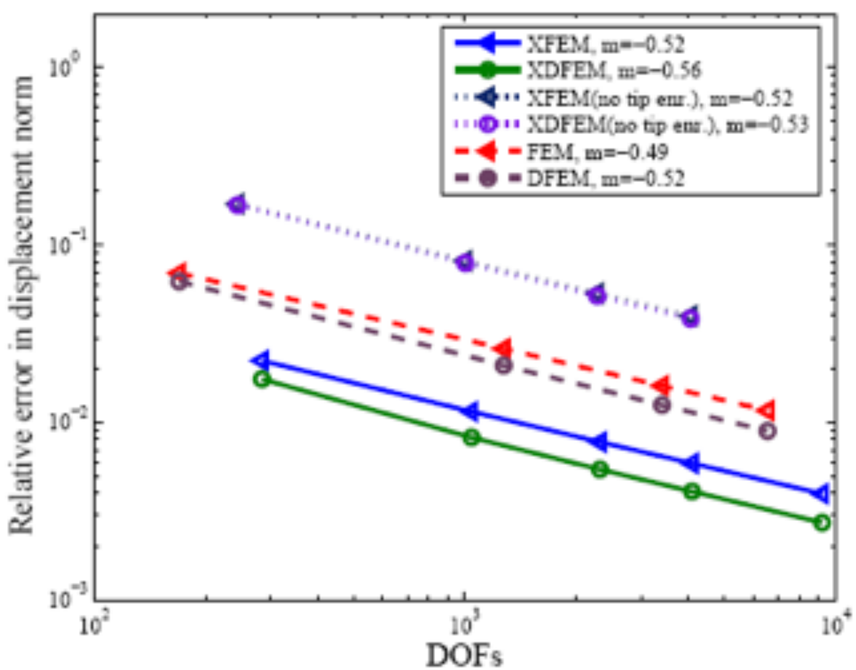

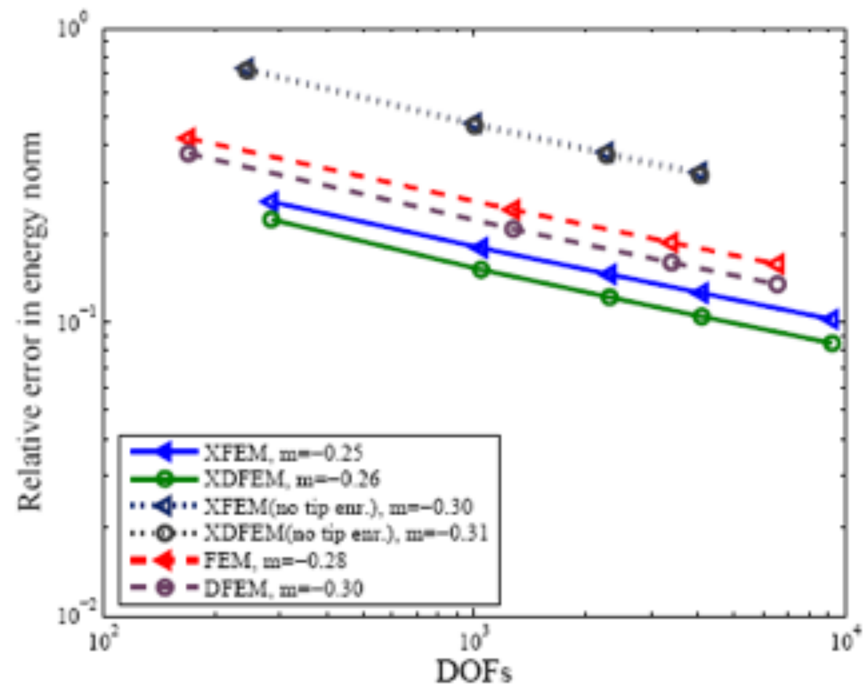

Numerical example of crack propagation

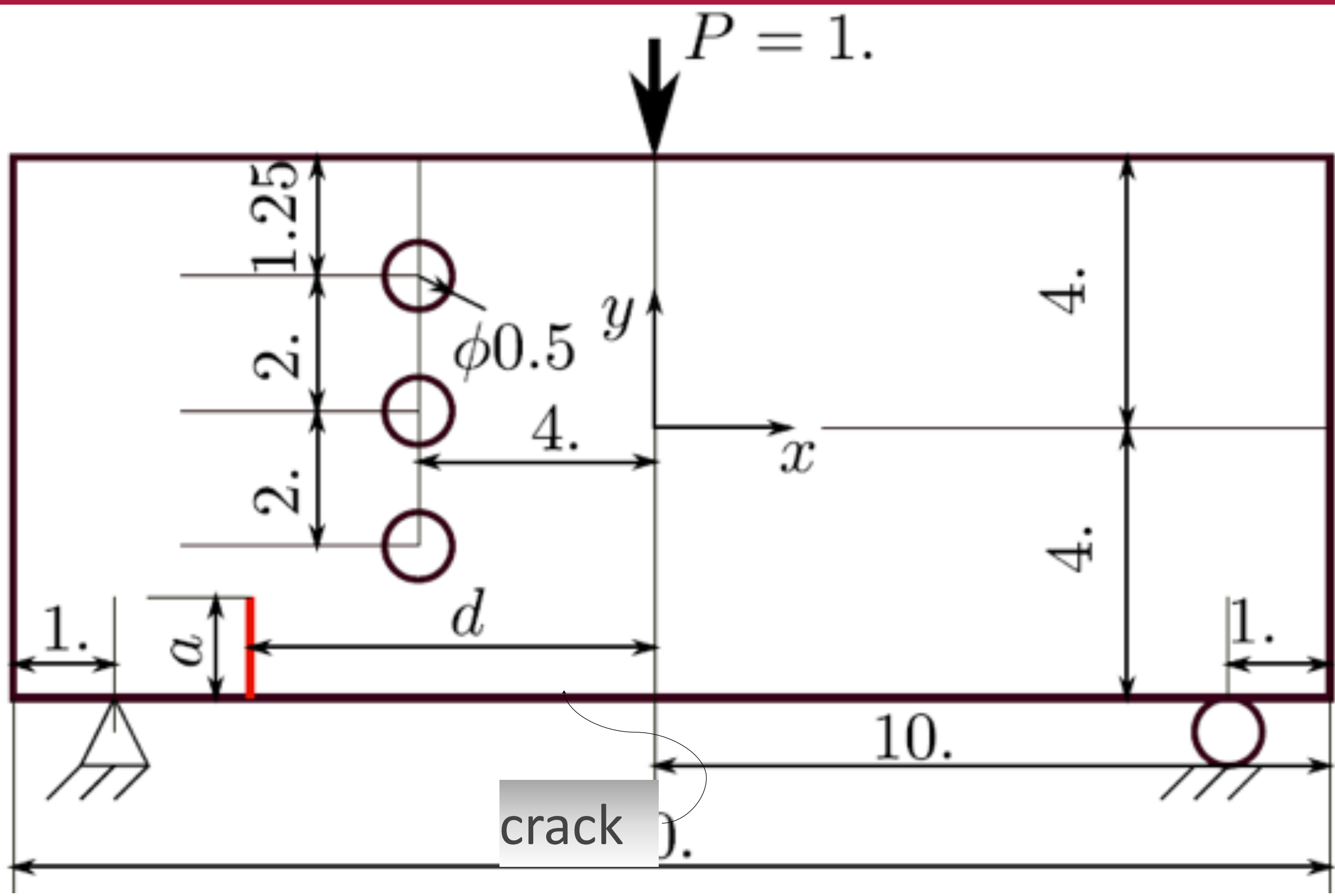

	d	a	crack increment	number of propagation
case 1	5	1.5	0.052	67
case 2	6	1.0	0.060	69
case 3	6	2.5	0.048	97

Numerical example of crack propagation

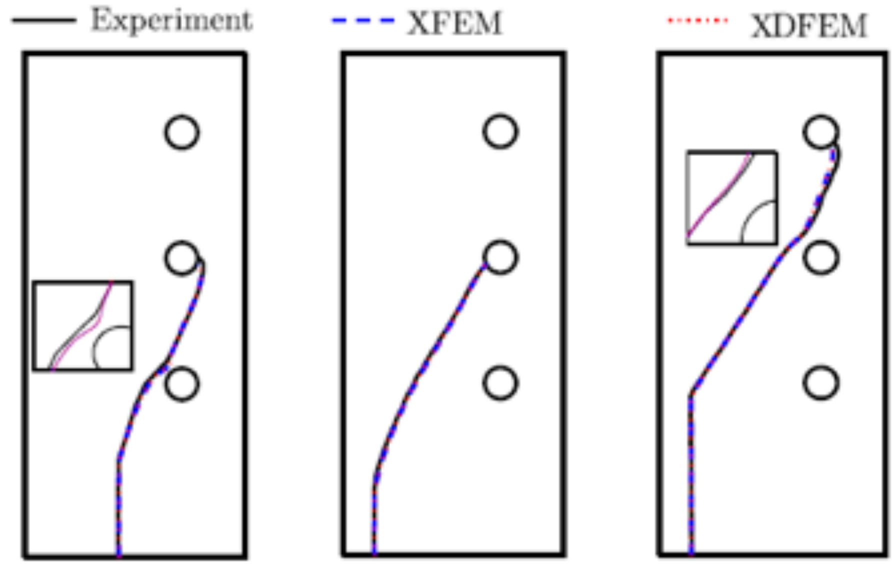

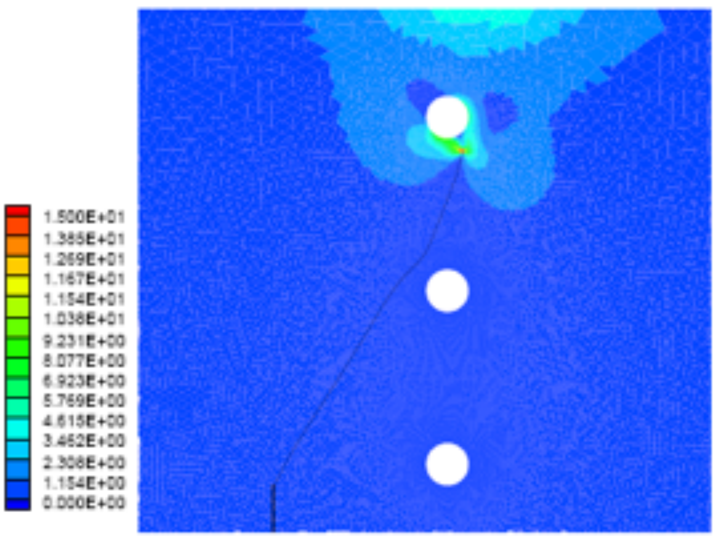

(c) XFEM, the 94th step

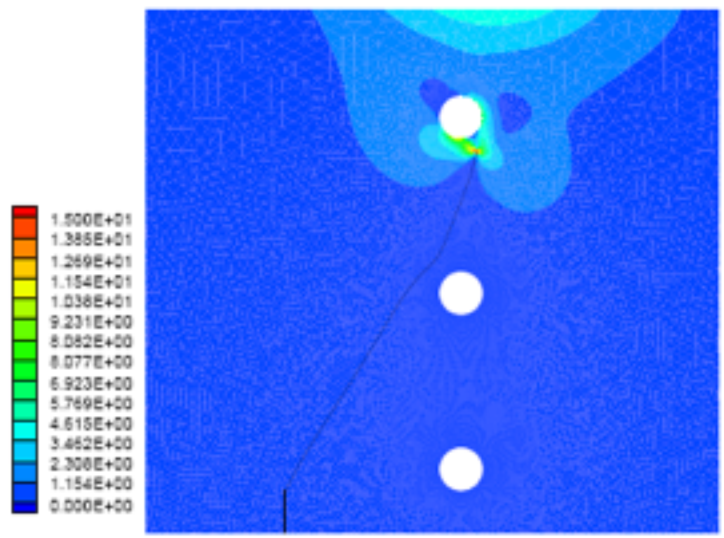

(d) XDFEM, the 94th step

Conclusions

✓Superconvergence in elasticity problems

✓Higher accuracy than XFEM in fracture problems

✓Consistent with XFEM in terms of crack evolution

✓Smooth nodal stress without post-processing

References

- Moës, N., Dolbow, J., & Belytschko, T. (1999). A finite element method for crack growth without remeshing. *IJNME*, *46*(1), 131–150.
- Melenk, J. M., & Babuška, I. (1996). The partition of unity finite element method: Basic theory and applications. *CMAME*, *139*(1-4), 289–314.
- Laborde, P., Pommier, J., Renard, Y., & Salaün, M. (2005). High-order extended finite element method for cracked domains. *IJNME*, *64*(3), 354–381.
- Wu, S. C., Zhang, W. H., Peng, X., & Miao, B. R. (2012). A twice-interpolation finite element method (TFEM) for crack propagation problems. IJCM, *09*(04), 1250055.
- Peng, X., Kulasegaram, S., Bordas, S. P.A., Wu, S. C. (2013). An extended finite element method with smooth nodal stress. http://arxiv.org/abs/1306.0536

Stabilised generalised/extended FEM

with Daniel Paladim, Marie Curie Fellow

Problem: In XFEM/GFEM, the enrichment function is not correctly reproduced in the elements that have enriched and non-enriched nodes (blending).

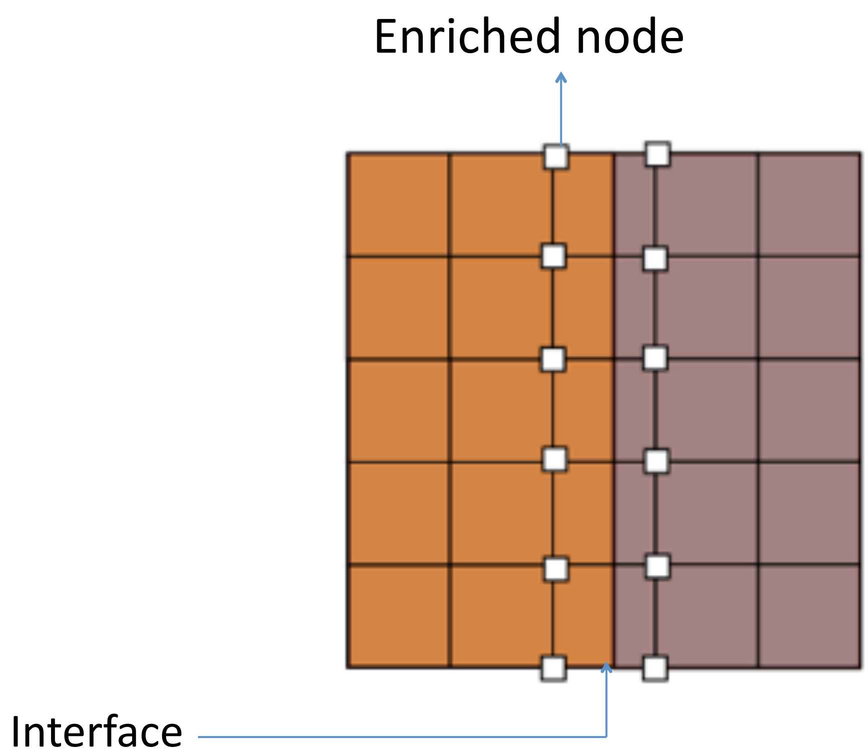

Solution: Corrected-XFEM by Fries (2008). Corrected XFEM, substitutes f(x) by R(x)f(x), where R(x) is the ramp function. A continuous function whose value is 1 in the enriched elements, 0 in the non-enriched elements and it varies continuously between 0 and 1.

Ramp function

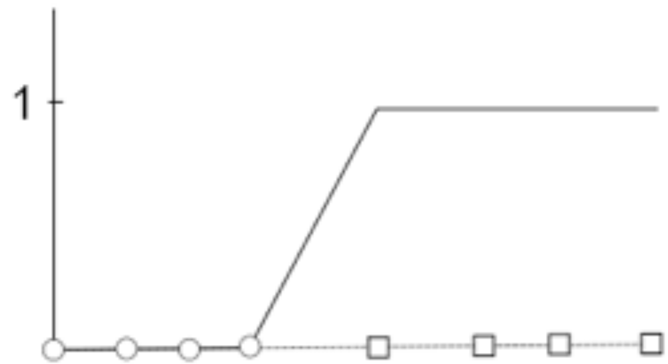

○ Non-enriched nodes

□ Enriched nodes

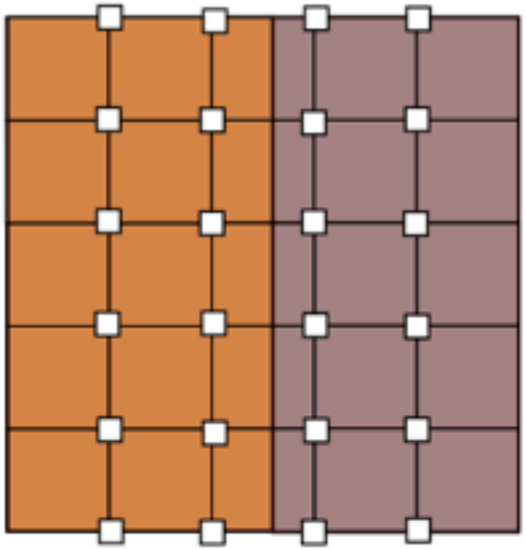

More solutions

•Suppressing blending elements by coupling enriched and standard regions. *Laborde et al. (2005) Gracie et al(2008)*

•Hierarchical shape functions in blending elements. *Chessa et al (2003) Tarancón et al. (2009)*

•Assumed strain blending elements. *Chessa et al. (2003) Gracie et al.*

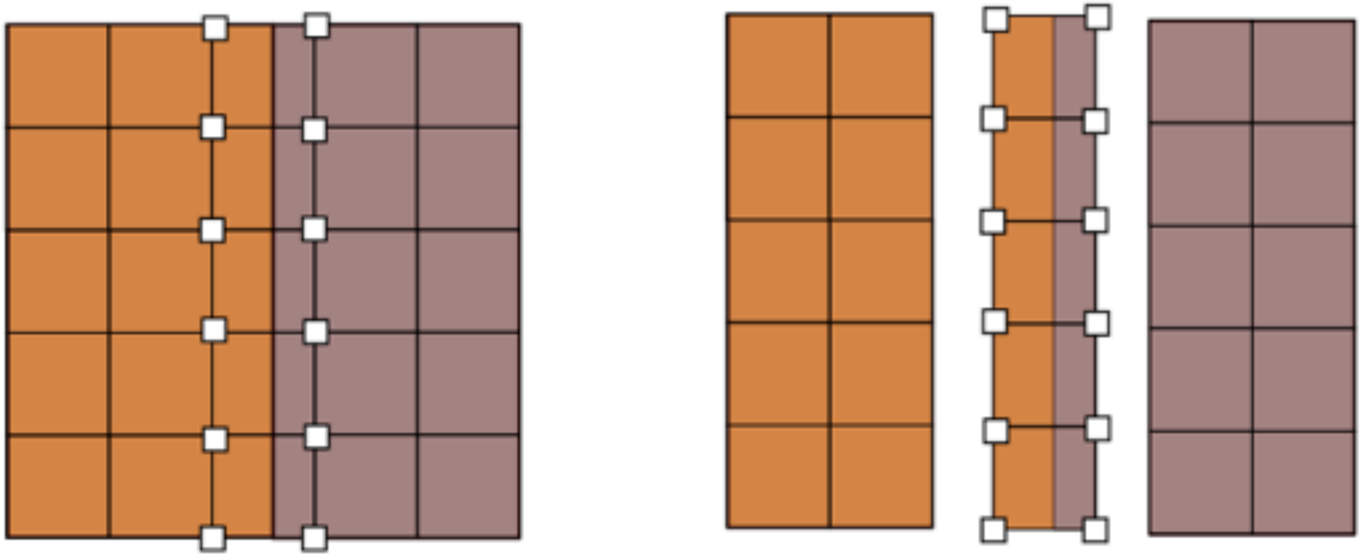

Another solution: Stable GFEM by Babuška and Banerjee (2012).

In SGFEM, the enrichment function f(x) is substituted by the following function $f(x)-\Sigma N_i(x)f(x_i)$. It is to say f minus its nodal interpolation.

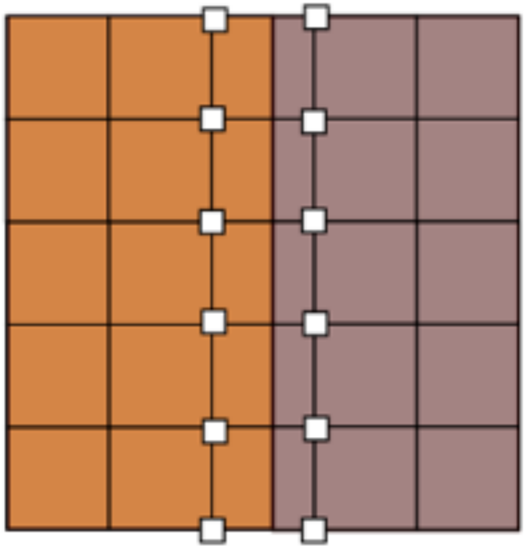

In the case that $f(x)=|\phi(x)|$, where ϕ is the level set of the interface we are trying to represent, we obtain the function introduced by Moës in 2003.

Problem: The stiffness matrix of GFEM/XFEM could be ill-conditioned. This is usually the case when the interface is very close to a node.

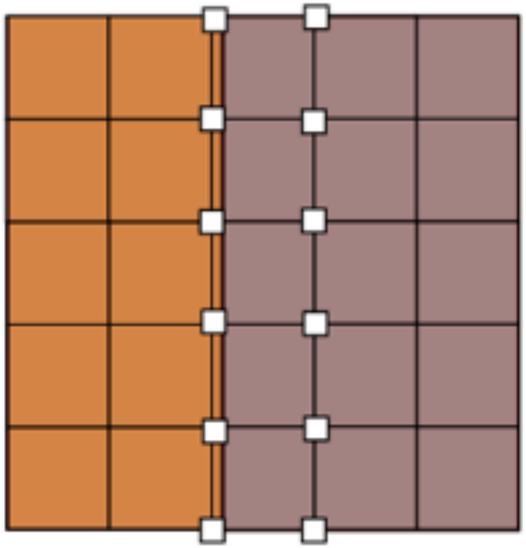

- Ill-conditioning reduces the accuracy when direct solvers are used (due to round-off errors).
- In iterative solvers, more iterations are required to bring the error

Solution: A preconditioner. Menk and Bordas (2011) proposed a preconditioner for GFEM/XFEM.

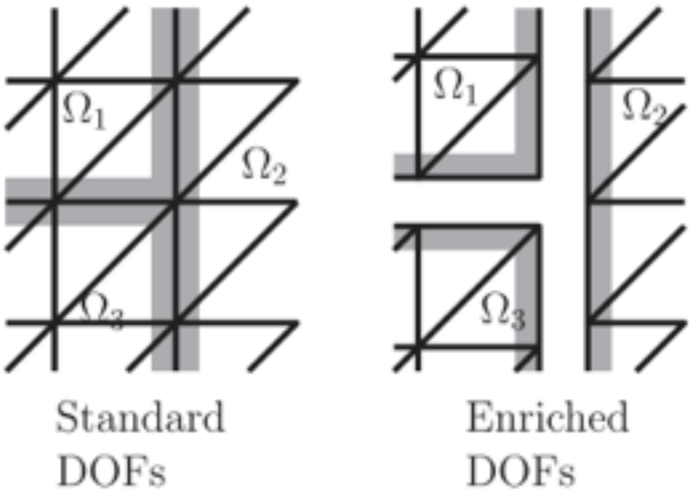

$$K = \begin{bmatrix} K_{\mathrm{FEM,FEM}} & K_{X,\mathrm{FEM}} \\ K_{\mathrm{FEM},X} & K_{X,X} \end{bmatrix}$$

$$P = \begin{bmatrix} P_{\mathrm{FEM}} & 0 & \\ 0 & P_X & 0 \\ & 0 & L^{-1} \end{bmatrix}$$

- Very robust to interfaces passing close to nodes.
- Can be parallelized.
- Not very easy to implement. Tuning is needed.

Basic idea The domain is divided only for the enriched DOFs.

$$K = \begin{bmatrix} K_{\mathrm{FEM,FEM}} & K_{X,\mathrm{FEM}} \\ K_{\mathrm{FEM},X} & K_{X,X} \end{bmatrix}$$

$$K = \begin{bmatrix} K_{\mathrm{FEM,FEM}} & K_{X,\mathrm{FEM}} & 0 \\ K_{\mathrm{FEM},X} & K_{X,X} & B^{\mathrm{T}} \\ 0 & B & 0 \end{bmatrix}$$

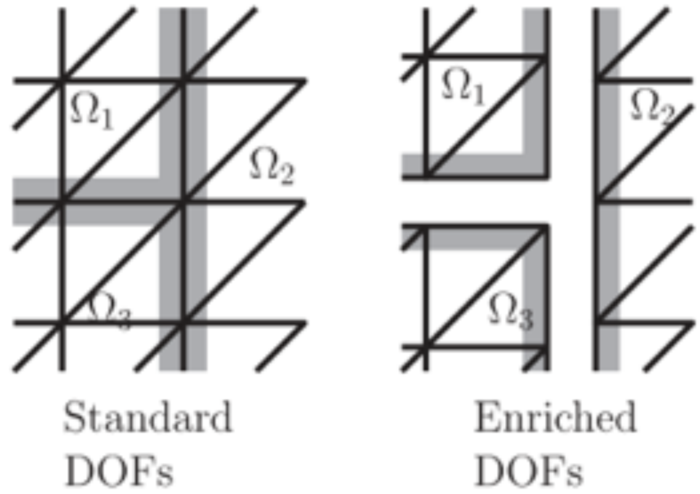

$$P = \begin{bmatrix} P_{\mathrm{FEM}} & 0 & \\ 0 & P_X & 0 \\ & 0 & L^{-1} \end{bmatrix}$$

$$P_X = \begin{bmatrix} C_1^{-1} & 0 & \\ 0 & C_2^{-1} & \\ & & \ddots \end{bmatrix}$$

$$\tilde{K} = \begin{bmatrix} \tilde{K}_{\mathrm{FEM,FEM}} & \tilde{K}_{X,\mathrm{FEM}} & 0 \\ \tilde{K}_{\mathrm{FEM},X} & I & Q^{\mathrm{T}} \\ 0 & Q & 0 \end{bmatrix}$$

Another solution

- *SGFEM, if 2 assumptions hold, a stiffness matrix with condition a number similar to FEM is generated*

- *Node clustering*

One 1-D bimaterial bar. The exact solution is in the finite domain

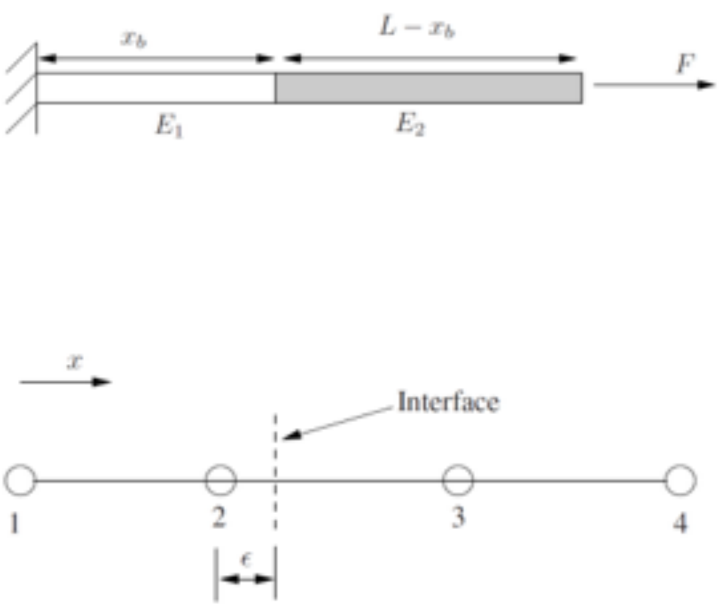

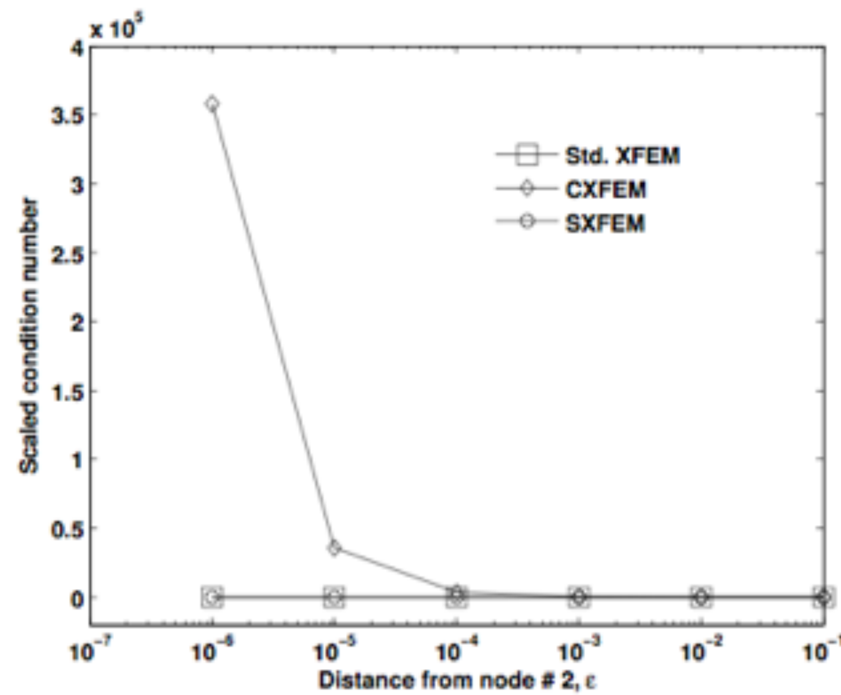

Circular inclusion

$$
u_r(r) = \begin{cases} \left[\left(1-\frac{b^2}{a^2}\right)\beta + \frac{b^2}{a^2}\right] r, & 0 \le r \le a, \\ \left(r - \frac{b^2}{r}\right)\beta + \frac{b^2}{r}, & a \le r \le b, \end{cases}
$$

$$
u_\theta(r) = 0,
$$

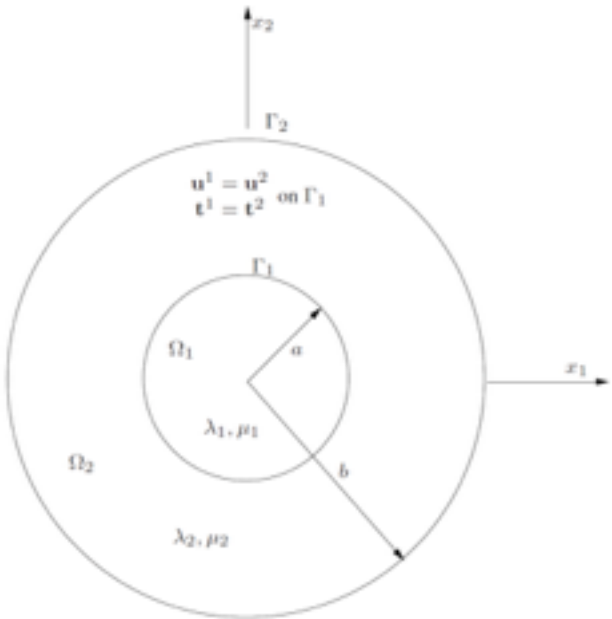

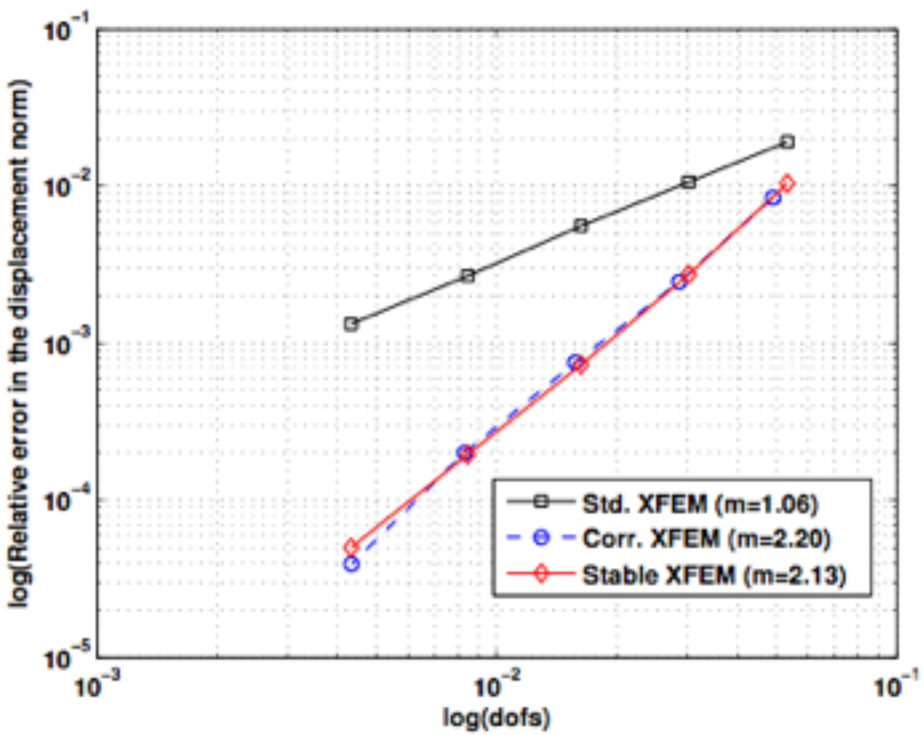

Infinite plate with crack in tension. Displacements prescribed along

$$u_x(r,\theta) = \frac{2(1+\nu)}{\sqrt{2\pi}}\frac{K_I}{E}\sqrt{r}\cos\frac{\theta}{2}\left(2-2\nu-\cos^2\frac{\theta}{2}\right)$$

$$u_y(r,\theta) = \frac{2(1+\nu)}{\sqrt{2\pi}}\frac{K_I}{E}\sqrt{r}\sin\frac{\theta}{2}\left(2-2\nu-\cos^2\frac{\theta}{2}\right)$$

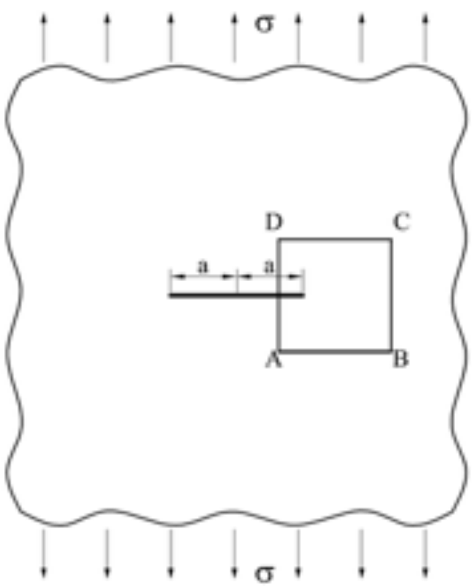

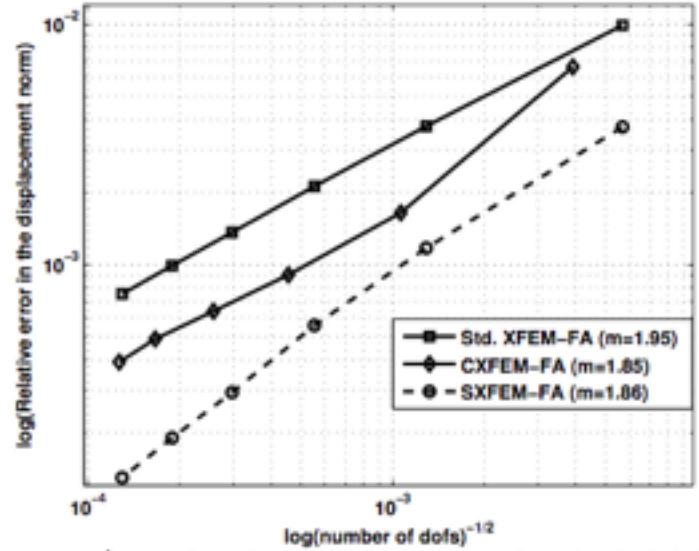

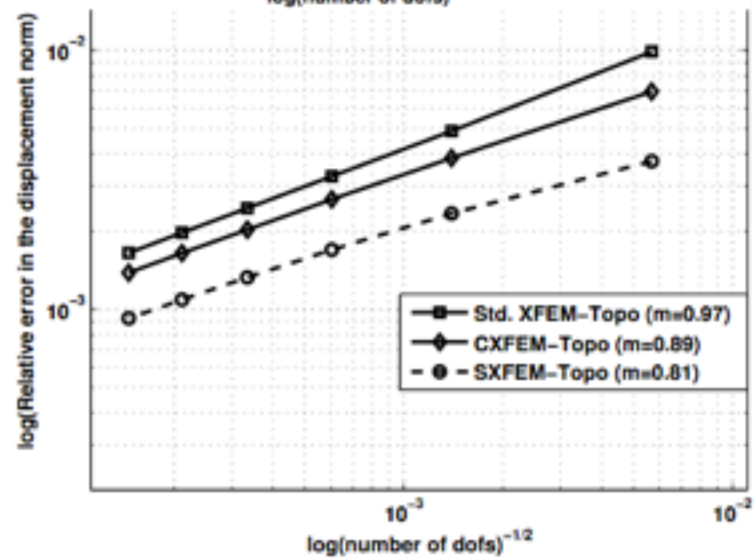

Edge crack in tension

$$K_I = F\left(\frac{a}{H}\right)\sigma\sqrt{\pi a}$$

$$F\left(\frac{a}{H}\right) = 1.12 - 0.231\left(\frac{a}{H}\right) + 10.55\left(\frac{a}{H}\right)^2 - 21.72\left(\frac{a}{H}\right)^3 + 30.39\left(\frac{a}{H}\right)^4$$

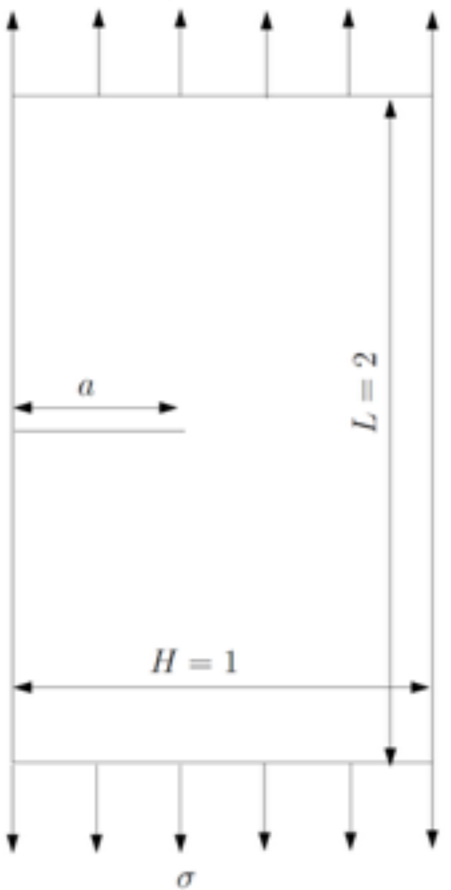

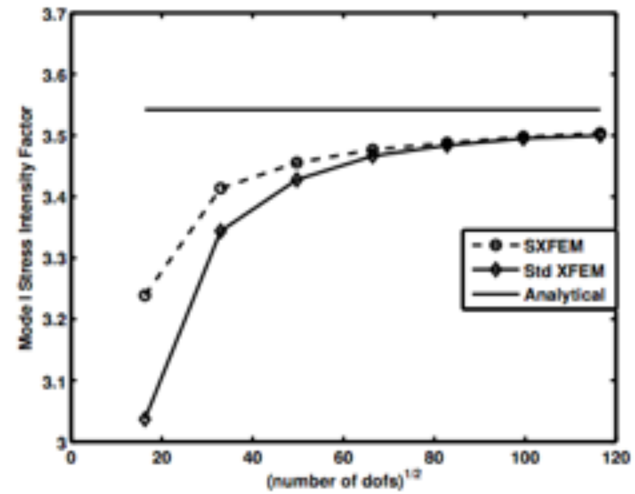

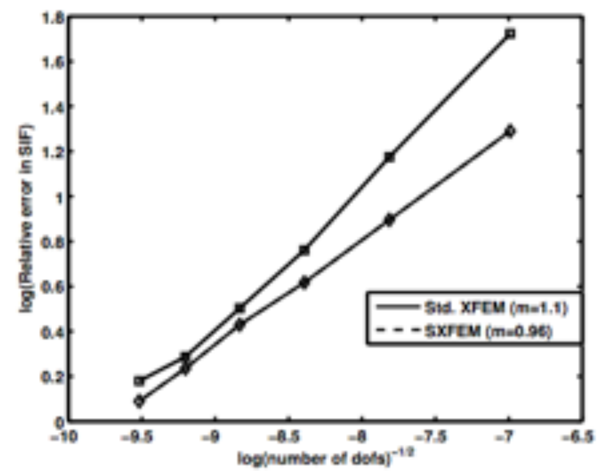

Work in progress

Development of 3D examples

- Spherical inclusion
- Several spherical inclusions
- Cracks in 3D

Stable generalized FEM

All those examples were implemented within Diffpack. Diffpack is a commercial software library used for the development numerical software, with main emphasis on numerical solutions of partial differential equations. It was developed in C++ following the object oriented paradigm.

The library is mostly oriented to the implementation of the finite element method, however it has tools for other methods, such as

Stable generalized FEM

- I. Babuška, U. Banerjee, Stable Generalized Finite Element Method (SGFEM), Computer Methods in Applied Mechanics and Engineering, Volumes 201–204, 1 January 2012, Pages 91-111, ISSN 0045-7825, 10.1016/j.cma.20

- Fries, T.-P. (2008), A corrected XFEM approximation without problems in blending elements. Int. J. Numer. Meth. Engng., 75: 503–532.

- Gracie, R., Wang, H. and Belytschko, T. (2008), Blending in the extended finite element method by discontinuous Galerkin and assumed strain methods. Int. J. Numer. Meth. Engng., 74: 1645–1669.

- Laborde, P., Pommier, J., Renard, Y. and Salaün, M. (2005), High-order extended finite element method for cracked domains. Int. J. Numer. Meth. Engng., 64: 354–381.

- Chessa, J., Wang, H. and Belytschko, T. (2003), On the construction of blending elements for local partition of unity enriched finite elements. Int. J. Numer. Meth. Engng., 57: 1015–1038.

- Tarancón, J. E., Vercher, A., Giner, E. and Fuenmayor, F. J. (2009), Enhanced blending elements for XFEM applied to linear elastic fracture mechanics. IJNME, 77: 126–148.

Part III. Application to multi-crack propagation

with Danas Sutula, President Scholar

Institute of Mechanics & Advanced Materials

Numerical Modeling of SOI Wafer Splitting

Physical process

Manufacturing process: *SmartCut*™

- H^+ ionization of a thin surface of Si
- Bonding to a handle-wafer (stiffener)
- High temperature thermal annealing
- Nucleation and growth of cavities filled with H_2
- Pressure driven micro crack growth
- Coalescence and post-split fracture roughness

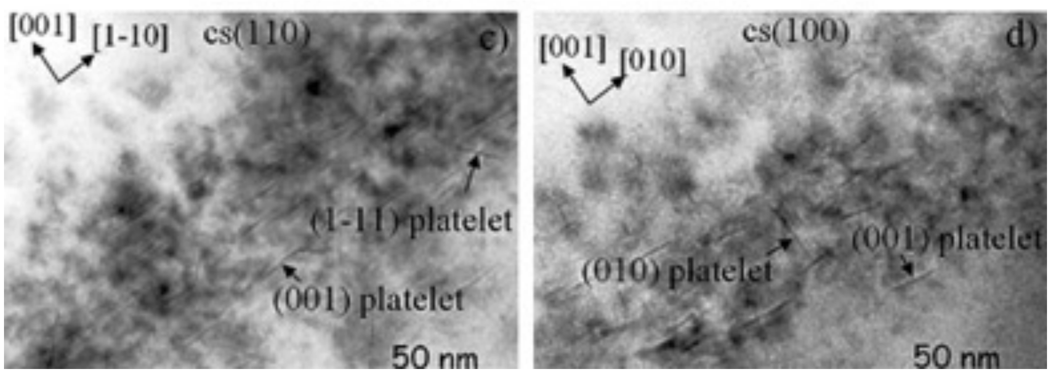

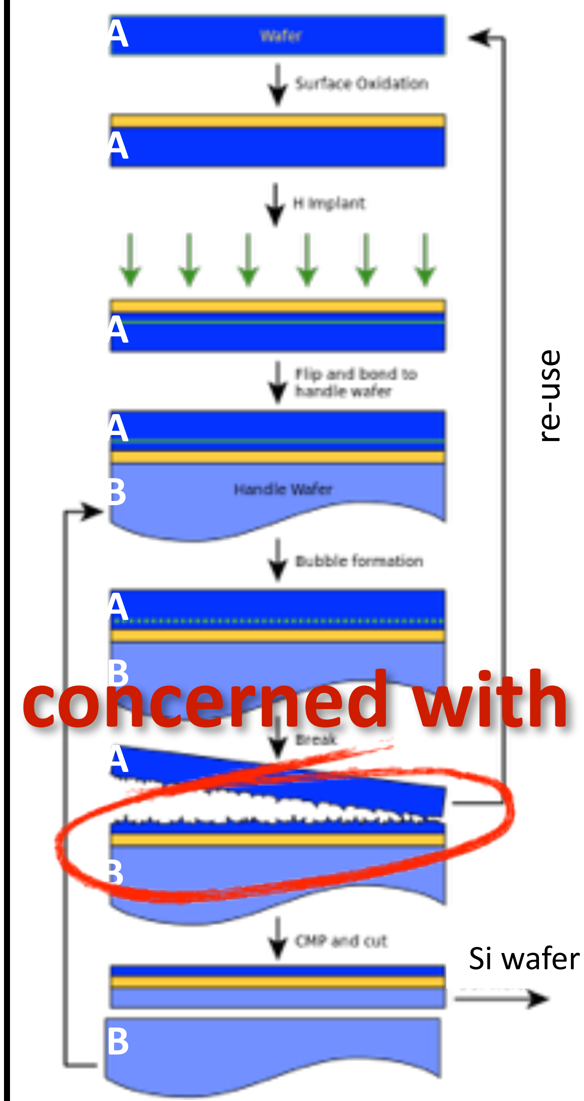

Objectives

Determine:

- micro crack nucleation points and direction
- multiple crack paths until coalescence
- time to complete fracture
- final surface roughness

Model

Modeling cavities by zero thickness surfaces

- discontinuities in the displacement field

Linear elastic fracture mechanics (LEFM)

- infinite stress at crack tip, i.e. *singularity*

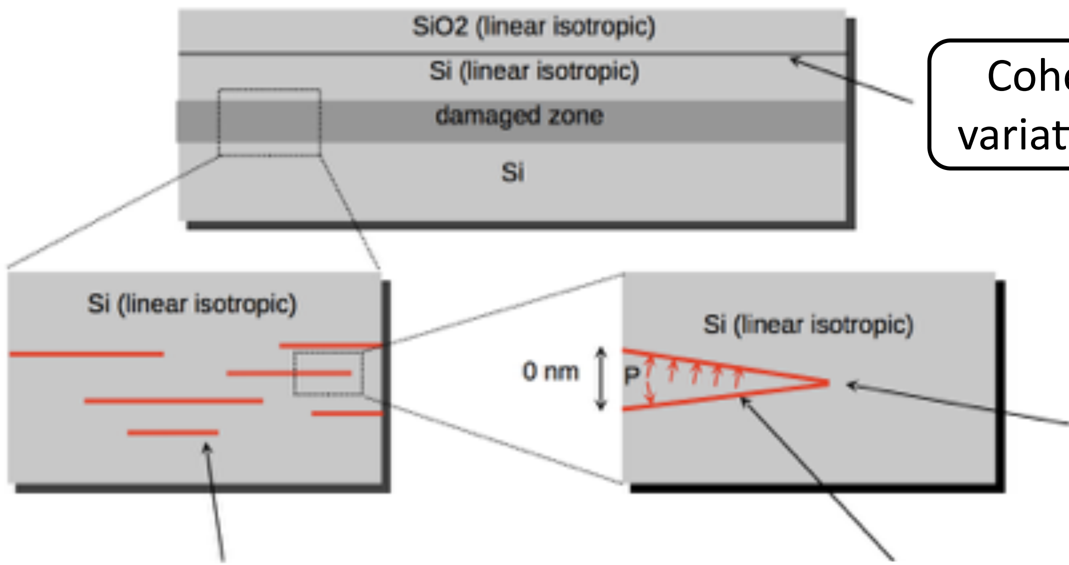

Cohesive interface with variation in surface energy

fracture criterion at the discontinuity tip

statistically distributed discontinuities

discontinuity subjected to H_2 pressure

XFEM formulation

Approximation function:

$$\mathbf{u}^h(\mathbf{x}) = \underbrace{\sum_{I \in \mathcal{N}_I} N_I(\mathbf{x})\mathbf{u}^I}_{\text{standard part}} + \underbrace{\sum_{J \in \mathcal{N}_J} N_J(\mathbf{x}) H(\mathbf{x}) \mathbf{a}^J}_{\text{discontinuous enrichment}} + \underbrace{\sum_{K \in \mathcal{N}_K} N_K(\mathbf{x}) \sum_{\alpha=1}^{4} f_\alpha(\mathbf{x}) \mathbf{b}^{K\alpha}}_{\text{singular tip enrichment}}$$

standard part

discontinuous enrichment

singular tip enrichment

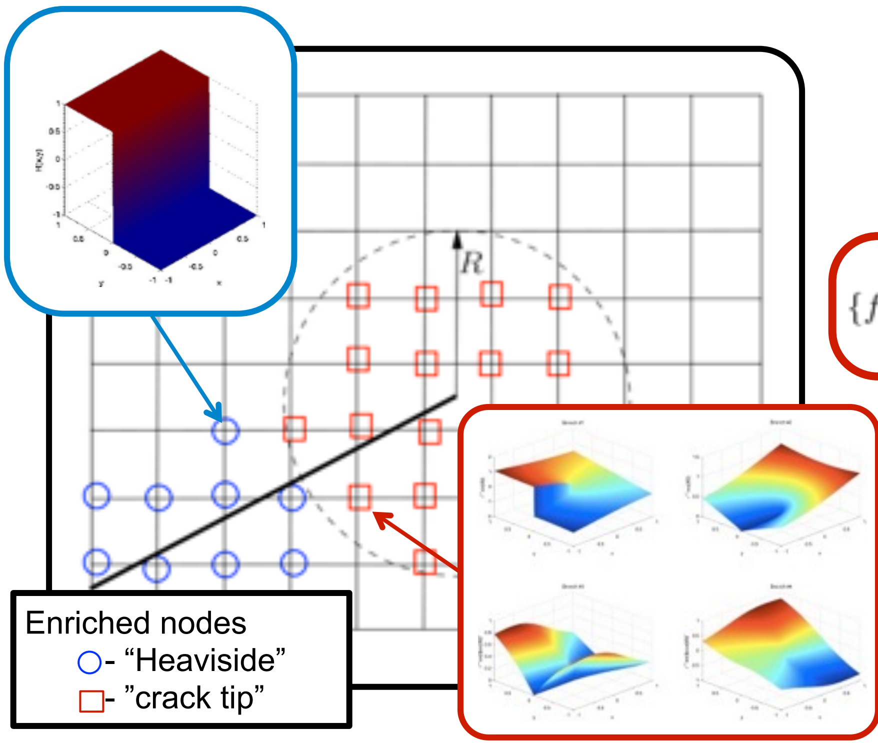

$$H(\mathbf{x}) = \begin{cases} +1 & \text{if } \mathbf{x} \text{ above crack} \\ -1 & \text{if } \mathbf{x} \text{ below crack} \end{cases}$$

$$\{f_\alpha(r,\theta), \alpha = 1,4\} = \left\{\sqrt{r}\sin\frac{\theta}{2}, \sqrt{r}\cos\frac{\theta}{2}, \sqrt{r}\sin\frac{\theta}{2}\sin\theta, \sqrt{r}\cos\frac{\theta}{2}\sin\theta\right\}$$

XFEM formulation

$$H(x) = \begin{cases} +1 & \text{if } x \text{ above crack} \\ -1 & \text{if } x \text{ below crack} \end{cases}$$

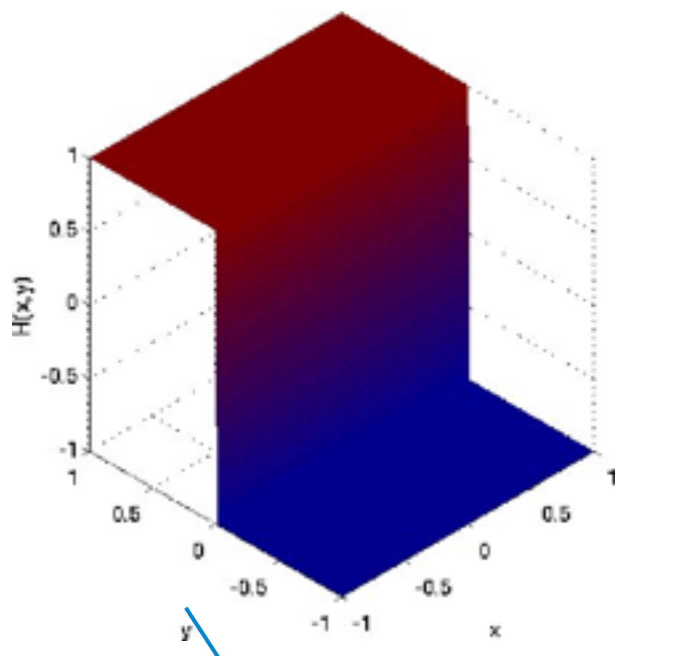

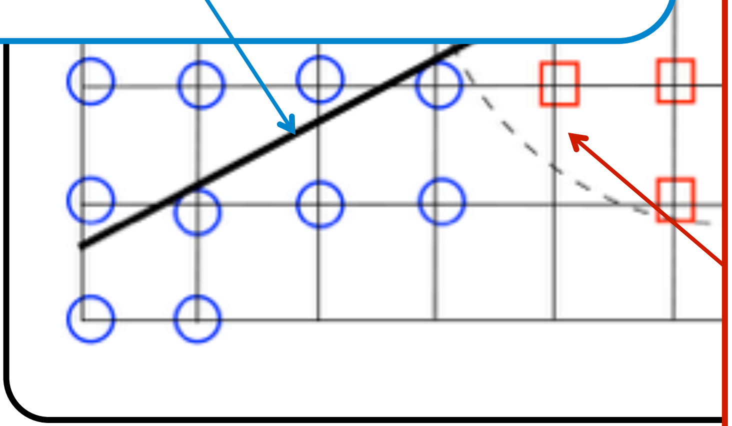

$$B(r,\theta) = \left\{ \sqrt{r}\cos\frac{\theta}{2} \quad \sqrt{r}\sin\frac{\theta}{2} \quad \sqrt{r}\sin\theta\,\sin\frac{\theta}{2} \quad \sqrt{r}\sin\theta\,\cos\frac{\theta}{2} \right\}$$

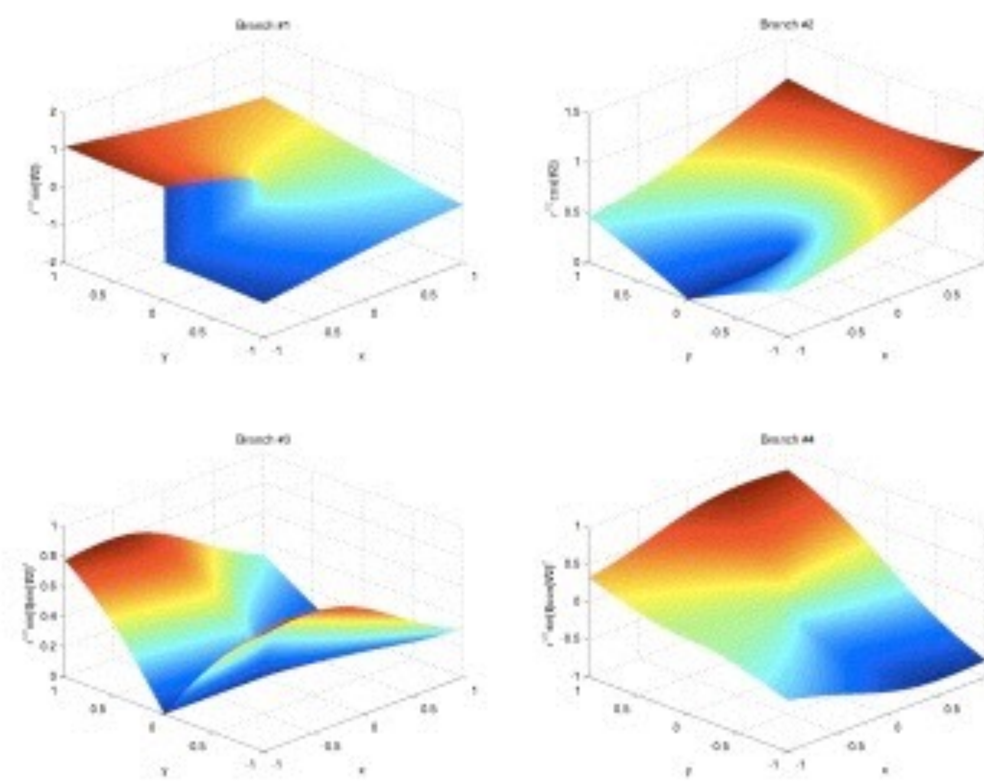

Discretization: XFEM

Extended Finite Element Method (XFEM)

- Introduced by Ted Belytschko (1999) for elastic problems

Fracture of "XFEM" using XFEM

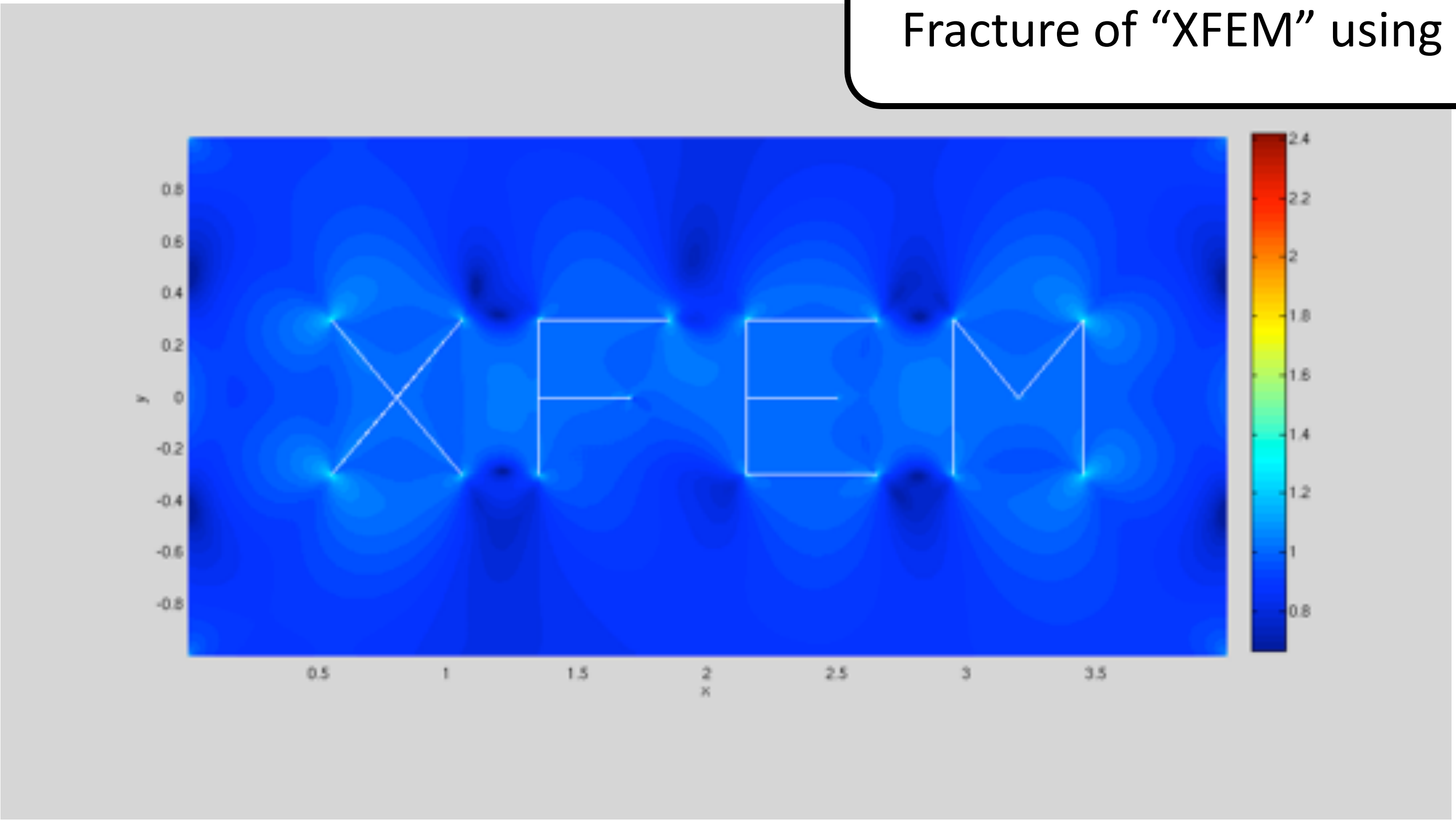

Plate with 300 cracks - vertical extension BCs

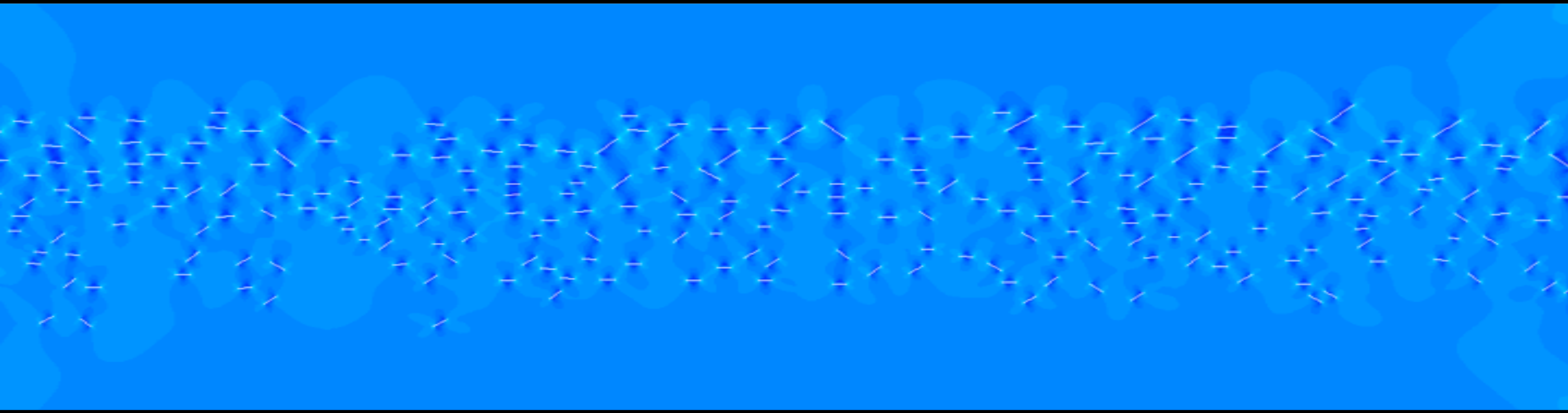

Example #1

Vertical extension of a plate with 300 cracks

Post-split roughness

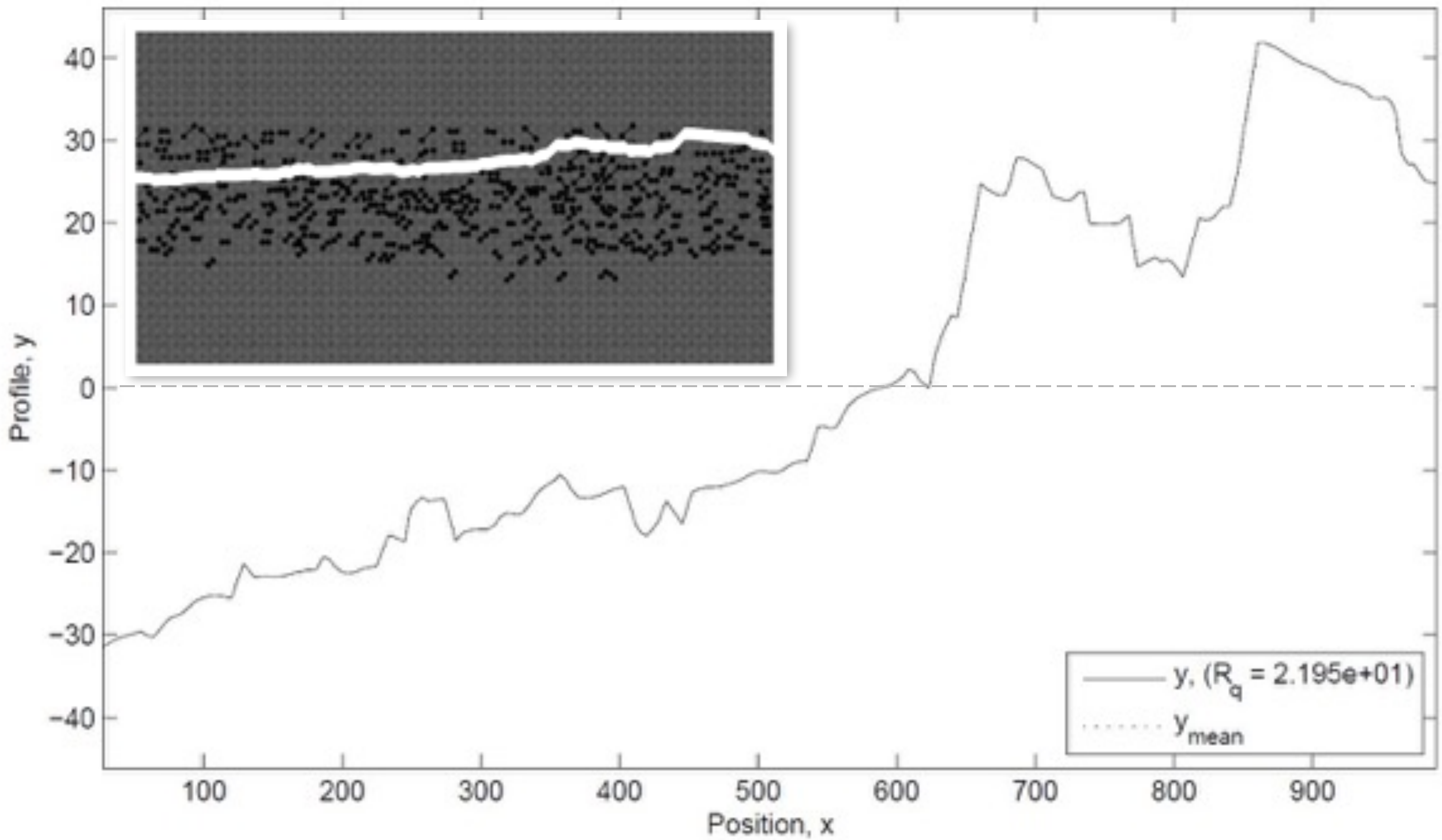

Example #2

Mechanical splitting of a wafer sample

- Post-split roughness as a function of micro crack distribution

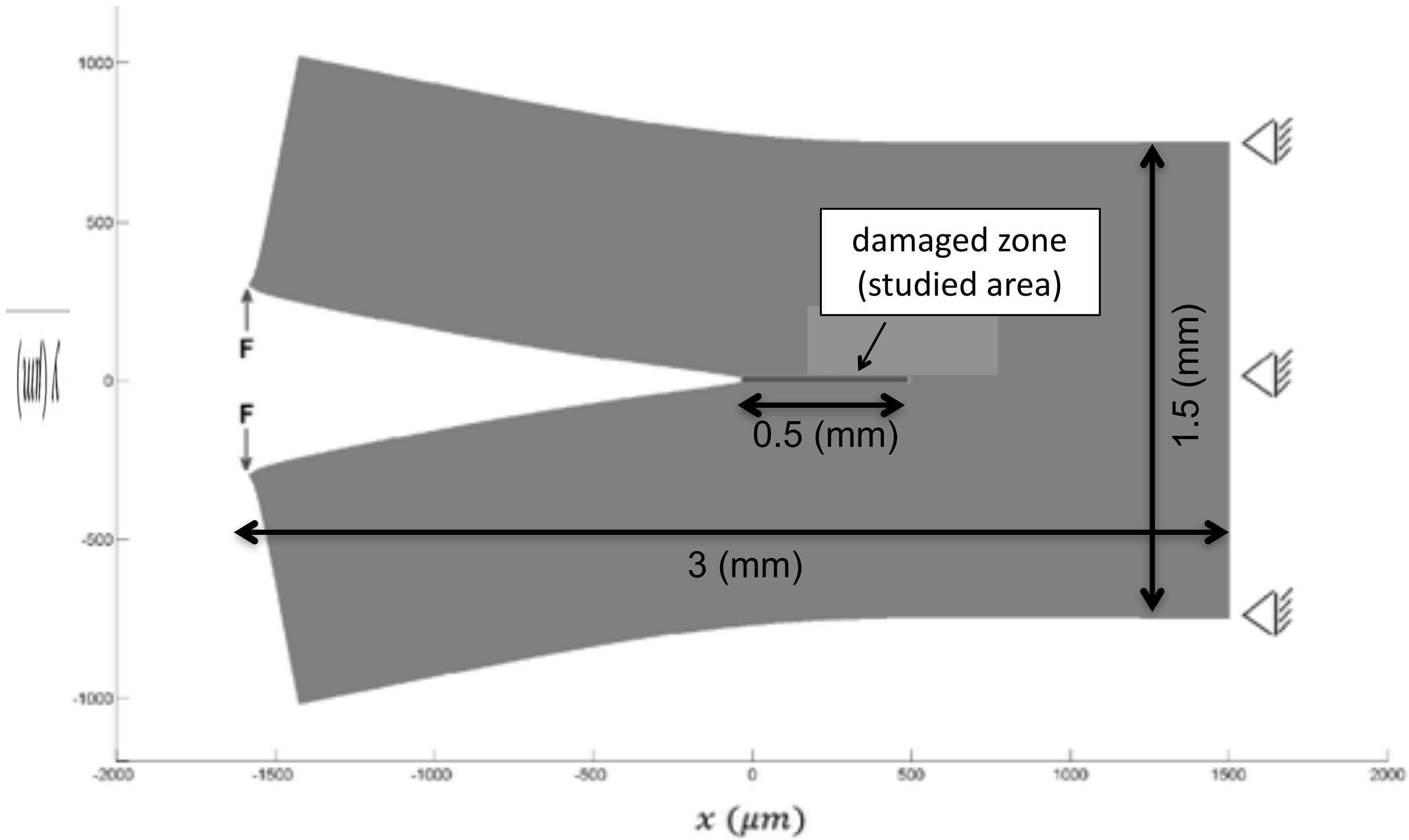

Example #2

Mechanical splitting of a wafer sample

- Discretisation (≈1mln. DOF, h_e = 150 nm)

Fracture control parameters

- initial cracked length: $\rho_{crk} = \{10, 30, 50, 70\}$ (%)
- damage thickness: $t_{dmg} = \{100, 300, 500\}$ (nm)

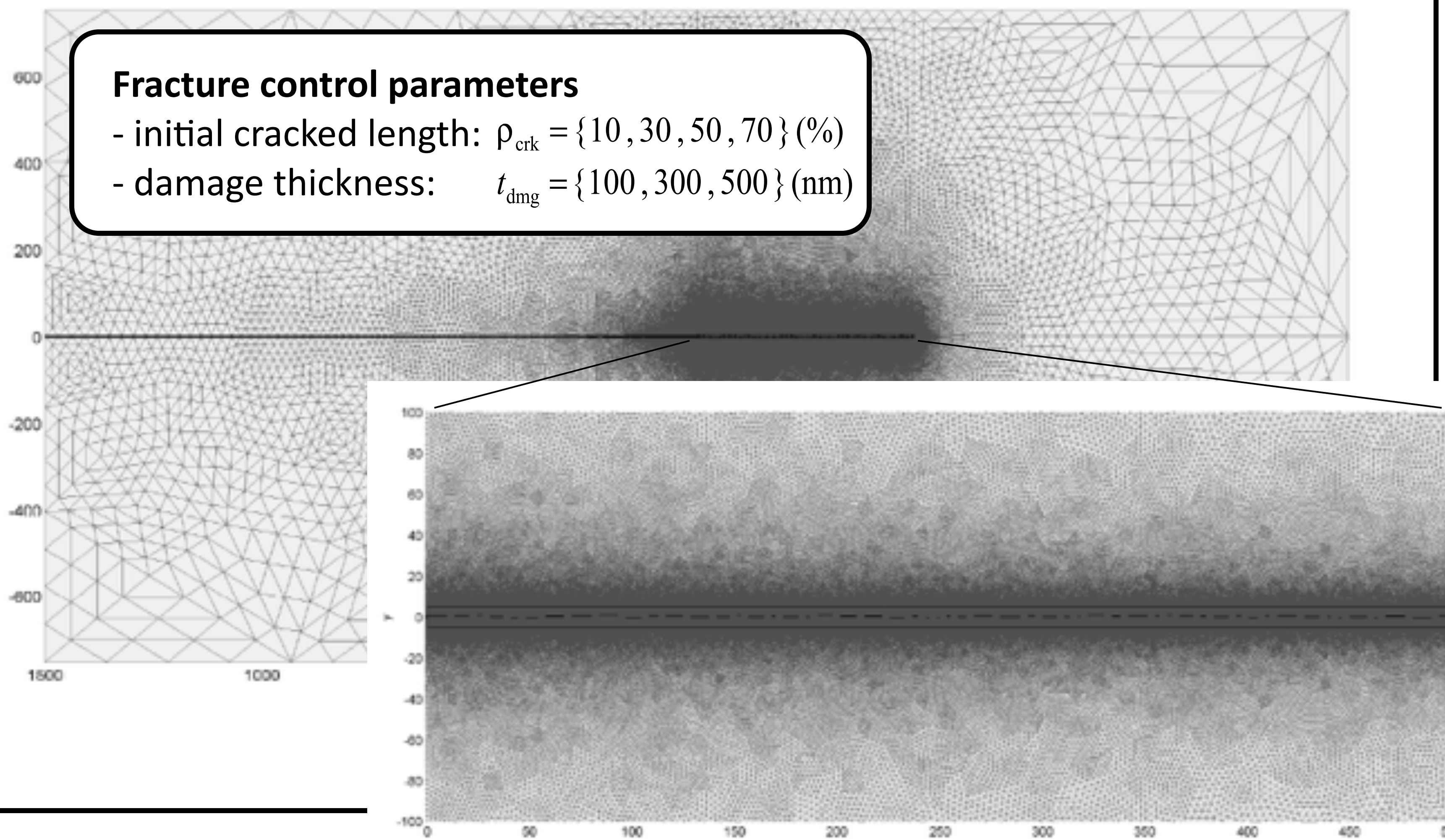

Example #2

Fracture ro

- Case exa

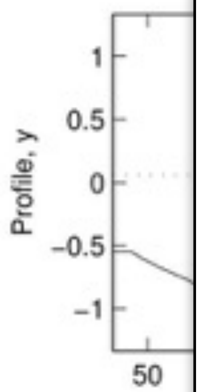

- Case exa

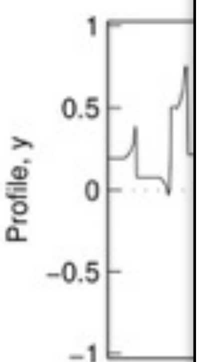

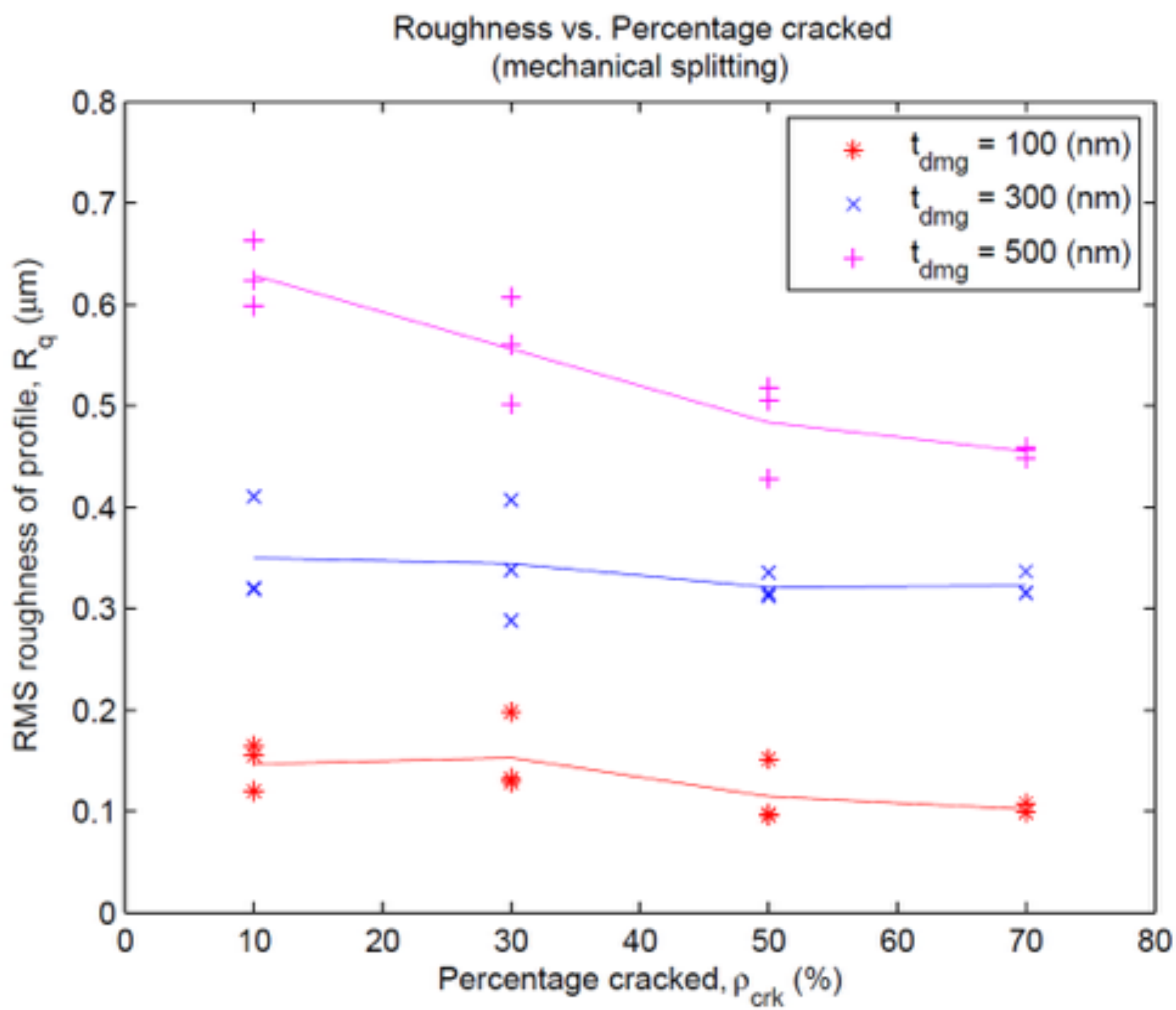

Summary

LEFM model

- Assuming mechanical interactions dominate during micro crack growth

Crack growth

- crack tip with max SIF in direction of max hoop stress

Discretization

- XFEM for efficient multiple fracture modeling

Part IV. Application to surgical simulation

with INRIA, France; Karol Miller, UWA.

RealTcut

Interactive multiscale cutting simulations

Institute of Mechanics & Advanced Materials

RealTcut

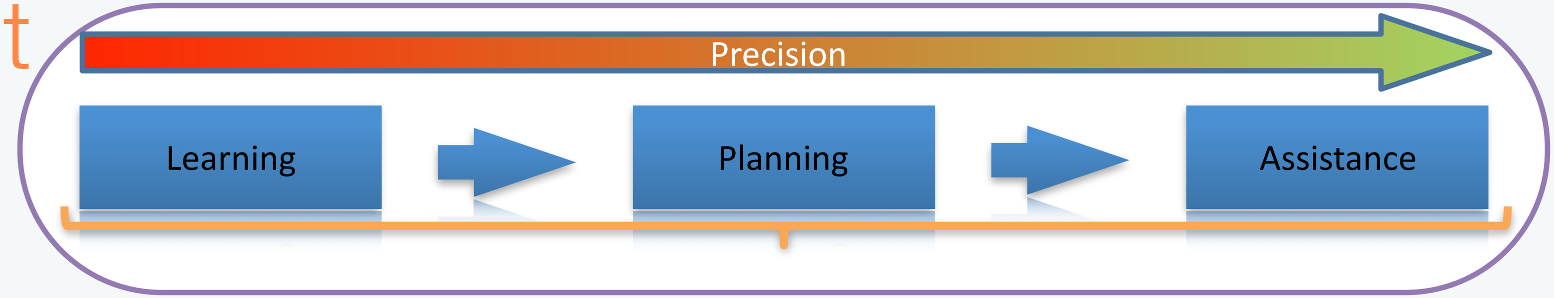

Surgical simulation (real time/interactivity)

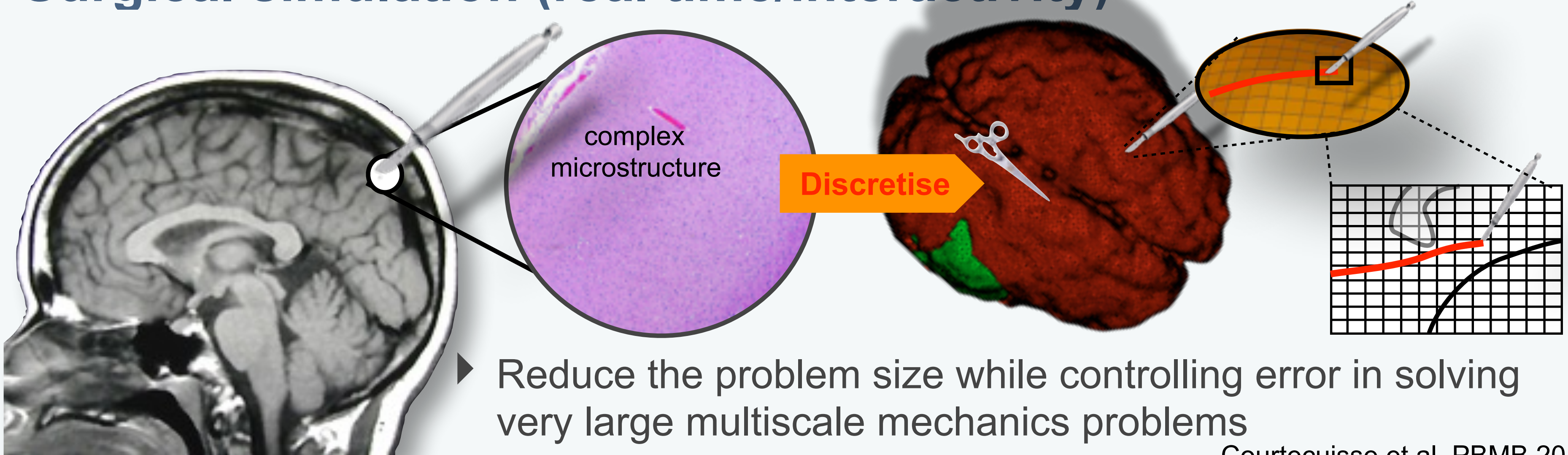

- Reduce the problem size while controlling error in solving very large multiscale mechanics problems

Courtecuisse et al. PBMB 2011

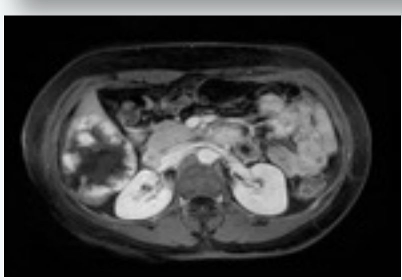
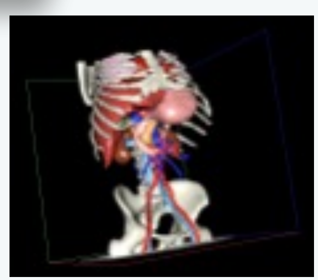
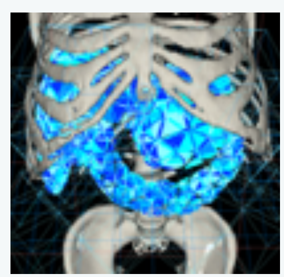
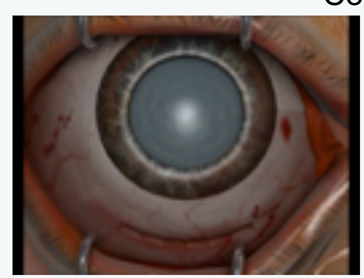


Interactive simulation of cutting in soft tissue

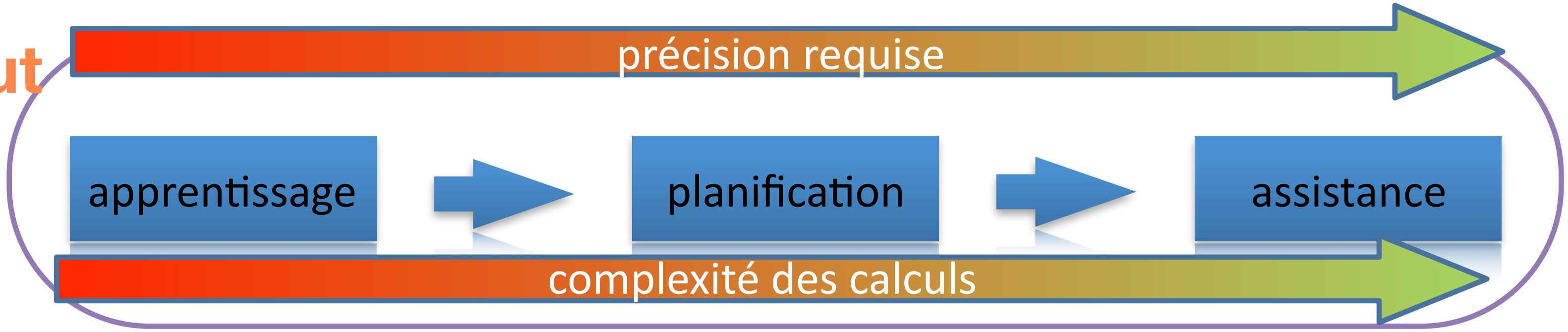

Real-time/interactivity for non-linear problems involving topological changes

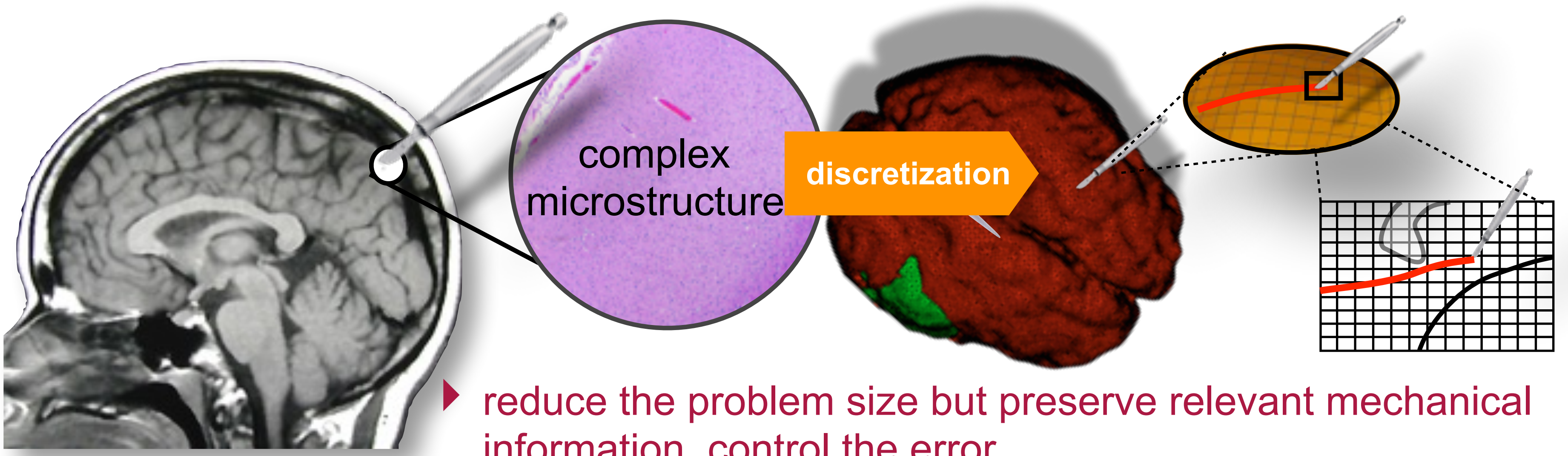

- reduce the problem size but preserve relevant mechanical information, control the error

Concrete objective: compute the response of organs during surgical procedures (including cuts) in real time (50-500 solutions per second)

Two schools of thought

- constant time
  - ➡ accuracy often controlled visually only
- model reduction or "learning"
  - ➡ scarce development for biomedical problems
  - ➡ no results available for cutting

First implicit, interactive method for cutting with contact

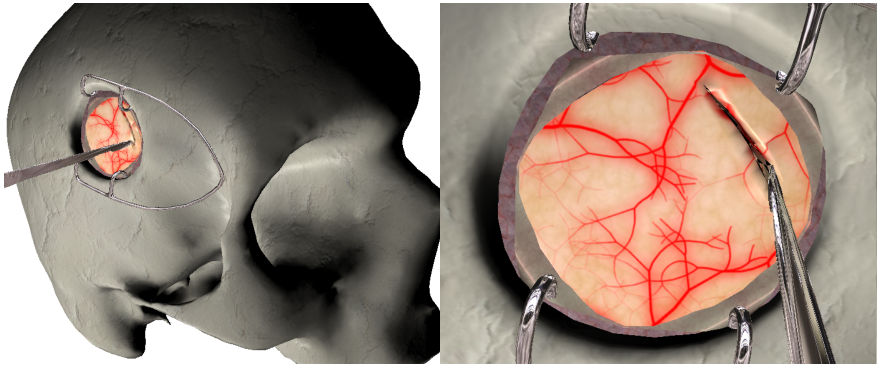

[Courtecuisse et al., MICCAI, 2013]
Collaboration INRIA

Proposed approach: maximize accuracy for given computational time. Error control

Complex geometries from medical images

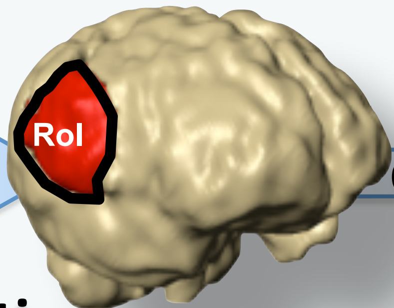

segmentation

Region of interest (RoI)

discretization

Topological changes & contact

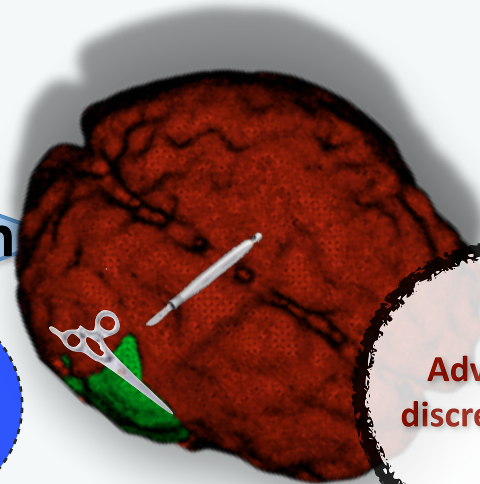

Model reduction

Advanced discretization

adaptivité

Error control

- interactivity
- space-time discretization?
- optimize use of compute resources

Verification & Validation

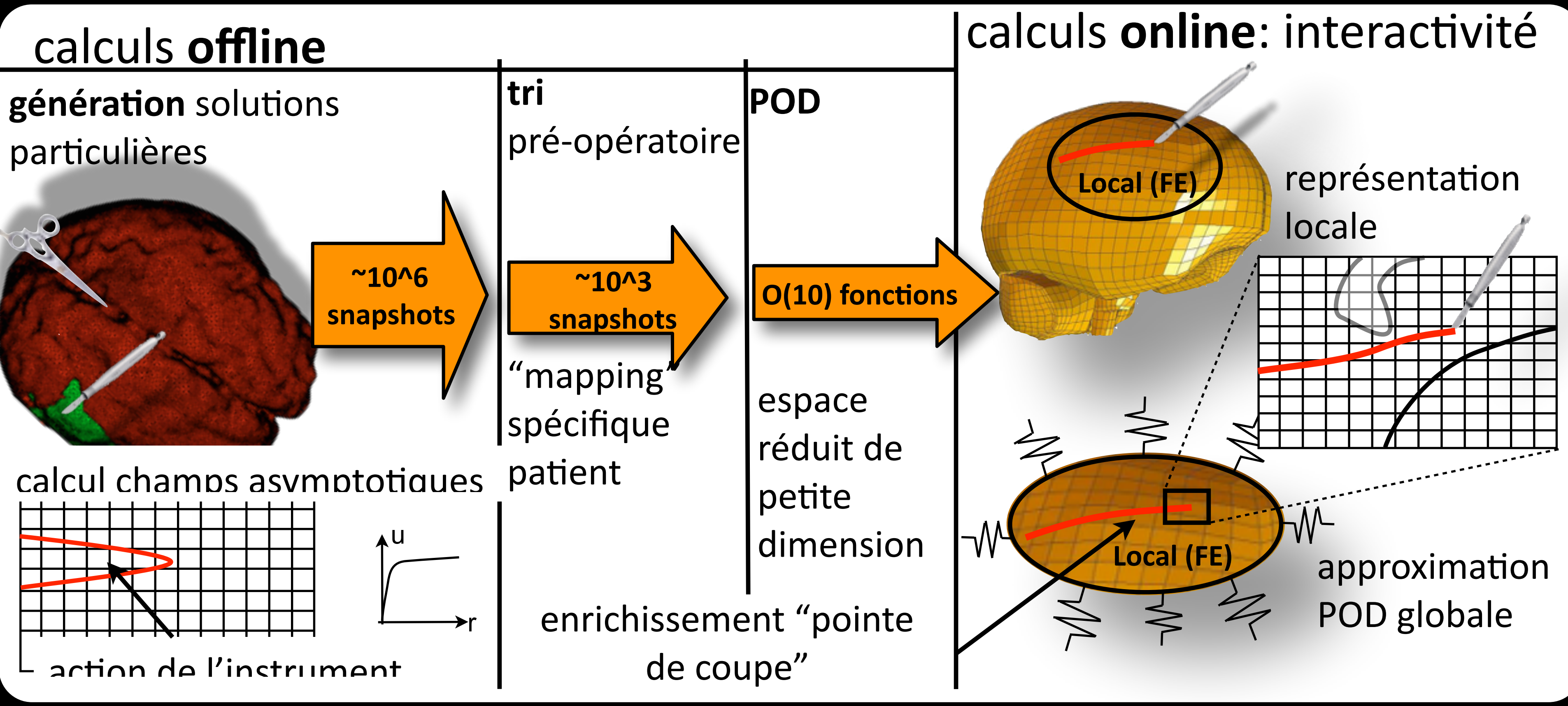

calculs offline
génération solutions particulières
~10^6 snapshots
calcul champs asymptotiques
u
r
action de l'instrument
tri
pré-opératoire
~10^3 snapshots
"mapping" spécifique patient
POD
O(10) fonctions
espace réduit de petite dimension
enrichissement "pointe de coupe"
calculs online: interactivité
Local (FE)
représentation locale
Local (FE)
approximation POD globale

A semi-implicit method for real-time deformation, topological changes, and contact of soft tissues

Paper ID : 269


There's a fine line between
wrong and visionary.
Unfortunately,
you have to be a
visionary to see it.
Sheldon Cooper,
The Big Bang Theory: The Pirate Solution

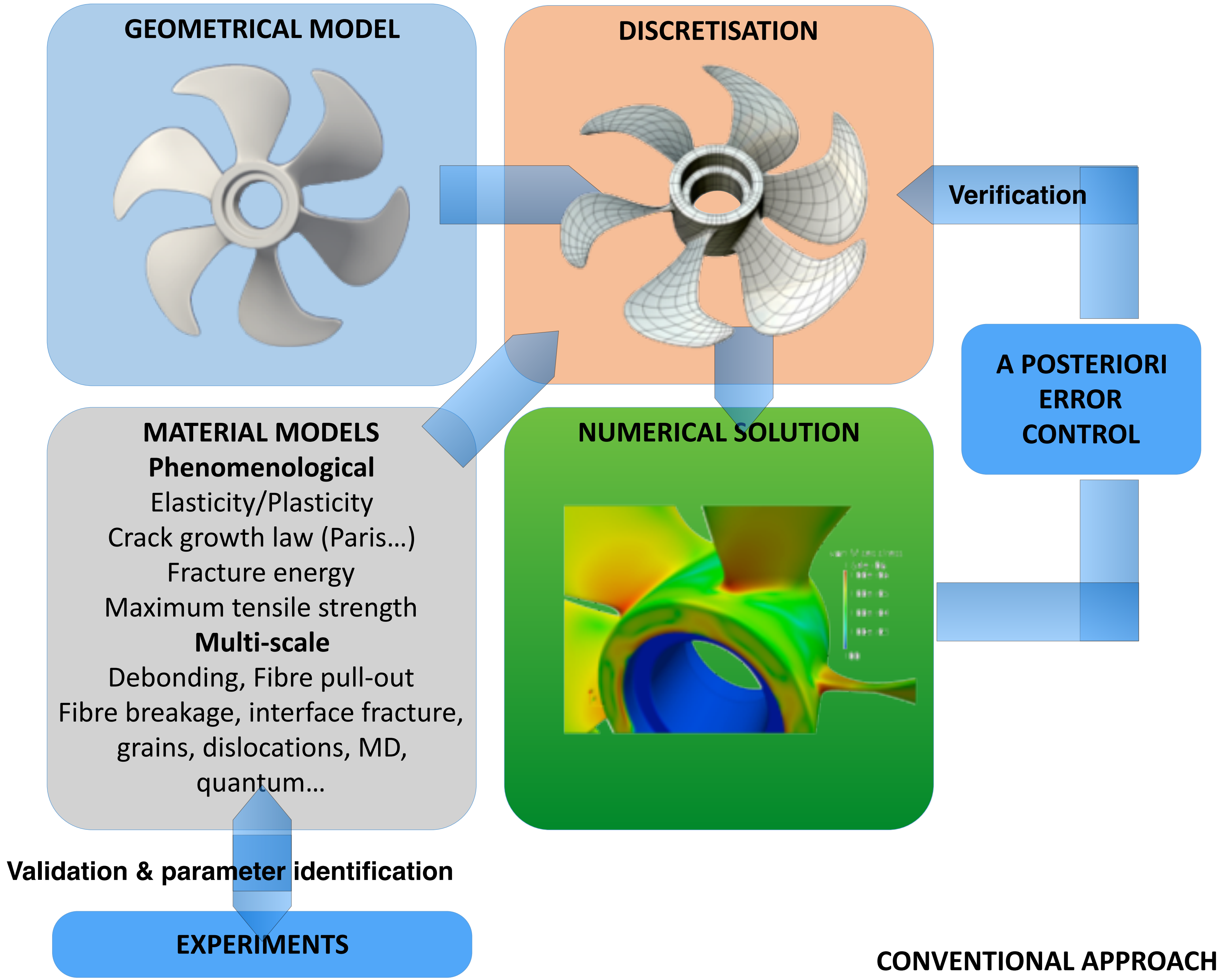

GEOMETRICAL MODEL
DISCRETISATION
Verification
A POSTERIORI ERROR CONTROL
MATERIAL MODELS
Phenomenological
Elasticity/Plasticity
Crack growth law (Paris...)
Fracture energy
Maximum tensile strength
Multi-scale
Debonding, Fibre pull-out
Fibre breakage, interface fracture, grains, dislocations, MD, quantum...
NUMERICAL SOLUTION
Validation & parameter identification
EXPERIMENTS
CONVENTIONAL APPROACH

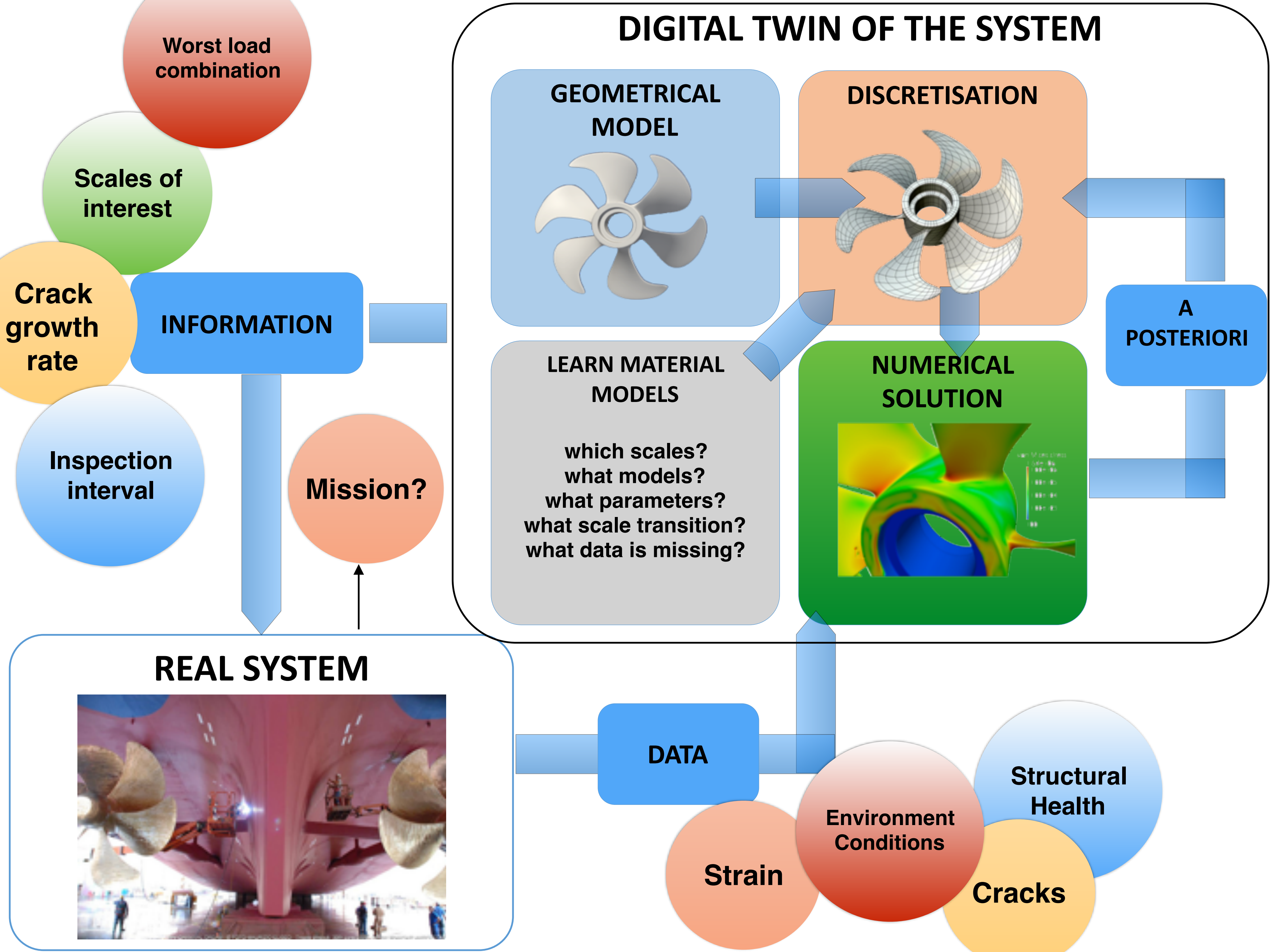
Worst load combination
Scales of interest
Crack growth rate
Inspection interval
INFORMATION
Mission?
DIGITAL TWIN OF THE SYSTEM
GEOMETRICAL MODEL
DISCRETISATION
A POSTERIORI
LEARN MATERIAL MODELS
which scales?
what models?
what parameters?
what scale transition?
what data is missing?
NUMERICAL SOLUTION
REAL SYSTEM
DATA
Strain
Environment Conditions
Structural Health
Cracks

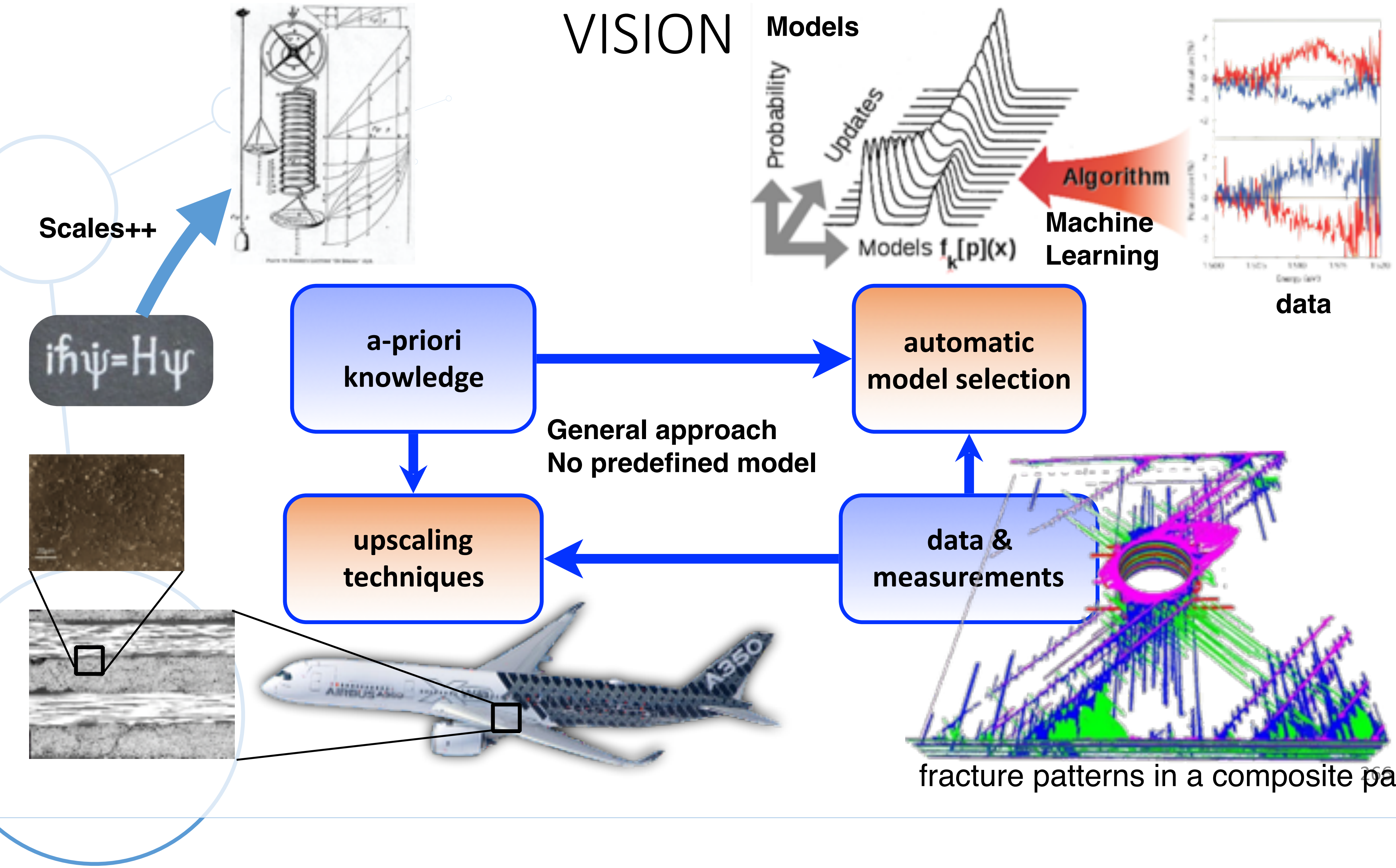
VISION
Models
Probability
Updates
Models f_k[p](x)
Algorithm
Machine
Learning
data
Scales++
iħψ=Hψ
a-priori
knowledge
automatic
model selection
General approach
No predefined model
upscaling
techniques
data &
measurements
A350
fracture patterns in a composite pa

Digital Twins...

Characterisation

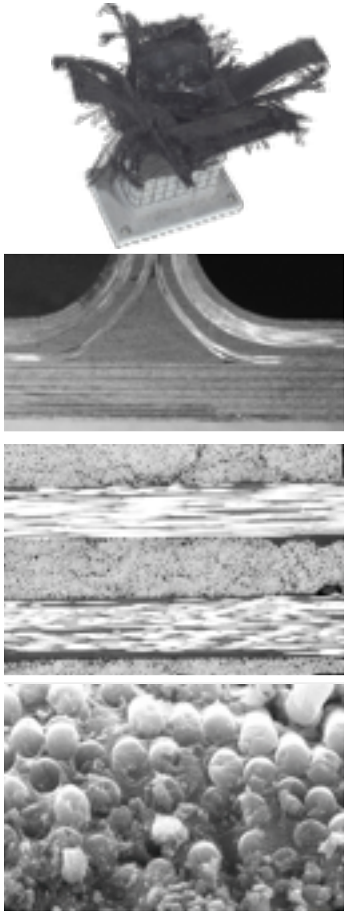

Monitoring

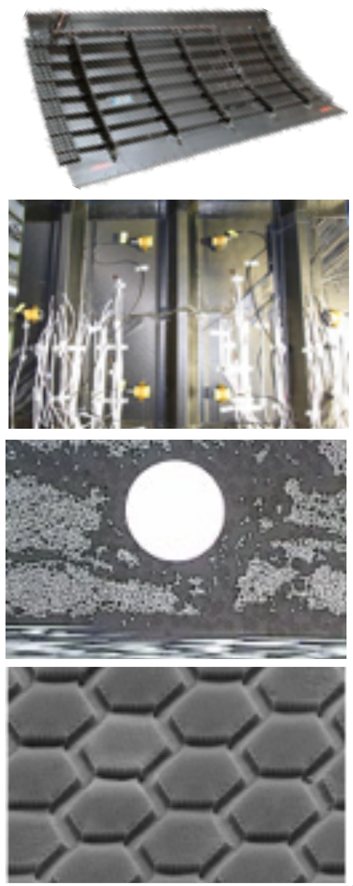

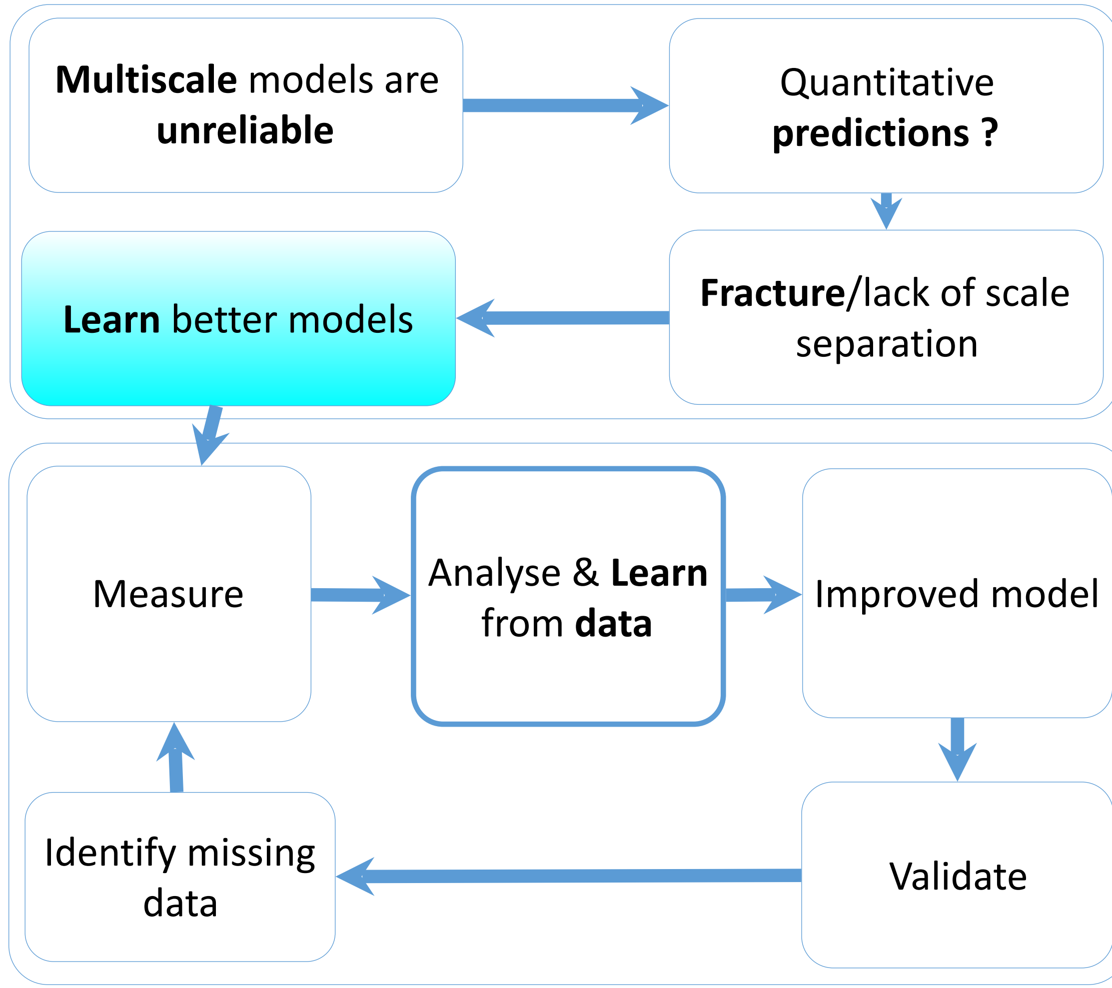

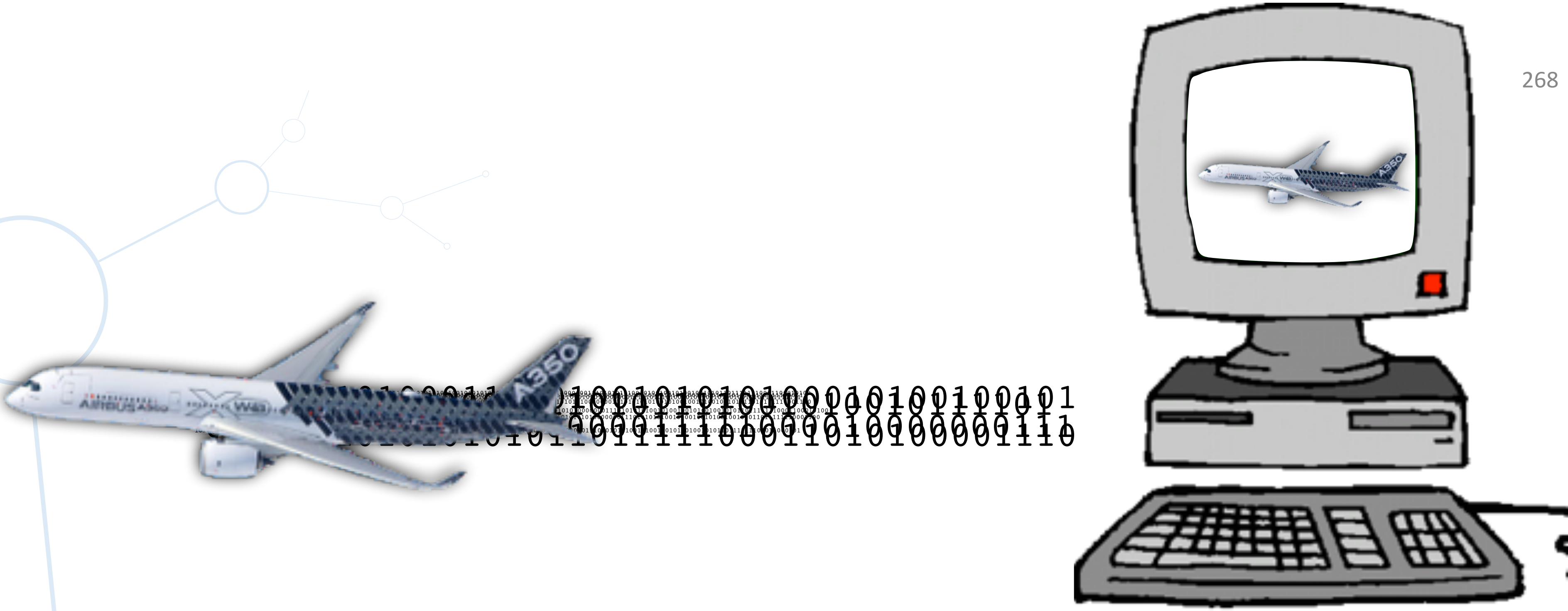
A350

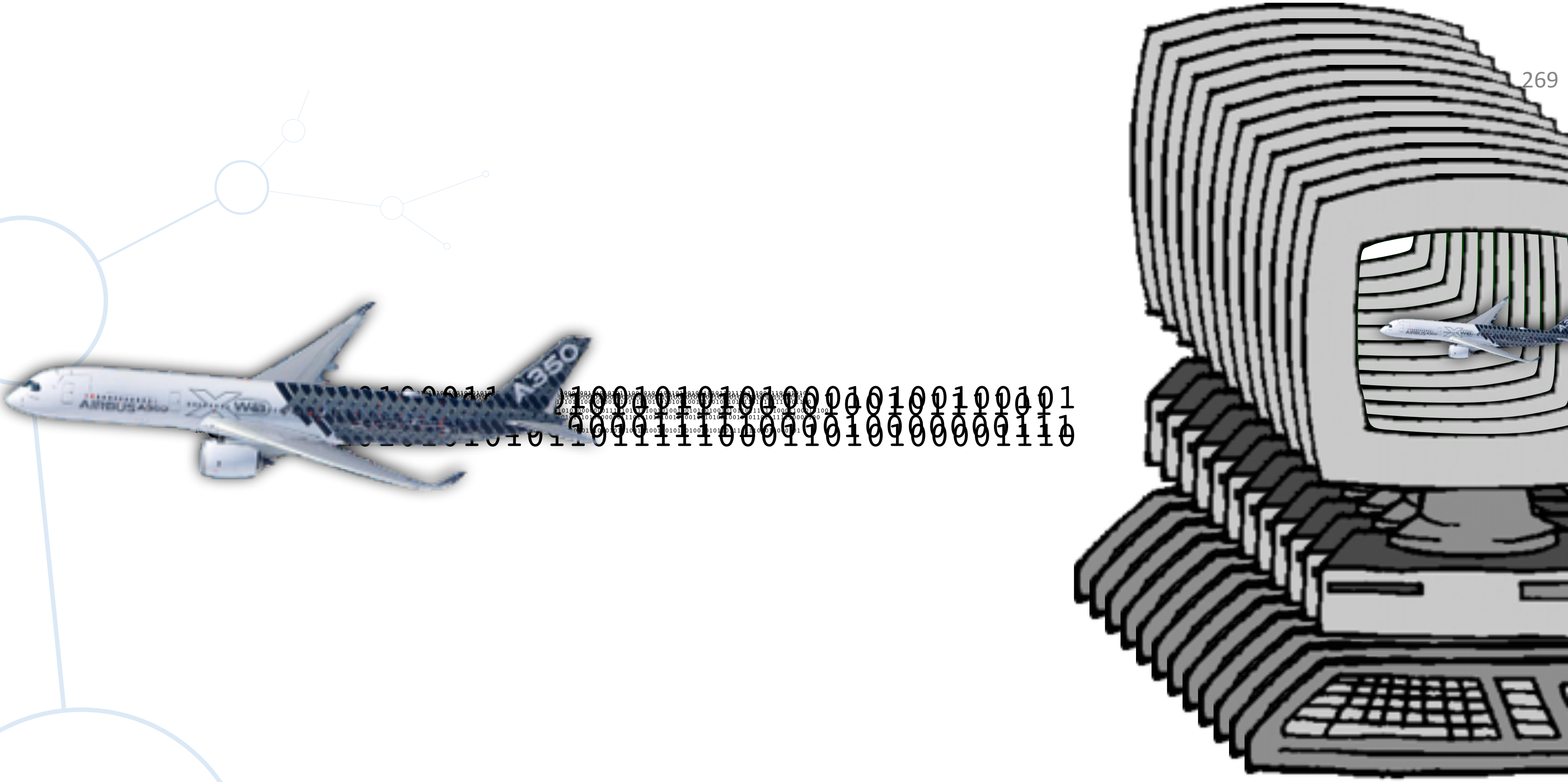

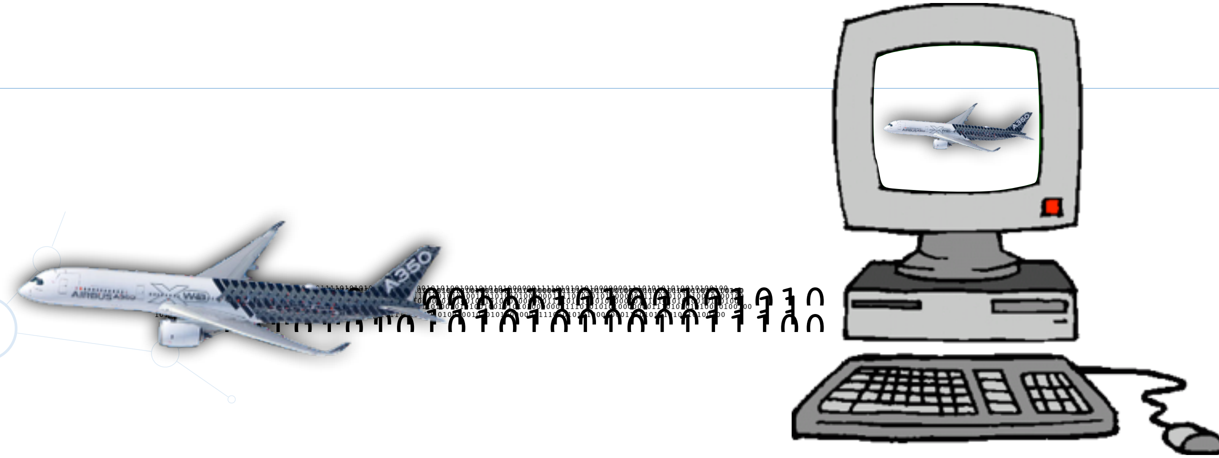

- Experience every event that its flying twin experiences
- Will revolutionise certification, fleet management and support (mirrors life of the “as-built” state)
- Will decrease weight
  - no reliance on statistical distribution of material properties
  - no reliance on heuristic design methods
  - less reliance on physical testing (environment?)
  - no assumed similitude between testing and operational conditions


www.imagespk.com www.imagespk.com www.imagespk.com www.imagespk.com

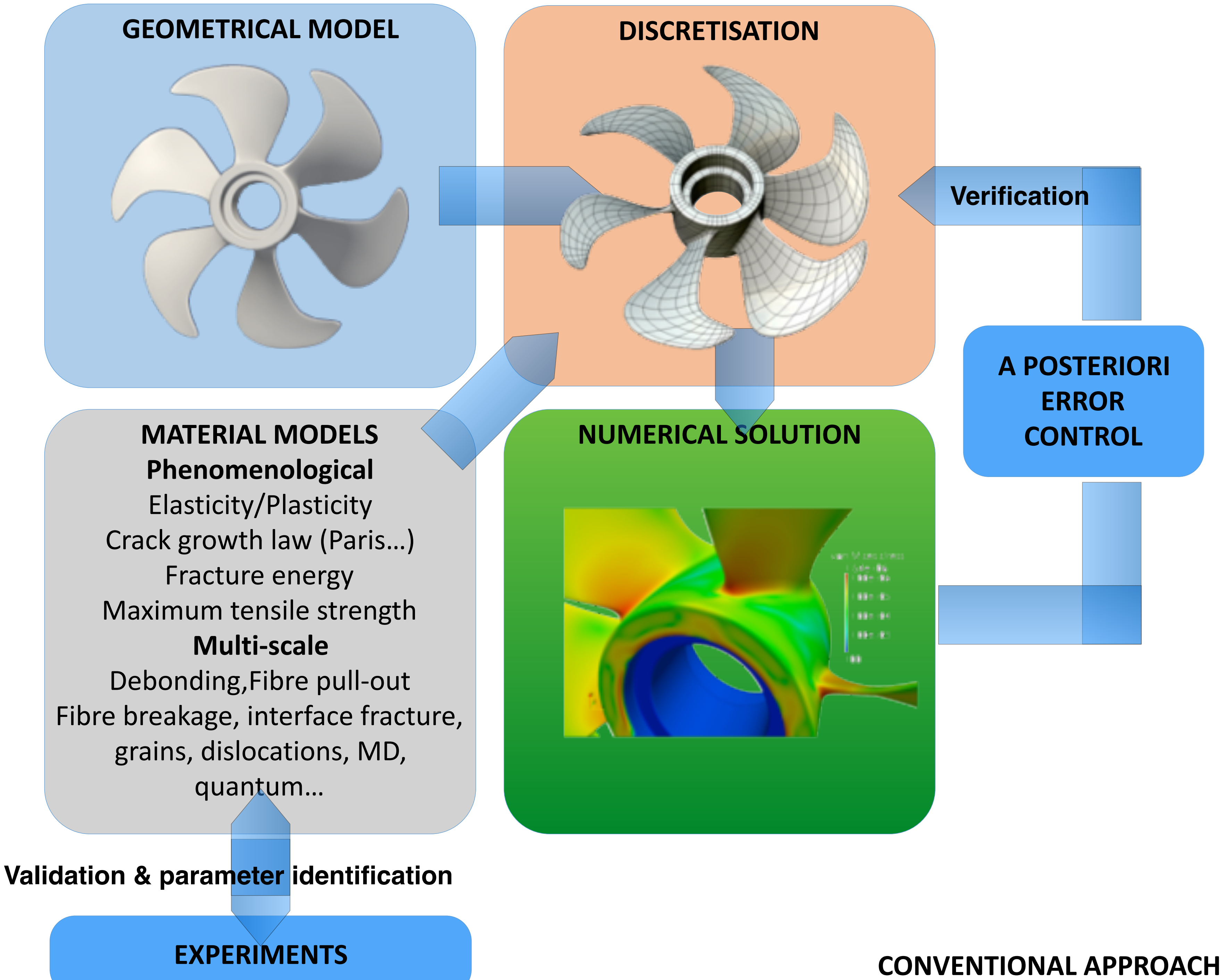
GEOMETRICAL MODEL
DISCRETISATION
Verification
A POSTERIORI ERROR CONTROL
MATERIAL MODELS
Phenomenological
Elasticity/Plasticity
Crack growth law (Paris…)
Fracture energy
Maximum tensile strength
Multi-scale
Debonding,Fibre pull-out
Fibre breakage, interface fracture, grains, dislocations, MD, quantum…
NUMERICAL SOLUTION
Validation & parameter identification
EXPERIMENTS
CONVENTIONAL APPROACH

When the material model is not known, this conventional approach is inadequate

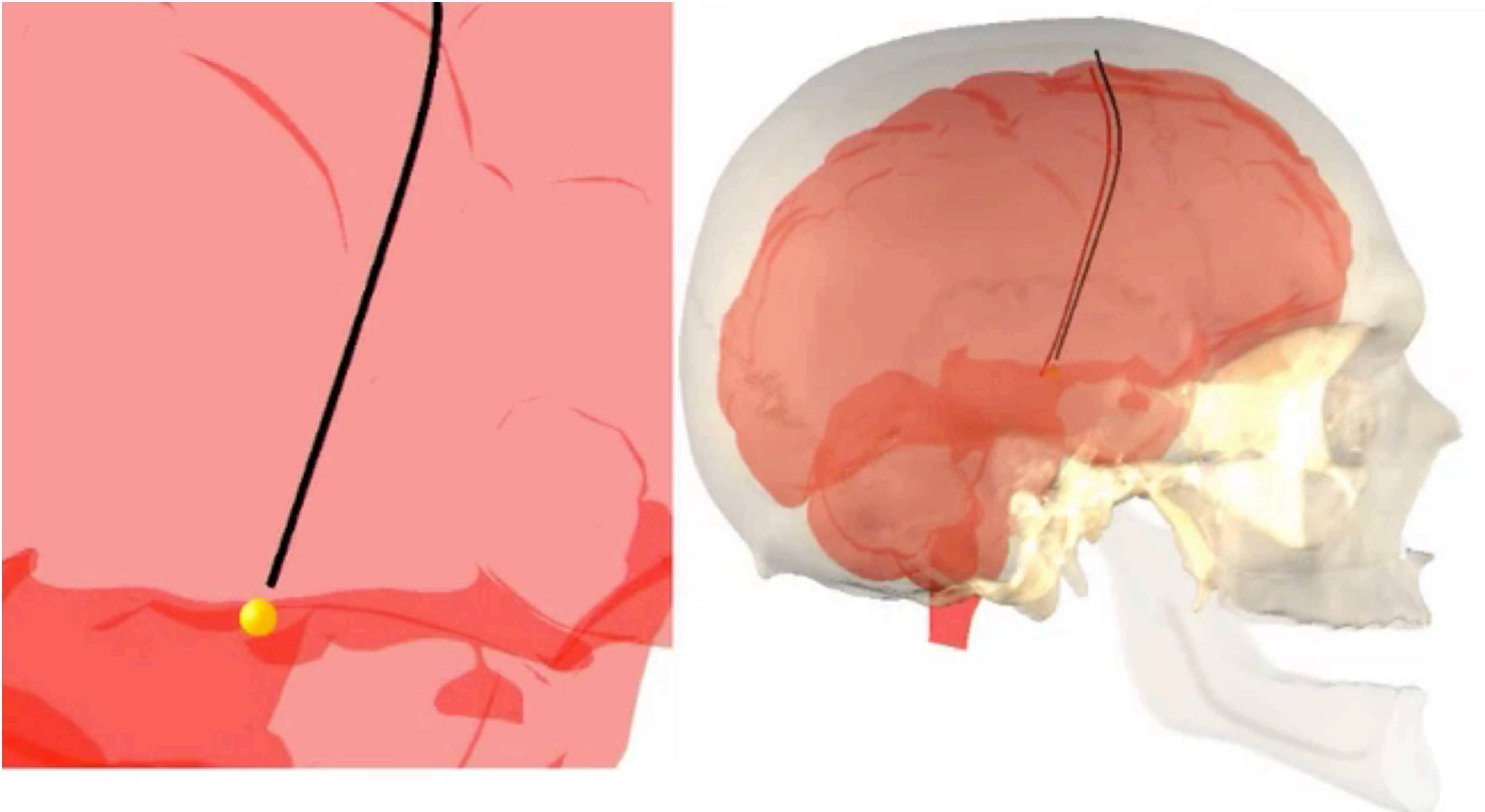

Deep-brain stimulation

Courtesy Alexandre Bilger, PhD thesis, Inria, 2014

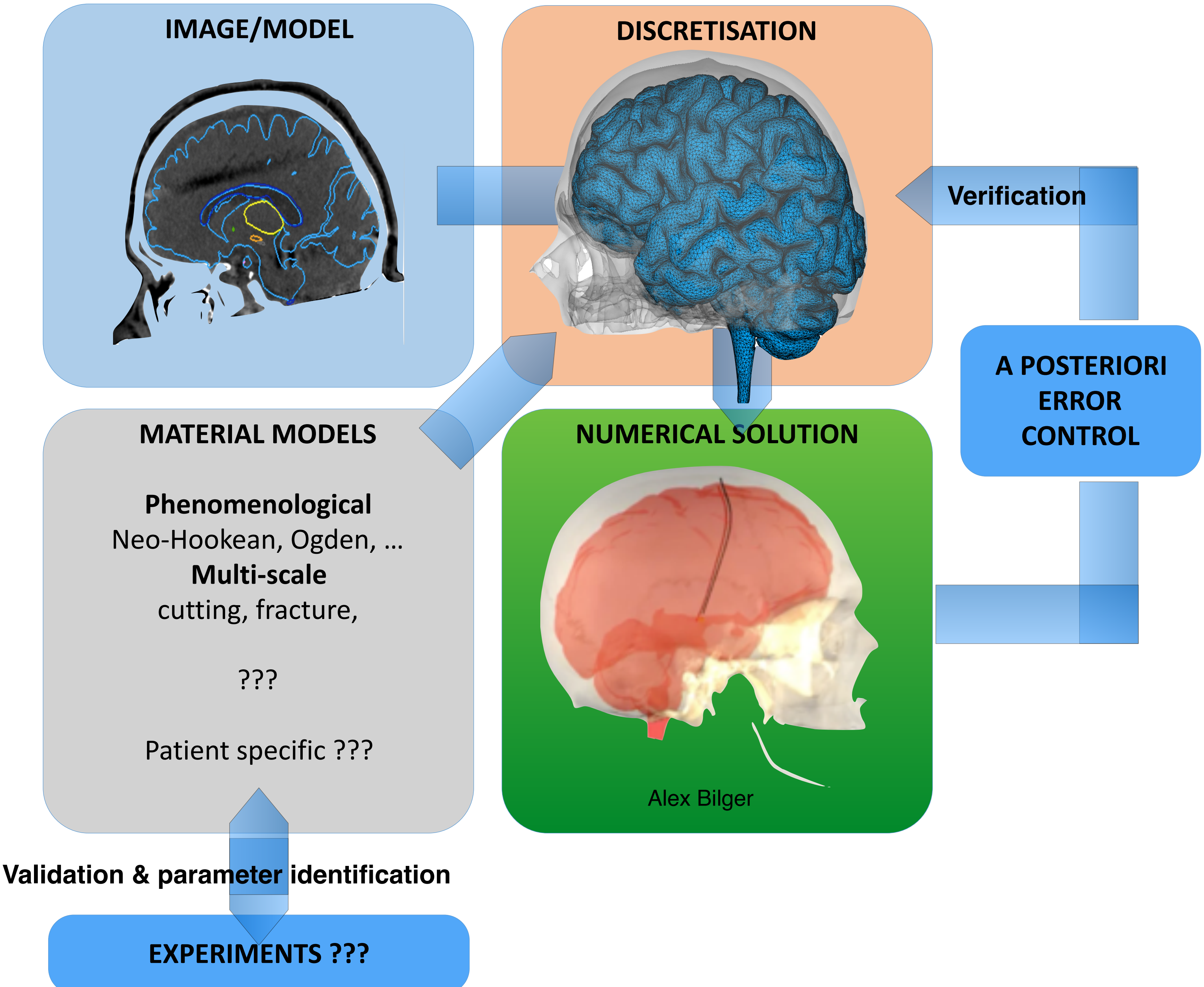
IMAGE/MODEL
DISCRETISATION
Verification
A POSTERIORI ERROR CONTROL
MATERIAL MODELS
Phenomenological
Neo-Hookean, Ogden, …
Multi-scale
cutting, fracture,
???
Patient specific ???
NUMERICAL SOLUTION
Alex Bilger
Validation & parameter identification
EXPERIMENTS ???

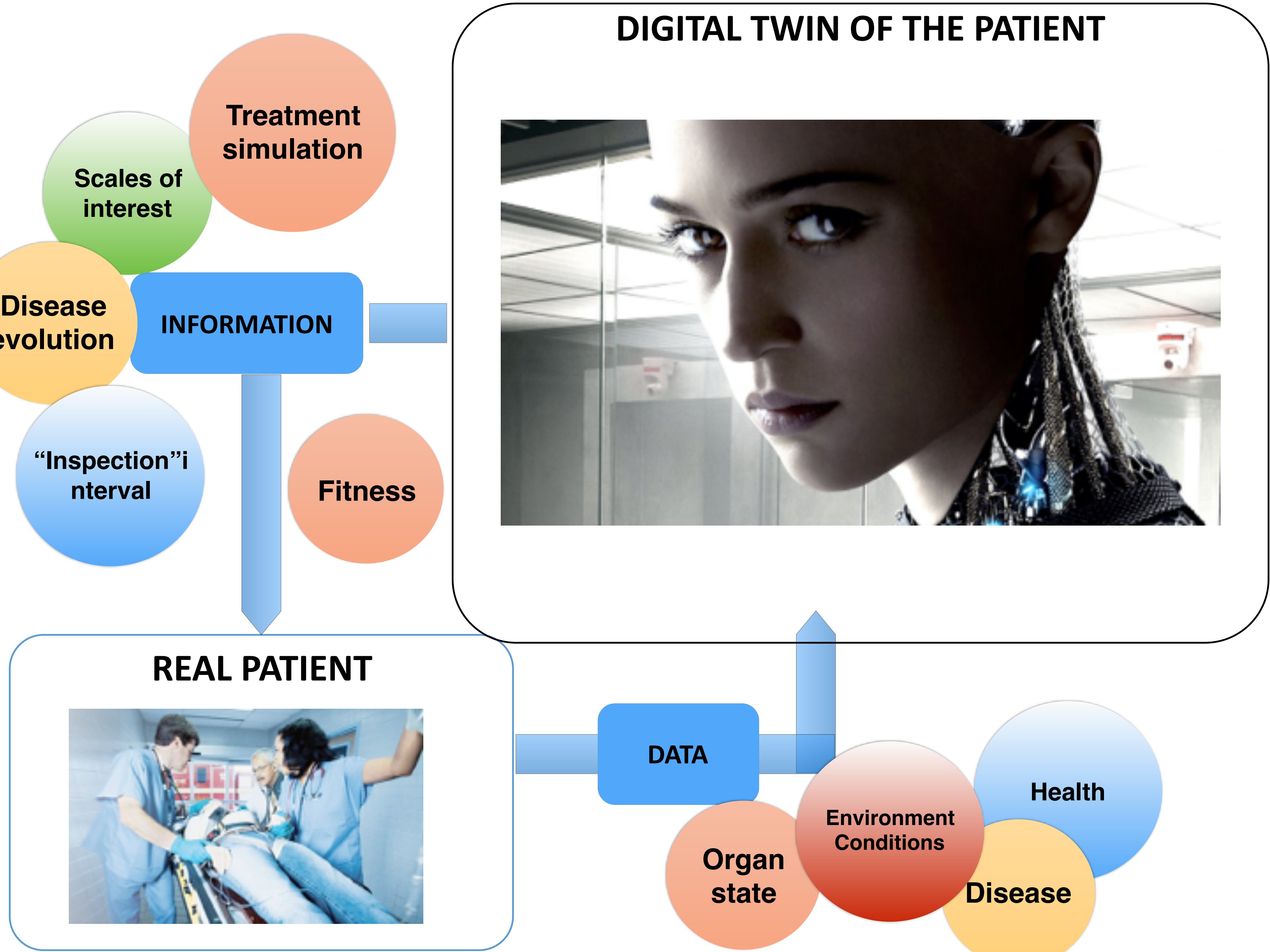
DIGITAL TWIN OF THE PATIENT
Treatment simulation
Scales of interest
Disease evolution
INFORMATION
"Inspection"i nterval
Fitness
REAL PATIENT
DATA
Health
Environment Conditions
Organ state
Disease

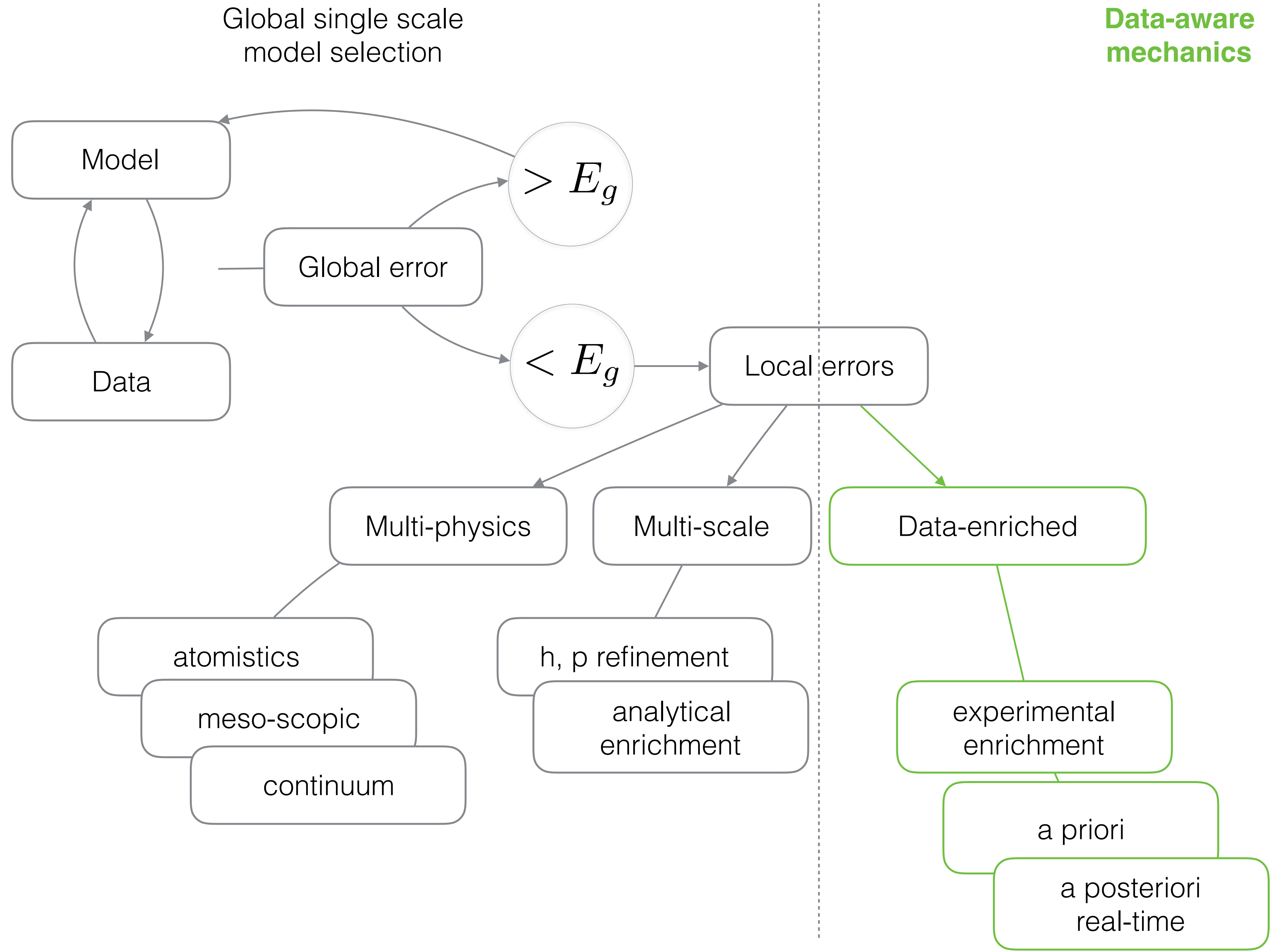

Global single scale
model selection
Data-aware
mechanics
Model
Data
Global error
$> E_g$
$< E_g$
Local errors
Multi-physics
Multi-scale
Data-enriched
atomistics
meso-scopic
continuum
h, p refinement
analytical
enrichment
experimental
enrichment
a priori
a posteriori
real-time

Papers on fracture

http://orbilu.uni.lu/handle/10993/26421

http://orbilu.uni.lu/handle/10993/22289

http://orbilu.uni.lu/handle/10993/20721

http://orbilu.uni.lu/handle/10993/24170

http://orbilu.uni.lu/handle/10993/21427

http://orbilu.uni.lu/handle/10993/21295
http://orbilu.uni.lu/handle/10993/16323

http://orbilu.uni.lu/handle/10993/22420

http://orbilu.uni.lu/handle/10993/19535

http://orbilu.uni.lu/handle/10993/21330

http://orbilu.uni.lu/handle/10993/18262

http://orbilu.uni.lu/handle/10993/19509

http://orbilu.uni.lu/handle/10993/19371

http://orbilu.uni.lu/handle/10993/17536

http://orbilu.uni.lu/handle/10993/17647

http://orbilu.uni.lu/handle/10993/14135

http://orbilu.uni.lu/handle/10993/16842

Papers on fracture

https://orbilu.uni.lu/bitstream/10993/22331/2/paper.pdf

http://orbilu.uni.lu/handle/10993/25048

http://orbilu.uni.lu/handle/10993/20721

http://orbilu.uni.lu/handle/10993/22420

http://orbilu.uni.lu/handle/10993/19960
http://orbilu.uni.lu/handle/10993/12316

http://orbilu.uni.lu/handle/10993/15109
http://orbilu.uni.lu/handle/10993/14067
http://orbilu.uni.lu/handle/10993/13879
http://orbilu.uni.lu/handle/10993/13876
http://orbilu.uni.lu/handle/10993/12523
http://orbilu.uni.lu/handle/10993/10965
http://orbilu.uni.lu/handle/10993/21442
http://orbilu.uni.lu/handle/10993/12107
http://orbilu.uni.lu/handle/10993/12026
http://orbilu.uni.lu/handle/10993/12026
http://orbilu.uni.lu/handle/10993/12089
http://orbilu.uni.lu/handle/10993/12113
http://orbilu.uni.lu/handle/10993/12116
http://orbilu.uni.lu/handle/10993/21337
http://orbilu.uni.lu/handle/10993/15234
http://orbilu.uni.lu/handle/10993/19960

Presentations

http://orbilu.uni.lu/handle/10993/15387